The Risk of Blepharoptosis in Contact Lens Wearers

Kun Hwang, MD, PhD and Joo Ho Kim, MD†*

Abstract: The aim of this systematic review was to summarize and evaluate the risk of blepharoptosis in contact lens wearers. In a PubMed search, 393 papers were found using the terms ''lens and ptosis.'' The abstracts were read and 16 full text articles were reviewed. Among them, 5 articles were analyzed. Five studies were subgrouped and a meta-analysis of these data suggested there is an increased risk of blepharoptosis in hard contact lens wearers over nonwearers (n = 7426, OR, 17.38, 95% CI = 3.71–81.29, $P < 0.00001$). One study was subgrouped and these data suggested there is also an increased risk of blepharoptosis in soft contact lens wearers over nonwearers (n = 90, OR, 8.12, 95% CI = 2.68–24.87, $P < 0.0002$). Patients wearing rigid contact lenses should be advised of the risk of ptosis, and a history of contact lens use should be sought in all patients who have acquired ptosis as the previous authors have recommended.

Key Words: Blepharoptosis, contact lenses, meta-analysis

Many plastic surgeons think that prolonged contact lens wear potentially causes acquired ptosis. Although several papers been written, only 1 study attempted to determine the risk of developing blepharoptosis due to wearing hard contact lenses.[1] Moreover, no systematic review of this subject is available.

The aim of this systematic review was to summarize and evaluate the risk of blepharoptosis in contact lens wearers.

METHODS

In a PubMed search, 393 papers were found using the terms "lens and ptosis." Studies that did not allow an evaluation of blepharoptosis due to contact lenses were excluded.

The abstracts were read and 16 full text articles were reviewed. Among them, 5 articles were analyzed (Fig. 1).[1–5] No restrictions on language and publication forms were imposed. However, the resulting full text papers were mostly in English. All articles were read by 2 independent reviewers who extracted data from the articles.

To summarize the effect of contact lens use on blepharoptosis, the data were summarized and the odds ratio (OR) between the contact lens wearers and nonwearers (control group) were calculated. Weighted mean differences (WMD) and 95% confidence intervals (CI) were also calculated. A statistical analysis was performed with Review Manager (The Nordic Cochrane Centre). In case the number of nonwearers was not written in the paper, it was calculated from the percent of the wearers and nonwearers of the general population of the nation reported.[6–8]

From the *Department of Plastic Surgery, Inha University School of Medicine; and †Department of Plastic Surgery, Inha University Hospital, Incheon, Korea.

Received September 24, 2014.
Accepted for publication April 7, 2015.

Address correspondence and reprint requests to Kun Hwang, MD, PhD, Department of Plastic Surgery, Inha University School of Medicine, 27 Inhang-ro, Jung-gu, Incheon 400-711, Korea;
E-mail: jokerhg@inha.ac.kr

The authors report no conflicts of interest.

Copyright © 2015 by Mutaz B. Habal, MD

ISSN: 1049-2275
DOI: 10.1097/SCS.0000000000001876

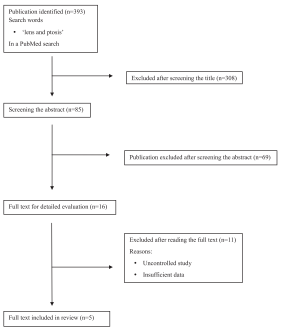

FIGURE 1. Flow chart of the selection process.

RESULTS

The 16 potentially relevant full text articles were reviewed, of which 5 articles met our inclusion criteria (Fig. 1).[1–5]

Effect of Hard Contact Lens Use on Blepharoptosis

Five studies were subgrouped and a meta-analysis of these data suggested there is an increased risk of blepharoptosis in hard contact lens wearers over nonwearers (n = 7426, OR, 17.38, 95% CI = 3.71–81.29, $Z = 3.63$, $P = 0.00003$, heterogeneity: $\chi^2 = 97.77$, $P < 0.00001$, $I^2 = 96\%$) (Table 1, Fig. 2A).

Effect of Soft Contact Lens Use on Blepharoptosis

One study was subgrouped and these data suggested there is also an increased risk of blepharoptosis in soft contact lens wearers over nonwearers (n = 90, OR, 8.12, 95% CI = 2.68–24.87, $Z = 3.70$, $P < 0.0002$) (Table 1, Fig. 2B).

DISCUSSION

All the studies analyzed were retrospective database studies because no randomized controlled study was available for contact lens use.

Kitazawa indicated that there was a significant association between hard contact lenses and blepharoptosis. The history of wearing hard contact lenses was significantly higher in patients (90.2%) versus controls (31.6%). Hard contact lens wearers had a 20 times increased risk of ptosis (odds ratio: 19.9; 95% confidence interval: 6.32–62.9) compared with the nonwearing subjects. In the other 4 papers, the number of nonwearers was not written in the paper, and therefore, the numbers were calculated from the percent of wearers and nonwearers of the general population of the nation reported. The criteria adopted in Kitazawa's study were based on the definition by Small who defined ptosis as an MRD of 1.5 mm or less since Japanese subjects at this level can exhibit a droopy eye look.[9] The criteria used by the other studies included an MRD of less than 2.8 or 2.5 mm.[4,10]

The mechanism as causation for the blepharoptosis in contact lens wearers has been postulated by Bosch: first, simultaneous, antagonistic action of the orbicularis, and levator muscle while squeezing the eyelids to remove the lens, second, forceful rubbing of the lens and subsequent stretching of upper eyelid structures during failed attempts at lens removal, third, repeated and similar although less forceful rubbing of the lens during blinking, fourth, irritation, leading to edema, and fifth, irritation leading to blepharospasms.[10] To date, most authors have agreed with the aponeurogenic etiology that chronic manipulation of the upper lid during

Copyright © 2015 Mutaz B. Habal, MD. Unauthorized reproduction of this article is prohibited.

TABLE 1. Summary of Retrospective Database Studies Included

	Author	(Year)	Total Group Size (n = eyelids)	Ptosis		Without Ptosis		Results (OR [CI])
				Intervention Group (n)	Control Group (n)	Intervention Group (n)	Control Group (n)	
Hard Lens	Kersten	1995	3652	61	96	25	3470	88.20 [53.08, 146.53]
	Thean	2003	1054	19	398	11	626	2.72 [1.28, 5.77]
	Bleyen	2011	316	31	12	9	264	75.78 [29.57, 194.18]
	de Silva	2011	2544	31	792	15	1706	4.45 [2.39, 8.29]
	Kitazawa	2013	178	92	10	24	52	19.93 [8.85, 44.91]
Soft Lens	Bleyen	2011	108	10	12	8	78	8.12 [2.68, 24.67]

CI, confidence interval; OR, odds ratio.

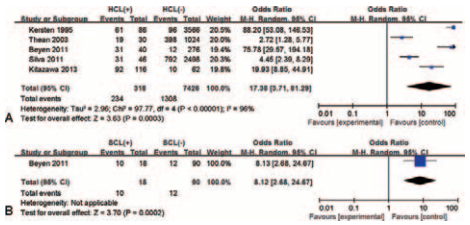

FIGURE 2. Meta-analysis of the effect of contact lens wearing on blepharoptosis. A, hard contact lens, B, soft contact lens.

rigid lens removal is responsible for inducing an aponeurotic disinsertion.[10–12]

Recently, Bleyen suggested that not only hard contact lens use but also soft contact lens use may be associated with ptosis. He insisted that the prolonged use of hard contact lenses most likely carries a higher risk than that for soft contact lenses for developing this disorder.[5] He recommend advising patients with blepharoptosis and contact lens users to discontinue contact lens use for 3 months and if the ptosis does not resolve, ptosis surgery can be planned.

Our meta-analysis implies that hard contact lens wearers (OR, 17.38) or a soft contact lens wearers (OR, 8.12) have an increased risk of blepharoptosis than nonwearers.

Patients wearing rigid contact lenses should be advised of the risk of ptosis, and the history of contact lens use should be sought in all patients with acquired ptosis as previous authors have recommended.[2,3]

ACKNOWLEDGMENT

This work was supported by a grant from INHA University (INHA-Research Grant).

REFERENCES

1. Kitazawa T. Hard contact lens wear and the risk of acquired blepharoptosis: a case-control study. *Eplasty* 2013;13:e30
2. Kersten RC, de Conciliis C, Kulwin DR. Acquired ptosis in the young and middle-aged adult population. *Ophthalmology* 1995;102: 924–928
3. Thean JH, McNab AA. Blepharoptosis in RGP and PMMA hard contact lens wearers. *Clin Exp Optom* 2004;87:11–14
4. de Silva DJ, Collin JR. Outcome following surgery for contact lens-induced ptosis. *Ophthal Plast Reconstr Surg* 2011;27:186–189
5. Bleyen I, Hiemstra CA, Devogelaere T, et al. Not only hard contact lens wear but also soft contact lens wear may be associated with blepharoptosis. *Can J Ophthalmol* 2011;46:333–336
6. Edwards K, Keay L, Naduvilath T, et al. A population survey of the penetrance of contact lens wear in Australia: rationale, methodology and results. *Ophthalmic Epidemiol* 2009;16:275–280
7. Nichols J. Contact Lenses 2008. Contact Lens Spectrum 2009; 1:24. Available at: http://www.clspectrum.com/article.aspx?article=102473. Accessed on: November 1, 2011
8. British Contact Lens Association. ACLM market report 2013: technical summary. Available at: https://www.bcla.org.uk/topics/aclm-releases-2013-contact-lens-market-report. Accessed on: September 1, 2014
9. Small RG, Sabates NR, Burrows D. The measurement and definition of ptosis. *Ophthalmic Plast Reconstr Surg* 1989;5:171–175
10. van den Bosch WA, Lemij HG. Blepharoptosis induced by prolonged hard contact lens wear. *Ophthalmology* 1992;99:1759–1765
11. Epstein G, Putterman AM. Acquired blepharoptosis secondary to contact-lens wear. *Am J Ophthalmol* 1981;91:634–639
12. Frueh BR. The mechanistic classification of ptosis. *Ophthalmology* 1980;87:1019–1021

Implant Site Under-Preparation to Compensate the Remodeling of an Autologous Bone Block Graft

Eduardo Anitua, DDS, MD,† Alia Murias-Freijo, DDS,*† and Mohammad Hamdan Alkhraisat, DDS, PhD*†

Abstract: Autologous bone block grafting is an efficient technique to thicken an atrophied residual alveolar ridge. A variable degree of resorption, however, occurs due to graft remodeling. In this study, we hypothesize that under-preparation of implant socket would permit the dental implant to act as a bone expansor and thus compensate for the contraction in the augmented ridge width.

From the *Private practice in oral implantology, Eduardo Anitua Foundation; and †Clinical Researcher, Eduardo Anitua Foundation, Vitoria, Spain.

Received February 4, 2015.
Accepted for publication March 1, 2015.

Address correspondence and reprint requests to Dr. Eduardo Anitua, Eduardo Anitua Foundation; C/ Jose Maria Cagigal 19, 01007 Vitoria, Spain. E-mail: eduardoanitua@eduardoanitua.com

E.A. is the Scientific Director of BTI Biotechnology Institute, Vitoria, Spain. He is the head of the Foundation Eduardo Anitua, Vitoria. A.M.-F. M.H.A. is a scientist at BTI Biotechnology Institute, Vitoria.
The authors report no conflicts of interest.

Copyright © 2015 by Mutaz B. Habal, MD

ISSN: 1049-2275
DOI: 10.1097/SCS.0000000000001839

Copyright © 2015 Mutaz B. Habal, MD. Unauthorized reproduction of this article is prohibited.

For that reason, 10 patients received an autologous bone block graft that was obtained from the ramus of the mandible. Residual alveolar ridge width was measured on CBCT scans obtained before surgery (T0), after 2 months of healing (T1), after 4 months of healing just before implant placement (T2), and after 4 months of implant placement (T3). The thickness of the alveolar ridge was initially increased from 2.5 ± 1.4 to 6.1 ± 2.0 mm. Before implant insertion, this width was decreased to 5.6 ± 2.1 mm. The last measurement after implant insertion indicated an increase to 7.3 ± 1.8 mm. In comparison to the measurements at T1, a loss of about 0.5 mm of the augmented width occurred. But, this loss was compensated by an increment of 1.2 mm at T3 (after implant insertion) if related to the measurement at T1. Neither gingival dehiscence nor block exposure was observed. Within the limitations of this study, under-preparation of implant socket could make the ridge expansion possible during implant insertion and thus to compensate the remodeling of autologous bone block graft.

Key Words: Autologous, block graft, bone graft, remodeling, ridge augmentation

Excessive mechanical load has been attributed to the likelihood of prosthetic complications such as abutment screw loosening/fracture, porcelain chipping, prosthesis fracture/failure, and crestal bone loss.[1] Improper implant positioning is one of the main factors that would result in excessive mechanical load because it complicates the prosthetic restoration.[2] For that reason, prosthetic-driven implant positioning has been established to minimize such a problem.[3]

In an atrophied alveolar crest, ridge bone augmentation is necessary to correctly position the implant. Bone block grafts are one of these procedures that are indicated when severe bone atrophy is present.[4] This reconstructive tool includes the harvesting of a bone block from a donor site and fixing the graft by screws at a recipient site. The main intraoral donor sites are the symphysis and the ramus of the mandible.

The easy access and the possibility of obtaining bone blocks without debilitating the mandible makes the symphysis a suitable donor area.[5–7] Donor site morbidity, although very much lower than extra-oral sites, was reported to include pain, functional limitations, swelling, and altered sensation in the mental and lower lip area.[8] Temporary paresthesia after chin graft harvesting surgery ranged from 10% to 50%[8,9] and in 1 study impaired nerve function was considered permanent in 15 out of 22 patients who suffered altered sensation.[8]

The ramus of the mandible is another target that allows easier surgery[10] and the possibility of obtaining bone blocks of sufficient dimensions to rehabilitate vertical and horizontal alveolar bone loss.[10] This donor site showed lesser postoperative complications than the symphysis area.[7,8] Patients could, however, suffer from swelling, and difficulty during mouth opening and chewing. Altered sensation was lower (ranged from 0% to 5%) and usually it was not persistent when compared with the symphysis.[8,9]

This study was conducted to test the hypothesis that implant insertion could serve to further expand the horizontal ridge augmentation and thus compensate for volume changes due to autologous graft remodeling. Patients in need of horizontal ridge augmentation were recruited. Bone surgery was performed to obtain a bone block graft from the ramus of the mandible. Alveolar ridge width was measured on CBCT scans obtained before surgery, before implant insertion and after implant insertion.

METHODS

This article was written following the Strengthening the Reporting of Observational Studies in Epidemiology (STROBE) guidelines[11] and included patients treated at private dental clinic in Vitoria, Spain. Patients included in the study fulfilled the following criteria: both sexes, patients with horizontal ridge atrophy that impair implant placement, and bone augmentation by an autologous bone graft. The exclusion criteria were the no insertion of dental implants at the augmented site, and ASA III–IV.

A retrospective cohort study design was used. Ten patients received a bone block graft in maxilla and mandible were included and evaluated.

Outcome Criteria

To challenge the hypothesis of the study, demographic and anamnesis data were obtained from patients' records. For residual alveolar ridge width, CBCT scans were imported to a visualizing software (BTI scan IV, BTI Biotechnology Institute, Vitoria, Spain). The CBCT scans were visualized in a sagittal section and ridge width was measured at a distance of 3–5 mm from the ridge crest. An anatomical landmark was identified for each scan. Measurements on the 3 CBCT scans were performed at the same distance from an anatomical landmark. CBCT scans were obtained using a Sirona GALILEOS 3D scanner (Sirona, Bensheim, Hesse, Germany) using the standardized positioning protocol (the occlusal plane parallel to the ground and the midsagittal plane perpendicular to the ground) and an irradiation protocol of 42 mAs and 80 kV. The scans were obtained before surgery (T1), after horizontal bone augmentation (T2), just before implant insertion (T3) and at several months after implant insertion (T4).

Early implant failure was evaluated by considering as failure any implant lost due to failure to achieve osseointegration, as indicated by implant mobility, radiolucency around the implant, pain, and/or supporation.

Surgical Procedures

Plasma rich in growth factors (PRGF-Endoret) was prepared from citrated whole blood according to the instructions of the manufacturer (BTI Biotechnology Institute).

Under local anesthesia, a full-thickness flap was reflected to expose the alveolar crest and to evaluate the amount the graft needed to be harvested. Then, a mucoperiosteal flap was reflected to expose the ramus of the mandible and a bone block was harvested by piezoelectric surgery (BTI-ultrasonic)[12] and copious irrigation. The removed bone block was stored in fraction 2 of PRGF-Endoret to increase cell survival and maintain the hydration of the bone.[13] The Onlay graft was screw-fixed at the recipient site. The space between the Onlay graft and the alveolar process was filled with autologous bone particulate mixed with fraction 2 of PRGF-Endoret. Otherwise, a PRGF-Endoret clot prepared from fraction 2 (F2) was used as the sole filling material.

PRGF membrane prepared from fraction 1 (F1) was then placed to cover the surgical site before flap closure with monofilament 5/0 suture. If tension was observed upon flap closure a periosteal relieving incision was practised to achieve tension-free flap suturing.

After several months of healing, the implant site was prepared by bone drilling at low velocity (150 rpm) without irrigation and the diameter of the last drill was inferior to the diameter of the implant to be placed. The implant was then inserted with a surgical motor at an insertion torque of 25 N cm and then continued manually to finish the implant placement.

© 2015 Mutaz B. Habal, MD

Copyright © 2015 Mutaz B. Habal, MD. Unauthorized reproduction of this article is prohibited.

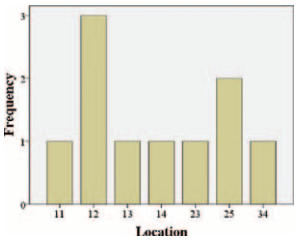

FIGURE 1. Changes in the thickness of the residual alveolar ridge. T0: preoperatice thickness, T1: thickness after 2 months of surgery, T2: thickness just before implant placement, and T3: after 4 months of implant placement.

Statistical Analysis

Descriptive statistics were performed when necessary considering the implant and the patient as a unit of analysis. Absolute and relative frequency distributions were calculated for qualitative variables and mean values and standard deviations for quantitative variables. SPSS v15.0 for Windows statistical software package (SPSS Inc, Chicago, IL) was used for the statistical analysis.

RESULTS

Ten patients participated in this study of whom 8 were women. The patients' mean age was 58 ± 16 years (range: 24–74 years). Bone ridge augmentation was performed in the maxillary anterior region (7 patients), maxillary premolar region (2 patients), and mandibular premolar region (1 patient) (Fig. 1). No graft exposure was observed during the healing period. The basal residual width was 2.5 ± 1.4 mm (range: 0.5– 4.10 mm). The augmented ridge width at T1 (2.5 ± 2.8 months since surgery) was 6.1 ± 2.0 mm (range: 2.9–9.9 mm) (Fig. 2). This width was 5.6 ± 2.1 mm (range: 2.7–8.4 mm) at T2 (4.0 ± 1.1 months since surgery). Dental implants were inserted in the augmented bone after 4.5 ± 1.2 months (range: 3–6 months) of surgery. The width of the augmented ridge was then measured after 4.2 ± 1.2 months (range: 2–5 months) since implant insertion (T3). The last width was 7.3 ± 1.8 mm (range: 5.1–9.1 mm). The time between the surgery and the last measurement was 8.7 ± 1.5 months (range: 7–11 months).

In comparison to the measurements at T1, a loss of about 0.5 mm of the augmented width occurred (Figs. 1 and 2). But, this loss was compensated by an increment of 1.2 mm at T3 (after implant insertion) if related to the measurement at T1 (Fig. 2).

DISCUSSION

The outcomes of this study confirm the efficiency of autologous bone block graft in horizontal ridge augmentation. Contraction in the augmented ridge, however, occurred during the healing process due to graft remodeling. Interestingly, the action of dental implant insertion into the augmented bone compensated the loss and caused a further increment in the width of the residual alveolar ridge.

The autologous bone block from the ramus of the mandible was efficient to thicken the residual alveolar ridge by approximately 4 mm. Volume changes due to graft remodeling are, however, one of the disadvantages of bone block grafts.[5,14] Graft remodeling could be influenced by the embryonic origin of the harvested bone. Intramembranous bone graft seems to maintain its volume, whereas endochondral bone graft undergoes variable degrees of resorption over a variable period of time.[9,15,16] In an analysis based on a cone beam computerized scan (CBCT) obtained after 10 and 180 days after graft placement, a mean graft resorption of 18.38% was reported.[17] In another study, the contraction in the horizontal bone augmentation with a bone block from the ramus of the mandible was from 4.6 ± 0.73 to 4.0 ± 0.77 mm.[18] In one meta-analysis of the volume changes after maxillary sinus augmentation, the weighted mean average resorption was $48 \pm 23\%$ when calculated for controlled studies and a wide variation in graft resorption was observed between individuals.[19]

These data would indicate the importance of taking measures to compensate for the loss in graft volume. Overaugmentation and the use of bone substitutes could be a useful tool for compensating graft remodeling.[19] In this study, we have tested the effect of implant insertion at the augmented bone to compensate for the loss in the augmented ridge width.

For that reason, under-preparation of the implant socket was performed so that the dental implant, when inserted into the bone socket, could act as a bone expansor. The last measurement of the alveolar ridge width indicated an increase of 1.2 mm when compared with the width after the placement of an autologous bone block graft. This outcome indicates the possibility of ridge expansion by implant insertion to compensate the dimensional loss in horizontal ridge augmentation.

The thickness of the alveolar ridge was measured on CBCT scans obtained at different time points. Different studies have documented that linear measurements on cone-beam CT scan are accurate and reproducible.[20,21]

One of the complications of bone ridge augmentation is graft exposure. The use of fibrin membrane has been efficient to prevent graft/implant exposure and to avoid undesirable outcomes.[22] Plasma rich in growth factors employs fibrin scaffold and endogenous growth factors that orchestrate tissue healing to promote adequate tissue regeneration and to reduce tissue inflammation.[23,24]

This study is limited by its retrospective design, sample size, and the absence of a control group. As for any retrospective study, there is a dependence on the availability and accuracy of medical/dental records and it is difficult to control bias and confounders. There is no randomisation nor blinding. This study is uncontrolled that put restrictions on the extrapolation of the results of this study. The outcomes, however, justify the performance of further studies with a larger sample size to establish sound conclusions about the efficacy of dental implant insertion to compensate the graft remodeling.

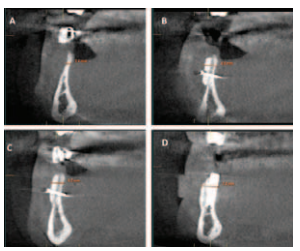

FIGURE 2. The thickness of the residual alveolar ridge measured on CBCT scans obtained before surgery (A), after surgery (B), before implant placement (C) and after implant placement (D).

REFERENCES

1. Anitua E, Alkhraist MH, Pinas L, et al. Implant survival and crestal bone loss around extra-short implants supporting a fixed denture: the effect of crown height space, crown-to-implant ratio, and offset placement of the prosthesis. *Int J Oral Maxillofac Implants* 2014;29:682–689
2. Brunski JB. Biomechanical factors affecting the bone-dental implant interface. *Clin Mater* 1992;10:153–201

© 2015 Mutaz B. Habal, MD

Copyright © 2015 Mutaz B. Habal, MD. Unauthorized reproduction of this article is prohibited.

3. Nevins M, Mellonig JT. The advantages of localized ridge augmentation prior to implant placement: a staged event. *Int J Periodontics Restorative Dent* 1994;14:96–111
4. Anitua E, Alkhraisat MH, Miguel-Sanchez A, et al. Surgical correction of horizontal bone defect using the lateral maxillary wall: outcomes of a retrospective study. *J Oral Maxillofac Surg* 2014;72:683–693
5. Koole R, Bosker H, van der Dussen FN. Late secondary autogenous bone grafting in cleft patients comparing mandibular (ectomesenchymal) and iliac crest (mesenchymal) grafts. *J Craniomaxillofac Surg* 1989;17(Suppl 1):28–30
6. Misch CM, Misch CE. The repair of localized severe ridge defects for implant placement using mandibular bone grafts. *Implant Dent* 1995;4:261–267
7. Raghoebar GM, Meijndert L, Kalk WW, et al. Morbidity of mandibular bone harvesting: a comparative study. *Int J Oral Maxillofac Implants* 2007;22:359–365
8. Clavero J, Lundgren S. Ramus or chin grafts for maxillary sinus inlay and local onlay augmentation: comparison of donor site morbidity and complications. *Clin Implant Dent Relat Res* 2003;5: 154–160
9. Brugnami F, Caiazzo A, Leone C. Local intraoral autologous bone harvesting for dental implant treatment: alternative sources and criteria of choice. *Keio J Med* 2009;58:24–28
10. Wood RM, Moore DL. Grafting of the maxillary sinus with intraorally harvested autogenous bone prior to implant placement. *Int J Oral Maxillofac Implants* 1988;3:209–214
11. von Elm E, Altman DG, Egger M, et al. The Strengthening the Reporting of Observational Studies in Epidemiology (STROBE) statement: guidelines for reporting observational studies. *Lancet* 2007;370:1453–1457
12. Anitua E. Implant Surgery and Prosthesis: A New Perspective Vitoria: Puesat al dia puplicaciones; 1996
13. Anitua E, Prado R, Orive G. Bilateral sinus elevation evaluating plasma rich in growth factors technology: a report of five cases. *Clin Implant Dent Relat Res* 2012;14:51–60
14. Kusiak JF, Zins JE, Whitaker LA. The early revascularization of membranous bone. *Plast Reconstr Surg* 1985;76:510–516
15. Breine U, Branemark PI. Reconstruction of alveolar jaw bone. An experimental and clinical study of immediate and preformed autologous bone grafts in combination with osseointegrated implants. *Scand J Plast Reconstr Surg* 1980;14:23–48
16. Zins JE, Whitaker LA. Membranous versus endochondral bone: implications for craniofacial reconstruction. *Plast Reconstr Surg* 1983;72:778–785
17. Alerico FA, Bernardes SR, Fontao FN, et al. Prospective tomographic evaluation of autogenous bone resorption harvested from mandibular ramus in atrophic maxilla. *J Craniofac Surg* 2014;25:e543–e546
18. Acocella A, Bertolai R, Colafranceschi M, et al. Clinical, histological and histomorphometric evaluation of the healing of mandibular ramus bone block grafts for alveolar ridge augmentation before implant placement. *J Craniomaxillofac Surg* 2010;38:222–230
19. Shanbhag S, Shanbhag V, Stavropoulos A. Volume changes of maxillary sinus augmentations over time: a systematic review. *Int J Oral Maxillofac Implants* 2014;29:881–892
20. Tchorz JP, Poxleitner PJ, Stampf S, et al. The use of cone beam computed tomography to predetermine root canal lengths in molar teeth: a comparison between two-dimensional and three-dimensional measurements. *Clin Oral Investig* 2014;18:1129–1133
21. Kosalagood P, Silkosessak OC, Pittayapat P, et al. Linear measurement accuracy of eight cone beam computed tomography scanners. *Clin Implant Dent Relat Res* 2014;doi: 10.1111/cid.12221
22. Torres J, Tamimi F, Alkhraisat MH, et al. Platelet-rich plasma may prevent titanium-mesh exposure in alveolar ridge augmentation with anorganic bovine bone. *J Clin Periodontol* 2010;37:943–951
23. Anitua E, Alkhraisat MH, Orive G. Perspectives and challenges in regenerative medicine using plasma rich in growth factors. *J Control Release* 2012;157:29–38
24. Anitua E, Sanchez M, Orive G. Potential of endogenous regenerative technology for in situ regenerative medicine. *Adv Drug Deliv Rev* 2010;62:741–752

What Is the Best Way to Handle the Involutional Blepharoptosis Repair?

Yoshitaka Wada, MD, PhD, Takahiro Hashimoto, MD,* Hirohiko Kakizaki, MD, PhD,† Noritaka Isogai, MD, PhD,* and Shinichi Asamura, MD, PhD**

Abstract: There are many different operations to correct involutional blepharoptosis (IB); however, the outcome of the corrective surgery is rather unpredictable, regardless of the procedure employed. A reasonably predictable outcome can be achieved with careful intraoperative evaluation of the condition, with measuring of the margin reflex distance-1 (MRD-1) in supine position of the patients. With these prepositions, we collected data that indicated that our approach can achieve a predictable outcome.

This was a prospective study of 21 consecutive patients (8 men and 13 women) involving 42 eyelids with IB. IB was defined as an MRD-1 of <2 mm. All 21 patients were informed of the purposes of the study, and underwent levator aponeurosis advancement. The MRD-1 was measured intraoperatively with the patients in a supine position and in the 3-month postoperative inspection with the patients in a sitting position. Statistical analyses using paired *t*-tests were performed.

From intraoperative measurement, mean MRD-1 values were 4.31 mm on the right side (range 3.0–4.5) and 4.29 mm on the left side (range 3.5–5.0). Three months after the operations, mean MRD-1 values were 3.07 mm on the right side (range 1.5–4.0) and 3.07 mm on the left side (range 2.0–4.0). Compared with the intraoperative MRD-1 measurements, those of the postoperatives were significantly 1.2 mm reduced (right: $P < 0.01$, left: $P < 0.01$).

The intraoperative measurement of MRD-1 without changing position of patients could result in successful outcome of the operation.

Key Words: Dry eye, involutional blepharoptosis, levator aponeurosis advancement, the margin reflex distance-1, visual field

Involutional blepharoptosis (IB) is a common complaint among the elderly population seeking plastic surgery. The definition of the IB is an excessively low-lying upper eyelid margin that can interfere with the visual field.[1] IB repair to obtain adequate visual field by levator aponeurosis advancement is successful in most

From the *Department of Plastic and Reconstructive Surgery, Kinki University Faculty of Medicine, Osaka-sayam, Osaka; and †Department of Ophthalmology, Aichi Medical University, Nagakute, Aichi, Japan.
Received February 5, 2015.
Accepted for publication March 1, 2015.
Address correspondence and reprint requests to Shinichi Asamura, Department of Plastic and Reconstructive Surgery, Kinki University Faculty of Medicine, 377-2 Ohno-higashi, Osaka-sayama, Osaka 5898511, Japan. E-mail: asamura@med.kindai.ac.jp
The authors report no conflicts of interest.
Copyright © 2015 by Mutaz B. Habal, MD
ISSN: 1049-2275
DOI: 10.1097/SCS.0000000000001840

Copyright © 2015 Mutaz B. Habal, MD. Unauthorized reproduction of this article is prohibited.

instances; however, the postoperative eyelid height is not uniformly predictable.[2–7]

The main factor in this unpredictable correction seems to be dependent upon insufficient intraoperative evaluation. If we can accurately predict postoperative eyelid height using measurement obtained during surgery, we could achieve an increase in the rate of steady outcomes.

Several reports have examined the relationship between the measurements of pre- and postoperative eyelid height.[5–11] Most surgeons recommended measuring eyelid height while patients are in the sitting position during surgery.[6–8,11,12] Conversely, some surgeons prefer to avoid the sitting position during surgery mainly because it is extremely difficult to maintain a sterile operative field as patients tend to shift about when transitioning to a sitting posture, leading to possible compromise of the sterile field and a consequent increase in the risk of bacterial exposure.

We examined intraoperative eyelid heights using the margin reflex distance-1 (MRD-1)[13] to investigate relationships between measurements of pre- and postoperative eyelid heights. Therefore, the establishment of MRD-1 results from our study can lead to the successful correction of the IB without changing patient's position from supine to upright position.

PATIENTS AND METHODS

This was a prospective study of 21 consecutive patients (8 men and 13 women) involving 42 eyelids with IB. IB was defined as an MRD-1 of <2 mm. The age range of patients was 70–94 years, with a mean age of 77 years. All 21 patients were informed of the purposes of the study, and underwent external levator superioris aponeurosis advancement.[7,14]

Local anesthesia was given using 1% lidocaine, 2 mL, with 1/100,000 epinephrine. The upper eyelid skin was incised for about 40 mm along the wrinkle line approximately 5 to 6 mm from the eyelid margin, and then the redundant skin, including orbicularis oculi muscle, was excised. The subcutaneous skin tissues and orbicularis oculi muscle were dissected, and then the edges of the external levator superioris aponeurosis and superior tarsus were identified. Orbital septum and preaponeurotic fat were dissected from the aponeurosis and retracted superiorly. The aponeurosis was detached from the tarsus, and the aponeurosis was separated from the Müller muscle. The aponeurosis was almost completely freed from their neighboring tissue. Then, the aponeurosis was advanced and fixed firmly at about half the height of the tarsus with a single 6–0 nylon horizontal mattress suture. In addition, the center of the aponeurosis was fixed on the slightly medial site of the fissure, that is, just over the pupil during eyelid opening. If adjusted undercorrection or overcorrection occurred, advancement was adjusted until an adequate eyelid height was obtained. Thereafter, 2 other sutures were added to obtain a natural curve of the eyelid. The intraoperative measurement was performed before skin closure, and amount of advancement was adjusted until adequate eyelid height, which was set to 3.5 to 5.0 mm of MRD-1, was achieved (Fig. 1). After establishing intraoperative MRD-1 with a central suture, another two 6–0 nylon sutures were added to fix the aponeurosis tightly to the tarsus. Fixation for a double fold was made, and the skin was closed 6–0 nylon interrupted sutures.

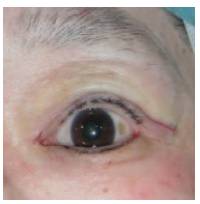

FIGURE 1. The intraoperative measurement was performed before skin closure, and amount of advancement was adjusted until adequate eyelid height, which was set to 5.0 mm of MRD-1, was achieved. MRD-1 = margin reflex distance-1.

The MRD-1, which represents the distance from the central papillary light reflex to the upper eyelid margin, was measured intraoperatively with the patients in a supine position and in the 3-month postoperative inspection with the patients in a sitting position. Statistical analyses using paired *t*-tests were performed to compare values of intraoperative measurement in the supine positions and values in the postoperative 3 months on the right and left sides, respectively. All operations and MRD-1 measurements were performed by a single surgeon (S.A.).

RESULTS

From intraoperative measurement, mean MRD-1 values were 4.31 mm on the right side (range 3.0–4.5) and 4.29 mm on the left side (range 3.5–5.0). Three months after the operations, mean MRD-1 values were 3.07 mm on the right side (range 1.5–4.0) and 3.07 mm on the left side (range 2.0–4.0) in Table 1. Compared with the intraoperative MRD-1 measurements, those of the postoperatives were significantly 1.2 mm reduced (right: $P < 0.01$, left: $P < 0.01$).

In terms of visual field, each patient was requested to answer the question, A–D, assessing the results of the procedure: A) excellent improved, B) moderately improved, C) slightly improved, D) same as before the operation. The survey result was as follows: A) 10 patients (47%), B) 7 patients (33%), C) 2 patients (10%), D) 2 patients (10%). For both the patients of Class C, technically it was almost impossible to establish the intraoperative MRD-1 to be 4.5 mm. The 2 patients who were classified to be Class D, and diagnosed to have astigmatism, much improved their visual field after changing the eyeglasses. Preoperative diagnosis performed by an ophthalomogist identified 8 patients with dry eyes, only 1 of which continuing to complain of dacryorrhea postoperatively; this was adequately resolved with simple eye drop treatment.

Preoperatively, 2 patients complained of persistent headache, which was much improved after the operation. Likewise, in the 5 patients complaining of stiff shoulders, all patients noticed marked improved postoperatively.

DISCUSSION

Throughout the operation, the patients with IB remained in the supine position and precise measurement of the MRD was done in this position. The postoperative MRD-1 was measured with the patient in the sitting position and the postoperative MRD-1 measurement is on average 1.2 mm less than the MRD-1 measured intraoperatively. Provided that the intraoperative measurement of the MRD-1 is 4.5 mm before suturing of the skin is completed, our approach proved to be effective in not only improving visual field, but also preventing ocular surface complications.

The etiology of IB may be multifactorial, and the histopathological findings show significantly excessive fatty tissue both of the levator palpebrae superioris aponeurosis and levator muscle that are observed at the time of corrective surgery.[15–21] Furthermore, it may be implicated as an etiological factor. Regardless of the operation used for this condition, some failures must be expected

TABLE 1. Pre-, Intra-, and Postoperative MRD-1. Compared with the Intraoperative MRD-1 Measurements, Those of the Postoperatives Were Significantly 1.2 mm Reduced

	Pre	Intra	Post
R (range, mm)	0.71 (-1.0–2.0)	4.31 (3.0–4.5)	3.07 (1.5–4.0)
L (range, mm)	0.93 (-1.0–2.0)	4.29 (3.5–5.0)	3.07 (2.0–4.0)

© 2015 Mutaz B. Habal, MD

Copyright © 2015 Mutaz B. Habal, MD. Unauthorized reproduction of this article is prohibited.

simply because the etiology is unknown at present. Ninety patients had MRD-1 intraoperative measurement greater than 4.5 mm; however, 2 patients had less than 4.5 mm MRD-1 in this study.

There are 3 main approaches to correct IB: the first is targeted on the external levator superioris aponeurosis, the second on Müller muscle, and the third involving both.[1–12] If the procedure is targeted on the Müller muscle, the lidocaine with epinephrine, which stimulates sympathetic nerves in the Müller muscle, is constricted with epinephrine so that the eyelid height decreases.[9,22,23] When the effect of the local anesthetic, however, fades away postoperatively, the upper eyelid droops and eyelid height are expected to increase. There may be possible overcorrection of IB, provided that this theory is correct. With the hypothesis, our choice of the IB surgery is mainly focused on the external levator superioris aponeurosis.

The results of surgical repair for IB were greatly improved over the years following the popularization of the technique of external levator superioris aponeurosis repair using local anesthesia by Jones et al.[2] Many surgeons deliberately overcorrect the ptotic eyelid by approximately 1 mm, expecting a modest decrease in eyelid height postoperatively with the resolution of the local anesthetic-induced paralysis of the orbicularis muscle and other associated muscles.[22] Nevertheless, infallible prediction of the final eyelid position remains an elusive goal.

MRD-1 needs to be considered in supine position during intraoperative measurement to obtain the desired postoperative eyelid height. Several years ago, the first author elected not to change the patient's position during IB repair, because not only it is cumbersome for some elderly patients, but also it seemed not to affect the final outcome. Swelling and weights of the anterior lamella of the eyelids may interfere with intraoperative MRD-1 measurement. After suturing the skin, as the MRD-1 is affected by swelling and weight of the anterior lamella, the operating surgeon must recognize the difference in MRD between standing and supine positions.[12,23] The swollen eyelids disappeared almost completely within 3 months, at which time we could ignore weight from the anterior lamella.[11,24] The MRD-1 measurement should be done when the effects of the surgery have subsided at least 3 months after the surgery.

The common pitfall of surgical intervention is postoperative dry eye, irrespective of the choice of the surgical method. An excessive advancement of levator aponeurosis frequently leads to an eyelid–eyeball dissociation.[24] The upper eyelid must move toward the lower corneal limbus going over the top of the corneal convex during eyelid closure, the upper eyelid with downward inclination toward the lower corneal limbus, and finally the upper and lower eyelids are approximated together. In normal physiological closure of the upper eyelid, after it reaches the apex of the eyeball, it moves backward along the curvature of the eyeball and maintains close contact between the 2 structures. Less careful attention is paid to dry eye symptomatology as an operator. Any surgeon dealing with IB must pay attention to this common complication when the surgical intervention is contemplating IB.[8,24,25]

Cosmetically, Japanese surgeons tend to be more interested in making larger eyes. In other words, the postoperative MRD-1 is more likely to be greater than 5 mm.[26] To accomplish this MRD-1 for the older generation with IB, it is not uncommon that their grandchildren frequently complain that the grandparent's facial feature is quite odd, given the faces of the older generation have wrinkled except the appearance of their eyes being much younger (Fig. 2). If MRD-1 is greater than 2.5 mm, there is no visual disturbance for routine daily living.[27] Among Japanese adults, the fissure height is 8.8 mm for men and is 8.2 mm for female, and in the senior population, it is 7.9 and 6.7 mm, respectively.[28] MRD-1 3 mm seems to be adequate for patients with IB (Fig. 3).

There are 2 common ways to evaluate IB; 1 is the levator function (LF) to judge the proper amount of fissure height in eyelid opening, and the other is assessing the MRD-1. In general, an LF more than 5 mm is an indication for levator advancement.[29,30] If less than 5 mm, alternative surgical methods must be used. In this study, IB is defined to satisfy 3 criteria: the MRD-1 is less than 2 mm, the LF is greater than 5 mm, and the age is older than 70.

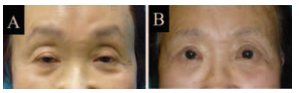

FIGURE 2. A, The preoperative view. B, The postoperative view. If MRD-1 is greater than 4.5 mm, it is not uncommon that their grandchildren frequently complain that the grandparent's facial feature is quite odd, given the faces of the older generation have wrinkled, except the appearance of their eyes being much younger. MRD-1 = margin reflex distance-1.

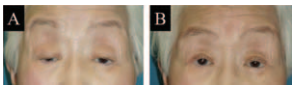

FIGURE 3. A, The preoperative view. B, The postoperative view. If MRD-1 is greater than 2.5 mm, there is no visual disturbance for routine daily living. MRD-1 = margin reflex distance-1.

Proportional to the increase of the aging population in developed countries, the incidence of IB is dramatically increasing. Also, the elderly population tends to have a reduced amount of lacrimal fluid and dysfunction of the Meibaum glands, incidentally increasing the risk of dry eyes. In terms of maintenance of the normal ocular surface condition, it may be a reasonable assumption that patients with IB can be a natural compensatory phenomenon to prevent the dry eye. The goal of IB treatment is not only the improvement of the visual field, but also the maintenance of the appropriate conditions of the ocular surface.

REFERENCES

1. Chang S, Lehrman C, Itani K, et al. A systematic review of comparison of upper eyelid involutional ptosis repair techniques: efficacy and complication. *Plast Reconstr Surg* 2012;129:149–157
2. Jones LT, Quickert MH, Wobig JL. The cure of ptosis by aponeurotic repair. *Arch Ophthalmol* 1975;93:629–634
3. Older JJ. Levator aponeurosis surgery for the correction of acquired ptosis: analysis of 113 procedures. *Ophthalmology* 1983;90: 1056–1059
4. Berris CE. Adjustable sutures for correction of adult-acquired ptosis. *Ophthal Plast Reconstr Surg* 1988;4:171–173
5. Liu D. Ptosis repair by single suture aponeurotic tuck: surgical technique and longterm results. *Ophthalmology* 1993;100: 251–259
6. Anderson RL, Dixon RS. Aponeurosis ptosis surgery. *Arch Ophthalmol* 1979;97:1123–1128
7. McCuuley TJ, Kersten RC, Kulwin DR, et al. Outcome and influencing factors of external levatorpalpebraesuperioris aponeurosis advancement for blepharoptosis. *Opthtal Plastic Reconstr Surg* 2003;19:388–393
8. Tucker SM, Verhulst SJ. Stabilization of eyelid height after aponeurotic ptosis repair. *Ophthalmology* 1999;106:517–522
9. Bartley GB, Lowry JC, Hodge DO. Results of levator-advancement blepharoptosis repair using a standard protocol: effect of epinephrine-induced eyelid position change. *Trans Am Ophthalmol Soc* 1996;94:165–173
10. Berlin AJ, Vestal KP. Levator aponeurosis surgery. A retrospective review. *Ophthalmology* 1989;96:1033–1037
11. Linberg JV, Vasquez RJ, Chao G. Aponeurotic ptosis repairunder local anesthesia. *Ophthalmology* 1988;95:1046–1052
12. Takahashi Y, Kakizaki H, Mito H, et al. Value of intraoperative eyelid height measurement in sitting and supine positions during blepharoptosis repair. *Opthtal Plastic Reconstr Surg* 2007;2:119–121
13. Karesh JW. Diagnosis and management of acquired blepharoptosis and dermatochalasis. *Facial Plast Surg* 1994;10:185–201
14. Sarver BL, Putterman AM. Margin limbal distance to determine amount of levator resection. *Arch Ophthalmol* 1985;103:354–356

© 2015 Mutaz B. Habal, MD

Copyright © 2015 Mutaz B. Habal, MD. Unauthorized reproduction of this article is prohibited.

15. Shirado M. Dyslipidaemia and age-related involutional blepharoptosis. *J Plastic Reconstr Aethentic Surg* 2012;65:e146–e150
16. Sanke RF. Relationship of senile ptosis to age. *Ann Ophthalmol* 1984;16:928–931
17. Shore JW, McCord CD Jr. Anatomic changes in involutional blepharoptosis. *Am J Ophthalmol* 1984;98:21–27
18. Cahill KV, Buerger GF Jr, Johnson BL. Ptosis associated with fatty infiltration of Müller's muscle and levator muscle. *Ophthal Plast Reconstr Surg* 1986;2:213–217
19. Watanabe A, Araki B, Noso K, et al. Histopathology of blepharoptosis induced by prolonged hard contact lens wear. *Am J Ophthalmol* 2006;141:1092–1096
20. Ahmadi AJ, Saari JC, Mozaffarian D, et al. Decreased carotenoid content in preaponeurotic orbital fat of patients with involutional ptosis. *Ophthal Plast Reconstr Surg* 2005;21:46–51
21. Pereira LS, Hwang TN, Kersten RC, et al. Levator superioris muscle function in involutional blepharoptosis. *Am J Ophthalmol* 2008;145:1095–1098
22. Older JJ. Upper lid blepharoplasty and ptosis repair using a transcutaneous approach. *Ophthal Plast Reconstr Surg* 1994;10:146–149
23. Castro E, Foster JA. Upper lid blepharoplasty. *Facial Plast Surg* 1999;15:173–181
24. Kakizaki H, Zako M, Mito H, et al. Intraoperative quantification using finger force for involutional blepharoptosis without postoperative lagophthalmos. *Jpn J Ophthalmol* 2006;50:135–140
25. Watanabe A, Kakizaki H, Selva D, et al. Short-term changes in tear volume after blepharoptosis repair. *Cornea* 2013;33:14–17
26. Yoza S. Blepharoplasty: surgical approach and indication. *Pepars(Japanese)* 2014;80:52–58
27. Meyer DR, Linberg JV, Powell SR, et al. Quantitating the superior visual field loss associated with ptosis. *Arch Ophthamol* 1989;107:840–843
28. Noda M. Age change of the eyelid and skin. Tubota K (ed), *Prac Ophthamol* (Japanese) 2008;18–22
29. Pobert GS, Nelson RS, Donna B. The measurement and definition of ptosis. *Ophthal Plast Reconstr Surg* 1989;5:171–175
30. Ettl A, Prinlinger S, Kramer J, et al. Functional anatomy of the levator palpebrae supriosus muscle and its connective tissue system. *Br J Ophthamol* 1996;80:702–707

Effectiveness and Safety of Selective Neck Dissection in Lymph Node-Positive Squamous Cell Carcinoma of the Head and Neck

Mustafa Polat, MD, Fatih Celenk, MD,* Elif Baysal, MD,* Cengiz Durucu, MD,* Seval Kul, PhD,† Semih Mumbuc, MD,* and Muzaffer Kanlikama, MD**

From the *Department of Otorhinolaryngology; and †Department of Biostatistics, Gaziantep University Faculty of Medicine, Gaziantep, Turkey.

Received February 10, 2015.
Accepted for publication March 7, 2015.

Address correspondence and reprint requests to Mustafa Polat, MD, ENT Specialist, Department of Otorhinolaryngology, Gaziantep University Faculty of Medicine, Gaziantep, Turkey;
E-mail: polatmusti@yahoo.com

The authors report no conflicts of interest.

Copyright © 2015 by Mutaz B. Habal, MD

ISSN: 1049-2275
DOI: 10.1097/SCS.0000000000001849

Abstract: The aim of this study was to investigate the effectiveness and safety of selective neck dissection in patients with lymph node-positive head and neck squamous cell carcinoma to determine regional control and survival rates. Eighty patients with lymph node-positive head and neck squamous cell carcinoma who underwent selective dissection were included in the study. Regional control, survival rates, and factors affecting survival were analyzed. Regional control was 90%, disease-specific survival was 93.4%, and the overall survival rate was 87.25%. T stage, N stage, age, and extracapsular spread were included in hazard regression models. None of the factors were statistically significant. Selective neck dissection is an effective and oncologically safe treatment option in selected cases. T stage, N stage, and extracapsular spread had no significant impact on disease-specific survival.

Key Words: Head and neck, recurrence, selective neck dissection, survival

Lymph node metastasis significantly affects the prognosis and survival of patients with head and neck squamous cell carcinoma. Radical or modified radical neck dissection has been the traditional surgical treatment for lymph node positive necks.[1] However, comprehensive neck dissection has several important effects on quality of life of patients, including cosmetic and functional problems. Selective neck dissection aims at dissecting only high-risk areas of the neck and offers less morbidity and functional loss and better cosmetic results.[2] Although the effectiveness of selective neck dissection has been well established in N0 head and neck cancers, its role remains controversial in cases with metastatic lymph nodes. There are published reports showing the effectiveness of selective neck dissection without compromising survival in the presence of lymph node metastasis.[1–4]

In this study, patients with histopathologically proven cervical lymph node metastasis from head and neck squamous cell carcinoma underwent selective neck dissection. The aim of this study was to investigate the effectiveness and safety of selective neck dissection in such a patient group to determine the regional control and survival rates. We also evaluated whether factors including T stage, N stage, and extracapsular spread were associated with regional failure and disease-specific survival.

MATERIALS AND METHODS

This retrospective study included 80 patients with lymph node-positive head and neck squamous cell carcinoma who underwent selective dissection between 2005 and 2011. Medical records of the patients were collected and included age, primary site of the tumor, follow-up period, stages of the primary and metastatic disease, recurrences, adjuvant therapies, and survival of the patients. All patients had clinically or histopathologically proven lymph node metastasis. However, staging of the necks was based on histopathologic examination. Histopathologic evaluation of the neck dissection specimen included presence of extracapsular spread, perineural and vascular invasion, and number of lymph node metastases.

All patients underwent a thorough head and neck examination and a flexible and/or rigid endoscopic examination. Preoperative computed tomography (CT) and ultrasonography were performed for lymph node staging. Distant metastases were ruled out by using positron emission tomography in suspicious cases. The type of selective neck dissection was determined according to the site of the primary tumor. In patients with oral cavity cancer, selective supraomohyoid neck dissection (levels I–III) was performed, whereas patients with laryngeal, oropharyngeal, or hypopharyngeal cancers

© 2015 Mutaz B. Habal, MD

Copyright © 2015 Mutaz B. Habal, MD. Unauthorized reproduction of this article is prohibited.

underwent selective lateral neck dissection (levels II–IV). In cases with multiple suspicious lymph nodes, lower levels (level IV and/or V) were also dissected and included in the specimen. The indication for unilateral or bilateral neck dissection was based on the site and stage of the primary tumor. Patients with stage N2, extracapsular spread, and perineural or vascular invasion received postoperative radiation therapy.

All patients were followed for at least 2 years. Patients were followed up once a month in the first year, 6 times a year in the second year, and 4 times a year in the third year. Patients were assessed for recurrences and distant metastasis during scheduled visits using chest X-ray, CT, and positron emission tomography. Patients with a follow-up less than 24 months, a history of prior treatment for head and neck malignancy, malignancies other than squamous cell carcinoma recurrence in the primary site, and N0 necks were excluded from the study. In addition, patients with N3 staged necks, obvious extracapsular extension, fixed metastatic lymph nodes, or invasion of surrounding structures underwent a comprehensive neck dissection and were also excluded from the study.

To compare 2 independent groups, Student's *t* tests or Mann-Whitney *U* tests (for continuous variables), and chi-squared tests (for categorical variables) were used. Survival probabilities were estimated using the Kaplan-Meier method. Hazard regression models were used for predictions for different factors. All univariate analyses were performed in SPSS for Windows version 22.0 (IBM Corp., Armonk, NY). A 2-sided P value <0.05 was defined as statistically significant. The study protocol was reviewed and approved by the institutional ethics committee.

RESULTS

Between 2005 and 2011, 80 patients with histopathogically proven lymph node metastasis underwent selective neck dissection for treating head and neck squamous cell carcinoma. Bilateral neck dissection was performed in 62 patients, and ipsilateral neck dissection was performed in 18 patients. The age of the patients ranged from 27 to 88 (mean 58.55 ± 12.33). There were 71 (88.8%) male and 9 (11.2%) female patients.

Primary tumor sites were the larynx in 57 (71.2%) patients, oral cavity in 16 (20%) patients, hypopharynx in 5 (6.25%) patients, and oropharynx in 2 (2.5%) patients. The primary tumor was clinically staged as T1 in 15 (18.75%) patients, T2 in 30 (37.5%) patients, T3 in 17 (21.25%) patients, and T4 in 18 (22.5%) patients. Regional metastasis was pathologically staged as N1 in 39 (48.75%) patients, N2a in 2 (2.5%) patients, N2b in 23 (28.75%) patients, and N2c in 16 (20%) patients. Extracapsular spread was observed in 18 (22.5%) patients. Demographic and clinical parameters of the patients are summarized in Table 1.

Mean follow-up period was 49.2 ± 27.3 months (range 24–98). During the follow-up period, we observed 8 (10%) patients with neck recurrence. Two of the patients with recurrence were female, whereas 6 patients with recurrence were male. One (12.5%) patient with neck recurrence was younger than 40 years, 4 (50%) patients were between 40 and 65 years, and 3 (37.5%) patients were older than 65 years. The primary site of neck recurrences was the oral cavity in 1 (12.5%) patient, larynx in 6 (75%) patients, and oropharynx in 1 (12.5%) patient. In patients with hypopharyngeal cancer no recurrence was observed. Neck recurrence occurred in 11% of the patients with laryngeal cancer and 6.6% of the patients with oral cavity cancer. The distribution of neck recurrences according to the primary tumor stage was 1 (6.7%) patient with T1 tumor, 2 (6.7%) patients with T2 tumor, 3 (17.6%) patients with T3 tumor, and 2 (11.1%) patients with T4 tumor (Table 2). No significant difference was found according to the primary tumor stage with respect to neck recurrence ($P = 0.667$). Distribution of neck recurrences according to neck stage was 3 (7.7%) patients with N1 neck, 3 (13%) patients with N2b neck, and 2 (12.5%) patients with N2c neck (Table 3). There was no significant difference according to the neck stage with respect to neck recurrence ($P = 0.849$). Neck recurrence was observed in 2 (11.1%) patients with extracapsular spread and 6 (9.7%) patients without extracapsular spread. Extracapsular spread was not a significant risk factor for neck recurrence ($P = 0.860$). Patients with neck recurrence were treated with additional surgery and/or radiation therapy. Details of the neck failure are described in Tables 2–4.

After 2 years follow-up, regional control was 90%, disease-specific survival was 93.4%, and overall survival rate was 87.25%. T stage, N stage, age, and extracapsular spread were included in hazard regression models. None of the factors were statistically significant. There was a marginally significant hazard ratio when T3 was compared with T1 (HR = 2.339 [0.978–5.595] $P = 0.056$).

TABLE 1. Demographic and Clinical Parameters of the Patients

Parameter	No. (%)
Mean age (range)	58.55 ± 12.33 (27–88)
Male	71 (88.8%)
Female	9 (11.2%)
Primary site	
Larynx	57 (71.25%)
Oral cavity	16 (20%)
Hypopharynx	5 (6.25%)
Oropharynx	2 (2.5%)
T staging	
T1	15 (18.75%)
T2	30 (37.5%)
T3	17 (21.25%)
T4	18 (22.5%)
N staging	
N1	39 (48.75%)
N2a	2 (2.5%)
N2b	23 (28.75%)
N2c	16 (20%)
Total	80 (100%)

TABLE 2. Distribution of Neck Recurrences According to the Primary Tumor and Neck Stages ($P = 0.667$ and 0.849, Respectively)

		Recurrence		
T Stage		Yes	No	Total
T1	n	1	14	15
	%	6.7%	93.3%	100.0%
T2	n	2	28	30
	%	6.7%	93.3%	100.0%
T3	n	3	14	17
	%	17.6%	82.4%	100.0%
T4	n	2	16	18
	%	11.1%	88.9%	100.0%
N1	n	8	72	80
	n	3	36	39
	%	7.7%	92.3%	100.0%
N2a	n	0	2	2
	%	0%	100.0%	100.0%
N2b	n	3	20	23
	%	13.0%	87.0%	100.0%
N2c	n	2	14	16

© 2015 Mutaz B. Habal, MD

Copyright © 2015 Mutaz B. Habal, MD. Unauthorized reproduction of this article is prohibited.

TABLE 3. Details of the Patients With Recurrence

Parameters	Neck Failures (%)
Gender	
Male	2 (25%)
Female	6 (75%)
Age	
<40 years	1 (12.5%)
40–65 years	4 (50%)
>65 years	3 (37.5%)
Primary site	
Larynx	6 (75%)
Oral cavity	1 (12.5%)
Oropharynx	1 (12.5%)
T staging	
T1	1 (12.5%)
T2	2 (25%)
T3	3 (37.5%)
T4	2 (25%)
N staging	
N1	3 (37.5%)
N2b	3 (37.5%)
N2c	2 (25%)
Extracapsular spread	
Present	2 (25%)
Absent	6 (75%)
Total	8 (100%)

DISCUSSION

Cervical metastasis is one of the most important factors associated with the prognosis, regional control, and survival rates of patients with head and neck squamous cell carcinoma. Accordingly, treatment of the neck should be a part of treatment, particularly in patients with lymph node metastasis. Comprehensive neck dissection is the standard treatment for node-positive cases. However, there is a trend toward reducing the extent of the neck procedures. There are many reports showing the efficacy and safety of selective neck dissection in patients with cervical metastasis. In a study comparing selective and comprehensive neck dissection in clinically positive necks, the authors found that the extent of neck dissection resulted in no difference in overall survival.[1]

Andersen et al[2] performed 129 selective neck dissections in 106 patients and reported a regional recurrence rate of 9% and a regional control rate of 94.3%. Chepeha et al[3] included 52 patients who underwent 58 selective neck dissections for cervical metastases from carcinoma of the upper aerodigestive tract and reported a 94% regional control rate. In a study conducted by Givi et al,[4] 108 patients underwent selective neck dissection and the authors reported 76.9% disease-specific survival and 14.8% regional recurrence rates. In this study, we investigated the role of selective neck dissection in the presence of metastatic lymph-node(s) in 80 patients with head and neck squamous cell carcinoma. After 2 years follow-up, regional control was 90%, disease-specific survival was 93.4%, and overall survival rate was 87.25%. Our results were similar to those reported in the literature.

Andersen et al reported that the primary tumor site, N stage, extracapsular spread, and postoperative irradiation have a significant impact on disease-specific survival.[1] Givi et al[4] found that T stage, oral cavity as the primary tumor site, number of positive nodes, surgical margins, and adjuvant treatment are significant predictors of disease-specific survival. We included T stage, N stage, age, and extracapsular spread in hazard regression models. None of the factors were significant predictors of disease-specific survival. T stage (T3 versus T1) had a marginally significant hazard ratio. The absence of a difference in survival between N stages and extracapsular spread status may be explained by the use of irradiation in patients with advanced stages and extracapsular spread. Another explanation is that we also added lower levels to the dissection specimen in cases with multiple suspicious lymph nodes.

In our experience, we do not recommend selective neck dissection in several circumstances, including N3-staged necks, obvious extracapsular extension shown by either preoperative CT or observed directly during the operation, fixed lymph nodes, and invasion of the surrounding structures. We excluded patients having these features from the present study. We believe that these conditions may increase regional recurrence rates. In addition, dissecting lower levels in cases with multiple suspicious lymph nodes may help to reduce recurrence.

This study has several limitations that should be considered. One of them is the limited number of neck recurrences. Although a limited number of neck recurrences does not affect survival and regional control rates, it is difficult to draw conclusions regarding the impact of factors on survival. The best way to determine whether patients who undergo selective neck dissection are oncologically safe is to compare them with those having comprehensive neck dissection. In this study, we did not include such a control group, which is another limitation of the study. However, the number of studies comparing comprehensive and selective neck dissection is very limited. In this study, we calculated regional control and survival rates and compared our results with those reported in the literature. Disease-specific survival, overall survival, and regional control rates were comparable with the literature.

TABLE 4. Distribution of Neck Recurrences According to the Primary Tumor Stage ($P = 0.667$)

		Recurrence		
T Stage		Yes	No	Total
T1	n	1	14	15
	%	6.7%	93.3%	100.0%
T2	n	2	28	30
	%	6.7%	93.3%	100.0%
T3	n	3	14	17
	%	17.6%	82.4%	100.0%
T4	n	2	16	18
	%	11.1%	88.9%	100.0%
Total	n	8	72	80
	%	10.0%	90.0%	100.0%

CONCLUSION

According to our results, selective neck dissection is an effective and oncologically safe treatment option in patients with lymph node-positive head and neck squamous cell carcinoma. T stage, N stage, and extracapsular spread had no significant impact on disease-specific survival. Several factors, including N3 stage, obvious extracapsular extension, invasion of the surrounding structures, and fixed nodes may compromise the success rates. Therefore, selective neck dissection is a safe and effective treatment option in selected cases.

REFERENCES

1. Patel RS, Clark JR, Gao K, et al. Effectiveness of selective neck dissection in the treatment of the clinically positive neck. *Head Neck* 2008;30:1231–1236
2. Andersen PE, Warren F, Spiro J, et al. Results of selective neck dissection in management of the node-positive neck. *Arch Otolaryngol Head Neck Surg* 2002;128:1180–1184

© 2015 Mutaz B. Habal, MD

Copyright © 2015 Mutaz B. Habal, MD. Unauthorized reproduction of this article is prohibited.

3. Chepeha DB, Hoff PT, Taylor RJ, et al. Selective neck dissection for the treatment of neck metastasis from squamous cell carcinoma of the head and neck. *Laryngoscope* 2002;112:434–438
4. Givi B, Linkov G, Ganly I, et al. Selective neck dissection in node-positive squamous cell carcinoma of the head. *Otolaryngol Head Neck Surg* 2012;147:707–715

Use of Postoperative Palatal Obturator After Total Palatal Reconstruction With Radial Forearm Fasciocutaneous Free Flap

Euicheol C. Jeong, MD, Young Ho Jung, MD,† and Jin-yong Shin, MD*‡*

Abstract: A 67-year-old-male patient visited our hospital for a mass on the soft palate of approximately 5.0 × 6.0 cm in size. He was diagnosed with adenoid cystic carcinoma and reconstruction after total palate resection was planned. After ablative surgery, a radial forearm free flap procedure was successfully performed to cover the hard and soft palates. However, wound disruption occurred twice during the postoperative period.

When a palate defect is reconstructed using a soft tissue free flap, flap drooping by gravitation and the flap itself can generate irregularity in the lower contour of the palate and, in the long-term, insufficiencies of velopharyngeal function, speech, and mastication. To complement such functional and aesthetic problems caused by flap drooping, conventional prosthetics and new operative techniques have been discussed. However, overcoming wound disruption caused by flap drooping in the acute postoperative period has not been discussed.

In this case, the temporary use of a palatal obturator during the postoperative period was beneficial after soft tissue reconstruction of the palate.

Key Words: Palatal obturator, palate reconstruction, radial forearm flap

From the *Department of Plastic Surgery, SMG-SNU Boramae Medical Center, Seoul, Republic of Korea; †Department of Otorhinolaryngology, Head and Neck Surgery, SMG-SNU Boramae Medical Center, Seoul, Republic of Korea; and ‡Department of Plastic and Reconstructive Surgery, College of Medicine, Seoul National University, Seoul, Republic of Korea.

Received February 16, 2015.
Accepted for publication March 22, 2015.

Address correspondence and reprint requests to Jin-yong Shin MD, Department of Plastic Surgery, SMG-SNU Boramae Medical Center, Department of Plastic and Reconstructive Surgery, College of Medicine, Seoul National University, SMG-SNU Boramae Medical Center, Borame-ro 5-gil, Dongjank-Gu, Seoul 156–707, Republic of Korea;
E-mail: gahaeja@naver.com

The authors report no conflicts of interest.

Copyright © 2015 by Mutaz B. Habal, MD

ISSN: 1049-2275
DOI: 10.1097/SCS.0000000000001856

INTRODUCTION

Most defects of the palate are generated by ablative surgery for head and neck cancer. These defects are challenging for reconstructive surgeons. Reconstruction options are dependent on the size and the location of the palatal defect. Generally, for both hard and soft palate defects, free tissue transfer has been shown to be stable and excellent.[1] If the resection involves only the soft and hard palates, with the alveolar ridge remaining, a radial forearm free flap procedure provides the best results. The radial forearm free flap is not bulky, is highly vascularized, has a long reliable pedicle, and can be folded over.[2–4] Although successful reconstruction using a radial forearm free flap was performed in our case, wound disruption occurred due to flap drooping, continuous movement, and bulkiness of the tongue. To protect the flap from gravitational force and external stimuli, we used a palatal obturator in the tertiary re-operation. The issue of wound disruption was solved after applying a palatal obturator; thus, we present the application of a palatal obturator as a novel method for protecting of radial forearm free flaps, which require stability.

CLINICAL REPORT

A 67-year-old male patient was admitted with the symptom of pain when swallowing. Malignant cancer invading the right nasal cavity, bilateral nasopharynx, and hard and soft palates was diagnosed (Fig. 1), and reconstruction after resection was planned.

A total palatal defect including the soft and hard palates was generated by the ablative surgery performed for the malignant cancer of the soft palate, and the soft and hard palates were immediately reconstructed with a radial forearm fasciocutaneous free flap to restore nasal and oral separation (Fig. 2). Vascular anatomoses were generated with facial vessels in the neck, and the donor site of the flap was closed with a split thickness skin graft. All suture wounds in the oral and nasal sides had healed primarily with no complications in the first 2 postoperative weeks.

However, wound disruption and downward prolapse of the flap were observed twice by oral examination in the postoperative follow-up period and both times they necessitated a revision operation. In the tertiary re-operation, a preformed palatal obturator for the protection of the repaired wounds and for anti-gravitational support was applied beneath the flap (Fig. 3).

After applying the obturator, no further disruption was reported in the additional follow-up evaluations (Fig. 4). The patient was able to swallow soluble foods 3 weeks after the tertiary re-operation and was prepared for radiation therapy.

DISCUSSION

In this case, the entire soft palate and the hard palate, except the tooth-bearing alveolus, were resected. The defect of the hard palate, excluding the tooth-bearing alveolus, was classified as Okay Class IA. For soft and hard palate reconstruction, the only currently

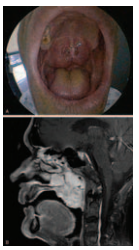

FIGURE 1. Preoperative view. (A) Large mass on the soft palate with multiple pits. (B) Heterogeneously enhanced large mass filling the right nasal cavity, bilateral nasopharynx, hard and soft palates, and right parapharyngeal space.

Copyright © 2015 Mutaz B. Habal, MD. Unauthorized reproduction of this article is prohibited.

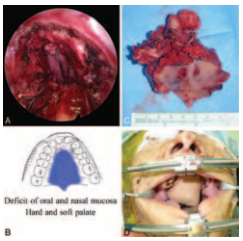

FIGURE 2. Resection of tumor. (A) Extent of defect area is a full layer of the hard and soft palates, and the lower half of the nasal septum. (B) Schematic drawing of the palate defect. (C) Resected hard and soft palates with adjacent soft tissue in nasal cavity. (D) Folded radial forearm free flap for the reconstruction of the nasal septum and oral surface of the palate.

FIGURE 3. (A, B) The obturator was designed to cover the entire palate.

FIGURE 4. (A) Application of the palatal obturator. (B) Adequate wound healing was obtained during the first 3 postoperative weeks without any further disruptions.

available materials are local flaps and prosthetic devices. The radial forearm fasciocutaneous free flap is versatile for soft tissue reconstruction of the palate and provides satisfactory separation between the oral and nasal cavity. In this case, a radial free flap was determined to be the appropriate reconstructive material, considering the size of defect and the desired functional outcome.[1–5]

Wounds after soft tissue reconstruction of the palate using a radial free flap are so fragile that they can be disrupted during the early postoperative period due to their bulkiness, stimulation by tongue movement, and gravitational flap drooping. Thus, the authors chose a palatal obturator for managing wound disruption in this case.

Palatal obturators completely occlude the nasal cavity from the oral cavity by maintaining a seal between the obturator bulb and the normal mucosal lining, thereby, restoring normal speech and swallow functions.

The palatal obturator used in this case is typically used in the treatment modality of small and medium-sized hard palate defects.[1,3,6] For the treatment of palatal defects, the advantages of the palatal obturator include a shorter operative time, shorter hospital stay, and complete visualization of the cavity.[7] A palatal obturator has often been used to compensate for hypernasality and nasal regurgitation in patients with cleft palates.[8]

Additionally, after maxillar reconstruction following maxillectomy, a palatal obturator is usually used for aesthetic and functional purposes. The contour of the lower soft tissues after maxillectomy is dependent on the underlying framework. When the framework is lost, it should be replaced by an artificial denture. A conventional prosthesis is used for preventing floating and drooping of the transferred flap after wound healing. If instability of the obturator prosthesis occurs due to a gradual increase in the drooping force, surgical debulking or the placement of a newly designed movable obturator prosthesis is necessary.[9]

Treatment options for preventing downward prolapse of reconstructed flaps have been discussed previously.

In 2003, a simple method of slit-shaped fenestration at the midline of the hard palate was performed in a maxillary reconstruction to gain the efficient function of the prosthesis. The dispersion of pressure generated by fenestration at the midline of the hard palate decreased the downward force acting on the transferred flap. This method has the advantages of being simpler, less invasive, and less expensive than other methods.[10] However, that method could not be used in the case presented here, because no remnant of the hard palate was present.

Improvement of velopharyngeal function by the palmaris longus tendon sling approach has also been described. The suspension approach also helps to prevent flaps from being drawn far from the posterior pharyngeal wall.[11] However, in the current case, no remnant tissues that could be used for the suspension of a tendon, such as levators or pharyngeal muscles, were present after the oncologic resection surgery.

The above procedures for preventing flap drooping have been shown to preserve the stability of prostheses and to allow for proper speech and mastication functions. However, the abilities of these procedures to manage wounds during acute postoperative care have not been discussed previously.

The palatal obturator has never been used for flap protection and wound management after palate reconstruction with free tissue transfer.

In this case, the palatal obturator superseded the role of splint. The stably fixed obturator with a tooth as a pivot supported flap without generating pressure to prevent downward prolapse. Additionally, inevitable stimulus of the wounds by movement of the bulky tongue was prevented, and the hygiene of the flap was improved by blocking contaminating substances, such as oral secretions.

No previous publications have discussed postoperative care for free flap reconstruction of the palate. Authors recommend the temporary use of a palatal obturator as a beneficial and unique option for preventing wound complications after this type of reconstruction.

REFERENCES

1. Gupta V, Cohan DM, Arshad H, et al. Palatal reconstruction. *Curr Opin Otolaryngol Head Neck Surg* 2012;20:225–230
2. Germain MA, Hartl DM, Marandas P, et al. Free flap reconstruction in the treatment of tumors involving the hard palate. *Eur J Surg Oncol* 2006;32:335–339
3. Genden EM, Wallace DI, Okay D, et al. Reconstruction of the hard palate using the radial forearm free flap: indications and outcomes. *Head Neck* 2004;26:808–814
4. Kim JH, Chu HR, Kang JM, et al. Functional benefit after modification of radial forearm free flap for soft palate reconstruction. *Clin Exp Otorhinolaryngol* 2008;1:161–165
5. Van der Sloot PG. Hard and soft palate reconstruction. *Curr Opin Otolaryngol Head Neck Surg* 2003;11:225–229
6. Tirelli G, Rizzo R, Biasotto M, et al. Obturator prostheses following palatal resection: clinical cases. *Acta Otorhinolaryngol Ital* 2010;30:33–39
7. Davison SP, Sherris DA, Meland NB. An algorithm for maxillectomy defect reconstruction. *Laryngoscope* 1998;108:215–219

© 2015 Mutaz B. Habal, MD

Copyright © 2015 Mutaz B. Habal, MD. Unauthorized reproduction of this article is prohibited.

8. Gümüş HO, Tuna SH. An alternative method for constructing an obturator prosthesis for a patient with a bilateral cleft lip and palate a clinical report. *J Esthet Restor Dent* 2009;21:89–94
9. Murakami M, Nishi Y, Umezono M, et al. Fabrication of a movable obturator following maxillary reconstruction with slit-shaped fenestration. *J Prosthodont* 2015;24:254–259
10. Sakuraba M, Kimata Y, Ota Y, et al. Simple maxillary reconstruction using free tissue transfer and prostheses. *Plast Reconstr Surg* 2003;111:594–598
11. Lee MC, Lee DW, Rah DK, et al. Reconstruction of a total soft palatal defect using a folded radial forearm free flap and palmaris longus tendon sling. *Arch Plast Surg* 2012;39:25–30

Frontal Sinolith

Dong Hoon Lee, MD, Tae Mi Yoon, MD, Joon Kyoo Lee, MD, and Sang Chul Lim, MD, PhD

Abstract: Sinolith in the paranasal sinus is still a rare entity. A sinolith in the frontal sinus is extremely rare, and only 2 patients have been reported in the English literature. Herein, the authors present an additional patient of frontal sinolith in a 78-year-old woman. The patient was preoperatively diagnosed with fungus ball of the frontal sinus, based on radio-opaque densities on computed tomography. Endoscopic surgery was performed and surgical biopsy was interpreted as sinolith. Clinical manifestations of frontal sinolith, including imaging study findings, are discussed with a review of the literature pertaining to this condition. Despite its rarity, frontal sinolith should be considered in the differential diagnosis of radio-densities in the frontal sinus.

Key Words: Frontal sinus, Sinolith, Computed Tomography

Sinolith is a term usually used to describe a calculus in the frontal, ethmoid, or sphenoid sinus, whereas the same pathology in the nasal cavity and maxillary sinus has been termed rhinolith or rhinolithiasis and antrolith or antrolithiasis, respectively.[1–3] Sinoliths are, however, extremely rare, compared with rhinoliths or antroliths.[1,3] Computed tomography (CT) findings of sinolith include a mass with metallic density or multiple calcifications, and sinolith should be considered in the differential diagnosis of calcified lesions in the paranasal sinuses on CT. To date, 2 patients of frontal sinolith have been reported in the English literature according to PubMed search. Herein, we present an additional patient of frontal sinolith mimicking fungus ball and a review of the literature pertaining to this condition.

From the Department of Otolaryngology-Head and Neck Surgery, Chonnam National University Medical School and Hwasun Hospital, Hwasun, South Korea.
Received January 15, 2015.
Accepted for publication March 24, 2015.
Address correspondence and reprint requests to Sang Chul Lim, MD, PhD, Department of Otolaryngology-Head and Neck Surgery, Chonnam National University Medical School and Hwasun Hospital, 160 Ilsimri, Hwasun, Jeonnam 519-809, South Korea. E-mail: limsc@chonnam.ac.kr
The authors report no conflicts of interest.
Copyright © 2015 by Mutaz B. Habal, MD
ISSN: 1049-2275
DOI: 10.1097/SCS.0000000000001858

CLINICAL REPORT

A 78-year-old woman with a left infra-auricular mass was referred to our hospital. We performed CT of the neck for evaluation of the left parotid gland and neck. On CT, multiple calcified lesions in the right frontal sinus were detected incidentally (Fig. 1). Although the patient had intermittent nasal symptoms, such as rhinorrhea, anosmia, and headache, her symptoms were not severe enough to necessitate a medical checkup. The patient had no history of nasal surgery and facial trauma. Nasal endoscopic examination showed purulent discharge from the right middle meatus draining into the choana.

A presumptive diagnosis of fungus ball in the frontal sinus was made, based on multiple calcifications on CT. Endoscopic sinus surgery was performed. The right frontal ostium was enlarged with powered instrumentation, and purulent secretion and a brittle mass were removed. Histopathological examination of the brittle mass in the right frontal sinus was consistent with sinolith. Histopathological findings obtained using Gomori methenamine silver (GMS) stain and periodic acid-Schiff (PAS) stain did not show fungi. No fungi were found to grow in the fungus culture. This patient was finally diagnosed as sinolith in the right frontal sinus. The postoperative course was uneventful. The patient was found to be free of lesions during follow-up examinations.

DISCUSSION

Contrary to rhinolithiasis of the nasal cavity, the occurrence of a sinolith is very rare.[1–3] Through literature search using PubMed with terms such as "frontal sinus," "sinolith," 'antrolithiasis," "antrolith," and combinations of these terms, 8 patients of sinoliths were retrieved from the English literature[1–7]; 4 patients of ethmoid sinus sinolith, 2 patients of sphenoid sinus sinolith, and 2 patients of frontal sinus sinolith.[7] Frontal sinus is an extremely rare location of a sinolith.

The etiology of sinolith has not been clearly established. It has been known that sinolith develops from an exogenous or endogenous nidus.[3] Endogenous niduses include tooth, bone chip, blood clots, purulent secretion, and mucus fungal element.[8] On the contrary, exogenous niduses include various foreign materials such as cotton, cellulose, and paper. Long-standing infection, fungal infection, poor sinus aeration and drainage, and presence of a foreign body are predisposing factors for sinolith.[1–3] During the review of the literature, previously reported patients of frontal sinolith were not related to the presence of a foreign body and the predisposing factors were radiation ($n = 1$) and chronic paranasal sinus inflammation ($n = 2$).

Most patients with sinoliths present with symptoms such as facial pain, nasal obstruction, purulent discharge, postnasal drip, epistaxis, and headache.[1,2,6] These symptoms and signs usually depend on coexisting infection of the involved sinus. Headache and postnasal drip were reported as symptoms of frontal sinolith.[5] Some patients can, however, be asymptomatic and are diagnosed incidentally by radiologic examination, as our patient.[4]

CT is very helpful to establish the diagnosis of sinolith.[1,6] CT may aid in the preoperative diagnosis of sinolith and provide useful information about the location, size, and relation to surrounding structures.[1,6] On CT, a dense, irregular, but a well-defined mass or masses are usually seen, as observed in the previously 2 reported patients. Our patient was, however, preoperatively diagnosed as fungal sinusitis due to multiple calcifications in the frontal sinus. It

FIGURE 1. Coronal CT scan with enhancement revealed multiple calcified lesions (red arrow) in the right frontal sinus.

© 2015 Mutaz B. Habal, MD

Copyright © 2015 Mutaz B. Habal, MD. Unauthorized reproduction of this article is prohibited.

should be kept in mind that frontal sinolith can show nonspecific findings of calcifications, and the diagnosis of frontal sinolith requires a high index of suspicion. The sinolith can be found along with chronic inflammatory changes within the paranasal sinuses, and occasionally it may be an incidental finding, as in this patient. The sinolith should be differentiated from fungal infection, ossifying fibroma, osteoma, osteoblastoma, benign odontoma, cementoma, primary or metastatic carcinoma, osteogenic sarcoma, fibrous dysplasia, calcified mucous, and retention cyst.[2] MRI findings of sinolith show low signal intensity or signal void on all sequences and variable signal intensity in the surrounding of the sinolith on T1- and T2-weighted images according to secretion or inflamed mucosa in the sinus. A mycetoma, dessicated secretions, an intrasinus tooth, or osteoma have similar findings on MRI.[9]

The treatment of choice for a sinolith is surgical drainage.[1–7] Surgical removal of the sinolith is usually performed along with appropriate treatment of the coexisting sinus disease.[1,2] The endoscopic approach is preferable and it offers advantages such as easy access to the lesion, perfect visualization, low morbidity, and low complications,[1] and external surgery is attempted if a sinolith cannot be removed with endoscopic surgery.

In conclusion, sinolith in the paranasal sinus is still a rare entity and the frontal sinus is a very unusual location of a sinolith. Despite its rarity, frontal sinolith should be considered in the differential diagnosis of radiodensities in the frontal sinus.

REFERENCES

1. Almaši M, Andrašovská M, Koval J. Sinolith in the ethmoid sinus: report of two cases and review of the literature. *Eur Arch Otorhinolaryngol* 2010;267:1649–1652
2. Özcan C, Vaysoğlu Y, Görür K. Sinolith: a rare isolated sphenoid sinus lesion. *J Craniofacial Surg* 2013;24:e104–e106
3. Nayak DR, Bhandarkar AM, Valiathan M, et al. Incidental 'ethmoid sinolith': an unusual cause of frontal recess obstruction. *BMJ Case Rep* 2014 doi: 10.1136/bcr-2014-204157
4. Grant DG, Hussain A, Burgel R. Frontal sinolith. *J Laryngol Otol* 1998;112:570–572
5. Mori S, Lee K, Fujieda S, et al. Antrolithiasis in the frontal sinus. *ORL J Otorhinolaryngol Relat Spec* 2000;62:335–337
6. Kanzaki S, Sakamoto M. Sinolith in the ethmoid sinus. *J Laryngol Otol* 2006;120:e11
7. Wyllie JW 3rd, Kern EB, Djalilian M. Isolated sphenoid sinus lesions. *Laryngoscope* 1973;83:1252–1265
8. Manjaly G, Pahor AL. Antral rhinolithiasis and tooth filling. *Ear Nose Throat J* 1994;73:676–679
9. Burgener FA, Meyers SP, Tan RK, Zaunbauer W. Paranasal sinus and nasal cavity. In: *Differential Diagnosis in Magnetic Resonance Imaging*. Stuttgart, Germany/New York: Georg Thieme Verlag; 2002;224–231.

A Lacrimal Sump Syndrome With a Large Intranasal Ostium

Zhenbin Qian, MD, Yunhai Tu, MD, Tianlin Xiao, MD, and Wencan Wu, MD

Abstract: Lacrimal sump syndrome is an uncommon cause of failed dacryocystorhinostomy. Small osteotomy was reported as the major cause of this syndrome. Here, the authors described the first case of a lacrimal sump syndrome with a large intranasal ostium following endoscopic endonasal dacryocystorhinostomy (EE-DCR). A 51-year-old women patient suffered recurrence of epiphora and dacryocystitis for 8 months following an EE-DCR. Examination showed a large intranasal ostium with a lot of purulent discharge and patent lacrimal irrigation. Lacrimal sump syndrome was diagnosed after passing a probe into the residual lacrimal sac under the aid of an endoscope. The residual sac was reopened and merogel was packed around the wound. The clinical symptoms disappeared after the surgery. It is indicated that lacrimal sump syndrome does happen not only in a small intranasal ostium, but also in a large intranasal ostium. Existing residual sac with bacterial infection may be related to this particular case.

Key Words: Endonasal dacryocystorhinostomy, lacrimal sump syndrome, large intranasal ostium

Endoscopic endonasal dacryocystorhinostomy (EE-DCR) is now widely considered a successful treatment for nasolacrimal duct obstruction. It has shown a number of advantages over external DCR (EX-DCR), including preservation of medial canthal tendon and pump function, direct visualization of nasal anatomy, and avoidance of cutaneous scar.[1–3]

Lacrimal sump syndrome is an uncommon cause of failed dacryocystorhinostomy. It was early described in 1993 in a case report by Jordan and McDonald.[4] The occurrence of lacrimal sump syndrome was reported from 0.3% to 4.8% of endonasal or external DCR patients.[2,4–6] The distinctive feature of the syndrome is the residual lacrimal sac formed after DCR, mostly present epiphora with or without mucopurulent discharge; however, lacrimal irrigation and dye disappearance may seem normal.

It has been reported that the small osteotomy is the main cause of lacrimal sump syndrome.[2,4–5] Here, we reported a case of lacrimal sump syndrome unusually with a large intranasal ostium and a patent lacrimal irrigation, which has been successfully treated after reopening the residual sac and packing the wound with merogel. As our knowledge, this is the first report about lacrimal sump syndrome having a large ostium following EE-DCR.

CLINICAL REPORT

A 51-year-old woman was referred with a 5-year history of epiphora in both eyes and 1-year history of purulent discharge in right eye. Since no significant improvement after 3 times of probing, a bilateral EEDCR was performed by a skilled surgeon. All the symptoms disappeared and lacrimal irrigation test easily passed after the surgery. But 8 months later, epiphora with purulent discharge in her left side recurred (Fig. 1A), especially in the morning. No remarkable change in her CT scan was found (Fig. 1B). Endoscopic examination showed a large intranasal ostium in a size around 5×3 mm,wildly opened but with a lot of purulent discharge (Fig. 1C-D); however, lacrimal irrigation was easily passed. Postoperative infection was first considered and then intravenous lavofloxacin lactate was recommended to apply after positive bacterial culture showing growth of *Klebsiella*

From the Department of Ophthalmology, Eye Hospital of Wenzhou Medical University, Wenzhou, China.
Received February 11, 2015.
Accepted for publication March 7, 2015.
Address correspondence and reprint requests to Wencan Wu, Department of Ophthalmology, Eye Hospital of Wenzhou Medical University, 270 Xue-Yuan West Road, Wen Zhou, Zhe Jiang 325000, China.
E-mail: wuwencan118@163.com
The authors report no conflicts of interest.
Copyright © 2015 by Mutaz B. Habal, MD
ISSN: 1049-2275
DOI: 10.1097/SCS.0000000000001864

Copyright © 2015 Mutaz B. Habal, MD. Unauthorized reproduction of this article is prohibited.

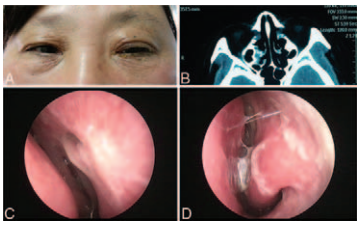

FIGURE 1. Recurrent dacrocysitis after EE-DCR. A 51-year-old women had recurrent epiphora with discharge after 8 months of EE-DCR. A, Shows purulent discharge covering her left eyelid; B, shows no remarkable finding with her CT scanning; and C and D, display a widely opened ostium with a lot of purulent discharge.

pneumoniae and *Streptococcus pneumonia*, which were sensitive to lavofloxacin lactate. The discharge around the eyelid decreased after 5 days of treatment, but it remained surrounding the ostium. Then, an endoscopic-guided probing was conducted, and a residual sac formed by the proliferated nasal mucosa was detected (Fig. 2A), which suggested a diagnosis of lacrimal sump syndrome. The residual sac was reopened under local anesthesia with the aid of an endoscope, and then merogel coverage was followed around the reopened wound (Fig. 2B-C). All symptom disappeared (Fig. 3A-B) and no recurrence after 1 year of follow-up.

DISCUSSION

Several reports have explained how is the lacrimal sump syndrome formed. Migliori and coworkers suggested inadequate bone removal or failure to completely open the lacrimal sac into the nose is the main cause of the lacrimal sump syndrome.[7] They illustrated that the residual sac was reformed either by nasal mucosa or adhesion between middle turbinate and lateral nasal wall, in which the residual sac was identified by passing a Bowman probe into the sac and tenting it away from common internal punctum. Fayet et al[2] demonstrated too small oseteotomy, or insufficient downward extension of the osteotomy may be related to lacrimal sump syndrome. Welham and Wulc[6] displayed the development of this syndrome was attributed to placing the nasal ostium too high, thus creating a blind pouch that retains tears and is vulnerable to infection.

In our case, the EE-DCR was performed by a skilled surgeon who made a large osteotomy with totally opened sac that maintained the lacrimal drainage system working anatomically and functionally for 8 months. If we defined a large intranasal ostium as 5 mm or more in any dimension, the ostium of 5 × 3 mm in our case belongs to the large one (Figs. 1A, 3B). However, the symptoms recurred after 8 months of postoperation when we thought it would never block the tears flow causing excess tearing again. We primarily thought those recurrent symptoms were induced by the postoperative infection since a lot of purulent discharge presented around the eyelid and intranasal ostium (Fig. 1A-C), especially when the bacterial culture showing positive result. Having not good response to antibacterial treatment, we finally realized it was lacrimal sump syndrome after we passed a probe into the residual sac under the guidance of an endoscope (Fig. 2A). Examination showed that the proliferated nasal mucosa formed the lower portion of residual sac.

FIGURE 2. Residual sac detection and resection. A, Shows a probe is used to detect the bottom of residual sac which reformed by proliferated nasal mucosa. Black arrow shows the large ostium opened. B, Shows the sac was reopened; C, shows merogel was covered around the wound.

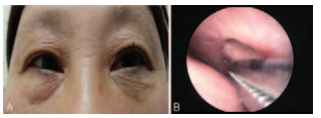

FIGURE 3. Photographs at 12 months of postoperation. A, Shows the discharge around her left eyelid disappeared; B, shows a 5 mm × 8 mm of intranasal ostium widely opened, which is measured by a marked tweezer. No discharge is noted around it.

As mentioned before, lacrimal sump syndrome mostly was related to a small osteotomy. Literature search has not found any case of lacrimal sump syndrome with a large ostium. We speculate the large ostium in our case drained the tears freely at first few months of postoperation; however, with the deposit of more and more bacteria to the bottom of residual sac, those bacteria quickly proliferated and produced a lot of purulent discharge that eventually blocked the whole lacrimal system and induced epiphora with discharge. It demonstrated not only a residual sac from the proliferated nasal mucosa contributed to this syndrome, but a lot of discharge from bacterial infection also participated in its blockage. Yazici and coworkers thought that the occurrence of lacrimal sump syndrome was underestimated; furthermore, not all of residual sac will induce lacrimal sump syndrome. They found 3 (7%) of residual lacrimal sac in 41 cases of successful Ex-DCR, but none of them having lacrimal sump syndrome. Thus, they speculated a lacrimal sump syndrome will not happen if the osteotomy is big and functional, even lower lacrimal sac existed.[8] Our observation is agreed with Yazici' finding, which means, excepting the residual sac, other factors may involve in the happen of lacrimal sump syndrome.

Since lacrimal sump syndrome is an uncommon complication of failed Ex- or EE-DCR, there are only few reporters described this syndrome. The detail description, for example, the relationship of the size of an ostium with lacrimal sump syndrome is still unclear. Linberg et al[9] observed mean final ostium diameter after Ex-DCR was only 1.8 mm under endoscopic study, and excellent functional results were obtained even when the intranasal ostium was quite small. Ben Simon et al[10] reported the mean (SD) postoperative ostium size was 9.6 mm^2, and the intraoperative osteotomy size correlated positively with the postoperative intranasal ostium size; however, there was no difference in either the intraoperative osteotomy size or the postoperative ostium size between failed and successful cases. Yazici et al used digital subtraction macrodacryocystography to assess the healed nasolacrimal ostium after ex-DCR. The average height of the healed ostium was 3.5 mm (range, 1.2–6.5 mm) for all 41 patients. Among 3 of nasolacrimal ostium located at the middle part of the regenerated sac, the height of ostium is 3.0, 2.1, and 1.6 mm, respectively, but none of them having lacrimal sump syndrome.[8] Comparing with our case, the postoperative ostium is larger than those reports, so it is truly a lacrimal sump syndrome with a large intranasal ostium.

Treatment for the lacrimal sump syndrome is not difficult. Jordan and McDonald[4] suggested that making a large osteotomy and opening the bottom of the lacrimal sac are considered can reduce the chance of the sump syndrome. Expand osteotomy and resect the lacrimal sac flaps and the surrounding nasal mucosa can be done in endoscopic revision surgery. Migliori[7] demonstrated that using contact Nd:YAG laser and implanting silicone stent is an effective method for treating lacrimal sump syndrome. In our case, the residual lacrimal sac was reopened under local anesthesia, and the wound was covered by the merogel. Merogel coverage helps early re-epithelialization of the ostium and inhibition of the fibrotic tissues, which may enhance the success rate of the surgery.[11] We consider that our method is minor invasive and highly efficient for the management of lacrimal sump syndrome with a large ostium.

© 2015 Mutaz B. Habal, MD

Copyright © 2015 Mutaz B. Habal, MD. Unauthorized reproduction of this article is prohibited.

Overall, we first describe a lacrimal sump syndrome with a large intranasal ostium following an EE-DCR. It demonstrated not only a small ostium is contributed to the lacrimal sump syndrome, but also a large ostium can involve in this syndrome. In this particular situation, we have to consider whether or not other factor participates in the process. Reopening of the residual sac and packing with merogel is an effective and minor invasive surgical treatment for the lacrimal sump syndrome with a large intranasal ostium.

REFERENCES

1. Yang JW, Oh HN. Success rate and complications of endonasal dacryocystorhinostomy with unciformectomy. *Graefes Arch Clin Exp Ophthalmol* 2012;250:1509–1513
2. Fayet B, Racy E, Assouline M. Complications of standardized endonasal dacryocystorhinostomy with unciformectomy. *Ophthalmology* 2004;111:837–845
3. Yüce S, Ali A, Doğan M, et al. Results of endoscopic endonasal dacryocystorhinostomy. *J Craniofac Surg* 2013;24:e11–e12
4. Jordan DR, McDonald H. Failed dacryocystorhinostomy: the sump syndrome. *Ophthalmic Surg* 1993;24:692–693
5. Fayet B, Katowitz WR, Racy E, et al. Endoscopic dacryocystorhinostomy: the keys to surgical success. *Ophthal Plast Reconstr Surg* 2014;30:69–71
6. Welham RA, Wulc AE. Management of unsuccessful lacrimal surgery. *Br J Ophthalmol* 1987;71:152–157
7. Migliori ME. Endoscopic evaluation and management of the lacrimal sump syndrome. *Ophthal Plast Reconstr Surg* 1997;13:281–284
8. Yazici B, Yazici Z. Final nasolacrimal ostium after external dacryocystorhinostomy. *Arch Ophthalmol* 2003;121:76–80
9. Linberg JV, Anderson RL, Bumsted RM, et al. Study of intranasal ostium external dacryocystorhinostomy. *Arch Ophthalmol* 1982;100:1758–1762
10. Ben Simon GJ, Brown C, McNab AA. Larger osteotomies result in larger ostia in external dacryocystorhinostomies. *Arch Facial Plast Surg* 2012;14:127–131
11. Wu W, Cannon PS, Yan W, et al. Effects of Merogel coverage on wound healing and ostial patency in endonasal endoscopic dacryocystorhinostomy for primary chronic dacryocystitis. *Eye* 2011;25:746–753

Extensive Inflammatory Gingival Tumor in a Young Nonsmoking Woman: Back to Basics

Farah Hajji, MD, Guillaume Beraud, MD,† Armel Genay, MD,* Gwenaël Raoul, PhD,* Karine Faure, PhD,‡ Benoit Guery, PhD,‡ and Joël Ferri, PhD**

Abstract: Tuberculous lesions of the oral cavity are rare and can be a diagnostic challenge, particularly in young immunocompetent patients. Most of the cases in the literature are secondary to pulmonary disease, whereas primary form is uncommon. This paper presents a case of gingival tuberculosis in a 26-year-old Indian female patient, manifesting as a rapidly extensive ulcer. The diagnosis was confirmed by histopathology and immunological investigations. Although oral manifestations of tuberculosis are rare, clinicians should include them in the differential diagnosis of various types of oral ulcers. An early diagnosis with a prompt treatment can prevent complications and potential contaminations.

Key Words: Extensive ulcer, gingiva, tuberculosis

CLINICAL REPORT

A 26-year-old woman, of Indian origin, was admitted for a painful ulcer of the gingiva facing the 45th tooth. The symptoms started 4 months prior the initial examination. She left India at the age of 13, and lived in the United States (Iowa). The medical history revealed tuberculosis in her grandmother. At first, she benefited from a simple dental treatment. The initial lesion evoluted toward a painful ulceration. Because an infection was suspected, she was treated with azithromicin then amoxicillin and clavulanic acid association, without any success. Clinical examination revealed a minor swelling of the cheek. Intraoral examination, limited by the important trismus, showed a painful ulcer with irregular and friable margin, bleeding on touch, affecting the right mandibular gingiva in the molar region, involving the cheek mucosa and tonsil region. Palpation of the neck revealed no palpable lymph nodes. The evolution of the disease was marked by the extension to the adjacent mandibula and to the soft tissues of the cheek, causing an orostoma (Fig. 1), probably aggravated by the iterative biopsies.

The progressive extension to the right mandibular region and the progressive loss of weight lead to a radiological assessment. The cervico-facial CT scan and MRI showed an infiltrating mandibular tumor with the involvement of masticatory muscles, the right tonsil, the osteolysis of the adjacent mandibula with medullar infiltration and multiple cervical bilateral lymph nodes (Fig. 2). Routine hematological and biochemical investigations and the chest x-ray did not reveal any abnormality, besides an inflammatory syndrome. Syphilis and HIV serology were negative. Tonsil and gingival biopsies only showed inflammation and necrosis. Several biopsies were performed under general anaesthesia to get a diagnostic.

We initially suspected a fungal or bacterial infection such as *Actinomycosis*, *Nocardia*, or a malignant process (lymphoma and oral squamous cell carcinoma). At first, the patient received only liposomal amphotericin, rapidly associated with voriconazole and broad-spectrum antibiotics (cephalosporins, then piperacillin–tazobactam, and finally carbapenems). After 3 months of medical treatment without any improvement, and no definitive diagnosis, we introduced a pentatherapy targeting atypical *mycobacterium* as salvage therapy. Her general condition dramatically improved starting the first week after antimycobacterial therapy introduction. After 2 months, the culture finally revealed a mycobacteria ultimately identified by PCR as *Mycobacterium tuberculosis*.

From the *Service de Chirurgie Maxillo-faciale et Stomatologie de l'Hôpital Roger Salengro du Centre Hospitalier Universitaire de Lille, Lille; †Service de Médecine Interne et Maladies Infectieuses du Centre Hospitalier Universitaire de Poitiers, Poitiers; and ‡Unité d'Infectiologie du Service de gestion du risque infectieux et des vigilances et infectiologie de l'Hôpital Huriez du Centre Hospitalier Universitaire de Lille, Lille, France.

Received February 15, 2015.
Accepted for publication March 16, 2015.

Address correspondence and reprint requests to Dr Farah Hajji, MD, Service de Chirurgie Maxillo-faciale et Stomatologie, Hôpital Roger Salengro du Centre Hospitalier Universitaire de Lille, BP 59000, Lille, France; E-mail: farah.h0412@yahoo.fr

The authors report no conflicts of interest.

Copyright © 2015 by Mutaz B. Habal, MD

ISSN: 1049-2275
DOI: 10.1097/SCS.0000000000001865

Copyright © 2015 Mutaz B. Habal, MD. Unauthorized reproduction of this article is prohibited.

FIGURE 1. A profile view showing the inflammatory ulcerative lesion of the cheek associated to a trismus.

FIGURE 2. An MRI image illustrating the extension of the tumor to soft tissues of the cheek, gingiva, and parapharyngeal space, with an osseous involvement.

The drugs given at first were rifampicin 600 mg, ethambutol 400 mg, and ciprofloxacin 500 mg during the first 3 months, associated to clarithromycin 1 g and amikacin during the first week. The response to this treatment was spectacular during the first weeks, locally and generally. Rifampin associated with izoniazid was continued for further 9 months. The ulcerative lesion was completely healed (Fig. 3) after 4 months of treatment with a progressive skin and mucosal cicatrization. Because of the retractile skin scar of the cheek, we made a platysmal flap to give much volume to the tissues. No recurrence was observed in the follow-up period of 6 months duration after the completion of full-course multidrug regimen.

DISCUSSION

Tuberculosis of oral cavity is a rare lesion.[1] It may be primary or secondary to pulmonary tuberculosis.[1] Oral manifestation of primary tuberculosis is uncommon, and most cases described in literature are case reports. Oral lesions occur in 0.05% to 5% of the patients with tuberculosis.[1] Because of its rapid evolution and to this particular localization, oral tuberculosis can be rapidly fatal if not diagnosed early and treated adequately. A notable feature in this case was the location in mandibular gingiva extending to the adjacent oral mucosa of the cheek and tonsil with an osseous infiltrating of the jaw. Involvement of these areas by primary oral tuberculosis is not often reported.[2]

Contrary to the secondary form of tuberculous oral lesions that is seen frequently in middle-aged persons and involves mainly the tongue and hard palate,[3] the primary form is commonly found in children and adolescents. It is usually affecting the gingiva and the mucobuccal folds and often associated to enlarged cervical lymph nodes.[4] Generally, the tongue and gingiva are the most common sites of infection in patients with oral tuberculosis, followed by tooth sockets, soft palate, floor of mouth, lips and buccal mucosa.[5]

The mechanism of primary inoculation is still unknown. However, it is thought that oral mucosa is affected by direct inoculation.[3] The intact oral mucosa membrane presents a natural resistance to *mycobacterium* invasion. This resistance is because of several local factors: the cleansing action of saliva, salivary enzymes, tissue antibodies, oral saprophytes, and the thickness of the protective epithelial covering. Any break or loss of this natural barrier, which may be a result of trauma, inflammatory conditions, tooth extraction, or poor oral hygiene, may provide a route of entry for *mycobacterium*.[6] In our case, we have considered that the *mycobacterium* invasion is secondary to the inoculation of *mycobacterium* during the dental treatment of the 45th tooth. We suppose that our patient presented a tuberculous primoinfection several years ago and that the inoculation occurred secondary to the dental treatment causing mucosal wound. This also suggests that our patient probably exhaled some *mycobacterium*, although considered having just latent tuberculosis.

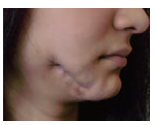

FIGURE 3. Spontaneous cicatrization of the ulceronecrotic lesion of the cheek after the medical treatment targeting *Mycobacterium tuberculosis*.

Clinical diagnosis is often difficult because of the variety of aspects of oral lesions of tuberculosis. They are nonspecific in their clinical presentation and are present before systemic symptoms become apparent. It usually consists of a stellate ulcer with undermined edges and a granulating floor.[7] Other lesions such as nodules, fissures, tuberculomas or granulomas also can be seen. The lesion may be single or multiple, painful or painless.[4] Skin, cervical lymph nodes, and salivary glands are also frequently involved.[8]

The differential diagnosis in an immunocompetent patient usually include malignant lesion, traumatic or aphtous ulcer, syphilis, sarcoidosis, and deep mycotic infections such as histoplasmosis.[1,4]

Diagnosis of oral tuberculosis is mainly based on histopathological examination and demonstration of acid-fast bacilli on Ziehl-Neelsen staining.[9] But because of the selective scarcity of bacilli within the tissues, mycobacteria can be harvested only in 27% to 60% cases.[2] The culture provides good results, but lacks sensitivity and last 4 to 6 weeks.[4] Sophisticated techniques such as PCR can be used alternatively, especially when the conventional methods of diagnosis render equivocal results.[10,11] Chest x-ray is indicated to exclude the possibility of pulmonary tuberculosis. We must highlight the importance of multiplying biopsies and collaborating with the histopathological laboratory.

The antibiotic regimen is effective even on extended lesions but must be given for longer periods. Drugs that are commonly used in quadri-therapy include rifampicin in combination with isoniazid, pyrazinamide, and ethambutol simultaneously administrated, usually for the first 2 months of treatment, followed by a rifampin-isoniazid combination for usually 4 months. The duration and regimen treatment is similar to the standard regimen used for pulmonary tuberculosis. In our case, the initial regimen was different because the initial hypothesis included atypical *mycobacterium*. It was extended to 9 months because of the extension of the ulcerative lesion to soft tissues of the cheek and the medullar bone infiltration. The medical treatment was sufficient to obtain a complete cicatrization of the orostoma.

Because it is still a worldwide health problem and because of its infrequent clinical intraoral manifestations, tuberculosis is more likely to be misdiagnosed, especially in nonendemic countries such as France. The clinician needs to be aware of these various lesions and should consider tuberculosis in the differential diagnosis of any nodular; ulcerated lesion of the oral cavity.

REFERENCES

1. Ito FA, De Andrade CR, Vargas PA, et al. Primary tuberculosis of the oral cavity. *Oral Dis* 2005;11:50–53
2. Rivera H, Correa MF, Castilli-Castillo S, et al. Primary oral tuberculosis: a report of a case diagnosed by polymerase chain reaction. *Oral Dis* 2003;9:46–48
3. Rauch MD, Friedman E. Systemic tuberculosis initially seen as an oral ulceration: report of a case. *J Oral Surg* 1978;36:387–389
4. Mignogna MD, Muzio LL, Favia G, et al. Oral tuberculosis: a clinical evaluation of 42 cases. *Oral Dis* 2000;6:25–30
5. Rodrigues G, Carnelio S, Valliathan M. Primary isolated gingival tuberculosis. *Braz J Infect Dis* 2007;11:172–173

© 2015 Mutaz B. Habal, MD

Copyright © 2015 Mutaz B. Habal, MD. Unauthorized reproduction of this article is prohibited.

6. Iype EM, Ramdas K, Pandey M, et al. Primary tuberculosis of the tongue: report of three cases. *Br J Oral Maxillofac Surg* 2001;39:402–403
7. Von Arx DP, Husain A. Oral tuberculosis. *Br Dent J* 2001;190:420–422
8. Zheng JW, Zhang QH. Tuberculosis of the parotid gland: report of 12 cases. *J Oral Maxillofac Surg* 1995;53:849–851
9. Karthikeyan V, Pradeep AR, Sharma CG. Primary tuberculous gingival enlargement: a rare entity. *J Can Dent Assoc* 2006;72:645–648
10. Goel MM, Ranjan V, Dhole TN, et al. Polymerase chain reaction vs. conventional diagnosis in fine needle aspirates of tuberculous lymph nodes. *Acta Cytol* 2001;45:333–340
11. Vargas PA, Villalba H, Passos AP, et al. Simultaneous occurrence of lymphoepithelial cycts, cytomegalovirus and mycobacterial infections in the intraparotid lymph nodes of a patient with AIDS. *J Oral Pathol Med* 2001;30:507–509

Giant Solitary Fibrous Tumor of Orbit

Goktekin Tenekeci, MD, Alper Sari, MD,* Yusuf Vayisoglu, MD,† and Onur Serin, MD‡*

Abstract: Solitary fibrous tumors (SFTs) have been reported in various locations in the body. Solitary fibrous tumors are extremely rare tumors, especially when located in the orbit. Diagnosis of SFT cannot be made based on histopathology only because it exhibits a variable microscopic appearance, and necessitates immunohistochemistry to confirm the diagnosis.

A 51-year-old man was admitted to our clinic for the evaluation of a mass bulging in his left eye. Clinical examination revealed a painless mass extruding out of the orbital cavity with dimensions of 8 × 7 cm. Exenteration of the left eye including the upper and lower eyelid and reconstruction of the orbital cavity using a temporoparietal fascia flap and a temporal muscle flap was performed.

SFT of orbital region is known as a slow growing and painless tumor. Based on previous studies, increased mitotic rate of the tumor gives the impression that the tumor has a malignant nature. Until now a small number or orbital SFTs were reported and none of them presented with a giant mass protruding out of the orbital cavity. We present a unique case of orbital SFT filling the whole orbital cavity and protruding outward as a giant mass. This case has been reported to expand our knowledge in this debated entity.

Key Words: Flap, immunohistochemistry, orbit, solitary fibrous tumor

From the *Department of Plastic Reconstructive and Aesthetic Surgery; †Department of Ear Nose and Throat; and ‡Department of Plastic Reconstructive and Aesthetic Surgery, Mersin University Hospital, Mersin University School of Medicine, Mersin, Turkey.

Received February 27, 2015.
Accepted for publication March 31, 2015.

Address correspondence and reprint requests to Goktekin Tenekeci, Mersin Üniversitesi Tıp Fakültesi Hastanesi, Plastik Rekonstruktif ve Estetik Cerrahi A.B.D, Mersin Üniversitesi, Çiftlikköy Kampüsü, Mezitli, Mersin, Turkey; E-mail: dr_tenekecig@hotmail.com

The authors report no conflicts of interest.

Copyright © 2015 by Mutaz B. Habal, MD

ISSN: 1049-2275
DOI: 10.1097/SCS.0000000000001868

Solitary fibrous tumor (SFT) is a rare mesenchymal spindle cell neoplasm that was originally described by Klemperer and Rabin[1] in pleura,[2,3] which then was identified in numerous extrathoracic sites too.[4–9] Rarely, it is found in the mediastinum, skin, meninges, orbit, upper respiratory tract, breast, thyroid, and peritoneum.[5] Solitary fibrous tumor exhibits a variable microscopic appearance, which necessitates immunohistochemistry to confirm the diagnosis. Definitive diagnosis is based on typical histopathologic and immunohistochemical features.[10,11] Solitary fibrous tumor forms a nodule secondary to spindle cell proliferation, mast cell, and multinucleated giant cells present in a collagenized stroma.[12,13] CD99, bcl-2, and CD34 positivity and negativity for epithelial, muscle, neural, and melanocytic markers confirm the diagnosis for SFT.[12,14,15]

Solitary fibrous tumors are extremely rare tumors, especially when located in the orbit. We present a unique case of orbital SFT filling the whole orbital cavity and protruding outward as a giant mass. This case has been reported to expand our knowledge in this debated entity.

CLINICAL REPORT

A 51-year-old man was admitted to our clinic for the evaluation of a mass bulging in his left eye (Fig. 1). The mass in his left eye was slowly enlarging and was first noticed 4 years ago; however, the patient did not apply to the hospital until he had a bleeding from the surface of the tumor. The patient has psychiatric disorders. His medical history was otherwise unremarkable. Clinical examination revealed a painless mass extruding out of the orbital cavity with dimensions of 8 × 7 cm. The mass was firm in consistency, and the left eye was blind on examination.

Orbital computed tomography scan (Fig. 2) revealed a 70 × 76 × 70 mm sized mass protruding from the left orbital cavity, which showed intense heterogenous contrast with regular borders and ovoid configuration. A cystic lesion with dimensions of 23 × 19 × 12 mm in ovoid configuration that contrasts from periphery was noted within it. Superolateral to this cystic lesion, an area with no contrast uptake and irregular borders and ovoid appearance (20 × 13 × 11 mm) was noticed. The extraocular structures within the orbit (the optic nerve and the extraocular muscles) were shifted to the periphery and thinned under the pressure of the enlarging mass. No apparent destructive changes were noted in the bony structures around the lesion and in the extraocular mucles.

Exenteration of the left eye including the upper and lower eyelid and reconstruction of the orbital cavity using a temporoparietal fascia flap and a temporal muscle flap was planned (Fig. 3). The temporoparietal fascia and temporal muscle flaps were harvested separately based on the superficial and the deep temporal vessels consecutively.

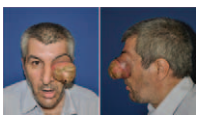

FIGURE 1. Frontal and lateral views of tumor before the operation. Note the mass extruding out from the left orbital cavity. The mass was firm in consistency, and the left eye was blind on examination.

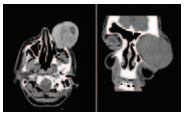

FIGURE 2. Preoperative axial (left side) and coronal (right side) computed tomography scan of the patient is seen. A mass with regular borders and ovoid configuration is noted. A cystic lesion in ovoid configuration is seen.

© 2015 Mutaz B. Habal, MD

Copyright © 2015 Mutaz B. Habal, MD. Unauthorized reproduction of this article is prohibited.

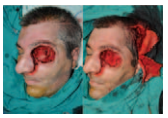

FIGURE 3. Patient is seen after the exenteration is completed (left side). Superficial temporal fascia flap and temporal muscle flap are elevated. The highly pliable temporoparietal fascia flap was set as a thin layer over the orbital bones in the orbital cavity.

The flaps were transferred to the orbital cavity through a subcutaneous tunnel under the intact temporal skin. The highly pliable temporoparietal fascia flap was set as a thin layer over the orbital bones in the orbital cavity (Fig. 3, right side) and the temporal muscle flap was then laminated as another layer over the temporoparietal fascia flap to fill the orbital cavity (Fig. 4). To cover the muscle a split thickness skin graft was used. Flap donor site was closed primarily.

The exenterated lesion weighed 213 g with dimensions of $9.5 \times 7 \times 6$ cm and was firm in consistency. Microscopically, the specimen was noted to have necrosis at the center. The tumor was formed of spindle cells with occasional myxoid degeneration, wide and short fascicles, thick-walled vascular structures, and occasional hyalinization. Mitotic rate was 7/10 Hydroxyl Radical and Peroxynitrite Sensor (HPF); however, significant atypia was noted occasionally. Cellularity was significantly high at some regions, whereas was lesser at some others. Amyloid accumulation was not noted with Congo Red. Positive staining with Epithelial Membrane Antigen (EMA), CD99, Caldesmon, Bcl-2, CD34 was noted. Proliferation index with Ki-67 was 5%. No staining of tumor cells was seen with S-100, melan-A, HMB 45, cytokeratin 8, P 40, smooth muscle antigen, desmin, cyclin-D, and progesterone receptor. Optic nerve was not invaded by tumor.

DISCUSSION

Ultrastructural and immunohistochemical studies indicate that SFTs arise from mesenchymal fibroblast like cells.[16] World Health Organization classifies SFT as a probable fibroblastic/myofibroblastic tumor.[2] Although SFT was originally reported to be located within the pleura,[1] case studies from extrapleural sites of SFT have also been reported.[4–9] As SFT is an extremely rare tumor, its long-term clinical behavior is not known. This case may enlighten the mostly unknown clinical behavior of this tumor.

Until now, a small number or orbital SFTs were reported and none of them presented with a giant mass protruding out of the orbital cavity. Solitary fibrous tumor of orbital region is known as a slow growing and painless tumor. This fact about the biologic behavior of the STFs was also recorded in our case as the slowly enlarging mass did not destruct the bony structures and protruded out. Although $\geq$4 years have passed since the tumor was first noticed and the tumor in this case is accounted as malignant, bony invasion or invasion to extraocular muscles did not substantiate. These data obtained by this patient are important because it provides us the information about the biologic behavioral pattern of the SFT. Bony invasion or extraocular muscle invasion does not occur even in malignant orbital SFTs before a lengthy period of time if occurs at all. An expansion of the eyelids overlying the enlarging mass was also seen. The SFTs including its orbital variant are usually recorded in adults within the ages of 24 to 72 years.[17,18]

FIGURE 4. Temporal muscle flap was laminated as another layer over the temporoparietal fascia flap to fill the orbital cavity after the muscle flap is tunneled under the intact skin (left side). On the right side, patient is seen at 3 months after the operation.

Solitary fibrous tumors or the orbit can be accompanied by decreased visual acuity along with impaired eye movements and a palpable mass.[16] Solitary fibrous tumors can arise anywhere within the orbit, including the intraconal or extraconal space, lacrimal gland fossa, lacrimal sac, and the eyelids.[19–22] Radiologic evaluation of orbital SFTs may reveal proptosis, compression of the extraocular muscles and lacrimal glands, displacement of the optic nerve, encasing of the eyeball, and bony changes within of the orbital wall.[16] The globe itself was enlarged in our case; however, there is no sign to identify from where exactly the tumor was originated. If the tumor would have been detected earlier, we would have an accurate information about the origin of the tumor.

The excised tumor in our case weighed 213 g with dimensions of $9.5 \times 7 \times 6$ cm. Although the mitotic rate was 7/10 HPF, cellularity was increased significantly in particular areas, along with significant atypia. Necrosis was noted in the central region of the tumor possibly due to ischemia. In a previous study, Blandamura et al[23] stated that tumors of $>$5 cm, showing hypercellularity, a mitotic rate $>$4/10 HPF and presence of necrosis, should be considered as potentially malignant. Based on this study, the tumor in our case was accounted as a malignant form of SFT.

Orbital SFTs, like SFTs elsewhere, are slow-growing tumors that follow an insidious and nonaggressive clinical course.[16] Solitary fibrous tumors originating within the orbit, are differentiated from other tumors of the orbital cavity by their histopathologic features and reactivity against specific immunohistochemical markers. Often the tumor is composed of a fibrocollagenous tissue. And orbital SFTs are nonencapsulated. Alternating hypocellular and hypercellular areas are present in SFTs[23] and are characterized by the proliferation of spindle-shaped cells arranged in fascicles in a patternless pattern[4] and have oval nuclei with finely dispersed chromatin.[23] They are composed of thick-walled, often branching vessels of variable size. The tumor cells are supported by a highly fibrous stroma showing hyalinized and keloidal collagen fibers, hemangiopericytoma-like vessels, myxoid change, and variable quantity of mast cells, mature adipocytes and multinucleated stromal cells.[13,14] Due to this variable histopathologic appearance, diagnosis of SFT cannot be made based on histopathology itself, and necessitates immunohistochemistry to confirm the diagnosis. Vimentin, CD34, CD99, Bcl-2, Ki-67 positivity, and specific muscle actin, smooth muscle actin, calponin, caldesmon, S-100 negativity is in favor of SFT diagnosis.[6] The case we report here is also diagnosed based on immunohistochemistry.

Benign fibrous histiocytoma, hemangiopericytoma, neurofibroma, solitary circumscribed neuroma, schwannoma, and giant cell angiofibroma must be remembered in the differential diagnosis of SFTs.[12,13] The patient demographics as well as the histopathologic and immunohistochemical features of giant cell angiofibromas and SFTs are quite similar.[3,24,25] In 2002, World Health Organization proposed that SFTs, giant cell angiofibromas and hemangiopericytomas to be considered as an interrelated group of neoplasms instead of different pathologic entities.[3,26]

In the management of SFT lesions, the treatment of choice is surgical excision of the tumor with wide margins with an objective of obtaining tumor-free margins. Incomplete excision of the tumor is considered as a predisposing factor for local recurrence.[23]

To the best of our knowledge, a SFT of the orbital region, originating from the globe itself, has never been reported in the literature until now. Reported orbital solitary fibrous tumors were originated from extraocular structures and caused proptosis, compression of the extraocular muscles and the lacrimal glands, displacement of the optic nerve, and encasing of the eyeball.[16]

© 2015 Mutaz B. Habal, MD

Copyright © 2015 Mutaz B. Habal, MD. Unauthorized reproduction of this article is prohibited.

This is probably the first case reporting that SFTs of orbital region may originate from and enlarge the globe itself.

REFERENCES

1. Klemperer P, Rabin CB. Primary neoplasm of the pleura: a report of 5 cases. *Arch Pathol* 1931;1:11–28
2. Guillou L, Fletcher JA, Fletcher CDM, et al. Extrapleural solitary fibrous tumour and haemangiompericytoma. In: Fletcher CDM, Unni KK, Mertens F, eds. *Pathology and Genetics of Tumors of Soft Tissue and Bone (WHO).* Lyon, France: IARC Press; 2002:86–90
3. Gengler C, Guillou L. Solitary fibrous tumour and haemangiopericytoma: evolution of a concept. *Histopathology* 2006;48:63–74
4. de Oliveira DH, Albuquerque AF, de Araujo Baretto MD, et al. Large solitary fibrous tumor of the oral cavity: report of a case. *Pathol Res Pract* 2014;210:1064–1067
5. Debs T, Kassir R, Amor IB, et al. Solitary fibrous tumor of the liver: report of two cases and review of the literature. *Int J Surg* 2014;12: 1291–1294
6. Carlos R, de Andrade BAB, Romanach MJ, et al. Solitary fibrous tumor of the upper lip: report of a pediatric case. *Int J Pediatr Otorhinolaryngol Extra* 2014;9:92–96
7. Lee JE, Hong HS, Chang KH, et al. Solitary fibrous tumor of the post-styloid parapharyngeal space. *Acta Radiol Short Rep* 2014;3:1–5
8. Polomsky M, Sines DT, Dutton JJ. Solitary fibrous tumor of the orbit with multiple cavities. *Ophthal Plast Reconstr Surg* 2013;29:117–119
9. Meyer TN, Matos BH, Oliviera LR, et al. Report of a case of solitary fibrous tumour of the orbit. *Oral Maxillofac Surg* 2013;17:225–227
10. Fama F, LeBouc Y, Barrande G, et al. Solitary fibrous tumor of the liver with IGF-II-related hyppoglycaemia. A case report. *Langenbecks Arch Surg* 2008;393:611–616
11. Novais P, Robles-Medranda C, Pannain VL, et al. Solitary fibrous liver tumor: is surgical approach the best option? *J Gastrointestin Liver Dis* 2010;19:81–84
12. Alawi F, Stratton D, Freedman PD. Solitary fibrous tumor of the oral soft tissues: a clinicopathologic and immunohistochemical study of 16 cases. *Am J Surg Pathol* 2001;25:900–910
13. O'Regan EM, Vanguri V, Allen CM, et al. Solitary fibrous tumor of the oral cavity: clinicopathologic and immunohistochemical study of 21 cases. *Head Neck Pathol* 2009;3:106–115
14. Jham BC, Salles JM, Soares JM, et al. Solitary fibrous tumour of the buccal mucosa: case report and review of the literature. *Br J Oral Maxillofac Surg* 2007;45:323–325
15. Vargas PA, Alves FA, Lopes MA, et al. Solitary fibrous tumour of the mouth: report of two cases involving the tongue and cheek. *Oral Dis* 2002;8:111–115
16. Yang BT, Wang YZ, Dong JY, et al. MRI study of solitary fibrous tumor in the orbit. *AJR Am J Roentgenol* 2012;199:506–511
17. Bernardini FP, de Concilis C, Schneider S, et al. Solitary fibrous tumor of the orbit: is it rare? Report of a case series and review of the literature. *Ophthalmology* 2003;110:1442–1448
18. Leoncini G, Maio V, Puccioni M, et al. Orbital solitary fibrous tumor: a case report and review of the literature. *Pathol Oncol Res* 2008;14:213–217
19. Scott IU, Tanenbaum M, Rubin D, et al. Solitary fibrous tumor of the lacrimal gland fossa. *Ophthalmology* 1996;103:1613–1618
20. Woo KI, Suh YL, Kim YD. Solitary fibrous tumor of the lacrimal sac. *Ophthal Plast Reconstr Surg* 1999;15:450–453
21. Krishnakumar S, Subramanian N, Mohan ER, et al. Solitary fibrous tumor of the orbit: a clinicopathologic study of six cases with review of the literature. *Surv Ophthalmol* 2003;48:544–554
22. Romer M, Bode B, Schuknecht B, et al. Solitary fibrous tumor of the orbit-two cases and a review of the literature. *Eur Arch Otorhinolaryngol* 2005;262:81–88
23. Blandamura S, Alaggio R, Bettini G, et al. Four cases of solitary fibrous tumor of the eye and orbit: one with sarcomatous transformation after radiotherapy and one in a 5-year-old child's eyelid. *J Clin Pathol* 2014;67:263–267
24. Rousseau A, Perez-Ordonez B, Jordan RC. Giant cell angiofibroma of the oral cavity: report of a new location for a rare tumor. *Oral Surg Oral Med Oral Pathol Oral Radiol Endod* 1999;88:581–585
25. Guillou L, Gebhard S, Coindre JM. Orbital and extraorbital giant cell angiofibroma: a giant cell-rich variant of solitary fibrous tumor? Clinicopathologic and immunohistochemical analysis of a series in favor of a unifying concept. *Am J Surg Pathol* 2000;24:971–979
26. Fletcher CD. The evolving classification of soft tissue tumours: an update based on the new WHO classification. *Histopathology* 2006;48: 3–12

Effect of Modified Fujita Technique Uvulopalatoplasty on Oxidative DNA Damage Levels in Patients With Obstructive Sleep Apnea Syndrome

Ebubekir Bakan, PhD, Vural Fidan, MD,† Hamit Hakan Alp, MD,‡ Nurcan Kilic Baygutalp, MD,* and Erdem Cokluk, MD‡*

Abstract: Snoring is a social hindrance problem and it can cause life threatening problems. Because of this it must be taken seriously and must be treated. Although there are many ways for treating this problem, still uvulopalatopharngoplasty (UPPP) which is an accepted classical method maintains its importance. Antioxidant status in patients with snoring have been investigated. All studies investigated the effect of CPAP treatment on the level of antioxidant agents. In this study we have examined the effect of UPPP on the level of antioxidant agents in patients with snoring.

Key Words: 8-OHdG, CBAP, DNA oxidation, lipid peroxidation, obstructive sleep apnea, oxidative stresses, UPPP

Snoring is a social problem affecting about one-fourth of the adult population,[1] which in addition results in obstructive sleep apnea (OSA) associated with high morbidity and mortality rates.[2] OSA is a syndrome that has characteristic upper airway obstruction and a decrease in blood oxygen saturation as sleeping.[2] Obstructive sleep apnea syndrome (OSAS) was first described by Willaim Hill in 1889.[1] The severity of apnea is defined with apnea–hypopnea index (AHI). AHI is the total number of apnetic and hypoapnetic sections per sleep-hour.[3] The OSAS severity can be divided into 3 categories: mild (AHI = 5–15), moderate (AHI = 15–30), and severe (AHI >30), and the value higher than 11 has been defined

From the *Department of Medical Biochemistry, Faculty of Medicine, Ataturk University, Erzurum; †Department of Otolaryngology, Eskişehir Yunus Emre State Hospital, Eskişehir; and ‡Department of Medical Biochemistry, Faculty of Medicine, Yuzuncu Yil University, Van, Turkey.

Received October 24, 2014.
Accepted for publication April 4, 2015.

Address correspondence and reprint requests to Hamit Hakan Alp, Department of Medical Biochemistry, Faculty of Medicine, Yuzuncu Yil University, 65100 Van, Turkey. E-mail: hamithakanalp@gmail.com

Clinical trials.gov identifier: NCT01635699
The authors report no conflicts of interest.

Copyright © 2015 by Mutaz B. Habal, MD

ISSN: 1049-2275
DOI: 10.1097/SCS.0000000000001870

Copyright © 2015 Mutaz B. Habal, MD. Unauthorized reproduction of this article is prohibited.

as cardiovascular risk factor.[4] Prevalence of OSAS alters between 1% and 10% of population and it affects men more than women.[5] Several therapy strategies may be traced, including 2 main categories. "Conservative therapy"—First aim of this therapy must be to reduce the risk factors such as cigarette, alcohol, overweight, and position during sleep.[6] Medications with drugs such as protriptilin and triptofan could be tried.[7] Mandibula repositioning or tongue retaining devices, nasal continuous positive airway pressure (CPAP), and bilevel positive airway pressure can be usefull.[8,9] "Surgical therapy"—Patients who are refractory to conservative therapy require some surgical approaches such as uvulopalatopharngoplasty (UPPP), laser-assisted uvulopalatoplasty (LAUP), tracheotomy, midline partial glossectomy, hyoid suspension, and nasal surgery.

Nocturnal obstruction of the upper airway in OSAS results in a marked decrease in arterial oxygen saturation, which rapidly normalizes after ventilation resumes. Although several mechanisms are involved, such fluctuations in oxygene saturation produce the reactive oxygen species (ROS).[10] ROS are highly reactive molecules that interact with nucleic acids, lipids, and proteins and are considered to have an increased DNA oxydation, giving rise to cytotoxic tissue damage. Lipid peroxidation caused by ROS results in several unstable, decomposed compounds, with the most important one being malondialdehyde (MDA), a good indicative of lipid peroxidation.[11] On the other hand, ROS are closely associated with DNA break and base modification. For this reason, the usage of any marker of DNA oxidation, such as 8-hydroxy-2 -deoxyguanosine [8-OHdG], to assess oxidative stress is of significance.[12]

It is well established that oxidative stress is correlated with OSAS, since the oxidative damage markers have been found high in this condition.[10,13] Although antioxidant levels were higher in patients with OSA than normal population, there is no report, as far as we are concerned, about the effect of UPPP on antioxidant status in patients with OSAS.

We performed the present study to confirm whether there is a relationship between the OSAS and serum MDA and leukocyte 8-OHdG levels before and after UPPP.

MATERIALS AND METHODS

The patients who underwent UPPP for OSAS between June 2008 and March 2011 at the otolaryngology department of our hospital were included in this study. The total number of the patients was 49 (29 male, age range being 34–58 years). All of the patients had snoring, daytime sleepiness, nasal obstruction, and apnea symptoms, indicating OSAS. All patients consented to participate in the study after being informed of the known benefits, risks, and complications of the procedure.

For all patients, an initial pretreatment evaluation was made, including a systematic clinical examination, muller maneuver, nasal, nasopharyngeal, pharyngeal and hypopharyngeal endoscopy, paranasal and nasopharyngeal computed tomography, acoustic rhinomanometry, and baseline diagnostic polysomnography. All patients had normal nasopharyngeal computed tomography, and only septal deviation on paranasal computed tomography was detected. All patients had minimally 10 or more AHI and more than 10 points at the epworth sleepiness scale. All the patients had OSAS and no chronic diseases such as diabetes mellitus, hypertension.

In preoperative period and 3 months after operation (UPPP application), AHI, sleepiness scala, body mass index (BMI), and O_2 saturation were recorded, and in both periods (pre- and postoperative) the blood samples were collected (2 mL serum for MDA determination, 3 mL whole blood for 8-OHdG/dG measurement). All samples were kept at -80°C up to test day.

Biochemical Analyses

DNA Isolation and Hydrolization

DNA isolation from leukocytes was made by the method of Miller and coworkers[14] and Adeli and coworkwers[15] after some modifications. For this purpose, 2 mL of whole blood (with ethylenediamine teraacetic acid (EDTA)) was mixed well with erythrocyte lysis solution, and the mixture was kept at $+4^{\circ}$C for 5 minutes. Then, it was centrifuged at 3500 rpm for 5 minutes. The resultant supernatant was discharged, and to the gray pellet at the bottom was added 0.1 mL of sodium dodesyl sulfate (10%), 40 μL of proteinase K, and 1.9 mL of WBC lysis solution, and the mixture was kept at 65°C for 1 hour. Following the last incubation, to the tube was added 0.8 mL of 9.5 M ammonium acetate, and the well-mixed tube was centrifuged at 3500 rpm for 25 minutes. Two milliliter from the supernatant was transferred into a steril tube carefully, and to this content was added 4 mL of 99% ethyl alcohol. The tube was stoppered immediately and mixed gently. The precipitated DNA was taken by means of a pipette tip. The condensed DNA was hydrolyzed by Kaur and coworkers' method. The hydrolyzed DNA was treated with 0.5 mL of formic acid (%60), and the tube was incubated at 150°C for 1 hour.[16]

HPLC Analysis of 8-OHdG and dG

For the high-pressure liquid chromatographic (HPLC) analysis, Agilent 1100 modular system was used.[17] The system included isogratic pump, autosampler, coloumn oven, RP-C18 coloumn (250 mm × 4.6 mm × 4.0 mm; Phenomenex, CA), electrochemical detector (ECD), and UV detector, with the latter being parallelly bound to the ECD. One milliliter of hydrolyzed DNA was used for HPLC analysis. Acetonitril-water (93:3, v/v) mixture stabilized with 0.5 M phosphate buffer was used as a mobile phase. The results obtained were mentioned as 8-OHdG/10^6dG.[18] The chromatographic conditions were as follows.

Pressure: 115 ± 10 bar
Injection volume: 100 μL
Coloumn oven: 32°C ECD: 600 mV UV: 245 nm

Serum MDA Analysis

Serum MDA analysis was executed by HPLC as defined by Khoschsorur et al[19] using fluorescence detector (HPLC-FLD). For this purpose, 50 μL of serum was mixed with 0.44 M H_3PO_4 and 42 mM thiobarbituric acit (TBA), and the mixture was incubated in boiling water bath for 30 minutes. Once incubation was ended, the tube was immediately cooled and was gently mixed after adding the same volume of alkaline methyl alcohol as the tube content. The resultant mixture was centrifuged at 3000 g for 3 minutes. The supernatant was removed by means of a pipette, from which

TABLE 1. The Comparison of Pre- and Postoperative Nonexperimental Characteristics of the Patients With OSAS

	Before UPPP N = 49	After UPPP N = 49
Age	46.08 ± 7.16	46.08 ± 7.16
Sex		
Male	29	29
Female	13	13
BMI	27.8 ± 3.6	26.9 ± 4.1
AHI	45.44 ± 12.51*	17.16 ± 12.51*
O_2 saturation (%)	79.32 ± 10.41*	88.1 ± 9.11*

OSAS = obstructive sleep apnea syndrome; UPPP = uvulopalatopharngoplasty.
*Statistically significant difference at the order of $P < 0.01$.

© 2015 Mutaz B. Habal, MD

Copyright © 2015 Mutaz B. Habal, MD. Unauthorized reproduction of this article is prohibited.

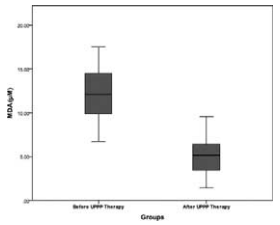

FIGURE 1. Pre- and postoperative MDA levels.

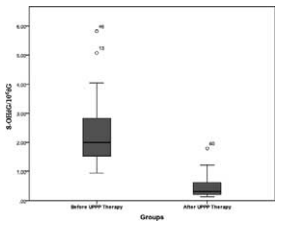

FIGURE 2. Pre- and postoperative 8-OHdG/10^6 dG levels.

100 μL was applied to HPLC-FLD system. The results were given in μmol. The chromatographic conditions were as follows.

Pressure: 75 ± 10 bar
FLD: Excitation 527 nm, emission 551 nm
Injection volume: 20 μL
Flow rate: 0.8 mL/min
Mobile phase: Methanol/50 nM KH_2PO_4 (40:60, v/v)
Coloumn: RP-C18 (5 μm, 4.6 × 160 mm, Eclipse VDB-C18 Agilent)

Statistical Analysis

IBM SPSS 19.0 was used for statistical analysis. Sample T-test was used, and $P < 0.05$ was considered statistically significant.

Findings

Three months after operation, epworth sleepiness scale was repeated, and 64.7% of patients had less than 10 points. While the AHI of patients were observed preoperatively as 10–93 and O_2 saturation as 60–93 %, the respective values were 2–35 and 69–98 at postoperative period. In other words, postoperative AHI gain was 54% (Table 1). Preoperatively, 7 patients had polyuria, while 2 patients had polyuria in postoperative phase. Preoperatively, 6 patients had sexual dysfunction, while 2 patients had sexual dysfunction in postoperative phase (Figs. 1–2).

The difference between the pre- and postoperative levels of MDA and 8-OHdG/10^6dG was statistically significant ($P < 0.05$), and it is shown in Table 2. Correlation analyses showed that statistically significant positive correlations were present between MDA and 8-OHdG/10^6dG and between MDA and AHI, and a statistically significant positive correlation between MDA and O_2 saturation ($R = 0.609$, $P < 0.01$; $R = 0.585$, $P < 0.01$; $R = -0.471$, $P < 0.05$, respectively). They are all shown in Figure 5, Figure 4 and Figure 7, respectively. On the other hand, a statistically significant negative correlation was found between 8-OHdG/10^6dG and AHI ($R = 0.359$, $P < 0.01$), and statistically significant negative correlation between 8-OHdG/10^6dG and O_2 saturation ($R = -0.241$, $P < 0.05$), and a statistically significant negative correlation was present between AHI and O_2 saturation ($R = -0.883$, $P < 0.01$) (Figs. 3 and 6).

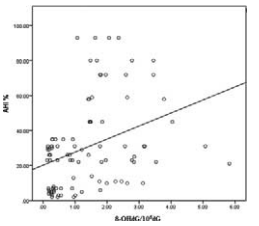

FIGURE 3. Correlation between 8-OhdG/10^6 dG and AHI levels.

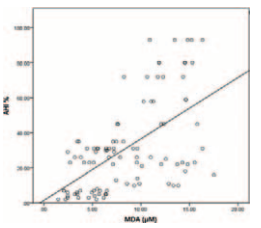

FIGURE 4. Correlation between MDA and AHI levels.

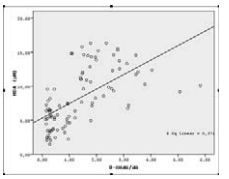

FIGURE 5. Correlation between MDA and 8-OhdG/10^6 dG levels.

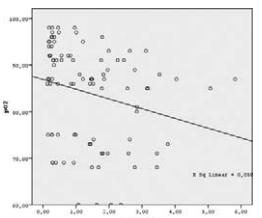

FIGURE 6. Correlation between pO_2 and 8-OhdG/10^6 dG levels.

TABLE 2. The Comparison of Pre- and Postoperative MDA and 8-OHdG/10^6dG Levels of the Patients With OSAS

		%95 CI of Means			%95 CI of Means	
	MDA (μM) Mean ± SD	Low	High	8-OHdG/10^6dG Mean ± SD	Low	High
Before UPPP (N = 49)	12.05 ± 2.85*	11.23	12.87	2.35 ± 1.03*	2.04	2.65
After UPPP (N = 49)	4.94 ± 1.96*	4.38	12.87	0.48 ± 0.36*	0.37	0.58

%95 CI (confidence interval). OSAS = obstructive sleep apnea syndrome; SD = standard deviation; UPPP = uvulopalatopharngoplasty.
*Statistically significant difference at the order of $P < 0.05$.

© 2015 Mutaz B. Habal, MD

Copyright © 2015 Mutaz B. Habal, MD. Unauthorized reproduction of this article is prohibited.

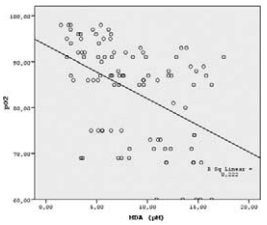

FIGURE 7. Correlation between pO_2 and MDA levels.

DISCUSSION

The present study was planned to investigate the possible effect of UPPP, used for OSAS therapy, on oxidative damage. There are several therapeutic modalities for OSAS. UPPP was first defined and applied by Ikematsu in 1964, and it was modified in 1981 by Fujita and coworkers.[20] In 1964, Ikematsu performed partial palatectomy and uvulectomy with mucousal resection of posterior plica. The author reported his results and his success rate was 81.6% with 152 patients.[21] In 1981, Fujita and coworkers performed UPPP for 66 patients and their success rate was 94% (improvement in snoring) and 50% in AHI (reduction of it).[20] As the UPPP was modified in the following years, the success increased. For instance, Fairbanks modified Fujita technique and performed for 43 patients. A success of 84% in snoring was obtained.[22] Surgeons can determine the success of operation only in postoperative 6th to 8th weeks. The success of UPPP in patients with severe OSAS has been reported to be low.[23,24]

UPPP is not a lonely applicable modality for OSAS. However, it can be performed in combination with other approaches.[25] The selection of the patient and postoperative follow-up are very critical for UPPP success.[26–28] We selected the patients for UPPP for whom we estimated that that approach would be successful, and we made a good, close follow-up for patient satisfaction. In addition, complication is an undesired situation in operations. Since in OSAS continuous positive airflow pressure (CPAP) is maintained, an increased ROS production is inevitable.[29,30]

ROS are produced in all aerobic cells. However, if an overproduction occurs and it becomes over antioxidant capacity, biomolecules such as DNA, lipids, proteins, and carbohydrates are oxidized, resulting in damage caused by this oxidative stress. ROS produce lipid hydroperoxides affecting polyunsaturated fatty acids. The breakdown of these hydroperoxides yields aldehyde groups, of which the majority is MDA. It is used as a marker for lipid peroxidation.[31] Several methods may be used for MDA determination, with the common one being spectrophotometric method based on the colored complex with TBA.[32] We measured MDA by the HPLC method, including FLD instead of UV detector because many studies are preset showing that the HPLC-FLD method is more reliable.[33,34]

It is well known that ROS are effective on the DNA. The base modification is the most important one. A well-known base modification is oxidation of D-guanosine residue to 8-OGdG, which is a good marker for DNA oxidation.[35] This oxidation product can be determined in body fluids such as serum and urine. Serum or urine 8-OGdG measurement can show the oxidative DNA damage. However, the determination of the oxidation on DNA molecule itself (not free ones) is more important. For this reason, in the present study, after we isolated DNA from leukocytes and hydrolyzed it with acid, 8-OGdG has been determined in that material. Although there are some disadvantages of acid hydrolysis, it is simply applied when compared to enzyme hydrolysis. In addition, during enzymatic hydrolysis, there may be some other oxidations due to pH changes, which may affect 8-OHdG measurement.[36] It is also well known that HPLC-ECD is the most convenient method for 8-OHdG measurement.[36]

It has been reported that ROS increase in patients with OSAS and that lipid peroxidation increases, resulting in decrease in antioxidant enzyme capacity.[37–39] The reverse reports are also present.[40] On the other hand, the majority of OSAS therapies are focused on pre- and postoperative CPAP treatment. Several studies have mentioned that CPAP treatment of OSAS patients may decrease the oxidative damage.[41]

Our results show that the preoperative MDA levels are higher than those in postoperative period ($P < 0.01$), which exhibits that UPPP decreases lipid peroxidation. Similarly, that the preoperative 8-OHdG levels are higher than those in postoperative period ($P < 0.01$) can be considered as lowering effect of UPPP on the DNA oxidative damage due to ROS. The significant positive correlation between AHI and DNA oxidation and between AHI and MDA ($P < 0.01$ for both) is also important with respect to our approach.

We can conclude from the results obtained that the patients with OSAS have high lipid peroxidation and oxidative DNA damage and that they have decreased AHI, increased O_2 saturation, and improvement in their snoring and sleeping when UPPP is carried out for the therapy. UPPP decreases both DNA oxidation and lipid peroxidation as well.

REFERENCES

1. Lugaresi E, Cirignotta F, Coccagna G, et al. Some epidemiological data on snoring and cardiocirculatory disturbances. *Sleep* 1980;3:221–224
2. Berry B. The International Classification of Sleep Disorders Manuel. 2nd ed. Lawrence, KS: Allen Press; 1991
3. Han S, Kern RC. Laser-assisted uvulopalatoplasty in the management of snoring and obstructive sleep apnea syndrome [review]. *Minerva Med* 2004;95:337–345
4. Shahar E, Whitney CW, Redline S, et al. Sleep-disordered breathing and cardiovascular disease: cross-sectional results of the Sleep Heart Health Study. *Am J Resp Crit Care* 2001;163:19–25
5. Young T, Palta M, Dempsey J, et al. The occurrence of sleep-disordered breathing among middle-aged adults. *N Engl J Med* 1993;328:1230–1235
6. Cartwright RD, Samelson CF. The effects of a nonsurgical treatment for obstructive sleep apnea. The tongue-retaining device. *JAMA* 1982;248:705–709
7. Smith PL, Haponik EF, Allen RP, et al. The effects of protriptyline in sleep-disordered breathing. *Am Rev Respir Dis* 1983;127:8–13
8. Clark GT, Blumenfeld I, Yoffe N, et al. A crossover study comparing the efficacy of continuous positive airway pressure with anterior mandibular positioning devices on patients with obstructive sleep apnea. *Chest* 1996;109:1477–1483
9. Ferguson KA, Ono T, Lowe AA, et al. A randomized crossover study of an oral appliance vs nasal-continuous positive airway pressure in the treatment of mild-moderate obstructive sleep apnea. *Chest* 1996;109:1269–1275
10. Yamauchi M, Nakano H, Maekawa J, et al. Oxidative stress in obstructive sleep apnea. *Chest* 2005;127:1674–1679
11. Esterbauer H, Schaur RJ, Zollner H. Chemistry and biochemistry of 4-hydroxynonenal, malonaldehyde and related aldehydes. *Free Radic Biol Med* 1991;11:81–128
12. Loft S, Fischernielsen A, Jeding IB, et al. 8-Hydroxydeoxyguanosine as a urinary biomarker of oxidative DNA-damage. *J Toxicol Env Health* 1993;40:391–404
13. Lavie L. Obstructive sleep apnoea syndrome: an oxidative stress disorder. *Sleep Med Rev* 2003;7:35–51
14. Miller SA, Dykes DD, Polesky HF. A simple salting out procedure for extracting DNA from human nucleated cells. *Nucleic Acids Res* 1988;16:1215
15. Adeli K, Ogbonna G. Rapid purification of human DNA from whole blood for potential application in clinical chemistry laboratories. *Clin Chem* 1990;36:261–264

© 2015 Mutaz B. Habal, MD

Copyright © 2015 Mutaz B. Habal, MD. Unauthorized reproduction of this article is prohibited.

16. Kaur H, Halliwell B. Measurement of oxidized and methylated DNA bases by HPLC with electrochemical detection. *Biochem J* 1996;318 (Pt 1):21–23
17. Armstrong D. Free Radical and Antioxidant Protocols. Totowa, NY: Human Press; 1998
18. Kasai H. Analysis of a form of oxidative DNA damage, 8-hydroxy-2 '-deoxyguanosine, as a marker of cellular oxidative stress during carcinogenesis. *Mutat Res Rev Mutat* 1997;387:147–163
19. Khoschsorur GA, Winklhofer-Roob BM, Rabl H, et al. Evaluation of a sensitive HPLC method for the determination of malondialdehyde, and application of the method to different biological materials. *Chromatographia* 2000;52:181–184
20. Fujita S, CW, Zurick F. Surgical correction of anatomic abnormalities in OSA UPPP. *Otolaryngol Head Neck Surg* 1984;89:923–924
21. Fujita S, Conway WA, Zorick FJ, et al. Evaluation of the effectiveness of uvulopalatopharyngoplasty. *Laryngoscope* 1985;95:70–74
22. Fairbanks DN. Snoring: surgical vs. nonsurgical management [comparative study]. *Laryngoscope* 1984;94:1188–1192
23. Utley DS, Shin EJ, Clerk AA, et al. A cost-effective and rational surgical approach to patients with snoring, upper airway resistance syndrome, or obstructive sleep apnea syndrome. *Laryngoscope* 1997;107:726–734
24. Zohar Y, Finkelstein Y, Talmi YP, et al. Uvulopalatopharyngoplasty: evaluation of postoperative complications, sequelae, and results [comparative study]. *Laryngoscope* 1991;101 (7 Pt 1):775–779
25. Fukuda N, Abe T, Katagiri M, et al. Effects of uvulopalatopharyngoplasty on patients with obstructive sleep apnea: the severity of preoperative tonsillar hypertrophy. *Nihon Kokyuki Gakkai Zasshi* 1998;36:34–40
26. Rodenstein DO. Assessment of uvulopalatopharyngoplasty for the treatment of sleep apnea syndrome. *Sleep* 1992;15(6 Suppl):S56–62
27. Wetmore SJ, Scrima L, Snyderman NL, et al. Postoperative evaluation of sleep apnea after uvulopalatopharyngoplasty. *Laryngoscope* 1986;96:738–741
28. Shimada A, Konno A, Isono S. Long-term result after UPPP for OSAS by evaluation of nocturnal oxygenation [review]. *Nihon Rinsho* 2000;58:1681–1684
29. Alonso-Fernandez A, Garcia-Rio F, Arias MA, et al. Effects of CPAP on oxidative stress and nitrate efficiency in sleep apnoea: a randomised trial. *Thorax* 2009;64:581–586
30. de Lima AM, Franco CM, de Castro CM, et al. Effects of nasal continuous positive airway pressure treatment on oxidative stress and adiponectin levels in obese patients with obstructive sleep apnea. *Respiration* 2010;79:370–376
31. Gawel S, WM, Niedworok E, Wardas P. Malondialdehyde (MDA) as a lipid peroxidation marker. *Wiad Lek* 2004;57:453–455
32. Draper HHHM. Malondialdehyde determination as index of lipid peroxidation. *Methods Enzymol* 1990;186:421–431
33. Mendes R, Cardoso C, Pestana C. Measurement of malondialdehyde in fish: a comparison study between HPLC methods and the traditional spectrophotometric test. *Food Chem* 2009;112:1038–1045
34. Fenaille F, Mottier P, Turesky RJ, et al. Comparison of analytical techniques to quantify malondialdehyde in milk powders. *J Chromatogr A* 2001;921:237–245
35. Mecocci P, Macgarvey U, Kaufman AE, et al. Oxidative damage to mitochondrial-DNA shows marked age-dependent increases in human brain. *Ann Neurol* 1993;34:609–616
36. Shigenaga MK, Aboujaoude EN, Chen Q, et al. Assays of oxidative DNA-damage biomarkers 8-oxo-2'-deoxyguanosine and 8-oxoguanine in nuclear-DNA and biological-fluids by high-performance liquid-chromatography with electrochemical detection. *Method Enzymol* 1994;234:16–33
37. Dyugovskaya L, Lavie P, Lavie L. Increased adhesion molecules expression and production of reactive oxygen species in leukocytes of sleep apnea patients. *Am J Resp Crit Care* 2002;165:934–939
38. Barcelo AM, Barbe F, Vila M, et al. Abnormal lipid peroxidation in patients with sleep apnoeawith sleep apnoea. *Eur Respir J* 2000;16:644–647
39. Grebe M, Eisele HJ, Weissmann N, et al. Antioxidant vitamin C improves endothelial function in obstructive sleep apnea. *Am J Resp Crit Care* 2006;173:897–901
40. Svatikova A, Wolk R, Lerman LO, et al. Oxidative stress in obstructive sleep apnoea. *Eur Heart J* 2005;26:2435–2439
41. Singh TD, Patial K, Vijayan VK, et al. Oxidative stress and obstructive sleep apnoea syndrome. *Indian J Chest Dis Allied Sci* 2009;51:217–224

Comparison of the Effects of Low-Level Laser Therapy and Ozone Therapy on Bone Healing

Hilal Alan, PhD, DDS, Nigar Vardi, PhD,†*
Cem Özgür, PhD, DDS, Ahmet Hüseyin, PhD, DDS,‡*
Ümit Yolcu, PhD, DDS, and Derya Ozdemir Doğan, PhD, DDS§*

Abstract: This study aims to compare the effect of low-level laser therapy (LLLT) and ozone therapy on the bone healing. Thirty-six adult male Wistar albino rats were used for this study. Monocortical defects were shaped in right femur of all rats. Defects were filled with nano-hydroxyapatite graft. The animals were divided into 3 groups and each group was than divided into 2 subgroups. Then, LLLT with a diode laser was applied to the first group (G1), ozone therapy was applied to the second group (G2), and no treatment was applied to the third group as a control group (G3). Animals were sacrificed after 4th and 8th weeks and the sections were examined to evaluate the density of the inflammation, the formation of connective tissue, the osteogenic potential, and osteocalcin activity. As a result, there were no significant differences among the groups of 4 weeks in terms of new bone formation. In the immunohistochemical assessment, the number of osteocalcin-positive cells was higher in the laser group compared to the other group of 4 weeks; this difference was statistically significant in the LLLT and ozone groups ($P < 0.05$). Histomorphometric assessment showed that the new bone areas were higher in the LLLT and ozone groups; furthermore, there was a statistically significant difference in the LLLT in comparison with the control group at 8th week ($P < 0.05$). At the same time immunohistochemical assessment showed that osteocalcin-positive cells were considerably higher in G2 than G1 at 8th week ($P < 0.05$). The findings of this study may be the result of differences in the number of treatment sessions. Further studies are therefore needed to determine the optimal treatment modality.

Key Words: Bone healing, low-level laser therapy, ozone, rat

Bone loss can result from various surgical procedures, traumas, or pathologies, and the process of bone healing has been broadly studied.[1] Bone regeneration is an extremely complex

From the *Department of Oral and Maxillofacial Surgery, Faculty of Dentistry, Inonu University, Malatya, Turkey; †Department of Histology and Embriology, Faculty of Medicine, Inonu University, Malatya, Turkey; ‡Department of Oral and Maxillofacial Surgery, Faculty of Dentistry, Bezmialem Vakif University, Istanbul, Turkey; and §Department of Prostodontics, Faculty of Dentistry, Cumhuriyet University, Sivas, Turkey.

Received July 18, 2014.
Accepted for publication April 5, 2015.

Address correspondence and reprint requests to Hilal Alan, PhD, DDS, Department of Oral and Maxillofacial Surgery, Faculty of Dentistry, Inonu University, 44280, Malatya, Turkey;
E-mail: hilalturker@hotmail.com

This project was funded by the Scientific Research Council of Inonu University (2012–156).
The authors report no conflicts of interest.

Copyright © 2015 by Mutaz B. Habal, MD

ISSN: 1049-2275
DOI: 10.1097/SCS.0000000000001871

Copyright © 2015 Mutaz B. Habal, MD. Unauthorized reproduction of this article is prohibited.

period, which comprises multiple biological reactions, such as the synthesis of DNA and the action of a great number of cells and proteins.[2] To enhance bone repair, various practices have been recommended, including the use of various types of grafts, fibrins, membranes, ozone, and bisphosphonates; low-level laser therapy (LLLT); hyperbaric oxygen therapy; and ultrasound.[3–5]

The biological effects of lasers were first studied in 1967 by Inyushin; Mester then applied lasers to accelerate the healing of chronic ulcers, ushering in the laser therapy model in 1971.[6] Contrary to other light sources, lasers produce monochromatic, harmonic, and collimated electromagnetic radiation. These features provide lasers with unique applications.[7] Light is first absorbed by photoreceptors in the cells when a laser is applied to the tissue. When absorbed, biochemical reactions can be regulated and mitochondrial respiration can be stimulated, producing molecular oxygen and ATP.[8] The synthesis of DNA, RNA, and cell-cycle regulatory proteins can be enhanced by these reactions, thus promoting cell proliferation.[9] There have been several studies describing the use of LLLT to stimulate wound healing,[10,11] nerve regeneration,[12] and collagen synthesis.[13,14]

Ozone (O3) is a triatomic molecule, consisting of 3 oxygen atoms; whereas it usually presents as a gas, it has been used in both gaseous and aqueous forms for medical purposes and can be dissolved in either water or oil.[15] The use of ozone medically is owed to its antimicrobial, disinfectant, and healing properties. Ozone is commonly used in restorative dentistry, endodontic procedures, oral surgery, and periodontology.[16] It can also be used during various clinical procedures, such as the management of early carious lesions, ulcerations, and herpetic lesions of the oral mucosa; the sterilization of cavities, root canals, and periodontal pockets; and the cleaning of dentures.[17]

Many investigations have attempted to quantitatively evaluate the influence of LLLT and ozone on bone constitution, but comparisons of both treatments are rare. The objective of the present investigation was to compare the influence of ozone and LLLT on grafted bone healing at 2 different times postsurgery.

MATERIALS AND METHODS

Ethical Statement

This study's experimental protocols were approved by the Experimental Animal Ethics Committee of Inonu University School of Medicine (2013/A14).

Experimental Animals

In total, 36 adult male Wistar albino rats were used. Their body weights ranged from 240 to 260 g at the beginning of the experiments. The animals were kept in individual cages in a room with 12-h day/night cycles, an ambient temperature of 21°C, and ad libitum access to water and a standard laboratory pellet diet. All experimental procedures followed the guidelines of the Animal Care and Use Committee of the Inonu University Faculty of Medicine Experimental Animal Center.

Study Design and Experimental Procedures

The experiment was designed with 36 rats. Monocortical defects were made in the right femurs of all rats. The defects were filled with nanohydroxyapatite (Bego oss s inject, Bremen, Germany). The animals were divided into 3 groups, and each group was then divided into 2 subgroups. LLLT with a diode laser was used in the first group (G1), ozone therapy was used in the second group (G2), and no treatment was used in the third group (control, G3). Animals were sacrificed after the 4th and 8th weeks.

Surgical Procedures

To prevent the postoperative infection, all rats were given intramuscular amoxicillin (50 mg/kg), every 24 h for 4 days, starting 1 day before surgery. They were also given an analgesic, every 24 h for 3 days, starting immediately after surgery.

All surgical procedures were performed under sterile conditions. All animals were anesthetized preoperatively with an intramuscular injection of ketamine (Eczacibasi Ilac Sanayi, Istanbul, Turkey; 40 mg/kg body weight). The right femoral region of the animals was shaved and the cutaneous surface was disinfected with a topical povidone–iodine solution before the operation. An incision, approximately 3 cm in length, was made on the skin surface and muscle. A monocortical defect, $3 \times 6\,cm^2$ in size, was made on the superior lateral side of the femur with a trephine bur used at low speed under irrigation with saline. After preparing the defect, graft material (nanohydroxyapatite) was implanted into the bone defect. The soft tissues were then repositioned and sutured with 4–0 polyglycolic acid sutures. The animals remained under observation until their full recovery.

LLLT with a Diode Laser

LLLT (CHEESE Dental Laser System, DEN4A) was applied immediately after operation and was repeated 3 times per week (every other day) during the experimental time of 4 weeks (12 sessions). The gallium–aluminum–arsenide diode laser device operates in the near-infrared spectrum at a continuous wavelength of 810 nm and a power output of 0.3 w. A dose of $12\,J/cm^2$ was applied around the defect per session yielding a total treatment dose of $144\,J/cm^2$.

Ozone Treatment

The ozone application device was a portable ozone delivery system (OzoneDTA generator, APOZA, Taiwan). A topical ozone application protocol was performed using an ozone generator (OzoneDTA, Taiwan) on the day of surgery at 80% concentration (4th grade) via a 90-degree probe for a duration of 30 s (as suggested by the manufacturer).

Specimen Preparation

After a 4 to 8-week healing period, rats were sacrificed by an overdose of general anesthetic. A surgical burr was used to harvest the bone containing the experimental area from the animal's femur postmortem.

The samples, including the surgical sites, were fixed in 10% neutral-buffered formalin, decalcified in ethylenediaminetetraacetic acid and embedded in paraffin. Five micron-thick sections were stained with hematoxylin and eosin.

For immunohistochemical analysis, thick sections were placed on polylysine-coated slides. After rehydration, the samples were transferred into citrate buffer (pH 7.6) and heated in a microwave oven for 20 min. After cooling for 20 min to room temperature, the sections were washed with phosphate-buffered saline (PBS). Then sections were placed in 0.3% H_2O_2 for 7 min and then washed with PBS. Sections were incubated with primary rabbit polyclonal anti-osteocalcine (Thermo, USA) antibody for 30 min, rinsed in PBS, and incubated with biotinylated goat anti-polyvalent antibody for 10 min and streptavidin peroxidase for 10 min at room temperature. Staining was terminated with the addition of chromogen plus substrate for 15 min; slides were then counterstained with Mayer hematoxylin for 1 min, rinse in tap water, and dehydrated.

Histologic and Histomorphometric Analysis

The sections were examined using a Leica DFC 280 light microscope by a histopathologist blinded to the status of the

© 2015 Mutaz B. Habal, MD

Copyright © 2015 Mutaz B. Habal, MD. Unauthorized reproduction of this article is prohibited.

animals. Four qualitative variables were examined during histological analyses:

1. The density of inflammation around the defect area was assessed. Grade 0 (no inflammation), grade 1 (mild; presence of < 25% of inflammatory cells in the area), grade 2 (moderate; presence of 26%–50% inflammatory cells in the area), and grade 3 (severe; presence of >51–100% inflammatory cells in the area).
2. The formation of connective tissue in the defect area was investigated. Grade 0 (no connective tissue), grade 1 (mild; presence of <25% connective tissue deposition in the area), grade 2 (moderate; presence of 26%–50% connective tissue deposition in the area), and grade 3 (severe; presence of >51% connective tissue deposition in the area).
3. The osteogenic potential, that is, the ratio of the area of new bone formation to the area of the total defect, was calculated as a percentage.
4. An estimation of osteocalcin activity in the defect was made. Qsteocalcin-positive cells (osteocalcin is produced by osteoblasts and is often used as a marker for the bone formation process) were counted in the area of the defect. The mean number of osteocalcin-immunopositive cells was determined.

All analyses were performed using a Leica Q Win Image Analysis System (Leica Micros Imaging Solution Ltd, Cambridge, UK). Histological assessments were performed in 5 randomly selected sites for each specimen at × 40 magnification.

Statistical Analysis

Statistical analysis was carried out using the SPSS for Windows version 13.0 (SPSS Inc., Chicago, IL, USA) statistical program. All data are expressed as the median (min–max). Normality for continued variables in groups was determined by the Shapiro-Wilk test. The variables did not show a normal distribution ($P < 0.05$). Kruskal-Wallis and Mann–Whitney U tests were used for comparison of variables among the studied groups. A $P < 0.05$ was regarded significant.

RESULTS

Histomorphometric and Immunohistochemical Assessment

At the end of 4 weeks:

G1: the lowest amount of new bone was found in the laser group but the differences were not statistically significant. The graft material was observed as a spherical, calcified structure in various forms and sizes in the defect area. Moreover, the graft material was surrounded by connective tissue (Fig. 1A). Osteocalcin-positive cells were observed in the connective tissue and on the surface of bone particles (Fig. 1B). The number of osteocalcin-positive cells was higher in this group than in any other groups after 4 weeks.

G2: although the amount of new bone formation was greater than that in the laser group, the differences were not statistically significant ($P > 0.05$; Fig. 1C). The localization of osteocalcin-positive cells in G2 was similar to that in G1 (Fig. 1D).

G3: the greatest amount of new bone was found in this group after 4 weeks, but the differences were not statistically significant ($P > 0.05$). However, bone marrow and graft material were observed among the bone fragments. The histology of the graft material was completely different from the existing bone, so it was easily differentiated within the defect area (Fig. 1E). Osteocalcin-positive cells were seen in the bone marrow (Fig. 1F).

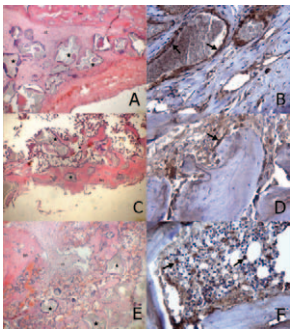

FIGURE 1. At the end of the 4th week: (A,B) laser group; (C,D) ozone group; (E,F) control group. bn:bone, ct: connective tissue, star: graft material, arrows: osteocalcin-positive cells. A,C,D: H-E X4; B,D,F: osteocalcin immune staining X40.

At the end of 8 weeks:

G1: the greatest amount of new bone formation was found in the laser group after 8 weeks. A great number of adipocytes and megakaryocytes in the bone marrow were observed (Fig. 2A). Moreover, hyaline cartilage and connective tissue were identified between the bone formation areas. Osteocalcin-positive cells were found in the bone marrow rather than on the surface of bone spicules (Fig. 2B).

G2: bone formation was similar to that observed in the laser group (Fig. 2C). In addition, statistically significant differences were not found in terms of connective tissue deposition or intensity of inflammation between the ozone and laser groups ($P > 0.05$). Osteocalcin-positive cells were higher in the ozone group than in the laser group ($P < 0.05$; Fig. 2D).

G3: the lowest amount of new bone formation was found in this group after 8 weeks (Fig. 2E). Many megakaryocytes were observed in the bone marrow. Osteocalcin-positive cells were identified on both the surfaces of bone spicules and in connective tissue (Fig. 2F).

Comparisons of new bone area among all groups are shown in Table 1. The intensity of inflammation and connective tissue deposition, and the number of osteocalcin-positive cells are shown in Table 2.

DISCUSSION

The present study examined and compared the impact of ozone and LLLT on bone tissue throughout the period of bone healing both histomorphologically and immunohistochemically. In this experimental work, we found that although the amount of new bone formation was greater in G2 than in G1, the difference was not statistically significant at early stages of regeneration (4 weeks after

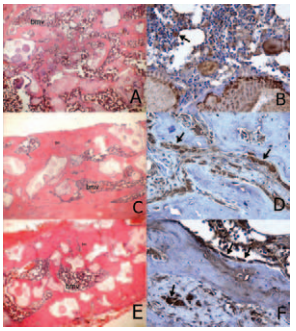

FIGURE 2. At the end of the 8th week: (A,B) laser group; (C,D) ozone group; (E,F) control group. bn:bone, ct: connective tissue, star: graft material, arrows: osteocalcin-positive cells. A,C,D: H-E X4; B,D,F: osteocalcin immune staining X40.

© 2015 Mutaz B. Habal, MD

Copyright © 2015 Mutaz B. Habal, MD. Unauthorized reproduction of this article is prohibited.

TABLE 1. Comparison of New Bone Area Among in all Groups (as a Percentage)

Groups/Time	New Bone Area	$P < 0.05$
4th week		
1. G1	14.7 (5.1–30.1)	(4) (5) (6)
2. G2	20.0 (17.4–25.7)	(4) (5)
3. G3	21.7 (17.0–30.0)	(4) (5)
8th week		
4. G1	37.0 (30.8–50.6)	(1) (2) (3) (6)
5. G2	34.6 (18.7–49.6)	(1) (2) (3)
6. G3	27.7 (0.0–36.6)	(1) (4)

surgery; $P > 0.05$). However, the amount of new bone formation was greater in both G1 and G2 compared with that in G3, but the only statistically significant difference was among G1 and G3 after 8 weeks with regard to new bone formation.

In this study, the Wistar rat experimental model was used because the animals are easily lodged and fed, they exhibit a rapid healing period, are a cost-effective model, and have been routinely utilized in other experimental studies[18] of bone regeneration.

Several types of bone graft materials exist to fill bone defects. Although autogenous grafts are the "criterion standard," they require substantial surgical time and are associated with donor site morbidity, which consists of hematoma formation, infection, and pain. Additionally, these grafts are frequently resorbed in large defects before osteogenesis is completed,[19] which has led to the development of various alternative graft materials.[20] Hydroxyapatite is the most investigated biomaterial both clinically and histologically, with regard to the process of bone healing.[21] Furthermore, nanohydroxyapatite bone grafts have been studied for the last 10 years. We thus chose a nanohydroxyapatite graft material to fill the defect areas.

Osteocalcin is an extracellular matrix protein synthesized and secreted via the process of osteoblastic differentiation and mineralization.[18] In our study, the number of osteocalcin-positive cells was higher in the ozone group than in the laser group at the end of 8 weeks.

Laser therapy is an effective, noninvasive stimulator of osteogenesis and osseointegration of graft materials, and may improve bone growth and functional recovery.[22] Results of our study are in line with those of other studies that have investigated bone regeneration in animals.[19,23] Ribeiro et al[24] used a gallium arsenide (GA–AS) laser (735 nm, 16J/cm^2) on grafted bones in the tibias of rats, observing improvements in bone repair with LLLT in the irradiated animals. However, other studies did not find any effects of LLLT on the repair of mineralized tissues.[22]

TABLE 2. Comparison of Intensity of Inflammation and Connective Tissue Deposition and Number of Osteocalcin-Positive Cells in all Groups

Groups/ Time	Intensity of Inflammation	Connective Tissue Deposition	Number of Osteocalcin
4th week			
1. G1	0.0 (0.0–2.0)	1.0 (0.0–3.0)	8.0 (3.0–17.0)
2. G2	1.2 (0.0–1.2)	0.0 (0.0–3.0)	5.7 (2.0–12.0)
3. G3	0.0 (0.0–2.0)	0.1 (0.0–3.0)	7.0 (2.0–25.0)
8th week			
4. G1	0.0 (0.0–1.0)	0.0 (0.0–3.0)	5.3 (0.0–12.0)
5. G2	0.0 (0.0–1.0)	0.0 (0.0–3.0)	9.0 (2.0–54.0)
6. G3	1.0 (0.0–3.0)	1.0 (0.0–3.0)	7.0 (1.0–26.0)
$P < 0.05$	2–3, 3–6, 2–5, 2–4	1–2, 1–3, 1–4, 1–5, 2–6, 4–6, 5–6	1–2, 1–4, 2–5, 4–5

The conflicting results of LLLT on biostimulation are primarily related to variations in radiation parameters.

To obtain excellent outcomes, the dose (frequency, dose, power, number of sessions, wavelength, and technique of applying) that is applied throughout the laser treatment is important.[20,25] There are controversial ideas about the ideal doses for LLLT: whereas some authors recommend a dose of 1 to 5 J/cm^2 to stimulate wound healing,[26] others argue that 16 J/cm^2 for each session more effectively increases the positive effects on bone metabolism.[27] In addition, others have suggested higher doses, so it is not yet possible to establish an ideal treatment protocol for lasers.[28,29] The LLLT dose for this study was chosen based on an earlier study regarding bone defect healing using an autogenous bone graft.[30]

Some studies were conducted daily for 1 to 2 weeks of LLLT. We chose to use 3 LLLT sessions/week to mimic the clinical treatment regimen. We can say that the dose for LLLT applied to the grafted bone in our protocol was sufficient to stimulate bone repair.

Systemic effects of LLLT have been defined by several authors.[31] Several growth factors and cytokines are released into the circulation after LLLT, which could affect the untreated side of an experimental animal.[19] We used different animals in the test and control groups to avoid bias owing to possible systemic effects of LLLT.

Ozone can have effects on oxygen metabolism, cell energy, antioxidant defenses, immunomodulation, and the vascular system.[32] As such, few authors have reported that ozone is beneficial for treating bone necrosis or areas of oral surgery in patients using drugs such as bisphosphonates, since they stimulate cell proliferation and soft tissue healing.[33]

Ozone can activate neutrophils and stimulate the synthesis of cytokines, leading to improvements in the immune system. In that way, ozone therapy positively affects the outcomes of some infectious diseases.

Ozone therapy can be applied via a range of methods, generally involving the mixing of ozone with a range of gases and liquids, and injecting these solutions into the body, including the vagina, rectum, muscle, and beneath the skin, or by autohemotherapy.[16] A few studies have applied ozone therapy during oral and maxillofacial surgery. Agrillo et al[33] cured 94 patients of bisphosphonate-related jaw osteonecrosis (BRONJ) and reported that if used twice weekly for 3 min, ozone therapy was effective. Petrucci et al[34] suggested that ozone therapy applied 15 days can successfully treat BRONJ. A separate study reported that ozone does not stimulate the osteoblastic activity of gingival cells during the regeneration of the periodontium around implants.[35] Ozone is known to have bactericidal and antioxidant characteristics, which might elucidate its positive effects on the healing process, enhancing wound healing and regulating the immune system. Ozdemir et al[5] investigated the impact of ozone therapy on bone defects treated with autogenous bone grafts in rats and reported improvements in bone regeneration and numbers of osteoblasts in autogenous bone. Kazancioglu et al[20] assessed the impact of LLLT and ozone on bone healing in rat calvaria. They formed critical size defects on 30 rat calvaria and separated the animals into 3 groups: a control group, an LLLT group, and an ozone therapy group. The authors sacrificed all the animals after 1 month. As a result of the study, they reported that the total area of new bone was significantly greater in the ozone group than in the control or LLLT groups. The differences between their study and our results may be because of the number of treatment sessions.

In conclusion, the present outcomes emphasize the stimulatory effects of laser and ozone therapies on the healing of grafted bone defects. However, there are no significant differences between ozone therapy and LLLT. The findings of this study may be the

© 2015 Mutaz B. Habal, MD

Copyright © 2015 Mutaz B. Habal, MD. Unauthorized reproduction of this article is prohibited.

result of differences in the number of treatment sessions. Further studies are therefore needed to determine the optimal treatment modality.

ACKNOWLEDGMENT

The authors thank Mr. Turgay Tastan for his kind assistance and support.

REFERENCES

1. Pinheiro ALB, Martinez Gerbi ME, Limeira FA, et al. Effect of low level laser therapy on the repair of bone defects grafted with inorganic bovine bone. *Braz Dent J* 2003;14:177–181
2. Sena K, Leven RM, Mazhar K, et al. Early gene response to low-intensity pulsed ultrasound in rat osteoblastic cells. *Ultrasound Med Biol* 2005;31:703–708
3. Ilgenli T, Dündar N, Kal BI, et al. Demineralized freeze-dried bone allograft and platelet-rich plasma vs platelet-rich plasma alone in infrabony defects: a clinical and radiographic evaluation. *Clin Oral Invest* 2007;11:51–59
4. Oliveira P, Sperandio E, Fernandes KR, et al. Comparison of the effects of low-level laser therapy and low-intensity pulsed ultrasound on the process of bone repair in the tibia. *Braz J Phys Ther* 2011;15:200–205
5. Ozdemir H, Toker H, Balcı H, et al. Effect of ozone therapy on autogenous bone graft healing in calvarial defects: a histologic and histometric study in rats. *J Periodont Res* 2013;48:722–726
6. Mester E, Spry T, Sender N, et al. Effect of laser ray on wound healing. *Amer J Surg* 1971;122:523–535
7. Deppe H, Horch HH. Laser applications in oral surgery and implant dentistry. *Lasers Med Sci* 2007;22:217–221
8. Kazem SS, Soleimanpour J, Salekzamani Y, et al. Effect of low-level laser therapy on the fracture healing process. *Lasers Med Sci* 2010;25:73–77
9. Renno AC, McDonnell PA, Parizotto NA, et al. The effects of laser irradiation on osteoblast and osteosarcoma cell proliferation and differentiation in vitro. *Photomed Laser Surg* 2007;25:275–280
10. Mester E, Mester AF, Mester A. The biomedical effects of laser application. *Lasers Surg Med* 1985;5:31–39
11. Luger EJ, Rochkind S, Wollman Y, et al. Effect of low-power laser irradiation on the mechanical properties of bone fracture healing in rats. *Lasers Surg Med* 1998;22:97–102
12. Anders JJ, Borke RC, Woolery SK, et al. Low power laser irradiation alters the rate of regeneration of the rat facial nerve. *Lasers Surg Med* 1993;13:72–82
13. Abergel RP, Meeker CA, Lam TS, et al. Control of connective tissue metabolism by lasers: recent developments and future prospects. *J Am Acad Dermatol* 1984;11:1142–1150
14. Bosatra M, Jucci A, Olliaro P, et al. In vitro fibroblast and dermis fibroblast activation by laser irradiation at low energy. An electron microscopic study. *Dermatologica* 1984;168:157–162
15. Bocci VA. Scientific and medical aspects of ozone therapy. State of the art. *Arch Med Res* 2006;37:425–435
16. Loncar B, Stipetic MM, Matosevic D, et al. Ozone application in dentistry. *Arch Med Res* 2009;40:136–137
17. Erdemci F, Gunaydin Y, Sencimen M, et al. Histomorphometric evaluation of the effect of systemic and topical ozone on alveolar bone healing following tooth extraction in rats. *Int J Oral Maxillofacial Surg* 2014;43:777–783
18. Loncar B, Mravak SM, Matosevic D, et al. Ozone application in dentistry. *Arch Med Res* 2009;40:136–137
19. Marques L, Holgado LA, Francischone LA, et al. New LLLT protocol to speed up the bone healing process—histometric and immunohistochemical analysis in rat calvarial bone defect. *Lasers Med Sci* 2014:1–6
20. Khadra M, Kasem N, Haanaes HR, et al. Enhancement of bone formation in rat calvarial bone defects using low-level laser therapy. *Oral Surg, Oral Med, Oral Pathol, Oral Radiol, and Endodontol* 2004;97:693–700
21. Obradović RR, Kesić LG, Pesevska S. Influence of low-level laser therapy on biomaterial osseointegration: a mini-review. *Lasers Med Sci* 2009;24:447–451
22. Guzzardella GA, Fini M, Torricelli P, et al. Laser stimulation on bone defect healing: an in vitro study. *Lasers Med Sci* 2002;17:216–220
23. Ribeiro DA, MAM. Low-level laser therapy improves bone repair in rats treated with anti-inflammatory drugs. *J Oral Rehab* 2008;35:925–933
24. Kazancioglu HO, Ezirganli S, Aydin MS. Effects of laser and ozone therapies on bone healing in the calvarial defects. *J Craniofac Surg* 2013;24:2141–2146
25. Barbosa D, de Souza RA, Xavier M, et al. Effects of low-level laser therapy (LLLT) on bone repair in rats: optical densitometry analysis. *Lasers Med Sci* 2013;28:651–656
26. Dörtbudak O, Haas R, Mailath-Pokorny G. Biostimulation of bone marrow cells with a diode soft laser. *Clinical Oral Implants Res* 2000;11:540–545
27. Saito S, Shimizu N. Stimulatory effects of low-power laser irradiation on bone regeneration in midpalatal suture during expansion in the rat. *Amer J Orthodontics Dentofacial Orthop* 1997;111:525–532
28. Fávaro-Pípi E, Feitosa SM, Ribeiro DA, et al. Comparative study of the effects of low-intensity pulsed ultrasound and low-level laser therapy on bone defects in tibias of rats. *Lasers Med Sci* 2010;25:727–732
29. Lirani-Galvão AP, Jorgetti V, da Silva OL. Comparative study of how low-level laser therapy and low-intensity pulsed ultrasound affect bone repair in rats. *Photomed Laser Surg* 2006;24:735–740
30. da Silva RV, Camilli JA. Repair of bone defects treated with autogenous bone graft and low-power laser. *J Craniofac Surg* 2006;17:297–301
31. Schindl A, Heinze G, Schindl M, et al. Systemic effects of low-intensity laser irradiation on skin microcirculation in patients with diabetic microangiopathy. *Microvasc Res* 2002;64:240–246
32. Azarpazhooh A, Limeback H. The application of ozone in dentistry: a systematic review of literature. *J Dent* 2008;36:104–116
33. Agrillo AM, Ungari C, Filiaci F, et al. Ozone therapy in the treatment of avascular bisphosphonate-related jaw osteonecrosis. *J Craniofac Surg* 2007;18:1071–1075
34. Petrucci MT, Gallucci C, Agrillo A, et al. Role of ozone therapy in the treatment of osteonecrosis of the jaws in multiple myeloma patients. *Haematologica* 2007;92:1289–1290
35. Matsumura K, Hyon SH, Nakajima N, et al. Effects on gingival cells of hydroxyapatite immobilized on poly(ethylene-*co*-vinyl alcohol). *J Biomed Mater Res* 2007;82:288–295

Split Cartilage Resection of Nasal Dome: A Solution to Ptotic Nasal Tips

Selahattin Tuğrul, MD, Remzi Doğan, MD,† Ilker Koçak, MD,‡ Sabri Baki Eren, MD,* and Orhan Ozturan, MD**

Objective: In ptotic noses, it is rather difficult to achieve the intended functional and cosmetic result without modifying the alar

From the *Faculty of Medicine, Department of Otorhinolaryngology, Bezmialem Vakif University, Fatih; †Department of Otorhinolaryngology, Bayrampasa State Hospital, Bayrampasa; and ‡Faculty of Medicine, Department of Otorhinolaryngology, Koç University, Fatih, Istanbul, Turkey.

Received August 6, 2014.
Accepted for publication April 5, 2015.

Address correspondence and reprint requests to Remzi Dogan, Department of Otorhinolaryngology, Bayrampasa State Hospital, Bayrampasa, Istanbul, Turkey; E-mail: dr.remzidogan@gmail.com

The authors report no conflict of interest.

Copyright © 2015 by Mutaz B. Habal, MD

ISSN: 1049-2275
DOI: 10.1097/SCS.0000000000001872

Copyright © 2015 Mutaz B. Habal, MD. Unauthorized reproduction of this article is prohibited.

cartilage and creating a new nasal tip. The split cartilage resection method was intended to create a new and permanent nasal tip to protect the physiologic and cosmetic appearance of the nose in the presence of long and ptotic nasal tip.

Method: A total of 53 patients who had nasal tip ptosis were included in the study: 26 patients (Group 1) who underwent lateral crural overlap because of the alar cartilage problem and 27 patients (Group 2) who underwent dome split cartilage resection. After at least 1 year of follow-up, the pre- and postoperative measurements of patients indicating their rotations and projections in their computerized images were compared and acoustic rhinometry was performed to determine the nasal valve function.

Results: There were no significant differences between the 2 groups with respect to the pre- and postoperative nasolabial angels, rotation angles, Goode index, and nasofacial angle. There were no significant differences between the nasal cavity volume values of the 2 groups; the volume increase in wide nasal cavity in Group 2 was higher. After the operation, the increase in minimum cross-sectional area values in Group 2 was significantly >1 in Group 1.

Conclusions: The nasal tip split resection method is a method that can be implemented and should be kept in mind as a technique, which must be considered as an alternative method for noses with ptotic and long nasal tip disorder.

Key Words: Cartilage resection, nasal tip, ptotic, split

The ptotic nasal tip means downward inclination of the tip of the nose and it is a disorder in which the nose becomes longer along with narrowed nasolabial angle.[1] In such noses, an esthetically undesirable appearance and an insufficiency in nasal functions are at stake. This situation becomes most visible as the patients say that they can breathe more comfortably when they raise their nostrils with their fingers.

The reasons behind ptotic nasal tip are primarily in 2 groups: the first group includes the intrinsic reasons and the second group includes the extrinsic reasons behind the nasal tip. Intrinsic reasons behind the nasal tip, which are accountable for the majority of such noses and are due to the abnormal cartilage structure, include extremely long lateral crura, vertically located and concave lateral crura, as well as short and weak medial crura. The extrinsic reasons include the nose being pushed or pulled to the inferior on account of externally effective forces in spite of the cartilage complex. These are long upper lateral cartilages, high anterior septal angle, overdeveloped caudal septum, thick and heavy nasal skin, extremely active depressor septi muscle, as well as increased nasal tip support due to old age and previous surgeries.[2] Most of these reasons enumerated for ptotic noses appear together; however, alar cartilage-related disorders constitute the great majority.

The correction of ptotic nasal tip depends on whether the underlying disorders are known and corrected. The objective is to recreate the alar cartilage tripod concept more cephalically.[3] For this purpose, it is necessary to make changes directly on the alar cartilage and to make some extrinsic interventions such as cropping the caudal ends of upper lateral cartilages, decreasing the anterior septal angle, and excising the caudal septal cartilage. In relation to the alar cartilages, techniques to modify the alar cartilages are implemented. The most frequently used techniques are known as the lateral crural steal (LCS),[4] lateral crural overlay (LCO),[5] and tongue in Groove (TIG) techniques.[6] In the LCS technique, a new type is created more laterally to the existing nasal dome; in the LCO technique, the lateral crux is incised, overlaid and sutured; and in the TIG technique, the medial crura are sutured to the caudal septum.

As ptotic noses frequently have asymmetry in addition to drooped nasal dome and weak cartilage, methods requiring resection are often needed. The main purpose of the split cartilage resection (SCR) method is to remove the weak part by performing a SCR in the nasal dome site and to create a new nasal tripod complex in a more cephalic position following reconstruction. It was considered that it would be more accurate to perform a comparison using especially the LCO method in which the alar cartilage is deconstructed and reconstructed to assess the results.

MATERIALS AND METHOD

A total of 53 patients in total made up of 26 LCO and 27 SCR patients, who had ptotic nasal tip due to long and deformed sites and were consequently operated, were included in the study.

The exclusion criteria were as follows: revision surgery, additional maxillofacial abnormalities, nonptotic septorhinoplasty patients, patients for whom no preoperative acoustic rhinometry measurements were taken, patients who were not preoperatively imaged, and patients who did not present to the follow-up in month 12 and tumor disorders.

To demonstrate the objective differences between pre- and postoperative (minimum 12 months) images, measurements identifying the nasal tip rotation and projection were made. To determine the nasal tip rotation, the nasolabial angle[7] and the tip rotation angle[8–10] were measured. The nasolabial angle is measured based on the intersection of the line between the columella point and subnasale and the line between the subnasale and labrale superior. As for the rotation angle, it is measured based on the intersection of the line between the tip and columella point and the line that is tangent to the columella. The nasal tip projection is calculated based on the measurement of the nasofacial angle and Goode index. The nasofacial angle is obtained as based on the intersection of the line between the glabella and pogonion and the line between the nasion and the tip. Finally, Goode index is obtained on the basis of the division of the distance between the alar point and the tip to the distance between the nasion and the tip.[7,9,11] Minimum 12 months after the operation, the nasal tip rotation and projection were reassessed and they were compared with the preoperative values.

To assess the nasal physiologic functions, all of the patients received acoustic rhinometry measurements before the operation and in month 12 at the earliest after the operation. Acoustic rhinometry (Acoustic Rhinometer A1; GM Instruments Ltd, Kilwinning, Scotland) was performed according to the standards established and prescribed by the standardization committee. For acoustic rhinometry, the patient was admitted into the room and allowed to rest for 15 minutes. A decongestant agent (Iliadin 0.05% 10 mL) was administered to both nasal cavities in 2 puffs. The patient was allowed to wait 15 minutes after the decongestant administration. An anatomic nose adaptor was applied for acoustic rhinometry. An ultrasound gel was used to protect against any potential leakage, if necessary. The patients were asked to hold their breath during the measurement. The mean value for the 3 curves was calculated. The unilateral minimum cross-sectional area (MCA) and unilateral nasal cavity volume was measured at 0 to 7 cm (volume of nasal cavity) away from the nostril.

Surgical Technique

All of the patients received surgery with open technique under general anesthesia. In nasal tip-related disorders, disorders of the alar cartilage can be viewed better, in an undistorted and natural fashion with the open technique rhinoplasty.[12] Thus, it is possible to perform the alar cartilage modification techniques under direct

© 2015 Mutaz B. Habal, MD

Copyright © 2015 Mutaz B. Habal, MD. Unauthorized reproduction of this article is prohibited.

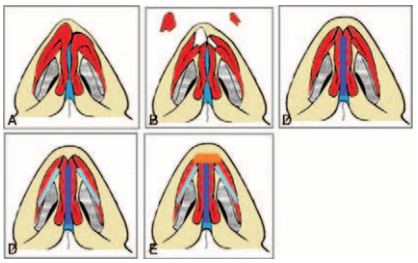

FIGURE 1. Split Cartilage Resection techniques: animation surgical steps.

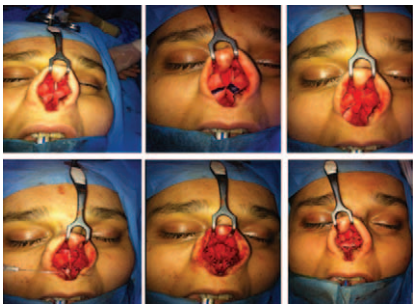

FIGURE 2. Split Cartilage Resection techniques: perioperative surgical steps.

visualization and in such a way that the results can be seen more precisely. For the external rhinoplasty incision, the bilateral alar marginal incisions were connected by a V-shaped transcolumellar incision at the beginning of the operation. The columellar skin flap was elevated from the medial crura, the operation was continued along the supraperichondrial avascular plane with subperiostal elevation on the dorsum until the radix. The dorsum-related modifications and osteotomies were defined before switching to the nasal tip surgery. For patients who needed it, the ULC caudal tip and scroll area were resected. Before any interventions on the alar cartilages, the length and concavity of the cartilages, curvatures of the tip, weakness or curvatures of the medial crura were examined (Fig. 1A). Then, cephalic resections were performed with 6 to 8 mm left from the alar cartilages. A strong columellar strut (Power cartilage septum) was placed (Fig. 1C). Infiltration was performed on the vestibule skin to which the alar cartilages were attached and the vestibule skin, that is, the underside of the lateral part of the cartilage, was elevated up to the medial crura. The parts to be excised from the nasal dome were marked and removed; their ends were equalized and primarily sutured (Fig. 1B). The prepared lateral crural struts were placed under the previously elevated alar cartilage lateral part and they were sutured with the vestibule skin (Fig. 1D). After the dome-equalizing sutures were removed, the cartilage parts removed via cephalic resection were placed on the newly created dome as both camouflage and tip grafts (Fig. 1E). Then, the conventional rhinoplasty stages were followed through to ensure appropriate closure. Split cartilage resection techniques-preoperative surgical steps (Fig. 2).

Statistical Analysis

Statistical analysis was carried out using the Statistical Package for the Social Sciences version 13.0 software for Windows (SPSS Inc, Chicago, IL). All of the quantitative variables were estimated using measures of central location (ie, mean and median) and measures of dispersion (ie, standard deviation [SD]). Data normality was checked using the Kolmogorov-Smirnov tests of normality.

The independent samples *t*-test was used to compare data among groups. For the pre- and postoperative comparisons of groups in themselves, the paired samples *t*-test was used. For the age distribution of the groups, the Kruskal-Wallis test was used and for the comparison of sex distribution, the chi-square test was used. $P < 0.05$ was considered as the level of significance.

RESULTS

A total of 53 (29 men, 14 women) people with low-nose deformity were included in the study. There are no significant differences between Group 1 (LCO) (n = 26, 17 men, 9 women, 26.08 ± 5.27 years) and group 2 (SCR) (n = 26, 12 men, 5 women, 27.14 ± 6.09 years) in terms of the number of patients, sex, and age ($P < 0.05$). The pre- and postoperative (mean value 13.35 ± 1.08 months) images of the patients were compared; the nasolabial angles and rotation angles were calculated and compared to identify the nasal tip rotation. The nasal tip projection was assessed on the basis of nasofacial angle and Goode index. To assess the nasal valve and nasal value, acoustic rhinometric measurements were taken.

Effects on Nasal Tip Rotation

There are no significant differences between the 2 groups with respect to the pre- and postoperative nasolabial and rotation angles ($P > 0.05$) (Table 1). Both groups had significant increases in the nasolabial and rotation angles following the operation as compared with the preoperative status ($P < 0.05$) (Fig. 3). There are no significant differences between the 2 groups with respect to the nasolabial and rotation angles (pre- and postoperative) ($P > 0.05$) (Fig. 4).

Effects on Nasal Tip Projection

There are no significant differences between the 2 groups with respect to the pre- and postoperative Goode index and nasofacial angle values ($P > 0.05$) (Table 1). Both groups had significant

TABLE 1. Effect of Lateral Crural Overlap and Split Cartilage Resection Techniques on the Nasal Tip

Technique		LCO (n = 26) Mean ± SD	SCR (n = 27) Mean ± SD	Student's paired *t*-test
Nazolabial angle	Preoperative	84.15 ± 3.24	83.23 ± 2.92	$P = 0.597^*$
	Postoperative	101.04 ± 3.29	102.78 ± 4.94	$P = 0.428^*$
Rotation angle	Preoperative	43.07 ± 2.99	43.58 ± 3.04	$P = 0.376^*$
	Postoperative	57.53 ± 2.48	58.96 ± 2.24	$P = 0.645^*$
Goode ratio	Preoperative	0.52 ± 0.54	0.54 ± 0.47	$P = 0.734^*$
	Postoperative	0.57 ± 0.39	0.61 ± 0.38	$P = 0.872^*$
Nazofacial angle	Preoperative	31.25 ± 3.24	31.61 ± 1.19	$P = 0.143^*$
	Postoperative	33.73 ± 3.47	34.85 ± 2.44	$P = 0.165^*$

LCO, lateral crural overlap; SCR, slip cartilage resection.
* $P > 0.05$.

© 2015 Mutaz B. Habal, MD
Copyright © 2015 Mutaz B. Habal, MD. Unauthorized reproduction of this article is prohibited.

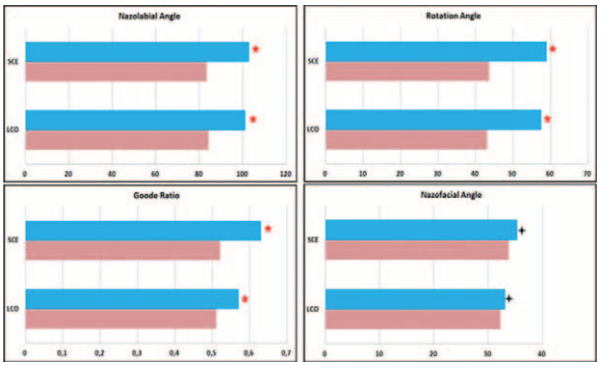

FIGURE 3. Rhinological assessments of groups within themselves.

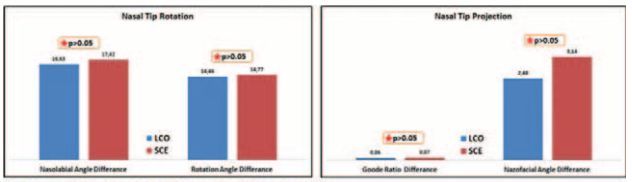

***LCO:** Lateral Crural Overlap, **SCE:** Split Cartilage Excision*

FIGURE 4. Effect of Lateral Crural Overlap and Split Cartilage Resection techniques on the nasal tip rotation and nasal tip projection.

increase in Goode index values following the operation as compared with the preoperative status ($P < 0.05$) (Fig. 3). But both groups had insignificant increase nasofacial angle values following the operation as compared with the preoperative status ($P > 0.05$) (Fig. 3). Even though Goode index and nasofacial angle values were increased more in Group 2 (SCR) as compared with Group 1 (LCE) (pre- and postoperative), there are no significant differences between them ($P > 0.05$) (Fig. 4).

Acoustic Rhinometric Measurements

There were no differences between the 2 groups before the operation in terms of both narrow and wide nasal cavity volumes ($P > 0.05$) (Table 2). Both groups had significant volume increases in both the narrow nasal cavity and the wide nasal cavity after the operation as compared with the postoperative status. Even though there were no significant differences between the nasal cavity volume values of the 2 groups, the volume increase in wide nasal cavity in Group 2 was higher ($P < 0.05$) (Table 2).

There were no significant differences between the 2 groups with respect to the preoperative MCA values ($p > 0.05$) (Table 2). After the operation, the increase in MCA values in Group 2 was significantly >1 in Group 1 for both nasal cavities ($P < 0.05$) (Table 2). Preop and postop views (Fig. 5).

FIGURE 5. Pre- and postoperative view.

DISCUSSION

It is not easy to achieve the desired results via surgery in long noses with drooped tips. The gold standard in achieving a successful result with such noses depends on the identification of the underlying anatomical distortion. Even though several disorders causing severe tip ptosis are present in the same patient, the essential problem for 85% of the patients is the presence of downward-slanted alar cartilages. Generally speaking, the presence of large lateral crura, weak and curved medial crura, or vertically oriented, lateral crura attached to the pyriform aperture at a high level is observed. Furthermore, the overprojection of the scroll site along with long lateral cartilages, high anterior septal angle, and thick and heavy skin of the nasal lobule are also deformities that are frequently present together. If identified, these additional coexisting deformities should be corrected with priority, such as conservative cephalic trim from the lateral crura, resection of the overdeveloped scroll site of lateral cartilages, and reduction of the high anterior septal angle. Such types of additional maneuvers are aimed at eliminating extrinsic forces that push downward; therefore, they allow the free upward movement of alar cartilages and they also enable them to remain at a more cephalic position during and after recovery.[2]

Medial and lateral crura are 2 essential cartilaginous structures anatomically forming the nasal tip. These are the essential structures forming the shape, length, and resistance of the nasal tip. The ligamentous cords between the medial crural footplates and caudal tip of the nasal septum, fibrous ligaments between the upper and lower lateral cartilages, and the interdomal ligament above the anterior septal angle constitute the resistance and projection of the

TABLE 2. Rhinologic Parameters of LCO and SCR groups*

Acoustic Rhinometric Values	LCO Narrow Side Mean ± SD	SCR Narrow Side Mean ± SD	Statistic Student's *t*-test	LCO Wide Side Mean ± SD	SCR Wide Side Mean ± SD	Statistic Student's *t*-test
VOL-Preoperative	6.27 ± 0.54	6.04 ± 0.65	$P = 0.072$	8.56 ± 0.57	8.93 ± 0.50	$P = 0.056$
VOL-Postoperative	8.18 ± 0.47	7.84 ± 0.80	$P = 0.068$	9.07 ± 0.09	11.06 ± 0.09	$P = 0.001$
Unpaired *t*-test	$P = 0.001$	$P = 0.001$		$P = 0.001$	$P = 0.001$	
MCA preoperative	0.34 ± 0.05	0.35 ± 0. 04	$P = 0.124$	0.48 ± 0.06	0.50 ± 0.05	$P = 0.054$
MCA postoperative	0.47 ± 0.06	0.54 ± 0.05	$P = 0.001$	0.57 ± 0.04	0.62 ± 0.04	$P = 0.023$
Unpaired *t*-test	$P = 0.001$	$P = 0.001$		$P = .001$	$P = .001$	

LCO, lateral crural overlap; MCA, minimal cross-sectional area; SCR, slip cartilage resection; SD, standard deviation; VOL, volume of nasal cavity. $P < 0.05$ was accepted statistically significant.

*Student's *t*-test was used for intergroup comparison. Paired *t*-test was used for within group comparison.

© 2015 Mutaz B. Habal, MD

Copyright © 2015 Mutaz B. Habal, MD. Unauthorized reproduction of this article is prohibited.

nasal tip.[13] Even though conservative methods and shaping with suture techniques are preferred methods in performing tip plasty, these techniques unfortunately often fall short in the long, deformed, and ptotic noses.[14] If the alar cartilage is malpositioned, long, and deformed, some changes need to be done on the cartilage. For that reason, cartilage modification techniques are needed to increase the tip rotation in a great majority of the patients. The decision as to which technique should be implemented in which case depends on the patient status as well as the surgeon's familiarity with these techniques; however, every technique has its applications in particular situations as well as some disadvantages and shortcomings.

According to the conventional nasal tip tripod theory, both lateral crura of the alar cartilage form the upper legs, whereas the medial crura form the lower leg of the tripod. Whereas the LCS technique, one of the most popular techniques, shorten the lateral legs of the tripod, the medial technique prolongs the leg, thereby the projection is increased as a primary aim and the rotation is increased as a secondary aim.[4] On the contrary, the lateral legs of the tripod are shortened, the nasal tip is pulled upward and downward in the lateral crural overlap technique, thereby increasing the rotation and decreasing the projection.[5] As for the TIG technique, the entire alar cartilage, namely, the tripod is moved upward and attached to the caudal septum, hence increasing the rotation.[6]

In our study, the LCO technique, the most popular one for ptotic noses according to the literature, and the SCR technique, which was implemented by the lead author of the study, were compared. The nasal tip rotation and projection ratios of both techniques were compared. With both techniques, there was a significant increase in the nasal tip rotation angles as compared with the preoperative status. The SCR technique allowed for more increase in rotation change values as compared with the LCO technique; however, the difference in between was not significant. These findings indicated that the SCR technique was as effective as LCO, the conventional technique, in creating the nasal tip rotation. To assess the nasal tip projection, Goode index and nasofacial angle are used according to the literature. In our study, Goode index values showed a significant increase with both techniques. Nasofacial angle values showed a insignificant increase with both techniques. This situation indicates that the SCR technique increases the nasal tip project at the same degree with the LCO technique based on the values measured 1 year on average after the surgery.

Although the SCR technique allows increased rotation and reduced projection as desired depending on the site of SCR from the nasal dome, it is also possible to increase only the rotation by performing resection at the point of intersection between the lateral crura and middle crura without resecting the middle crura. After the cartilages on both trimmed ends are equalized, they are sutured end-to-end to assure better and symmetrical nasal tip precision, the tip support should definitely be assured with a strong columellar strut.[15] The reason for this is that the weakness of medial crura in ptotic noses is prominent. The ptotic noses with alar cartilage abnormality generally have lateral crura in long and concave shapes.[16] In this case, the vestibule skin is dissected from lateral crura to mobilize it and a strut (lateral crural strut) is placed underneath to assure its stability, thereby preventing it from curved or pitted again over time.[16] One or, as need be, 2 cartilage pieces excised via cephalic trim may also be sutured onto the newly created nasal tip to be used as both camouflage graft and a cap graft assuring a smooth surface for people with thin skin.[17] This technique, which can be used in patients with long and ptotic alar cartilage, may be used to operate not only primary, but also, eligible, secondary patients (ptotic noses with large alar cartilages).

One of the most important structures on which the techniques performed after rhinoplasty operations is the nasal valve. In ptotic noses, one of the essential structures constituting the nasal valve is the point where the lateral crura are attached to the middle crura. In our study, acoustic rhinometric measurements were taken to assess the effect on the nasal valve during the creation of the nasal tip. With both techniques that were implemented, there were significant increases in the MCA and volume of nasal cavity values as compared with the preoperative status; however, the increase with the SCR technique we performed was significantly higher as compared with that of the LCO technique. In ptotic noses, the weakest site is generally the point where the lateral crura are attached to the middle crura due to degenerations in the lower lateral cartilages. No procedures are performed on this site with the LCO technique. With the slip cartilage resection technique, this site is resected and connected with the medial crura, the more intact piece of lateral crura. Therefore, we believe that the MCA values showed a higher increase in the SCR group.

One of the limitations of our study is that the noses have only been followed for 1 year, and that nasal shape can continue to evolve over the span of many years, and so the final results are still uncertain.

CONCLUSIONS

The nasal tip split resection method is a method that can be implemented and should be kept in line as a technique, which must be considered as an alternative method for noses with ptotic and long nasal type disorder.

REFERENCES

1. Simons R. Nasal tip projection, ptosis, and supratip thickening. *Ear Nose Throat J* 1982;61:452
2. Foda HM. Management of the droopy tip: a comparison of three alar cartilage-modifying techniques. *Plast Reconstr Surg* 2003;112:1408–1417
3. Anderson JR. The dynamics of rhinoplasty. Proceedings of the 9th International Congress in Otolaryngology. Amsterdam: Excerpta Medica;1969. pp. 708–710
4. Kridel RWH, Konior RJ, Shumrick KA, et al. Advances in nasal tip surgery: the lateral crural steal. *Arch Otolaryngol Head Neck Surg* 1989;115:1206–1212
5. Konior RJ, Kridel RWH. Lateral crural techniques for repositioning of the nasal tip. *Oper Techn Otolaryngol Head Neck Surg* 1990;1:158–165
6. Kridel RWH, Scott BA, Foda HMT. The tongue-in-groove technique in septorhinoplasty: a ten year experience. *Arch Facial Plast Surg* 1999;1:246–256
7. Powell N, Humpherys B. Proportions of the Aesthetic Face. New York: Thieme- Stratton; 1984
8. Sheen JH, Sheen AP. Aesthetic Rhinoplasty. 2nd ed. St. Louis: Mosby; 1987:25–45
9. Daniel RK. The nasal tip: anatomy and aesthetics. *Plast Reconstr Surg* 1992;89:216–224
10. Stal S. Rotating the nasal tip. In: Gunter JP, Rohrich RJ, Adams WP, editors. Dallas Rhinoplasty: Nasal Surgery by the Masters. Vol 1. St. Louis: Quality Medical Publishers; 2002. pp. 402–409.
11. Foda HMT, Kridel RWH. Lateral crural steal and lateral crural overlay: an objective evaluation. *Arch Otolaryngol Head Neck Surg* 1999;125:1365–1370
12. Foda HMT. External rhinoplasty: a critical evaluation of 500 cases. *J Laryngol Otol* 2003;117:473–477
13. Arden RL, Crumley R. Cartilage grafts in open rhinoplasty. *Facial Plast Surg* 1993;9:285–294
14. Toriumi DM, Johnson CMJ. Open structure rhinoplasty: featured technical points and long term follow-up. *Facial Plast Surg Clin North Am* 1993;1:1–22
15. Gunter JP, Rohrich RJ. External approach for secondary rhinoplasty. *Plast Reconstr Surg* 1987;80:161–174

© 2015 Mutaz B. Habal, MD

Copyright © 2015 Mutaz B. Habal, MD. Unauthorized reproduction of this article is prohibited.

16. Gunter JP, Friedman RM. Lateral crural strut graft: technique and clinical applications in rhinoplasty. *Plast Reconstr Surg* 1997;99: 943–952
17. Rohrich] RJ, Deuber MA. Nasal tip refinement in primary rhinoplasty: the cephalic trim cap graft. *Aesthet Surg J* 2002;22:39–45

Surgical Management of Giant Scalp Neurofibroma After Ultra-Selective Embolization of Nutrient Artery

Si-Ming Yuan, MD, Yao Guo, MD, Lei Cui, MD, Jun Wang, MD, Xin-Bao Hu, MD, Ji-Hong Zhou, MD, Hui-Qing Jiang, MD, and Zhi-Jian Hong, MD

Objectives: Neurofibroma, a common benign tumor in soft tissue, continues to grow, so it often appears to be giant. Surgical management of giant neurofibroma is a challenge due to the risk of excessive bleeding. Embolization of tumor's nutrient artery may reduce the blood loss in operation. This study introduces the surgical management of giant scalp neurofibroma with preoperative ultra-selective embolization of nutrient artery.

Methods: From January 2006 to December 2013, 9 patients with giant scalp neurofibroma were enrolled into the study. Digital subtraction angiography (DSA) showed tumor's nutrient artery. Ultra-catheter was inserted into the nutrient artery and its branches as close as possible to the tumor. Then ultra-selective embolization was performed with gelatin sponge particles. Surgical removal of tumor was performed in 3 days after embolization. The wound was repaired by skin graft.

Results: All of the 9 patients underwent successful DSA and ultra-selective embolization. Among them, occipital artery was embolized in 3 patients (left side in 1 patient and right side in 2 patients). Both occipital artery and superficial temporal artery were embolized in 6 patients (left side in 2 patients, right side in 3 patients, and both side in 1 patient). No complications, such as ectopic embolism, occurred in the patients. All of the tumors were resected completely without blood transfusion. The skin graft survived very well on the wounds.

Conclusions: Preoperative ultra-selective embolization of nutrient artery is a feasible, safe, and effective method to reduce the blood loss in operation and facilitate the surgical management of giant scalp neurofibroma.

From the Department of Plastic Surgery, Jinling Hospital, School of Medicine, Nanjing University, Nanjing, Jiangsu, China.
Received September 10, 2014.
Accepted for publication April 5, 2015.
Address correspondence and reprint requests to Zhi-Jian Hong, Department of Plastic Surgery, Jinling Hospital, School of Medicine, Nanjing University, 305 East Zhongshan Road, Nanjing, Jiangsu 210002, China; E-mail: hongzj384@sohu.com
Si-Ming Yuan and Yao Guo are co-first authors.
This work was supported by the National Natural Science Foundation of China (No. 81272989).
The authors report no conflicts of interest.
Copyright © 2015 by Mutaz B. Habal, MD
ISSN: 1049-2275
DOI: 10.1097/SCS.0000000000001873

KeyWords: Interventional embolization, neurofibroma, nutrient artery, scalp

Neurofibroma, a common benign tumor, may occur anywhere in the body, including skin and soft tissue, nervous system, muscle, skeleton, and visceral organs.[1] The tumor continues to grow, so it often appears to be giant. For the giant neurofibroma, surgical management still is the best option,[2] although it is always a challenge due to the risk of excessive bleeding in operation.[3] In this study, we introduced the surgical treatment of 9 patients with giant scalp neurofibroma. Interventional embolization of tumor's nutrient arteries was made preoperatively, which effectively reduce the bleeding in the operation. Clinical observation demonstrated this is a safe and effective way to facilitate the surgical removal of giant scalp neurofibroma.

PATIENTS AND METHODS

This research was approved by the Committee on Clinical Investigation of Jinling Hospital. Informed consent was provided for the patients, according to the Declaration of Helsinki. From January 2006 to December 2013, 9 patients with giant scalp neurofibroma were enrolled into the study, 5 of which were men. Ages of patients at admission ranged from 12 to 60 years. The area of the tumors ranged from 300 to 500 cm^2. Among them, 7 patients had solitary tumors and 2 patients were diagnosed as neurofibromatosis type 1 (NF-1).

All of the patients underwent routine laboratory examinations and were proved with normal renal functions. Magnetic resonance imaging was performed to show the extent of tumor. Angiography was carried out on GE DSA (LCV+) (General Electric, Fairfield, Connecticut). The contrast media was Iopromide (trade name Ultravist, 100 mL/bottle, 300 mg I/mL, Schering AG, Germany). The puncture pore at the right groin was made with local anesthesia. Percutaneous puncture into the right femoral artery was done with the technique of Seldinger. Then a 5F Cobra catheter was inserted into the right femoral artery, passed through the external iliac artery, the common iliac artery and the aorta, and arrived at the external carotid artery finally. Then angiography was performed. According to angiography images, as well as the location of the tumor, nutrient arteries were located. Then ultra-catheter was inserted into the nutrient arteries and its branches as close as possible to the tumor. Ultra-selective embolization of the nutrient arteries and the branches were performed with gelatin sponge particles. After that, angiography was repeated and the results confirmed that the nutrient artery's branches in the tumor were not displayed, which indicated the successful embolization. The catheter was then pulled out and the puncture pore was pressed by bandage. Patients were observed for 10 minutes and sent back to the ward if no adverse reactions occurred.

Surgical removal of the tumor was performed in 3 days after embolization. Saline solution with adrenaline at the concentration of 1 : 200,000 was injected into the edge of the tumor. Then the scalp was incised and dissection was made over the periosteum. All of the tumors did not invade the periosteum, so the dissection was smooth. The wound was repaired by split-thickness skin graft acquired from the lateral thigh.

RESULTS

All of the 9 patients underwent successful DSA. No contrast media-related adverse reactions were observed. Angiographies showed that these scalp neurofibromas were supplied by occipital

Copyright © 2015 Mutaz B. Habal, MD. Unauthorized reproduction of this article is prohibited.

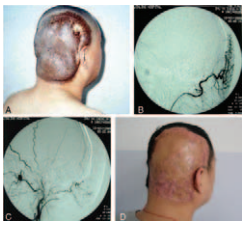

FIGURE 1. Case 1: a 45-year-old man had a giant neurofibroma on the right scalp (A). Digital subtraction angiography examination showed that the right occipital artery was the main nutrient artery (B). Ultra-selective embolization of the branches of right occipital artery was performed. After that, angiography confirmed that most of the branches in tumor were not displayed (C). Surgical removal of the tumor was performed 2 days after embolization. The tumor was resected completely and the wound was repaired by skin graft (D).

artery, superficial temporal artery, or both. The nutrient arteries branched into the tumors network-likely. Ultra-selective embolization of the nutrient artery and the branches were performed. In our cases, occipital artery was embolized in 3 patients (left side in 1 patient and right side in 2 patients). Both occipital artery and superficial temporal artery in 6 patients (left side in 2 patients, right side in 3 patients, and both side in 1 patient). No complications, such as ectopic embolism and ischemic necrosis of the normal scalp, occurred in the patients. Three days after embolization, all of the tumors were completely removed surgically. In the operation, part of the tumor was seen to be ischemic and degenerated. The blood loss remained under control and all of the patients did not need blood transfusion. Skin graft on the wound survived well. The follow-up period ranged from 6 to 36 months. No tumor recurrence was observed. Figures 1-3 show three typical cases with giant neurofibromas treated by the methods above mentioned.

DISCUSSION

Most of neurofibromas are sporadic, which may occur anywhere in the body. Systemic multiple neurofibroma, NF, is an autosomal dominant disorder that arises from abnormal differentiation of neural crest cells. Neurofibromatosis appears as 3 types, including NF1, NF2, and schwannomatosis.[4–6] The genes mutations responsible for them were located in 17q11.2, 22q11.2-q12, and SMARCB1, respectively.[7–9]

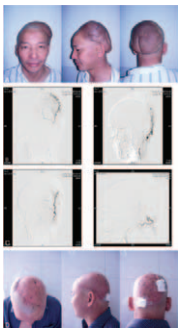

FIGURE 2. Case 2: a 52-year-old man had a giant scalp neurofibroma (A). Digital subtraction angiography examination showed that the top branch of superficial temporal artery (B) (left image) and the occipital artery (B) (right image) were the main nutrient arteries. Ultra-selective embolization of the top branches of superficial temporal artery and occipital artery was performed. After that, angiography confirmed that almost all of the branches in tumor were not displayed (C). Surgical removal of the tumor was performed 3 days after embolization. The tumor was resected completely and the wound was repaired by skin graft (D).

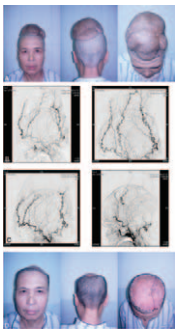

FIGURE 3. Case 3: a 60-year-old woman had a giant scalp neurofibroma on the top of head (A). Digital subtraction angiography examination showed that superficial temporal artery and occipital artery on both sides (B) were the main nutrient arteries. Ultra-selective embolization of the branches of bilateral superficial temporal artery and occipital artery was performed. After that, angiography confirmed that most of the branches in tumor were not displayed (C). Surgical removal of the tumor was performed 3 days after embolization. The tumor was resected completely and the wound was repaired by skin graft (D).

Neurofibroma grows invasively with ill-defined boundary. There are abundant malformed vessels in the tumor, including abnormal venous sinuses, aneurism, and arteriovenous fistula.[10] Giant neurofibroma is a challenge for surgeon due to the risk of massive bleeding in the operation. With endovascular techniques and new embolic agents, preoperative embolization has become a useful adjuvant method for the surgical management of giant neurofibroma.[11,12]

Feeding arteries of the scalp include superficial temporal artery, posterior auricular artery, occipital artery, supraorbital artery, and supratrochlear artery. Among them, superficial temporal artery and occipital artery are the major feeding vessels. These arteries have clear distribution and regular anatomical position. It is easy to perform an interventional embolization. In this study, ultra-catheter was inserted into the nutrient artery and its branches as close as possible to the tumor. Then ultra-selective embolization was performed. After that, angiography was repeated. The branches in the tumor were not displayed, which confirmed the successful embolization. In operation, the blood loss was largely reduced. All of the tumors were removed successfully without blood transfusion.

In summary, preoperative ultra-selective embolization of nutrient artery is a feasible, safe, and effective method to reduce the blood loss in the surgical resection of giant scalp neurofibroma. In this study, the wounds were repaired by skin graft. We will correct the baldness deformity by skin expander treatment in the future.

REFERENCES

1. Korf BR. Neurofibromatosis. *Handb Clin Neurol* 2013;111:333–340
2. Janes LE, Sabino J, Matthews JA, et al. Surgical management of craniofacial neurofibromatosis type 1 associated tumors. *J Craniofac Surg* 2013;24:1273–1277
3. Vélez R, Barrera-Ochoa S, Barastegui D, et al. Multidisciplinary management of a giant plexiform neurofibroma by double sequential preoperative embolization and surgical resection. *Case Rep Neurol Med* 2013;2013:987623
4. Ferner RE, Gutmann DH. Neurofibromatosis type 1 (NF1): diagnosis and management. *Handb Clin Neurol* 2013;115:939–955
5. Lloyd SK, Evans DG. Neurofibromatosis type 2 (NF2): diagnosis and management. *Handb Clin Neurol* 2013;115:957–967
6. Chen SL, Liu C, Liu B, et al. Schwannomatosis: a new member of neurofibromatosis family. *Chin Med J* 2013;126:2656–2660
7. Ledbetter DH, Rich DC, O'Connell P, et al. Precise localization of NF1 to 17q11.2 by balanced translocation. *Am J Hum Genet* 1989;44:20–24
8. Hulsebos TJ, Bijlsma EK, Geurts van Kessel AH, et al. Direct assignment of the human beta B2 and beta B3 crystallin genes to

© 2015 Mutaz B. Habal, MD

Copyright © 2015 Mutaz B. Habal, MD. Unauthorized reproduction of this article is prohibited.

22q11.2-q12: markers for neurofibromatosis 2. *Cytogenet Cell Genet* 1991;56:171–175
9. Plotkin SR, Blakeley JO, Evans DG, et al. Update from the 2011 International Schwannomatosis Workshop: from genetics to diagnostic criteria. *Am J Med Genet A* 2013;161A:405–416
10. Oderich GS, Sullivan TM, Bower TC, et al. Vascular abnormalities in patients with neurofibromatosis syndrome type I: clinical spectrum, management, and results. *J Vasc Surg* 2007;46:475–484
11. Jones RG, Kiatisevi P, Morris DC, et al. Intravascular embolisation and surgical resection of a giant neurofibroma with intratumoural haemorrhage. *Br J Radiol* 2010;83:e225–e229
12. Tomei KL, Gupta V, Prestigiacomo CJ, et al. Spontaneous hemorrhage of a facial neurofibroma: endovascular embolization before surgical intervention. *J Craniofac Surg* 2013;24:e514–e517

Hatchet Flap: Clinical Evaluation of Results in Reconstruction of Lateral Nasal Region Defects

Candemir Ceran, MD, Fatih Tekin, MD,† Duriye D. Demirseren, MD,‡ Soner Tezcan, MD,* Ersin Aksam, MD,§ and Mustafa E. Demirseren, MD**

Abstract: Hatchet rotation-advancement flap is a well-known flap design, which is a worthwhile option in the reconstruction of lateral nasal region skin defects. In this study, the author's experience with 3 different designs of hatchet flaps, for the reconstruction of the defects in 3 different parts of the lateral nasal region, has been presented. All flaps in 31 clinical cases were planned from the cheek and nasolabial region. For the defects in the upper 1/3 part, flaps were planned in advancement type, for the middle 1/3 part, flaps were planned in rotation-advancement type, and for the lower 1/3 part, flaps were planned in rotation type. Satisfactory results were achieved in all patients except in patients having defects in the lower 1/3 part.

In reconstruction of lateral nasal region defects, hatchet flap has different advantages such as versatility, better tissue match, and short final scar in the nasolabial fold. When planned in rotation type, for the lower 1/3 part, the ratio of complications increases significantly, which necessitates considering other flap options as the first-line choice of reconstruction for this region.

Key Words: Hatchet flap, lateral nasal region, rotation-advancement flap

From the *Plastic Reconstructive and Aesthetic Surgery Department, Ankara Ataturk Training and Research Hospital; †Plastic Reconstructive and Aesthetic Surgery Department, Ankara Kecioren Training and Research Hospital; ‡Dermatology Department, Ankara Ataturk Training and Research Hospital, Ankara; and §Plastic Reconstructive and Aesthetic Surgery Department, Akhisar State Hospital, Manisa, Turkey.

Received September 17, 2014.
Accepted for publication April 5, 2015.

Address correspondence and reprint requests to Ersin Aksam, Akhisar State Hospital, Plastic Reconstructive and Aesthetic Surgery Department, 45200 Manisa, Turkey; E-mail: ersinaksam@gmail.com

The authors report no conflict of interest.

Copyright © 2015 by Mutaz B. Habal, MD

ISSN: 1049-2275
DOI: 10.1097/SCS.0000000000001874

INTRODUCTION

The lateral nasal region is the transition zone between important facial anatomic landmarks such as the cheek, periorbital region, glabella, nasal dorsum, and nasal tip. The upper 1/3 of the region, which includes medial canthal region, has thinner skin, the middle 1/3 has thicker skin, and the lower 1/3 has thick skin, which is strongly adhered to the underlying alar cartilages. Defects in the lateral nasal region commonly occur after malign tumor excisions. Using different modifications of local flaps in reconstruction is generally accepted as the best option.[1] When choosing the local flap, the tissue characteristics of the donor area and the type of movement must be taken into consideration. With this in mind, hatchet flaps can be designed according to the location of the defect in the lateral nasal region. The hatchet flaps, which are rotation-advancement flaps, are well-known modifications of V-Y advancement flaps with one side of the "V" being left intact.[2] This study details our experience in the reconstruction of lateral nasal region defects with different designs of hatchet flaps made according to the location of the defect.

MATERIALS AND METHODS

Thirty-one patients whose lateral nasal region defects were reconstructed with hatchet flaps between May 2010 and June 2013 were included in this study. Eighteen patients were men (58%) and 13 were women (42%). The patients' age ranged from 36 to 78 years with the median age of 59 years. The borders of the lateral nasal region were accepted as the intercanthal line superiorly, alar rim inferiorly, and nasofacial junction laterally. The region was divided into 3 equal parts, each having different tissue characteristics. The locations of the defects were in the upper 1/3 region in 12 patients, the middle 1/3 region in 13 patients, and the lower 1/3 region in 6 patients.

In all patients, the reason for the defect was malign tumor excisions. The mean defect size was 1.4×2.1 cm with a range of 1×1.2 to 2.3×2.5 cm. Pathological examination of the specimens showed a basal cell carcinoma with clear margins in all the patients. The mean follow-up time was 21 months.

The Surgical Technique

Operations were performed under local anesthesia. The design of the hatchet flap was made according to the size and exact location of the defect in the lateral nasal region. All the flaps were elevated from the cheek and nasolabial region. The donor site, which is to be closed primarily in V-Y fashion, was kept in the nasolabial fold area.

In the upper 1/3 part, the axial length of the flap was designed to be approximately 3 times the diameter of the defect. To achieve more advancement, the flap was totally elevated in subcutaneous plane and only cutaneous component was kept intact as the main nourishment source. In the middle 1/3 part, the axial length of the flap was designed to be approximately 2.5 times the diameter of the defect. The upper border of the flap was planned more convex than the upper 1/3 region flap, to add more rotational movement. In the lower 1/3 part, the axial length of the flap was designed to be approximately twice the diameter of the defect. The upper border of the flap was more convex than the middle 1/3 flap, since rotation was the main aimed movement. Both the cutaneous component and the subcutaneous perforators were kept intact, which allows double nourishment to the flap. In all 3 regions, to achieve nasofacial definition and better inset, the edges of the flap were partially trimmed. The planning details of the flap for each region are summarized in Figures 1–3.

Copyright © 2015 Mutaz B. Habal, MD. Unauthorized reproduction of this article is prohibited.

FIGURE 1. Illustration of hatchet flap design for defects in the upper 1/3 of the lateral nasal region.

FIGURE 2. Illustration of hatchet flap design for defects in the middle 1/3 of the lateral nasal region.

FIGURE 3. Illustration of hatchet flap design for defects in the lower 1/3 of the lateral nasal region.

RESULTS

In the early postoperative period, no complications such as hematoma, infection, suture dehiscence, and partial or total flap necrosis were observed. All the donor sites healed uneventfully independent of the movement type of the flaps. In the follow-up period, no recurrences of basal cell carcinoma (BCC) were observed. In all patients with defects in the upper and middle 1/3 parts, satisfactory results with regard to tissue match and final scar were achieved. However, trap-door deformity was noted in the lower 1/3 region in 3 patients. Additionally, all patients were asked to evaluate their satisfaction with respect to overall surgical outcome and the final scar appearance. Only 4 patients with trap door deformity were concerned about the scar, but none of the patients wanted to have revision surgery, when they were offered. Gentle massage on the flap was suggested to these patients. Slight improvement has been noted with time (Figs. 4–7).

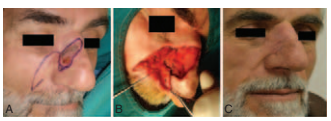

FIGURE 4. (A) Preoperative view of a middle 1/3 BCC in lateral nasal region with plan for excision, note the previous glabellar transposition flap for medial canthal BCC. (B) Intraoperative view of flap elevation, dorsal part of the defect was primarily closed. (C) Postoperative 2-year view of the patient.

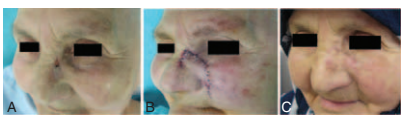

FIGURE 5. (A) Preoperative view of the middle 1/3 BCC in lateral nasal region. (B) Intraoperative view after adaptation of the flap. (C) Postoperative 1-year view of the patient.

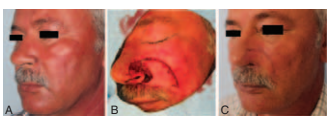

FIGURE 6. (A) Preoperative view of a lower 1/3 BCC in lateral nasal region. (b) Intraoperative view after adaptation of the flap. (C) Postoperative view of the patient.

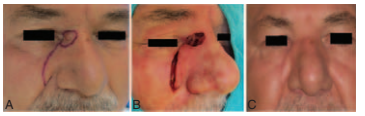

FIGURE 7. (A) Preoperative view of an upper 1/3 BCC in lateral nasal region with plan for excision. (B) Intraoperative view after flap elevation. (C) Postoperative view of the patient.

DISCUSSION

Reconstructive surgeons need to keep the subunit principle in mind when making the decision concerning the reconstruction of lateral nasal region skin defects, but many authors have demonstrated equally good results using reconstruction with "defect-only" approach.[3] In our cases, we preferred the defect-only approach. Better color and tissue match and minimal scar are the main concerns of skin-only defect reconstruction of the lateral nasal region. Local flaps are generally accepted as the most suitable option when these concerns are considered.[4] Glabellar region as a donor site is commonly used for the upper 1/3 of lateral nasal region defects; however, it has the disadvantage of tissue bulk, which may not be the best match for the thin neighboring skin of the region.[5] Meanwhile, cheek and nasolabial regions have the advantages of skin laxity and camouflage of donor site scar in the nasolabial fold.[6,7] In addition to the chosen donor site, the design of local flaps, which allows the transposition, rotation, or advancement of the flap, is also important.[8] Among these designs, the rotation-advancement flaps have the advantage of using the most adjacent skin, which is generally the best match. When cheek and nasolabial region are chosen as the donor site of the rotation-advancement flap, final scar would be parallel to the relaxed skin tension lines and camouflaged in the nasolabial fold.[9]

Hatchet flap was first described by Emmett et al.[4] Since then, this flap has been widely accepted and used in different body parts, such as the face, helix, eyelid, scalp, trochanter, sacral region, extremities, and fingertip.[2,4,10,11] Although the hatchet flaps have the cutaneous pedicle and subcutaneous perforators as the 2 sources of nourishment, it has been shown that one of the pedicles could be sacrificed depending on the defect and the region.[12] This means that the subcutaneous perforators could be kept intact making the hatchet flap a more rotation-type flap or the subcutaneous perforators could be sacrificed in which case the hatchet flap would be a more advancement-type flap. In lateral nasal region defects, we were able to reconstruct defects up to 2 cm in diameter with these designs of hatchet flaps.

Although our results were found to be satisfactory for the defects in the upper and middle 1/3 part, some of our patients had trap-door deformity in the lower 1/3 part, which could be explained by the thick and inelastic tissue characteristics of the region and the curvilinear incision.[13,14] In the lower 1/3 part, the overall results were not satisfactory when compared with the other parts.

In conclusion, hatchet flap in lateral nasal region reconstruction has advantages of versatility, better tissue match since the most adjacent tissue is used, and short final scar, which is camouflaged in nasolabial fold. However, the occurrence of a trap-door deformity and poor results in flaps applied to the lower 1/3 part can be considered as the main drawback of the hatchet flap in the lateral nasal region.

ACKNOWLEDGMENTS

We thank Nebil Yesiloglu, MD, for illustrations in Figures 1–3.

REFERENCES

1. Guida RA, Rubach B. Aesthetic restoration of acquired nasal defects. *Operative Techniques in Otolaryngology-Head and Neck Surgery* 2000;11:102–109

© 2015 Mutaz B. Habal, MD

Copyright © 2015 Mutaz B. Habal, MD. Unauthorized reproduction of this article is prohibited.

2. Elshahat A. The versatility of the hatchet flap in soft tissue reconstruction and a proposed new classification. *Eur J Plast Surg* 2011;35:351–357
3. Thornton FT, Griffin JR, Constantine FC. Nasal reconstruction: an overview and nuances. *Semin Plast Surg* 2008;22:257–268
4. Zhi-guo W, Quan-chen X, Rui-xia K, et al. Principles of hatchet-skin flap for repair of tissue defects on the cheek. *Aesth Plast Surg* 2012;36:163–168
5. Turgut G, Ozcan A, Yesiloglu N, et al. A new glabellar flap modification for the reconstruction of medial canthal and nasal dorsal defects: "flap in flap" technique. *J Craniofac Surg* 2009;20:198–200
6. Driscoll BP, Baker SR. Reconstruction of nasal alar defects. *Arch Facial Plast Surg* 2001;3:91–99
7. Fader DJ, Baker SR, Johnson TM. The staged cheek-to-nose interpolation flap for reconstruction of the nasal alar rim/lobule. *J Am Acad Dermatol* 1997;37:614–619
8. Dinehart SM. The rhombic bilobed flap for nasal reconstruction. *Dermatol Surg* 2001;27:501–504
9. Pan Y, Ai Y, Li H, et al. Local hatchet flap for facial skin defects reconstruction in special areas. *Dermatol Surg* 2004;30:1256–1260
10. Sowerby JL, Taylor SM, Corey C, et al. The double hatchet flap a workhorse in head and neck local flap reconstruction. *Arch Facial Plast Surg* 2010;12:198–201
11. Demirseren ME, Gökrem S, Ozdemir OM, et al. Hatchet-shaped tensor fascia lata musculocutaneous flap for the coverage of trochanteric pressure sores: a new modification. *Ann Plast Surg* 2003;51:419–422
12. Jósvay A. Clinical experience with the hatchet-shaped gluteus maximus musculocutaneous flap. *Ann Plast Surg* 2005;55:179–182
13. Hosokawa K, Susuki T, Kikiu T, et al. Sheet of scar causes trapdoor deformity: a hypothesis. *Ann Plast Surg* 1990;25:134–135
14. Kaufman AJ, Kiene KL, Moy RL. Role of tissue undermining in the trapdoor effect of transposition flaps. *J Dermatol Surg Oncol* 1993;19:128–132

Long-Term Outcome of Combined Lateral Tarsal Strip With Temporal Permanent Tarsorrhaphy for Correction of Paralytic Ectropion Caused By Facial Nerve Palsy

Kye Yoon Kwon, MD, Sun Young Jang, MD,† and Jin Sook Yoon, MD, PhD**

From the *Institute of Vision Research, Department of Ophthalmology, Yonsei University College of Medicine, Seoul; and †Department of Ophthalmology, Soonchunhyang University Bucheon Hospital, Soonchunhyang University College of Medicine, Bucheon, Kyunggido, Korea.

Received July 24, 2014.
Accepted for publication April 7, 2015.

Address correspondence and reprint requests to Jin Sook Yoon, Department of Ophthalmology, Yonsei University College of Medicine, 50-1 Yonsei-ro, Seodaemun-gu, 120-752, Seoul, Korea;
E-mail: yoonjs@yuhs.ac

The authors report no conflicts of interest.

Copyright © 2015 by Mutaz B. Habal, MD

ISSN: 1049-2275
DOI: 10.1097/SCS.0000000000001875

Abstract: Paralytic ectropion caused by facial nerve palsy often requires surgical intervention for cornea protection. In this study, the authors intended to investigate the long-term surgical outcome of their surgical technique of correcting paralytic ectropion, which is a combined lateral tarsal strip and minimal temporal permanent tarsorrhaphy. The authors performed a retrospective chart review of patients who underwent paralytic ectropion repair by combined lateral tarsal strip with minimal temporal permanent tarsorrhaphy (5 mm) from January 2010 to December 2012. Patients with at least 1 year of follow-up were included. An analysis of preoperative and postoperative measurements included the extent of lagophthalmos, grade of superficial punctate keratopathy (SPK), and tear break-up time (tBUT). The study included 22 patients and a total of 22 eyes. The lagophthalmos, grade of SPK, and tBUT at both 1 month and 1 year of postoperative follow-up were all significantly improved compared with preoperatively (all $P < 0.01$). At 1 year after surgery, the mean SPK grade and tBUT were slightly, but not significantly, worse than at 1 month after surgery ($P = 0.716$ and $P = 0.632$, retrospectively). Three patients were not satisfied with the aesthetic appearance; however, no patient required additional surgery to enhance eyelid closure because of ectropion recurrence or to reopen the tarsorrhaphy during long-term follow-up. Combined lateral tarsal strip with minimal temporal permanent tarsorrhaphy is a quick, safe, and effective surgical technique for the treatment of lower eyelid paralytic ectropion. It produces minimal cosmetic disfigurement and low morbidity during long-term follow-up.

Key Words: Facial nerve palsy, lateral tarsal strip, paralytic ectropion, permanent tarsorrhaphy

Paralytic ectropion is a common ocular sequela of facial nerve palsy, which may cause various problems because of poor cornea protection. These problems include exposure keratopathy, dry eye, tearing, and conjunctivitis.[1,2] Facial nerve palsy decreases the function of the orbicularis oculi muscle and thereby impairs eyelid blinking and closure. Eyelid retraction, even with cicatricial entropion of the upper eyelid, can develop during the long-term follow-up in patients with chronic, persistent facial nerve palsy.[3] Lack of lubrication and poor eyelid closure may even cause corneal ulceration and eventual visual loss. When conservative treatment does not effectively protect the cornea, surgical strategies to improve eyelid closure, such as gold or platinum weight insertion, tightening of the lower eyelid, palpaberal springs, or tarsorrhaphy, are essential.[4,5]

The most common surgical techniques for repair of a substantial ectropion are lateral tarsal strips and lateral tarsorrhaphy, both of which are quick and easy procedures to reduce lower lid laxity and enhance eyelid closure.[6] Unfortunately, the lateral tarsal strip procedure alone cannot sufficiently elevate the lower eyelid to provide corneal protection, and the permanent lateral tarsorrhaphy may produce disappointing cosmetic results.[7,8] Chang and Olver[9] described an augmented lateral tarsal strip tarsorrhaphy, which requires a long strip (10–15 mm) to maximize elevation of the lower eyelid. In this technique, the lateral tarsal strip was draped over the posterior lamella of the lateral part of the upper eyelid and sutured to the outer aspect of the superolateral orbital rim and periosteum. This improved corneal signs in 93% of patients, while producing low morbidity. In 2009, Kahana and Lucarelli[10] introduced a novel surgical technique, adjunctive transcanthotomy

Copyright © 2015 Mutaz B. Habal, MD. Unauthorized reproduction of this article is prohibited.

lateral suborbicularis fat lift and orbitomalar ligament resuspension with a lateral tarsal strip, which resulted in resolution of symptoms and satisfactory aesthetic outcomes in 12 patients with severe ectropion. Both of these innovative augmented lateral tarsal strip techniques provide strong, optimal tightening, and elevating of the lower eyelid; however, they require blunt dissection over the superolateral or inferolateral orbital rim in the preperiosteal plane, which may cause bleeding and damage to zygomaticofacial nerves. As Asians have thicker orbicularis muscles and a greater tendency towards bleeding than Caucasians, more time and experience would be required to dissect a large area of the lateral orbital rim in Asians. Moreover, Asians are more enophthalmic than Caucasians; therefore, suturing tarsal strips over the anterior aspect of the rim in the preperiosteal plane may still pull the eyelid away from the eye laterally. The lateral tarsal strip should be carefully attached to the posterior aspect of the lateral orbital rim, especially in Asians because of their typical enophthalmic features.

At our institution, we perform a lateral strip procedure, which involves anchoring the strip to the posterior orbital rim, combined with a small lateral permanent tarsorrhaphy to correct paralytic ectropion caused by facial nerve palsy. Although this procedure is a simple combination of a lateral tarsal strip and small lateral permanent tarsorrhaphy, the long-term results with respect to cornea protection, improved eyelid closure, and aesthetic satisfaction appear to be comparable with those obtained using an augmented procedure. The aim of this study was to investigate and compare both short-term and long-term surgical outcomes of the combination of lateral tarsal strip and permanent tarsorrhaphy for correction of paralytic ectropion in patients with facial nerve palsy.

MATERIALS AND METHODS

We performed a retrospective chart review of patients who underwent paralytic ectropion repair by lateral tarsal strip combined with minimal (5 mm) lateral permanent tarsorrhaphy from January 2010 to December 2012. The indications for surgery were lagophthalmos causing keratitis and lower eyelid sagging due to facial nerve palsy, which were not effectively improved by conservative treatment (including aggressive lubrication). Only those patients with at least 1 year of follow-up were included in this study. The study was approved by the institutional review board of Severance Hospital.

Surgical Method

After injecting local anesthetic into the lateral canthus and posterolateral aspect of the inferolateral orbital rim, a 5- to 7-mm horizontal lateral canthal skin and orbicularis incision was made, followed by a lower limb lateral canthotomy and cantholysis. The inner and lateral aspect of the rim was dissected by spreading with blunt scissors. A portion of the tendon was then shortened and resutured to the periorbita at Whitnall tubercle at the inner aspect of lateral rim using double-armed 5-0 nylon sutures. The tarsal strip was attached slightly higher than the medial canthal tendon, to form a slight upward slant of the lateral canthus. After fixing the tarsal strip, the upper lid and lower lid margins along the gray line for 5-mm lateral eyelids were incised, using a number 15 blade. Approximately 5 mm of anterior and posterior lamella were separated using Westcott scissors (Miltex, York, PA) proximal to the lid margins. After de-epithelialization of posterior upper lid margin, the posterior lamellas were sutured together between the upper and lower eyelids using 5-0 Vicryl (Ethicon, Cincinnati, OH) sutures. The lateral canthal angle was reformed using a buried 6-0 Vicryl (Ethicon, Cincinnati, OH) suture. The orbicularis and skin were closed in 2 layers in an interrupted fashion using 6-0 nylon sutures (Fig. 1).

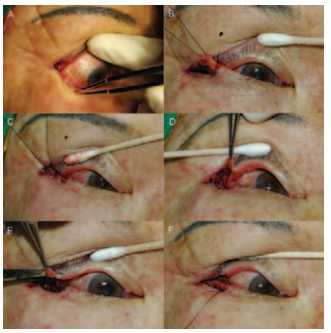

FIGURE 1. Photographs demonstrating the technique for combined lateral tarsal strip and tarsorrhaphy. A, A horizontal lateral canthal skin and orbicularis incision is made, followed by a lower limb lateral canthotomy and cantholysis. B, Formation of the lateral tarsal strip. C, Anchoring the lateral tarsal strip to the rim of the periosteum near the Whitnall lateral orbital tubercle. D, Anterior and posterior lamellas of the upper eyelid after they were split. E, Excision of a small triangular area of anterior lamella of upper eyelid is performed. F, Overlapping the 2 posterior lamella (tarsal plate of upper eyelid and tarsal strip of lower eyelid).

Outcome Measurements

Preoperative and postoperative measurements included the extent of lagophthalmos, grade of superficial punctate keratopathy (SPK), and tear break-up time (tBUT). Tear break-up time was measured by instilling fluorescein stain into the lower fornix and measuring the time required for the tear to dissipate. This was performed 3 separate times, and the average of these 3 times was recorded. After instillation of fluorescein to determine the tBUT, the cornea was evaluated for SPK by looking for the presence of stain uptake. Preoperative and postoperative SPK was graded from 0 to 3 as follows: 0, none or trace; 1, mild; 2, moderate; or 3, severe.[11] Postoperative symptoms and measurements were routinely assessed at 1 month and 1 year after surgery. Complications were also recorded.

Statistics

PAWS statistical software, version 19.0 (SPSS, Inc., IBM Corp., Armonk, NY), was used to conduct the data analyses. Paired *t*-tests were used to compare initial values of lagophthalmos, tBUT and SPK with those measured at 1 month and 1 year. A P value < 0.05 was considered statistically significant.

RESULTS

The study included 22 patients and involved a total of 22 eyes. The mean age of the patients was 54.6 years (range, 12–87 years); 10 were men and 12 were women. Of the affected eyes, 12 were right and 10 were left. The mean duration of facial palsy from the onset of symptoms until surgery was 9.7 months (range, 2–120 months), and the mean postoperative follow-up was 16.5 months (range, 12–73 months). The cause of the facial nerve palsy was post-tumor surgery in 14 cases, traumatic in 3 cases, infectious in 2 cases, and idiopathic in 3 cases (Table 1).

The mean preoperative lagophthalmos was 3.44 mm (standard deviation [SD], 1.27), which was reduced to 0.36 mm (SD, 0.54) at 1 month postoperatively. At 1 year postoperatively, the mean lagophthalmos increased slightly to 0.56 mm (SD, 0.54) (Fig. 2A). The mean preoperative SPK grade was 2.77 (SD, 0.43), which decreased to a mean of 0.11 (SD, 0.32) at 1-month postoperatively and 0.22 (SD, 0.42) at 1 year after surgery (Fig. 2B). The mean preoperative tBUT was 2.91 seconds (SD, 1.63), which improved to 9.76 seconds (SD, 2.53) at 1-month postoperatively and

© 2015 Mutaz B. Habal, MD

Copyright © 2015 Mutaz B. Habal, MD. Unauthorized reproduction of this article is prohibited.

TABLE 1. Patient Characteristics

Patients (eyes)	22 (22)
Age (y) (mean, [range, SD])	54.6 (12–87, 28)
Sex, men (%)	10 (45.4%)
Affected eye, right : left	12 : 10
Postoperative follow-up (mo) (mean, [range])	16.5 (12–73)
Cause of facial nerve palsy	
Idiopathic	3
Traumatic	3
Post-tumor surgery	14
Infectious	2
Duration of facial nerve palsy (mo) (mean, [range])	9.7 (2–120)

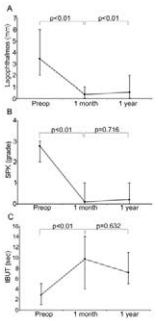

FIGURE 2. Plots demonstrating the mean change in lagophthalmos, superficial punctate keratopathy and lagophthalmos, and tear break-up time. A, lagophthalmos, B, superficial punctate keratopathy (SPK), C, tear break-up time (tBUT). The parameters were evaluated preoperatively, at 1 month and 1 year after surgery.

7.15 seconds (SD, 1.55) at 1 year after surgery (Fig. 2C). The improvements in lagophthalmos, SPK, and tBUT at 1 month and 1 year after surgery, compared with the preoperative values, were statistically significant (all $P < 0.01$). At 1-year postoperatively, allof the parameters worsened slightly compared with the values at 1 month after surgery, but the changes in SPK and tBUT were not statistically significant ($P = 0.716$, $P = 0.632$). Figure 3 shows representative preoperative and postoperative photographs of 1 of our patients.

During this study, none of the patients required reoperation or developed eyelid retraction. Three patients were not satisfied with the aesthetic appearance; however, no patient required additional surgery during our long-term follow-up to improve eyelid closure or to re-open the tarsorrhaphy.

DISCUSSION

Facial nerve paralysis produces loss of muscle tone of the orbicularis oculi muscle, resulting in outward turning of the eyelid margin.[10] Severe lower eyelid ectropion often results in conjunctival keratinization, tearing, pain, and reduced visual acuity secondary to ocular exposure. For laxity of the lower lid, various techniques can achieve horizontal lower eyelid tightening. Since 1979, when Anderson and Gordy[7] originally described the lateral tarsal strip and recommended its use for entropion resulting from lateral canthal laxity, a lateral tarsal strip procedure is now most frequently performed to treat paralytic ectropion[1]; however, the lateral tarsal strip does not effectively elevate the lower eyelid height in the long term.[8,9] Permanent lateral tarsorrhaphy of the lateral one-third or one-half of the eyelid is the most effective surgical method to treat severe exposure keratopathy; however, it can produce a markedly unacceptable cosmetic appearance and block lateral vision, and it does not improve lateral laxity.

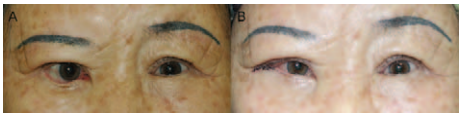

FIGURE 3. Representative preoperative and postoperative photographs of a patient. A, Preoperative lower lid ectropion resulting from facial nerve palsy. B, One-week postoperative appearance showing significantly corrected lower lid ectropion.

Previous authors have described modified techniques for the lateral tarsal strip. In 1989, Jordan and Anderson[12] described the enhanced tarsal strip, which differed from the original lateral tarsal strip by not involving a splitting of the lid. Corin et al[13] suggested resection of the orbicularis with lateral tarsal strip if overriding of the orbicularis is present. Charonis and Gossman[14] proposed the formation of a periosteal strip to strengthen the posterior lamella of the tarsal strip. Chang and Olver[9] described the augmented lateral tarsal strip tarsorrhaphy mentioned earlier, which consisted of a long strip attached to a point higher than the attachment site for the conventional lateral tarsal strip; however, all of the augmented lateral canthoplasties require dissection of a large area of the orbital rim, which can produce bleeding and other morbidity. Moreover, Asians tend to have enophthalmic anatomic features, so tight anchoring of the lateral canthal tendon or tarsus to the posterior Whitnall ligament is mandatory, which does not require dissection over the orbital rim in the preperiosteal plane.

Our current results demonstrated that in Asians, a procedure involving simple combined lateral tarsal strip and small permanent tarsorrhaphy, when performed appropriately, significantly improves lagophthalmos and prevents corneal breakdown during long-term postoperative follow-up. This technique also tightened the upper eyelids through shortening of the lateral part of the upper eyelid, which is not possible with the conventional lateral tarsal strip. All but 3 of our patients were satisfied with the cosmetic appearance. And our technique also has the advantage of allowing easy and fast opening of the tarsorrhaphied eyelid if facial nerve function recovers.

Because this study was retrospective, it had intrinsic limitations, which include the lack of direct comparison with control or other treatment groups. As well, the number of patients was relatively small. Nevertheless, the clinical effectiveness of this simple technique involving lateral tarsal strip and small permanent tarsorrhaphy during 1 year of postoperative follow-up was confirmed in our study by significant and consistent improvements in lagophthalmos, SPK, and tBUT. Complications, recurrence of ectropion requiring reoperation, or chronic eyelid retraction did not occur during follow-up.

In conclusion, combined lateral tarsal strip with minimal temporal permanent tarsorrhaphy is a safe and effective surgical technique for the treatment of severe lower eyelid ectropion due to facial nerve palsy. This technique not only provides significant improvement of symptoms and signs of exposure keratopathy and lagophthalmos, but it also minimizes the risk of cosmetic disfigurement and complications.

REFERENCES

1. Tucker SM, Santos PM. Survey: management of paralytic lagophthalmos and paralytic ectropion. *Otolaryngol Head Neck Surg* 1999;120:944–945
2. Kersten RC, Kulwin DR. Paralytic ectropion of the lower eyelid. *Plast Reconstr Surg* 1995;96:991–992
3. Hassan AS, Frueh BR, Elner VM. Mullerectomy for upper eyelid retraction and lagophthalmos due to facial nerve palsy. *Arch Ophthalmol* 2005;123:1221–1225

© 2015 Mutaz B. Habal, MD

Copyright © 2015 Mutaz B. Habal, MD. Unauthorized reproduction of this article is prohibited.

4. Kinney SE, Seeley BM, Seeley MZ, et al. Oculoplastic surgical techniques for protection of the eye in facial nerve paralysis. *Am J Otol* 2000;21:275–283
5. Patipa M. Ophthalmic surgical management of facial paralysis. *J Fla Med Assoc* 1990;77:839–842
6. Becker FF. Lateral tarsal strip procedure for the correction of paralytic ectropion. *Laryngoscope* 1982;92:382–384
7. Anderson RL, Gordy DD. The tarsal strip procedure. *Arch Ophthalmol* 1979;97:2192–2196
8. Olver JM. Surgical tips on the lateral tarsal strip. *Eye (Lond)* 1998;12 (pt 6):1007–1012
9. Chang L, Olver J. A useful augmented lateral tarsal strip tarsorrhaphy for paralytic ectropion. *Ophthalmology* 2006;113:84–91
10. Kahana A, Lucarelli MJ. Adjunctive transcanthotomy lateral suborbicularis fat lift and orbitomalar ligament resuspension in lower eyelid ectropion repair. *Ophthal Plast Reconstr Surg* 2009;25: 1–6
11. Efron N, Morgan PB, Katsara SS. Validation of grading scales for contact lens complications. *Ophthalmic Physiol Opt* 2001;21:17–29
12. Jordan DR, Anderson RL. The lateral tarsal strip revisited. The enhanced tarsal strip. *Arch Ophthalmol* 1989;107:604–606
13. Corin S, Veloudios A, Harvey JT. A modification of the lateral tarsal strip procedure with resection of orbicularis muscle for entropion repair. *Ophthalmic Surg* 1991;22:606–608
14. Charonis GC, Gossman MD. Involutional entropion repair by posterior lamella tightening and myectomy. *Ophthal Plast Reconstr Surg* 1996;12:98–103

Ideal or Young-Looking Brow Height and Arch Shape Preferred by Koreans

Se Jin Hwang,[*†] *Hun Kim, BHS,*[‡] *Kun Hwang, MD, PhD,*[‡] *Seong Kee Kim, MD,*[‡§] *Young Suk Kim, BA,*[‡] *and Yeon Soo Kim, MD, PhD*[‡]

Abstract: The aim of this study is to see which brow height and arch shape is preferred as ideal or young-looking by Koreans.

A survey was conducted between June and Dec 2014 on 186 women who visited the brow bar (''Benefit'' of Incheon city). They were asked to choose which they believed ideal and youngest amongst the 3 brow archetypes according to their height and 4 types of modification of Anastasia (rotation of medial and lateral arms), which was illustrated.

Approximately half (52.5%) of the respondents answered that their brow matches them very well or well. Most (81.2%) believed there might be a method to yield an ideal brow archetype and almost all (97.3%) would change the brow shape if the expert advised. The most preferred ideal brow height was of a middle height (63.2%, the distance from the lateral canthus to the lateral end of eyebrow, which was 2/3 of the eye width). The most preferred ideal brow arch shape was the arched type (57.6% arches on a line drawn from the center of the nose through the center of the pupil). The most preferred young-looking brow height was of an upper height (46.2%, the distance from the lateral canthus to the lateral end of eyebrow was 3/4 of the eye width) followed by a middle height (39.7%). The most preferred young-looking brow arch shape was the head-up position (53.3%, medial arm of the brow was rotated upward to the horizontal plane).

The result of this study might be useful in facial rejuvenation surgeries as well as in brow esthetics or tattooing of the eyebrows.

From the *King's College London, London, UK; †Inha Research Institute for Medical Science; ‡Department of Plastic Surgery, Inha University School of Medicine; and §Dr Kim's Aesthetic Surgical Plastic Clinic, Seoul, Korea.

Received November 4, 2014.
Accepted for publication April 7, 2015.

Address correspondence and reprint requests to Kun Hwang, MD, PhD, Department of Plastic Surgery, Inha University School of Medicine, 27 Inhang-ro, Jung-gu, Incheon, 400-711, Korea.
E-mail: jokerhg@inha.ac.kr

This work was supported by a grant from INHA University (INHA-Research Grant).
The authors have no conflict of interest to declare.

Copyright © 2015 by Mutaz B. Habal, MD

ISSN: 1049-2275
DOI: 10.1097/SCS.0000000000001877

Key Words: Beauty, eyebrows, rhytidoplasty

Eyebrows play the role of ''conductor'' in an orchestra named ''facial expression''. Brow-lift procedures are performed by plastic surgeons to counteract the effects of aging and to optimize facial aesthetics.

There are several competing methods for ideal brow design; most designs have resulted from the analyses of plastic surgeons or makeup artists.[1–4] According to our previous article, Anastasia was the most preferred (44.8%, brow starts on a perpendicular line drawn from the middle of the nostril, arches on a line drawn from the center of the nose through the center of the pupil, and ends on a line drawn from the edge of the corresponding nasal ala through the outer edge of the eye) by Korean women.[5]

The preferred height of the eyebrow or arch shape has, however, not yet determined.

The aim of this study is to see which brow height and arch shape is preferred as ideal or young-looking by Koreans.

METHODS

Brow Archetypes According to Their Height

From our previous article, the most preferred brow archetype, the Anastasia was chosen: Brow starts on a perpendicular line drawn from the middle of the nostril, arches on a line drawn from the center of the nose through the center of the pupil, and ends on a line drawn from the edge of the corresponding nasal ala through the outer edge of the eye (Fig. 1).

1. Upper height: the distance from the lateral canthus to the lateral end of eyebrow was 3/4 of the eye width.
2. Middle height: the distance from the lateral canthus to the lateral end of eyebrow was 2/3 of the eye width.
3. Lower height: the distance from the lateral canthus to the lateral end of eyebrow was 3/5 of the eye width.

Brow Archetypes According to the Arch Shape

1. Arched: arches on a line drawn from the center of the nose through the center of the pupil.
2. Head-up: medial arm of the brow was rotated upward to the horizontal plane.

© 2015 Mutaz B. Habal, MD

Copyright © 2015 Mutaz B. Habal, MD. Unauthorized reproduction of this article is prohibited.

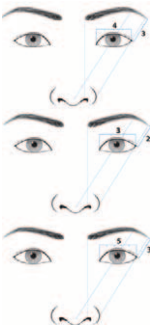

FIGURE 1. Brow archetypes according to their height. (Upper) Upper height: the distance from the lateral canthus to the lateral end of eyebrow was 3/4 of the eye width. (Middle) Middle height: the distance from the lateral canthus to the lateral end of eyebrow was 2/3 of the eye width. (Lower) Lower height: the distance from the lateral canthus to the lateral end of eyebrow was 3/5 of the eye width.

3. Tail-up: lateral arm of the brow was rotated upward to the horizontal plane.
4. Horizontal: medial arm and lateral arm of the brow were rotated upward to the horizontal plane (Fig. 2).

Data Collection

A survey was conducted between June 1 and October 30, 2014, on 186 women who visited the brow bar ("Benefit" of Incheon city).

They were asked whether they think there might be a method, which produces an ideal brow archetype. In cases where they said yes, they were asked to choose amongst the 3 brow archetypes according to their height illustrated and choose which they think ideal and young.

They were also asked to choose the youngest and ideal among the 4 types of modification of Anastasia (rotation of medial and lateral arms).

Population Sample

Before completing the survey, each participant provided background information, including age, occupation, income, marital status, and level of education.

Sensitivity Following the Trend (Fashion) Among the Groups

Sensitivity following the trend was asked on a Likert scale (5: definitely yes, 4: yes, 3: neither yes or no, 2: no, 1: definitely no).

Statistical Analysis

A χ^2 test and paired *t*-test were used. *P*-values less than 0.05 were considered significant.

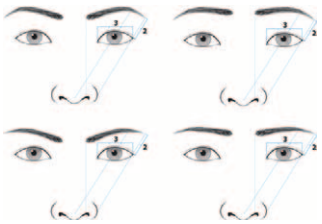

FIGURE 2. Brow archetypes according to the arch shape. (Left upper) Arched: arches on a line drawn from the center of the nose through the center of the pupil. (Right upper) Head-up: medial arm of the brow was rotated upward to the horizontal plane. (Left lower) Tail-up: lateral arm of the brow was rotated upward to the horizontal plane. (Right lower) Horizontal: medial arm and lateral arm of the brow were rotated upward to the horizontal plane.

RESULTS

Satisfaction to the Present Brow Shape

Among the 186 valid responses for this item, 20 (10.8%) answered their brow matches them very well, 79 (42.5%) well, 73 (39.2%) neither matches nor clashes, 14 clashes (7.5%). The score of the satisfaction to the present brow shape was 3.59 ± 0.78 (5: definitely yes, 4: yes, 3: neither yes or no, 2: no, 1: definitely no).

Presence or Absence of the Ideal Brow Archetype (16th Item)

Among the 186 respondents, 151 (81.2%) believed there might be a method to yield an ideal brow archetype, whereas 35 (18.8%) answered they did not.

Intention to Change the Brow Shape if an Expert Advises

Among the 185 valid responds, almost all (97.3%, 180) answered they will change the brow shape if an expert advises it. Only a few (5, 2.7%) answered they will not change despite an expert's recommendation.

Ideal Brow Height

The preference for the ideal brow height was different among the 3 heights queried ($P < 0.01$, 1.385×10^{-19} [χ^2]).

The middle height (63.2%, 115) was the most preferred followed by the upper height (29.7%, 54). The lower height was the least preferred (7.1%, 13).

The middle height was significantly preferred over the upper height ($P < 0.01$, [paired *t*-test]). The upper height was significantly preferred over the lower height ($P < 0.01$, [paired *t*-test]) (Fig. 3).

Young-Looking Brow Height

The preferences for the young-looking brow height were different among the 3 heights ($P < 0.01$, 1.303×10^{-17} [χ^2]).

The upper height (46.2%, 85) looked youngest followed by the middle height (39.7%, 73). The lower height was least preferred as a young brow (14.1%, 26).

The upper height and middle height was significantly preferred over the lower type as younger looking ($P = 0.001$, [paired *t*-test]), respectively. There were, however, no significant differences between the higher height and the middle height ($P = 0.341$, [paired *t*-test]) (Fig. 4).

Ideal Arch Shape

The preferences for the ideal brow arch shape were different among the 4 shapes ($P < 0.01$, 3.566×10^{-25} [χ^2]).

Among the 184 valid responses for this item, most (57.6%, 106) preferred the "arched" type as an ideal shape followed by the "head-up" (23.4%, 43). Fewer respondents choose the "horizontal" (14.1%, 26) or the "Tail-up" (4.5%, 9).

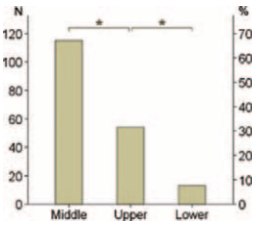

FIGURE 3. Ideal brow height,* $P < 0.01$; *N*, number of responses.

Copyright © 2015 Mutaz B. Habal, MD. Unauthorized reproduction of this article is prohibited.

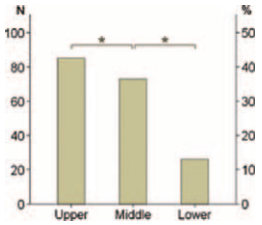

FIGURE 4. Young-looking brow height,* $P < 0.01$; *N*, number of responses.

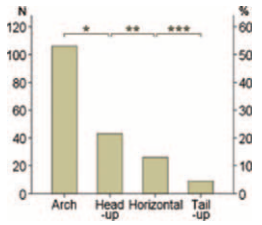

FIGURE 5. Ideal arch shape,* $P < 0.01$,** $P = 0.04$,*** $P = 0.004$; *N*, number of responses.

The arched was significantly preferred over the head-up ($P < 0.01$, [paired *t*-test]). The head-up was significantly preferred over the horizontal ($P = 0.04$, [paired *t*-test]). The horizontal was significantly preferred over the tail-up ($P = 0.004$, paired *t*-test]) (Fig. 5).

Young-Looking Arch Shape

The preferences for the young-looking brow arch shape were different among the 4 shapes ($P < 0.01$, 1.295×10^{-25} [χ^2]).

The head-up (53.3%, 98) looked the youngest followed by the horizontal (33.7%, 62). The arched was less preferred as a young-looking brow (12.0%, 22). The tail-up was the least preferred as a young-looking brow (1.0%, 2).

The head-up was significantly preferred over the horizontal ($P = 0.004$, [paired *t*-test]). The horizontal was significantly preferred over the arched ($P < 0.01$, [paired *t*-test]). The arched was significantly preferred over the tail-up ($P < 0.01$, [paired *t*-test]) (Fig. 6).

Preference of an Ideal and Young-Looking Brow Height and Arch Shape With the Score of the Sensitivity Following the Trend

Regarding the question whether the subjects follow trends, 23 (12.4%) answered definitely yes (score 5), 74 (39.8) answered yes (score 4), 80 responded neither yes or no, 8 (4.3%) wrote no, and only 1(0.5%) stated definitely no. Thereafter, the score of the sensitivity following trends (fashion) was 3.56 ± 0.78.

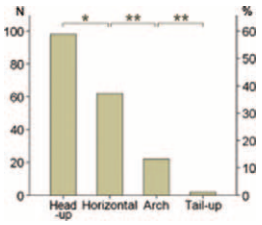

FIGURE 6. Young-looking arch shape,* $P = 0.004$, ** $P < 0.01$; *N*, number of responses.

There was no significant correlation between the preference for the ideal brow height and the score of the sensitivity following the trend ($P = 0.376$, [χ^2]).

There was also no significant correlation between the preference for the young-looking brow height and the score of the sensitivity following the trend ($P = 0.451$, [χ^2]).

There was a significant correlation between the preference for the ideal arch shape and the score of the sensitivity following the trend ($P = 0.040$, [χ^2]). All the score groups, however, answered "arch type" as the ideal arch shape.

There was also a significant correlation between the preference for the young-looking brow arch shape and the score of the sensitivity following the trend ($P = 0.036$, [χ^2]). Score 5, 3, 2 groups answered the "head-up type" as a young-looking arch shape.

Effect of Brow Shape on Face Image

Among the 186 valid responses for this item, most (92%, 171) answered that brow shape effects the face image. Only 1 (0.55) denied, and 14 (7.5%) answered they have no idea.

Ranking of the Important Structures Affecting Face Image

Among the 181 valid responses for this item, most (65.7%, 119) answered that the eye affects the face image most, followed by the brows (25.4%, 46), nose (13, 7.2%), and lips (3, 1.7%).

Eyes were significantly greater than brows ($P < 0.01$, [paired *t*-test]). Brows were significantly greater than the nose ($P < 0.01$, [paired *t*-test]). The nose was significantly greater than the cheeks ($P = 0.012$, [paired *t*-test]) (Fig. 7).

Eyebrow Makeup or Trimming

Among the 186 valid responses for this item, most (55.4%, 103) answered they apply makeup or trim eyebrows sometimes. Over one-third (68, 36.6%) trim or apply makeup frequently.

Preference of Brow Height and Arch Shape According to the Experience of Imitating the Makeup of Famous Stars

Over half (58.1%, 108) had an experience of imitating the makeup of famous stars whereas less than half (41.8%, 78) did not have any experience.

There was no significant correlation between the preference for the ideal brow height and the experience of imitating the makeup of famous stars ($P = 0.799$, [χ^2]). There was also no significant correlation between the preference for the young-looking brow height and the experience of imitating the makeup of famous stars ($P = 0.262$, [χ^2]). There was no significant correlation between the preference for the young-looking arch shape and the experience of imitating the makeup of famous stars ($P = 0.556$, [χ^2]).

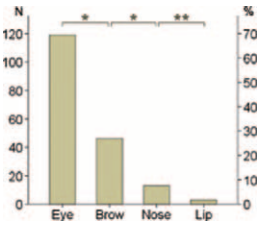

FIGURE 7. Ranking of the important structures affecting face image, * $P < 0.01$,** $P = 0.012$; *N*, number of responses.

© 2015 Mutaz B. Habal, MD

Copyright © 2015 Mutaz B. Habal, MD. Unauthorized reproduction of this article is prohibited.

There was a significant correlation between the preference for the ideal brow arch shape and the experience of imitating the makeup of famous stars ($P = 0.003$, [χ^2]). In the imitation experienced group, over half (74.1%, 54) preferred the arched as an ideal brow arch shape. In the imitation not-experienced group, the sum (48.0%, 50) of the head-up (28.8%, 30) and the horizontal (19.2%, 20) types exceeded that of the arched (46.2%, 48).

Preference of Brow Archetypes According to Age

Among the 186 respondents, 138 (74.2%) were younger than the age of 30, and 48 (25.8%) were older than 31 years of age.

There was no significant correlation between the preference for the ideal brow height and age groups of younger than 30 and older than 30 ($P = 0.512$, [χ^2]). There was also no significant correlation between the preference for the young-looking brow height and the age groups of younger than 30 and older than 30 ($P = 0.531$, [χ^2]). There was no significant correlation between the preference for the ideal arch shape and age groups of younger than 30 and older than 30 ($P = 0.054$, [χ^2]). There was also no significant correlation between the preference for the young-looking brow arch shape and the age groups of younger than 30 and older than 30 ($P = 0.089$, [χ^2]).

Preference of Brow Archetype According to Occupation

Among the 186 respondents, 49 (26.3%) were students, 90 (39.7%) were office workers, 15 (8.1%) were housewives, 22 (11.8%) were specialized workers, and 10 (5.4%) were others (unclassified occupations).

There was no significant correlation between the preference for the ideal brow height and occupation ($P = 0.277$, [χ^2]). There was also no significant correlation between the preference for the young-looking brow height and occupation ($P = 0.114$, [χ^2]). There was no significant correlation between the preference for the ideal arch shape and occupation ($P = 0.801$, [χ^2]).

There was a significant correlation between the preference for the young-looking brow arch shape and occupation ($P = 0.042$, [χ^2]). All the occupation groups, however, answered the head-up as a young-looking arch shape.

Preference of Brow Archetypes According to Level of Education

Among the 186 respondents, 19 (10.2%) were high school graduates, 53 (28.5%) were college students, 107 (57.5%) were college graduates, and 7 (3.8%) were in graduate school.

There was no significant correlation between the preference for the ideal brow height and level of education ($P = 0.884$, [χ^2]). There was also no significant correlation between the preference for the young-looking brow height and level of education ($P = 0.179$, [χ^2]). There was no significant correlation between the preference for the ideal arch shape and the level of education ($P = 0.347$, [χ^2]).

There was a significant correlation between the preference for the young-looking brow arch shape and the level of education ($P = 0.044$, [χ^2]). The graduate school group answered the horizontal as a young-looking arch shape whereas other groups chose the head-up as a young-looking shape.

Preference of Brow Archetypes According to Marital Status

Among the 186 respondents, 42 (22.6%) were married and 144 (77.4%) were single.

FIGURE 8. The most preferred ideal brow. Middle height and arched.

There was no significant correlation between marital status and the preference for the ideal brow height ($P = 0.299$, [χ^2]), or the preference for the young-looking brow height ($P = 0.909$, [χ^2]), or the preference for the ideal arch shape ($P = 0.594$, [χ^2]), or the preference for the young-looking brow arch shape ($P = 0.108$, [χ^2]).

Preference of Brow Archetypes According to Income

Among the 183 valid responses, 128 (69.9%) had a monthly income less than $3500 and 55 (30.1%) had an income greater than $3500.

There was no significant correlation between monthly income and the preference for the ideal brow height ($P = 0.237$, [χ^2]), or the preference for the young-looking brow height ($P = 0.370$, [χ^2]), or the preference for the ideal arch shape ($P = 0.388$, [χ^2]), or the preference for the young-looking brow arch shape ($P = 0.413$, [χ^2]).

DISCUSSION

In our previous study, Anastasia was the most preferred (44.8%, brow starts on a perpendicular line drawn from the middle of the nostril, arches on a line drawn from the center of the nose through the center of the pupil, and ends on a line drawn from the edge of the corresponding nasal ala through the outer edge of the eye) by Korean women.[5]

In this current study, we searched for the ideal and young-looking brow height and arch shape using modifications of the Anastasia type.

Approximately, half (52.5%) of the respondents answered their brow matches them very well or well. Most (81.2%) believed there might be a method to yield an ideal brow archetype and almost all (97.3%) would change the brow shape if an expert advised.

The most preferred an ideal brow height of middle height (63.2%, the distance from the lateral canthus to the lateral end of eyebrow was 2/3 of the eye width). The most preferred ideal brow arch shape was the arched (57.6% arches on a line drawn from the center of the nose through the center of the pupil) (Fig. 8).

The most preferred young-looking brow height was the upper height (46.2%, the distance from the lateral canthus to the lateral end of eyebrow was 3/4 of the eye width) followed by the middle height (39.7%). The most preferred young-looking brow arch shape was the head-up (53.3%, medial arm of the brow was rotated upward to horizontal plane) (Fig. 9).

Feser compared 3 different variations of eyebrows by interviewing 357 subjects in Germany and assumed the trend at the time (2007) appears to be moving away from arched eyebrows and toward lower positioned eyebrows with a maximum height in the lateral third.[6] His moving trend "with a maximum height in the lateral third" is very similar to the "arch at two-thirds of its length" in Hwang of our previous study. In our previous result, the

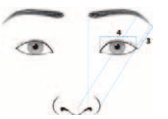

FIGURE 9. The most preferred young-looking brow. Upper height and head-up.

© 2015 Mutaz B. Habal, MD

Copyright © 2015 Mutaz B. Habal, MD. Unauthorized reproduction of this article is prohibited.

preference of the Anastasia exceeded that of Hwang in which the brow starts on a perpendicular line drawn from the middle of the nostril, arches at two-thirds of its length, and ends on an oblique line drawn from the middle of the nostril through the lateral canthus.[5]

Close-set eyes can be made to seem farther apart by starting the medial brow lateral to the medial canthus whereas wide-set eyes can be counteracted by starting the medial brow medial to the medial canthus.[7] The preference for Anastasia (44.8%, the brow starts on a perpendicular line drawn from the middle of the nostril) is believed to be the wide-set eyes of the Koreans than Caucasians.

Roth devised an aesthetic model for eyebrow arch position in 100 magazine photographs of fashion models. He measured eyebrow arch positions in a line through the medial canthus and lateral limbus parallel to the midline and they were compared with eye width.[8] In our study, we used the distances from the lateral canthus to the lateral end of eyebrow relative to the eye width. For the convenience of the responders in the brow bar, we used the simple ratios (3/4; upper height, middle height; 2/3, lower height; 3/5) and their drawings in the questionnaires.

Griffin suggested that the ideal modern female brow aesthetic is becoming lower, flatter, and with a more lateral peak.[7] In the current study, we saw Koreans who preferred the middle height (63.2%) and the arched (57.6%) as an ideal brow. They, however, believed the upper height (46.2%) and the head-up (53.3%) were young-looking brow.

Women with long faces should have lower and straighter eyebrows to prevent adding to the impression of an already long face. For square faces, typically heralded by a broad, angular jawline, the brow peak should be very gradual and the lateral brow segment should point more inferiorly, which softens the otherwise angular face.[9] There might be a possible explanation for the differences between our current study and Griffin's review. Finally, we have to quote Knize's article that "Given the wide variation in facial and eye dimensions, there is no mathematical solution to determine a universally beautiful female eyebrow."[10]

The result of this study might be useful in facial rejuvenation surgeries as well as in brow esthetics or tattooing of the eyebrows.

ACKNOWLEDGMENT

We are grateful to Kwan Hyun Youn, PhD, (medart@medart.co.kr), medical illustrator, for drawing of illustrations. We also thank Ye Seul Moon, cosmetic therapist, and So Hyun Choi, brow artist Benefit Cosmetics Korea, LTD., Incheon, for collecting data.

REFERENCES

1. Westmore MG. Facial cosmetics in conjunction with surgery. Paper presented at: Aesthetic Plastic Surgical Society meeting, May 7, 1974, Vancouver, BC, Canada; 1974.
2. Lamas P, Pemberton C. Eyebrows 101. How can you create beautiful eyebrows. 2013. Available at: http://www.lamasbeauty.com/beauty/november00/eyebrows-101.htm. Assessed December 31, 2013.
3. Anastasia SA. 1997. Available at: http://www.anastasia.net. Assessed December 31, 2013.
4. Schreiber JE, Singh NK, Klatsky SA. Beauty lies in the "eyebrow" of the beholder: a public survey of eyebrow aesthetics. *Aesthet Surg J* 2005;25:348–352
5. Kim SK, Cha SH, Hwang K, et al. Brow archetype preferred by Korean women. *J Craniofac Surg* 2014;25:1207–1211
6. Feser DK, Gründl M, Eisenmann-Klein M, et al. Attractiveness of eyebrow position and shape in females depends on the age of the beholder. *Aesthet Plast Surg* 2007;31:154–160
7. Griffin GR, Kim JC. Ideal female brow aesthetics. *Clin Plast Surg* 2013;40:147–155
8. Roth JM, Metzinger SE. Quantifying the arch position of the female eyebrow. *Arch Facial Plast Surg* 2003;5:235–239
9. Baker SB, Dayan JH, Crane A, et al. The influence of brow shape on the perception of facial form and brow aesthetics. *Plast Reconstr Surg* 2007;119:2240–2247
10. Knize DM. Anatomic concepts for brow lift procedures. *Plast Reconstr Surg* 2009;124:2118–2126

Optimization of Cranio-Orbital Remodeling: Application of a Mathematical Model

Kathryn V. Isaac, MD, Jochen Koenemann,† Ricardo Fukasawa,† David Qian, MMath,† Andre Linhares,† Nikoo R. Saber, PhD,‡ James Drake, MD,§ Christopher R. Forrest, MD,|| John H. Phillips, MD,|| and Phuong D. Nguyen, MD||*

Abstract: Cranio-orbital remodeling aims to correct the dysmorphic skull associated with craniosynostosis. Traditionally, the skull is reconstructed into a shape that is subjectively normal according to the surgeon's perception. We present a novel technique using a mathematical algorithm to define the optimal location for bony osteotomies and to objectively reshape the fronto-orbital bar into an ideal normal skull contour.

Using pre-operative computed tomography images, the abnormal skull contour at the frontal-orbital region was obtained for infants planned to undergo cranio-orbital remodeling. The ideal skull shape was derived from an age- and sex-matched normative skull library. For each patient, the mathematical technique of dynamic programming (DP) was applied to compare the abnormal and ideal skull shapes. The DP algorithm identifies the optimal location of osteotomy sites and calculates the objective difference in surface area remaining between the normative and dysmorphic skull shape for each solution applied. By selecting the optimal solution with minimal objective difference, the surgeon is guided to reproducibly recreate the normal skull contour with defined osteotomies.

The DP algorithm was applied in 13 cases of cranio-orbital remodeling. Five female and 8 male infants with a mean age of 11 months were treated for craniosynostosis classified as metopic (n = 7), unicoronal (n = 4), or bicoronal (n = 2). The mean OR time was 190.2 min (SD 33.6), mean estimated blood loss 244 cc (SD

From the *Division of Plastic and Reconstructive Surgery, University of Toronto, Toronto; †Department of Combinatorics & Optimization, Faculty of Mathematics, University of Waterloo, Waterloo; ‡Centre for Image Guided Innovation and Therapeutic Intervention; §Division of Neurosurgery; and ||Division of Plastic and Reconstructive Surgery, Centre for Craniofacial Care and Research, The Hospital for Sick Children, Toronto, Canada.

Received November 29, 2014.
Accepted for publication April 7, 2015.

Address correspondence and reprint requests to Kathryn V. Isaac, 909 Bay street, Unit 2305, Toronto Ontario, Canada M5S 3G2;
E-mail: kathryn.isaac@mail.utoronto.ca

The authors report no conflicts of interest.

Copyright © 2015 by Mutaz B. Habal, MD

ISSN: 1049-2275
DOI: 10.1097/SCS.0000000000001878

Copyright © 2015 Mutaz B. Habal, MD. Unauthorized reproduction of this article is prohibited.

147.6), and 10 infants required blood transfusions. Compared with a historical crania-orbital remodeling group treated without application of the algorithm, there was no significant difference in OR time, estimated blood loss, or transfusion rate.

This novel technique enables the craniofacial surgeon to objectively reshape the fronto-orbital bar and reproducibly reconstruct a skull shape resembling that of normal infants.

Key Words: bicoronal craniosynostosis, cranial vault reconstruction, Cranio-orbital remodeling, craniosynostosis, metopic craniosynostosis, unicoronal craniosynostosis

INTRODUCTION

Cranio-orbital remodeling aims to correct the malformed skull shape of infants with craniosynostosis, specifically the metopic, unilateral, and bilateral coronal synostoses. The surgeon must deconstruct the anterior cranium and reassemble irregular bone fragments to recreate an anatomically normal-appearing skull. The fronto-orbital bar (bandeau) is the foundation of this construct. Osteotomies may be performed at an infinite number of locations along the fronto-orbital bar to alter the curvature of the abnormal skull. However, the number of osteotomies is limited by the need to maintain its structural integrity. Reshaping the fronto-orbital bar relies on the surgeons' ability to correctly place osteotomies to create a normal curve based on their subjective perception or using templates.[1,2]

Other techniques for the correction of craniosynostosis include strip craniectomy procedures. The strip craniectomy procedures only resect the abnormal fused suture (suturectomy) and are usually combined with postoperative manipulation.[3–5] Spring-assisted or distractor-assisted postoperative manipulation enables expansion of the cranial vault, whereas external headbands or helmets apply restrictive forces post-strip craniectomy.[6] By contrast, the cranial vault remodeling procedures necessitate removing and rearranging sections of the cranial vault to recreate a normal shaped skull, based on the foundation of the fronto-orbital bar. Remodeling procedures are effective in correcting the shape and expanding the cranial vault volume. Cranial vault remodeling enables the surgeon to correct both the abnormal regions of overgrowth and regions of restricted undergrowth.[6] It is a highly effective and the most widely used procedure for the surgical correction of metopic, unilateral, and bilateral coronal synostoses.

Shaping of the front-orbital bandeau is challenging and critical as the foundation of rest of the cranial vault reconstruction. The intraoperative use of generic templates for shaping the fronto-orbital bandeau has been described.[1,2] These templates were contoured according to the surgeon's subjective perception of a normal skull shape. The osteotomies in the fronto-orbital bandeau were then performed to best recreate the curve of the subjectively contoured template. Subsequently, computer-aided design and manufacturing (CAD/CAM) templates derived from an age- and sex-matched normative skull library have been developed.[7–9] The prefabricated templates provide an intraoperative guide for the ideal normal curve at the fronto-orbital region, thereby eliminating the need for the subjective creation of the curve. During the cranial vault remodeling, the prefabricated template provides the surgeon with the ideal curve to reconstruct. However, attempting to recreate the ideal curve by performing multiple osteotomies to reshape a dysmorphic fronto-orbital bar is time-consuming, unpredictable, and, despite expert perceptive skills, may inaccurately reconstruct the desired template shape.

In this article, we present a simple and reproducible way of reshaping the fronto-orbital bandeau using mathematical programming to identify the optimal locations for performing the bony osteotomies.

TECHNIQUE

Prefabricated CAD/CAM bandeau templates help to guide the fronto-orbital reshaping and result in a reproducible correction of cranial dysmorphology.[7–9] The CAD/CAM bandeau templates are derived from an age- and sex-matched normative skull library generated for infants of 8 to 12 months.[7] This present study utilizes the construct of the ideal skull shape and seeks to optimize the attainment of the ideal contour by objectifying the steps to reshape the bone. The bandeau curve of the abnormal skull shape is obtained from the preoperative computed tomography (CT) scan for infants scheduled for cranio-orbital remodeling surgery. The abnormal fronto-orbital curve of the skull is compared with the normal curve of a sex- and age-matched normal skull, derived from the normative database.

The mathematical technique of dynamic programming (DP) is employed to determine the optimal location of osteotomy sites required to reshape the abnormal fronto-orbital bar into a normal skull shape.[10,11] DP determines where to position cuts (osteotomies) using a multistage decision process, in which each sequential optimal cut is based on the location of the previous one. Utilizing this backward recursive problem-solving technique, the optimal solution for transforming the dysmorphic shaped fronto-orbital bar into a normative skull shape is predictably determined. The curves of the deformed skull and normal skull are compared and the DP algorithm is applied to generate the optimal location of osteotomy sites based on the number of cuts the surgeon desires to perform (Fig. 1A-D).

The algorithm enumerates the location of the candidate osteotomies and each solution determined by the algorithm contains a specific number of cuts. For each solution, the algorithm performs a quantitative assessment of the area difference remaining between the normal and abnormal skull curves. This calculated objective difference in surface area (mm^2) remaining between the normative and abnormal skull shapes at the bandeau level is defined as the area under the curve (AUC). The AUC value represents the amount of deviation or "error" remaining between the ideal normal skull curve and patient's skull shape following the simulated osteotomies applied with the algorithm. A larger AUC value denotes a greater difference between the ideal normal skull and the dysmorphic skull

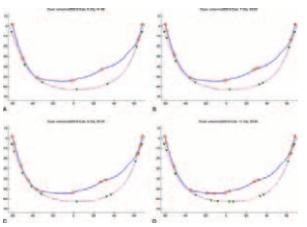

FIGURE 1. (A–D). Graphical representation of the algorithm applied to case of unicoronal craniosynostosis.[10] The curves of the normal (blue) and abnormal (red) skull shapes are shown with blue X marks on the red skull representing the entire set of candidate cut locations. The algorithm provides a unique solution for each incremental increase in the number of desired cuts; 5 cuts (A), 7 cuts (B), 9 cuts (C), 11 cuts (D). In each diagram, the red triangles represent cut locations on the abnormal skull, and the green triangles represent where they map to on the ideal skull. The appearance of the abnormal skull after osteotomies, rotation, and interposition is represented as the red curve overlapping the blue ideal skull to demonstrate how well the curves match. The area between the red and blue curves, representing the area of difference between the reshaped skull and the ideal is listed as the objective measure (AUC) in mm^2.

© 2015 Mutaz B. Habal, MD

Copyright © 2015 Mutaz B. Habal, MD. Unauthorized reproduction of this article is prohibited.

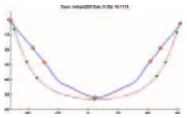

FIGURE 2. Solution derived from dynamic programming algorithm for correction of dysmorphology in the case of metopic craniosynostosis using 5 osteotomy sites.[10]

undergoing alterations with simulated cuts. As the number of cuts increases, the objective difference (AUC) between the reshaped and ideal skull diminishes, nearing perfection. Thus, the surgeon can determine the optimum number of cuts based on the improvement (decreasing AUC) with the addition of more cuts.

Three-dimensional stereophotographic images were obtained before and after surgery for assessment of the surgical outcome. The use of CT imaging for routine postoperative assessment of surgical correction following cranial vault remodeling has been discontinued in our practice due to the radiation-associated risks. The 3D images serve as a surrogate for objectively comparing the native dysmorphic contour and the reconstructed skull contour. Postoperative 3D images for 4 patients have been obtained to date.

CLINICAL REPORT

An infant with metopic craniosynostosis scheduled for cranio-orbital remodeling surgery underwent a standard preoperative CT scan. At the anatomical level of the bandeau site, the shape of the infant's skull was compared with an age- and sex-matched control normative skull shape. Preoperatively, the DP algorithm was applied and solutions derived for incremental number of cuts. Based on the minimal differential improvement in dysmorphology correction between the solutions for 5 and 7 cuts, a total of 5 osteotomy sites were selected (Fig. 2). The planned osteotomy site locations are marked on the patient-specific template to be used as a guide intraoperatively (Fig. 3A-B).

Intraoperatively, the marked template is fixed to the fronto-orbital bandeau and the identified locations for the wedge osteotomies are translated onto the skull.

The unicortical wedge osteotomies are performed, the inner table and diploe are removed and the fronto-orbital bandeau is conformed to the normative skull shape template (Fig. 4A-B). The reshaped fronto-orbital bandeau is then fixed on the external surface with absorbable hardware. Once the reshaping of the fronto-orbital bandeau is completed and it is secured to the skull, the remainder of the frontal and temporal region reconstruction is built upon the shape of the bandeau as the base.

RESULTS

The DP algorithm was applied in 13 cases of cranio-orbital remodeling. Five female and eight male infants with a mean age of 11 months were treated for craniosynostosis classified as metopic (n = 7), unicoronal (n = 4), or bicoronal (n = 2). For each case, the number of osteotomies performed was determined by selecting the algorithm solution with the greatest incremental drop in AUC for a given number of cuts. For this series of patients, the selected number of osteotomies ranged from 5 to 9.

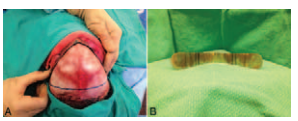

FIGURE 3. Intraoperative application of template (A) with planned osteotomy site locations (B). A midline osteotomy is performed and implied in all algorithm solutions.

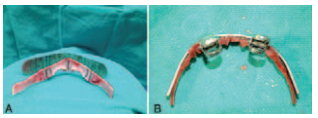

FIGURE 4. Intraoperative marking of fronto-orbital bandeau with osteotomy locations (A) and reshaped skull conforming to normative skull template (B).

The mean OR time was 190.2 min (SD 33.6), mean estimated blood loss was 244 cc (SD 147.6), and mean transfusion volume of 100 cc (SD 75.9). A comparison was performed with a historical cranio-orbital remodeling group. This historical group was similarly treated with the intraoperative use of the prefabricated CAD/CAM bandeau templates but without application of the DP algorithm to guide the osteotomies. For the historical group, the mean OR time was 218 min (SD 64.5), estimated blood loss 230 cc (SD 65.3), and required transfusion volume of 81.7 cc (SD 91.8). In this comparison, there was no significant difference observed in OR time, estimated blood loss, or transfusion volume.

A comparison of the pre-operative and post-operative 3D stereophotographic images demonstrates a qualitative improvement in the contour at the level of the fronto-orbital bar (Fig. 5). In these cases of metopic craniosynostosis correction, 9 cuts (Fig. 5A) and 7 cuts (Fig. 5B) were performed based on the selected algorithm solution for minimizing the objective difference between the ideal curve and the patients' dysmorphic curve.

DISCUSSION

This study describes the novel application of a mathematical algorithm to identify the optimal location of osteotomy sites in the fronto-orbital bandeau and reshape the deformed skull in craniosynostosis corrective surgery. We sought to devise an efficient method to reliably minimize the difference between the ideal skull shape and postoperative shape achieved. This algorithm enables the craniofacial surgeon to efficiently and reproducibly reconstruct a skull shape resembling that of normal infants.

The application of the algorithm results in an improved contour relative to a normative ideal skull. In this small case series, we demonstrated the successful preoperative application of the algorithm, intraoperative performance of the optimal solution, and postoperative result of an improved contour. The algorithm may be applied to all dysmorphic skull shapes of varying severity. It reliably calculates the multitude of potential solutions and instantly demonstrates the expected postoperative curve. The application of the algorithm in the preoperative planning provides the surgeon with an accurate depiction of the predicted postoperative shape. It offers the flexibility of selecting any number of cuts to achieve the desired shape, while minimizing the objective difference (AUC) between the ideal and reconstructed contour. Intraoperatively, this technique provides both the template of the ideal shape combined with guidance on number and location of osteotomies required to

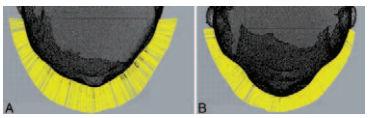

FIGURE 5. 3D stereophotographic bird's eye view of 2 patients (A and B) with metopic craniosynostosis treated with application of the dynamic programming algorithm. The preoperative skull contour is represented by the black wire mesh surface. The postoperative contour following remodeling with the application of the algorithm is represented by the outer yellow contour. The postoperative images were acquired 3 months (A) or 6 months (B) following surgery. The yellow surface area between the preoperative and postoperative skull contours represents the change in skull morphology secondary to both the remodeling procedure and physiologic growth of the skull.

© 2015 Mutaz B. Habal, MD

Copyright © 2015 Mutaz B. Habal, MD. Unauthorized reproduction of this article is prohibited.

achieve it. This technique minimizes the subjectivity, which is traditionally applied to reconstruct a perceived normal skull.

With the new application of this algorithm in our case series, there has been no demonstrated significant difference in OR time, estimated blood loss, or transfusion volume compared with a historical control group. Given the learning curve with the application of a new technique, we expect a reduction in the OR time with increasing experience, as all decisions required for reshaping the fronto-orbital bandeau are made preoperatively.

The AUC value is critical in the preoperative planning. It represents the objective difference or "error" remaining between the ideal curve and the expected postoperative curve achieved with a given number and location of osteotomies. The surgeon selects the algorithm solution based on the reduction of the AUC for a given number of osteotomies. These calculations are performed with CT-derived images of the osseous cranial vault. Our postoperative assessment performed with 3D imaging includes the soft tissues overlying the osseous skull. The 3D images provide a detailed depiction of the achieved result; however, these are not appropriate for comparison with the CT-derived images and calculated AUC. The time lapse between the preoperative and postoperative 3D images ranges from 3 to 9 months and the soft tissues overlying the remodeled skull precludes our ability to objectively compare the AUC preoperatively and postoperatively. This limitation due to skull growth and differing imaging modalities currently prevents accurate assessment of the postoperative result with objective numerical values. However, the 3D images provide a true representation of the postoperative contour achieved and offer a non-invasive low-risk modality for monitoring growth and contour correction at repeated intervals in the long term.

The novel application of this algorithm for the surgical correction of metopic, unilateral, and bilateral coronal synostoses enables the surgeon to predictably and reliably reshape the fronto-orbital bandeau. By eliminating the need to subjectively reshape the bandeau and select sites for the osteotomies, an improved contour relative to a normative, image data-derived ideal skull is achieved.

REFERENCES

1. Pappa H, Richardson D, Webb AAC, et al. Individualized template-guided remodelling of the front-orbital bandeau in craniosynostosis corrective surgery. *J Craniofac Surg* 2009;20:178–179
2. Burstein F, Eppley B, Hudgins R, et al. Application of the spanning plate concept to fronto orbital advancement: techniques and clinical experience in 60 patients. *J Craniofac Surg* 2006;17:241–245
3. Panchal J, Marsh JL, Park TS, et al. Sagittal craniosynostosis outcome assessment for two methods and timings of intervention. *Plast Reconstr Surg* 1999;103:1574–1584
4. Marsh JL, Jenny A, Galic M, et al. Surgical management of sagittal synostosis: a quantitative evaluation of two techniques. *Neurosurg Clin N Am* 1991;2:629–640
5. Jimenez DF, Barone CM. Endoscopic craniectomy for early surgical correction of sagittal craniosynostosis. *J Neurosurg* 1998;88:77–81
6. Fearon JA. Evidenced-based medicine: craniosynostosis. *Plast Reconstr Surg* 2014;133:1261–1275
7. Saber NR, Phillips J, Looi T, et al. Generation of normative pediatric skull models for use in cranial vault remodeling procedures. *Childs Nerv Syst* 2011;28:405–410
8. Burge J, Saber NR, Looi T, et al. Application of CAD/CAM pre-fabricated agematched templates in cranio-orbital remodeling in craniosynostosis. *J Craniofac Surg* 2011;22:1810–1813
9. Khechoyan D, Saber NR, Burge J, et al. Surgical outcomes in craniosynostosis reconstruction: The use of pre-fabricated templates in cranial vault remodeling. *JPRAS* 2014;67:9–16
10. Qian, D. (2013). Dynamic Programming: Salesman to Surgeon. University of Waterloo. Unpublished Master's Thesis, The University of Waterloo, Ontario
11. Bellman R. Dynamic Programming. New Jersey: University Press; 1957

Aging as the Impact Factor on Septoplasty Success

Mehmet Habesoglu, MD, Osman Kilic, MD, Basak Caypinar, MD, and Serap Onder, MD

Objective: The aim of the study was to discuss the impact of aging on septoplasty success.

Study Design and Setting: This prospective case control study was conducted at the Umraniye Education and Research Hospital.

Methods: Our study group consists of 23 patients older than 60-year-old who have septal deviation and have previously been postponed for this surgery due to various reasons. Twenty-six patients under 40-year-old are randomly chosen as the control group who were running to septoplasty. Postoperative Glasgow Benefit Inventory Index, preoperative and postoperative NOSE score, and nasal mucociliary clearance time (MCCt) were noted for both the groups. All collected data were compared between the groups.

Results: In both the groups, postoperative NOSE scores decreased significantly compared to preoperative values ($P < 0.01$). This decrease was not significantly different between the groups. In both the groups, a significant decrease was noted in nasal MCCt with surgery ($P = 0.004$). However, this difference between two groups was not statistically significant. In addition, the Glasgow Benefit Inventory (GBI) index of control group was notably higher than the study group and this was statistically significant ($P = 0.027$). Also, the decrease of NOSE scores was conversely related to high GBI indexes and this is statistically significant ($P = 0.005$).

Conclusion: For many surgical procedures, aging is considered as one of the important prognostic factors on success. To date no study in the literature discussed this relationship between aging and the success of septoplasty. At this point, our results showed that septoplasty is a successfully performed procedure in all ages. But, satisfaction of patients is statistically decreasing with aging.

Key Words: Age, Glasgow benefit inventory, nasal mucociliary clearance, success of septoplasty

Nasal obstruction is one of the major symptoms in otolaryngology practice.[1] The etiology of nasal obstruction can vary such as septal deviation, turbinate hypertrophy, concha bullosa, nasal polyps, and other sinonasal disorders.[2,3] Septal deviation is the most frequent cause of nasal dysfunction and nasal blockage.[3] Even small deviations in key areas have been shown to adversely affect nasal airflow, mucociliary clearance, and the external appearance of the nose.[4]

From the Department of Otorhinolaryngology, Umraniye Education and Research Hospital, Istanbul, Turkey.

Received February 21, 2015.
Accepted for publication April 7, 2015.

Address correspondence and reprint requests to Mehmet Habesoglu, MD, Department of Otorhinolaryngology, Umraniye Education and Research Hospital, Istanbul, Turkey; E-mail: mhabesoglu@yahoo.com

The authors report no conflicts of interest.

Copyright © 2015 by Mutaz B. Habal, MD

ISSN: 1049-2275
DOI: 10.1097/SCS.0000000000001879

Copyright © 2015 Mutaz B. Habal, MD. Unauthorized reproduction of this article is prohibited.

Septoplasty is the first preferred procedure performed for the treatment of the septal deviation. Improving nasal airflow is the primary goal of this operation. Epistaxis, sinusitis, obstructive sleep apnea, and headaches are other rare indications for septoplasty.[4] There are many studies and reviews about the improving effect of septoplasty on quality of life (QOL). Many methods such as rhinomanometry, acoustic rhinometry, QOL questionnaires, NOSE score, and nasal mucociliary clearance time (MCCt) have been used to evaluate indication and outcomes of surgeries for nasal obstruction.

In this study, we aimed to discuss the age factor for the success of the operation considering improvement on QOL after the operation. Here, we investigated the efficacy of septoplasty on the QOL even in advanced-age patients compared to earlier decades in the light of NOSE score, nasal MCCt, and Glasgow Benefit Inventory index.

MATERIAL AND METHODS

Study Objectives and Design

Our objective was to determine the efficacy of septal surgery on the QOL in different age groups by evaluating NOSE score, nasal MCCt, and Glasgow Benefit Inventory (GBI) index before and 6 months after the surgery.

Setting

This prospective study was conducted at the Umraniye Education and Treatment Hospital in Turkey. It was approved by the Umraniye Education and Treatment Hospital Ethical Committee and informed consent was obtained from the participants. The present study received no industrial support.

Subjects and Patient Characteristics

Individual investigators were responsible for allocating patients into the appropriate study groups. A total of 49 patients were enrolled in the study, whose completed surgery was analyzed. Twenty-three of the patients were over 60-year-old (study group) and 26 were under 40-year-old (control group). Patients were excluded based on the following criteria: (1) a history of previous endonasal surgery, (2) a history of underlying immunologic diseases that might interfere with wound healing, including acquired immunodeficiency syndrome, cystic fibrosis, immotile cilia syndrome, and systemic diseases, (3) heavy smokers, and (4) patients with chronic sinusitis or nasal polyposis. Outcome assessors were blinded.

Surgical Procedure

All septoplasties were performed by the same surgery team, under local anesthesia. Diazepam and atropine were used for premedication, 30 to 45 minutes before operation. Anesthesia with 2% lidocaine with 1:200.000 epinephrine was infiltrated submucosally before incision. Standard septoplasty was performed with the mucoperichondrial flap kept intact. We placed Doyle internal nasal splint and kept 2 days in nasal cavities before removal. Postoperatively, to prevent infection and pain, all patients in both groups were given the same systemic antibiotics and analgesics. In both the groups, patients were instructed to use normal saline nasal spray in both nostrils 10 times per day.

Outcome Measures

Both the groups were subjected to the same NOSE score, saccharine time test to measure nasal MCCt, and Glasgow Benefit Inventory index.

Subjective Symptom Determining With NOSE Score

Nasal obstruction symptom evaluation was performed with NOSE score: nasal congestion or stuffiness, nasal blockage or obstruction, trouble breathing through nose, trouble sleeping, and unable to get enough air through the nose during exercise or exertion.

We determined patients with the NOSE score before and after the surgery.

Objectively Measurement of Nasal Mucociliary Clearance

The nasal mucociliary activity was evaluated with saccharin time (ST) measurement for both nasal sides. Saccharin time measurement was performed as Stanley described on both sides inferior to inferior conchae without the use of a topical anesthetic agent to evaluate nasal mucociliary activity before and after septoplasty. The mean and standard deviation of ST were obtained.[5]

Glasgow Benefit Inventory Index

The GBI index measures QOL in 3 sections: social, general, and physical. It involves 18 questions; 12 of them evaluate general QOL improvement, whereas 3 of them relate to social and physical improvement. Each question has 5 possible options, wherein a score of 5 shows most favorable outcome and 1 least favorable outcome. A score of 3 shows no change. In our study, the GBI index was the subjective and patient-dependent tool used to measure the QOL of patients who were operated for septal deviation.[6]

Statistical Analysis

The IBM SPSS Statistics 22.0 program was used for all statistical analyses. Although study data were being determined, descriptive statistical methods (mean, standard deviation, and median) were used as the Mann-Whitney U test to compare the parameters which do not show normal distribution between the two groups and the Wilcoxon Signed Rank test for comparing in each group. Spearman rho correlation analysis was used to observe the relations between parameters. Results were determined in the safety zone of %95 and significance at $P<0.05$ level.

RESULTS

Preoperative and postoperative NOSE scores in the study group were 14.74 ± 2.82 and 2.83 ± 3.54, respectively ($P=0.001$). Also, preoperative NOSE scores were evaluated as 14.54 ± 2.83 in the control group and noted as 3.23 ± 4.55 after the operation ($P=0.001$). Although, in both of the groups, postoperative NOSE scores decreased significantly after the surgery, this decrease was not significantly different between the groups ($P=0.809$), (Table 1), (Fig. 1).

In both the groups, a significant decrease was noted in nasal MCCt with surgery ($P=0.004$). But the difference between two groups was not statistically significant ($P=0.566$) (Table 1), (Fig. 2).

Glasgow Benefit Inventory indexes of the control group were notably higher than the study group and this was statistically significant ($P=0.027$) (Fig. 3). When we compared the relationship between the decrease of NOSE score and MCCt with GBI indexes, decrease of NOSE score were statistically significant with high GBI indexes ($P=0.005$), (Fig. 4). But, when we evaluated the decreases of nasal MCCt and GBI indexes, there was no statistically significant connection ($P=0.759$).

DISCUSSION

Septal deviation is the most frequently detected reason of nasal blockage and septoplasty is one of the most commonly performed

© 2015 Mutaz B. Habal, MD

Copyright © 2015 Mutaz B. Habal, MD. Unauthorized reproduction of this article is prohibited.

TABLE 1. Differences of NOSE, MCCt and Glasgow Inventory Scores between the Groups

		Study Group	Control Group	†P
		Mean ± SD (Median)	Mean ± SD (Median)	
Nose	Preop	14.74 ± 2.82 (15)	14.54 ± 2.83 (14)	0.740
	Postop	2.83 ± 3.54 (2)	3.23±4.55 (2)	0.903
	Difference	11.91 ± 4.56 (13)	11.31 ± 4.96 (12)	0.809
	Preop–Postop ‡P	‡0.001**	‡0.001**	
MCCt§	Preop	12.78 ± 4.12 (12)	10.69 ± 4.93 (10.5)	0.145
	Postop	9.83 ± 7.71 (7)	7.27 ± 3.96 (7)	0.144
	Difference	2.95 ± 8.73 (3)	3.42 ± 5.05 (3)	0.566
	Preop–Postop ‡P	‡0.004**	‡0.002**	
Glasgow		71.87 ± 6.77 (71)	74.42 ± 8.92 (77.5)	0.027*

† Mann-Whitney U test.
‡ Wilcoxon Signed Ranks test.
§ MCCt, mucociliary clearance time.
* $P < 0.05$.
** $P < 0.01$.

surgeries by otolaryngologists.[1] Septoplasty can be performed by a traditional way or directed endoscopically.[4]

There are some factors affecting septoplasty success as –perop bleeding, fracture of quadrangular cartilage according to previous traumas, technique of septoplasty (close, open, and endoscopically approach) and nasal packing material.[7,8] Although aging is important for success of many surgical procedures, it is still not discussed in the present literature for septoplasty.

In the literature, the NOSE score and MCCt are usually used to evaluate the success of septoplasty. Nowadays different kinds of QOL questionnaires were described for the evalution of satisfaction of patients for the procedure. The Glasgow Benefit Inventory index is a well-designed questionnaire to determine the benefit of patient from the operation. It is sensitive and patient-dependent for the changes in health.[6]

Gandomi et al evaluated outcomes of septoplasty by the NOSE score and found significant improvement 3 months after surgery.[1] Bezerra et al investigated any difference in gender for septoplasty success and determined disease-specific QOL by the NOSE questionnaire. They found significant improvement with NOSE score

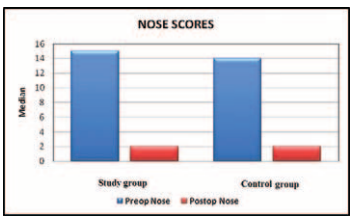

FIGURE 1. Evaluation of NOSE scores comparing preoperative values with postoperative values in the study groups.

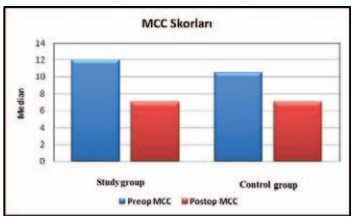

FIGURE 2. Decrease in nasal mucociliary clearance between the groups.

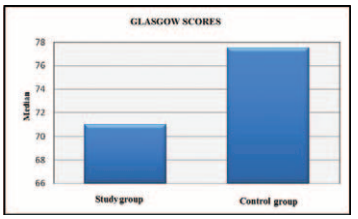

FIGURE 3. Evaluation of Glasgow benefit inventory scores in the study and control groups.

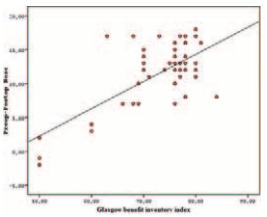

FIGURE 4. Comparison of relationship between the decrease in the NOSE score and Glasgow benefit inventory indexes.

but did not detect any difference in gender.[9] In our study, NOSE scores showed improvement for both the groups regardless of age according to data.

Uslu et al showed the decrease of MCCt after septoplasty and connected this data with the success of operation.[10] Sakallıoğlu et al declared that septoplasty operation positively affects the MCC mechanism.[11] We also found MCC time significantly decreased after septoplasty for both the groups. Improvement in MCCt after septoplasty is independent from the age factor.

Hytönen et al reported in 2012 an investigation about septoplasty for enhancing the QOL. They used a generic 15-dimension (15D) and the 22-item sinonasal outcome test (SNOT-22) questionnaires before and 6 months after surgery. They found that total SNOT-22 score was reduced, showing that the nasal symptoms decreased with septoplasty by the way health-related QOL became poorer. They claimed septoplasty enhances the QOL if the nasal symptoms are moderate or severe, but if the symptoms are mild and the patient is elderly, the surgeon has to be more careful to decide to operate.[12] We used the GBI index as QOL questionnaire after septoplasty individually for both the groups and found that the GBI index was statistically significant postoperatively. However, when we compared the groups, the GBI index of control group was statistically higher than the study group ($P = 0.027$). According to these data, we claim that septoplasty is a successfully performed procedure for all ages but satisfaction of patient for this procedure is higher in earlier ages than elderly. Also we have seen that decrease of NOSE scores is more effective subject on the QOL according to the decrease of nasal MCCt related to the GBI indexes. We think that the subjectively determining both NOSE score and GBI index personalizes the benefit of operation.

Septal deviation could be neglected by the younger people because of their intensive work schedule. So, physicians can receive these people at an advanced age. In this case, the physician should consider that septoplasty is a successfully performed procedure regardless of age but has better results for satisfaction of patient in earlier ages.

CONCLUSION

Sometimes physicians may consider septoplasty as an negligible procedure for the advanced-age patients. But they also should know QOL is valuable for all ages. At this point, our study supposed that

© 2015 Mutaz B. Habal, MD

Copyright © 2015 Mutaz B. Habal, MD. Unauthorized reproduction of this article is prohibited.

septoplasty is a successfully performed procedure at all ages but subjectively has more satisfactory results in early-age patients.

REFERENCES

1. Gandomi B, Bayat A, Kazemei T. Outcomes of septoplasty in young adults: the Nasal Obstruction Septoplasty Effectiveness study. *Am J Otolaryngol* 2010;31:189–192
2. Stewart MG, Smith TL, Weaver EM, et al. Outcomes after nasal septoplasty: results from the Nasal Obstruction Septoplasty Effectiveness (NOSE) study. *Otolaryngol Head Neck Surg* 2004;130:283–290
3. Stewart MG, Witsell DL, Smith TL, et al. Development and validation of the Nasal Obstruction Symptom Evaluation (NOSE) scale. *Otolaryngol Head Neck Surg* 2004;130:157–163
4. Van Olphen AF. The septum. In: Scott-Brown's otorhinolaryngology. *Head Neck Surg* 2008;2:1582–1588
5. Stanley P, MacWilliam L, Greenstone M, et al. Efficacy of a saccharin test for screening to detect abnormal mucociliary clearance. *Br J Dis Chest* 1984;78:62–65
6. Banerjee AS, Johnson IJ. Intratympanic gentamicin for Ménière's disease: effect on quality of life as assessed by Glasgow benefit inventory. *J Laryngol Otol* 2006;120:827–831
7. Karlsson TR, Shakeel M, Al-Adhami A, et al. Revision nasal surgery after septoplasty: trainees versus trainers. *Eur Arch Otorhinolaryngol* 2013;270:3063–3067
8. Konstantinidis I, Triaridis S, Triaridis A, et al. Long term results following nasal septal surgery. Focus on patients' satisfaction. *Auris Nasus Larynx* 2005;32:369–374
9. Bezerra TF, Stewart MG, Fornazieri MA, et al. Quality of life assessment septoplasty in patients with nasal obstruction. *Braz J Otorhinolaryngol* 2012;78:57–62
10. Uslu H, Uslu C, Varoglu E, et al. Effects of septoplasty and septal deviation on nasal mucociliary clearance. *Int J Clin Pract* 2004;58:1108–1111
11. Sakallioğlu O, Düzer S, Kapusuz Z, et al. The evaluation of nasal mucociliary activity after septoplasty and external septorhinoplasty. *Indian J Otolaryngol Head Neck Surg* 2013;65(Suppl 2):360–365
12. Hytönen ML, Lilja M, Mäkitie AA, et al. Does septoplasty enhance the quality of life in patients? *Eur Arch Otorhinolaryngol* 2012;269: 2497–2503

Efficacy of *N*-Acetylcysteine on Wound Healing of Nasal Mucosa

Beyhan Yilmaz, MD, Gül Türkçü, MD,† Engin Şengül, MD,* Aylin Gül, MD,* Fazil Emre Özkurt, MD,* and Mehmet Akdağ, MD**

Abstract: Postoperative nasal mucosa healing is a highly complex and organized process, and the success rates of endoscopic sinus surgery and septoplasty surgeries are closely associated with the postoperative wound healing processes. In this experimental study, the authors' aim was to use histopathologic examination to investigate the effects of *N*-Acetylcysteine (NAC) on the wound healing of rat nasal mucosa after mechanical trauma. Twenty-one Sprague-Dawley rats were randomly divided into 3 groups: the nontreated group (N = 7), the control saline group (N = 7), and the NAC group (N = 7). No treatment was given to the nontreated group for 15 days. The control saline group received intraperitoneal injection of saline (2.5 mL/kg, intraperitoneal) for 15 days and the NAC group was intraperitoneally injected with NAC at a dose of 300 mg/kg/day for 15 days. At the beginning of the study, unilateral mechanical nasal trauma was induced with an interdental brush inserted through the right nostril in all rats. Samples were stained using hematoxylin and eosin solution, and were examined by a pathologist using a light microscope. The severity of inflammation was milder in the NAC group compared with that in the nontreated and saline groups ($P < 0.05$). The subepithelial thickness index was lower in the experimental group ($P < 0.05$). Goblet cell loss was reduced in the experimental group compared with the nontreated and saline groups ($P < 0.05$). NAC decreases inflammation and goblet cell loss. Therefore, NAC has potential beneficial effects on the wound healing of nasal mucosa in rats.

Key Words: *N*-Acetylcysteine, nasal mucosa, wound healing

Nasal mucosa provides many functions such as temperature regulation by warming and humidifying the incoming air and preventing foreign bodies from occluding the airway.[1] To perform these functions, a healthy mucociliary clearance mechanism and normal cell structure are needed, because the nasal mucosa is lined by respiratory epithelium. The function of mucociliary clearance mechanism is easily disrupted by a number of conditions including trauma, surgery or foreign body exposure, and the wound healing is a time-taking process.[2] Postoperative nasal mucosa healing is a highly complex and organized process and it has been investigated by a limited number of studies.[3,4]

Endoscopic sinus surgery and septoplasty are commonly performed otorhinolaryngologic surgeries and the success rates of these surgeries are closely associated with the postoperative wound healing processes. The effects of anti-inflammatory drugs such as corticosteroids and caffeic acid phenethyl ester (CAPE) on postoperative nasal mucosa healing have been investigated in previous studies.[5,6]

N-Acetylcysteine (NAC), a thiol compound, is the *N*-acetyl derivative of L-cysteine, which has anti-inflammatory, antioxidant, and mucolytic properties. These properties have been investigated by numerous studies.[7–9] To our knowledge, however, no study has been reported regarding the potential histopathologic effects of NAC on nasal mucosa healing. Thus, the current study was aimed to present the potential histopathologic effects of intraperitoneally administered NAC on nasal mucosa healing in traumatized rats.

MATERIALS AND METHODS

The current study was conducted in accordance with Guide for the Care and Use of Laboratory Animals issued by the National Institutes of Health, Commission on Life Sciences, and the National Research Council.[10] Twenty-one Sprague-Dawley rats weighing 180 to 220 g were randomly divided into 3 groups: the nontreated group (N = 7), the control saline group (N = 7), and the NAC group

From the *Departmant of ENT; and †Departmant of Pathology, Dicle University Medical School, Diyarbakir, Turkey.
Received February 23, 2015.
Accepted for publication April 7, 2015.
Address correspondence and reprint requests to Beyhan Yilmaz, MD, Department of ENT, Dicle University, School of Medicine, Diyarbakir 21280, Turkey. E-mail: drbeyhanyilmaz@gmail.com
The authors report no conflicts of interest.
Copyright © 2015 by Mutaz B. Habal, MD
ISSN: 1049-2275
DOI: 10.1097/SCS.0000000000001880

Copyright © 2015 Mutaz B. Habal, MD. Unauthorized reproduction of this article is prohibited.

(N = 7). The rats were kept under standard environmental conditions (12-hour light/dark cycles, temperature between 22 and 24°C, and relative humidity at 50%). The rats were allowed free access to water and normal diet until they were sacrificed. The rats were anesthetized by intraperitoneal injection of ketamine hydrochloride (50 mg/kg; Ketalar, Pfizer, Istanbul, Turkey) and 2% xylazine hydrochloride (10 mg/kg; Rompun, Bayer, Istanbul, Turkey). Unilateral mechanical nasal trauma was induced with an interdental brush inserted through the right nostril in all rats.

No treatment was given to the nontreated group for 15 days. The control saline group received intraperitoneal injection of saline (2.5 mL/kg, intraperitoneal) for 15 days and the NAC group was intraperitoneally injected with NAC (Asist 10% ampoule, 300 mg/3 ml, Hüsnü Arsan, Turkey) at a dose of 300 mg/kg/day for 15 days. This dose was chosen based on the findings of the study by Sadowska et al[11] who reported that the in vitro antioxidant and anti-inflammatory efficacy of NAC is best achieved at a dose ranging between 150 and 500 mg/kg/day. The authors also found that the intravenous or intraperitoneal administration of NAC has a beneficial influence on inflammatory response compared with the more commonly performed oral administration. Depending on this finding, we preferred intraperitoneal administration of NAC in all the rats. The study was concluded on day 15, because the studies have shown that the inflammation in rat nasal mucosa reaches the highest level after 14 days.[4]

Tissue Preparation

All surgical procedures were carried out under nonsterile but clean conditions. At the end of 15 days, following the induction of anesthesia all rat noses were removed by microdissection. The noses were fixed in 10% formalin solution for 48 hours and decalcified in 10% formic acid solution for 4 days. Following the decalcification, samples were taken from the specimens and all specimens were embedded in paraffin after the routine histologic tissue preparation. The paraffin blocks were sliced with a microtome (Microm HM 360) in 4 to 5 mm thickness and stained with routine hematoxylin and eosin (H&E) method. All the stained specimens were evaluated by the same pathologist under a light microscope (Olympus BX53, Japan).

Histopathologic evaluations were performed according to the scoring system reported by Kinis et al.[6] The injured side was compared with the healthy side, which enabled the assessment of the loss in goblet cells and ciliated cells. The intensity of inflammation was evaluated just subjectively. The scoring system used for the histologic evaluation of the severity of inflammation, goblet cell loss, and ciliated cell loss is as follows: (0) none, (+) mild, (++) moderate, and (+++) severe. The epithelial thickness index (ETI) and subepithelial thickness index (STI) were scored as positive (+) or negative (−). These evaluations and scorings were made based on the scoring systems described in 2 previous studies on wound healing processes.[3,6]

The calculation of ETI and STI scores was performed based on the ratio of the average height of the regenerated epithelium or subepithelial tissue at the wound site to the height of the average epithelium or subepithelium in the contralateral side. The ratio was considered positive (+) if it was higher than 1, and negative (−) if lower than 1.

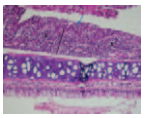

FIGURE 1. Severe loss of goblet cells and ciliated cells is shown in the nontreated group (blue arrow). Increased inflammation is present in subepithelial layer (asterisk). Thickness because of hypertrophy is present in the subepithelial layers (black arrow) (H&E, 200×).

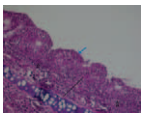

FIGURE 2. Severe loss of goblet cells and ciliated cells is shown in the in the saline (control) group (blue arrow). Increased inflammation is present in subepithelial layer (asterisk). Thickness because of hypertrophy is present in the subepithelial layers (black arrow) (H&E, 200×).

Statistical Analysis

All data were analyzed using the SPSS 15.0 software package for Windows (SPSS Inc. Chicago, IL). A χ^2 test was used for the comparison of the variations in the histologic categories between the nontreated, control saline, and NAC groups. The Kruskal-Wallis test was used for comparing continuous variables among the 3 groups, and the Mann-Whitney *U* test was used for intragroup distributions. A *P* value of <0.05 was considered significant.

RESULTS

The groups were compared for severity of goblet cell loss, ciliated cell loss, and inflammation. A significant difference was found between the groups in severity of goblet cell loss and inflammation, whereas no difference was found in ciliated cell loss (Table 1, Figs. 1-3).

Intragroup comparison of goblet cell loss revealed a significant difference between the nontreated and NAC groups ($P = 0.020$) and between the control saline and NAC groups ($P = 0.032$) (Table 2, Figs. 1-3). Similarly, intragroup comparison of severity of inflammation revealed a significant difference between the nontreated and NAC groups ($P = 0.019$) and between the control saline and NAC groups ($P = 0.019$) (Table 3, Figs. 1-3).

The comparison of STI values showed that the NAC had lower values compared with the nontreated and control saline groups and the difference was statistically significant ($P = 0.032$) (Table 4, Figs. 1-3). The comparison of ETI values, however, demonstrated that the nontreated and control saline groups had similar values and both of these values were slightly higher than those in the NAC group, but this difference was not statistically significant ($P = 0.366$) (Table 4).

TABLE 1. Comparison of Nontreated, Saline and NAC Groups by Means of Severity of Inflammation, Goblet Cell Loss and Ciliated Cell Loss

Variables	Nontreated Group Mean ± SD	Saline Group Mean ± SD	NAC Group Mean ± SD	*P* Value
Severity of inflammation	1.57 ± 0.53	1.57 ± 0.53	1.33 ± 0.57	0.030
Goblet cell loss	2.28 ± 0.75	2.00 ± 0.57	1.28 ± 0.72	0.028
Ciliated cell loss	1.71 ± 0.75	1.42 ± 0.53	1.33 ± 0.73	0.078

P value; Kruskal-Wallis test. NAC, *N*-Acetylcysteine.

© 2015 Mutaz B. Habal, MD

Copyright © 2015 Mutaz B. Habal, MD. Unauthorized reproduction of this article is prohibited.

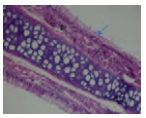

FIGURE 3. Mostly preserved goblet cells and ciliated cells are shown in the NAC group (blue arrow). A small number of inflammatory cell infiltration is present in subepithelial layer (asterisk). Significantly decreased subepithelial thickness (black arrow) (H&E, 200×).

DISCUSSION

Wound healing has been investigated in numerous studies. Most of these studies have investigated the wound healing processes in skin, and also Dorset-Martin et al reported a review in 2004.[12] In addition, there are a number of clinical studies conducted on nasal and paranasal sinus mucosal wound healing processes.[5,13–15] There are, however, a limited number of studies regarding the potential histopathologic effects of the agents on the nasal mucosal wound healing after mechanic trauma.[3,6,16] Some of these studies were performed by Khalmaturova et al,[3] Kinis et al,[6] and Şimşek et al,[16] who analyzed the effects of corticosteroids, CAPE, and phenytoin, respectively.

NAC has anti-inflammatory and antitoxic effects and it exerts these effects by inhibiting the release of LPS-induced lipid peroxidation, proinflammatory cytokines, and nitric oxide. Moreover, NAC also inhibits the proinflammatory transcription factor NF-κB and thus downregulates the expression of several proinflammatory genes.[7] Literature shows that NAC provides a number of preventive and protective effects against the toxic effects of several drugs in various tissues, including red blood cells, cochlea, kidney, tympanic membrane, brain, and heart.[17–21] To our knowledge, however, no study has been reported regarding the potential histopathologic effects of NAC on nasal mucosal wound healing. In the current study, we aimed to investigate the potential histopathologic effects of intraperitoneally administered NAC on nasal mucosa healing in traumatized rats.

The mucociliary clearance mechanism has a major role in the clearance and defense of upper respiratory airways. This mechanism filters the inhaled particles through the nasal mucosa layer. The nasal mucus consists of 2 layers: the outer layer, which is viscous and thick, and the inner sol layer, which is serous and relatively thinner. The serous fluid is secreted by the serous cells and the mucous fluid is secreted by the goblet cells. In mucous secretion, some mucins are produced and the most well-known mucins are glycoproteins, which are produced by the goblet cells and provide mucus with their viscous and elastic properties. By producing mucins, the goblet cells play an important role in mucociliary clearance.[22] Cilia are found in the sol layer and their tips connect the gel layer. Cilia move in the gel layer and push the entrapped particles toward the nasopharynx, thereby performing mucociliary clearance. Therefore, both cilia and the goblet cells have a major role in mucociliary clearance. The functions of cilia and the mucociliary clearance mechanism, however, can be easily disrupted by a number of conditions such as inflammation, mechanical trauma, respiratory tract infections, and toxic substances (such as cigarette smoke).[23,24]

Kinis et al[6] found that goblet cell loss and ciliated cell loss was lower in the CAPE group compared with the nontreated and control saline groups and thus suggested that CAPE has a protective effect on the mucociliary clearance mechanism.

Khalmaturova et al[3] reported that the number of regenerated goblet cells and ciliated cells in the control group was higher than the one in the dexamethasone group, which showed that the steroids have a negative effect on the mucociliary clearance mechanism because they lead to delayed mucosal regeneration of ciliated and goblet cells.

In our study, goblet cell loss, similar to the one in the study by Kinis et al,[6] was lower in the NAC group compared with the nontreated and control saline groups. We consider that this finding can be associated with the active role of NAC in the preservation of postoperative nasal mucociliary clearance.

Unlike the findings in study by Kinis et al,[6] however, the ciliated cell loss in our study was lower in the NAC group, but the difference was not statistically significant. This result may be related to the ciliary regeneration, which was also emphasized in the study by Khalmaturova et al.[3] The authors found that the ciliary regeneration did not end on day 28 after mucosal trauma and the process was still continuing. They suggested that 28 days are not sufficient for total ciliary regeneration; thus, longer observation time is needed. Athanasiadis et al[25] investigated the wound healing in sheep and found that reciliation was complete on the 84th day in a sheep model. Therefore, a rat model is not suitable and a longer observation time is needed.

TABLE 2. Severity of Goblet Cell Loss

Variables	No Infiltration (0) N	Mild (+) N	Moderate (++) N	Severe (+++) N	*P*1 Value	*P*2 Value
Nontreated	–	1	3	3		
Saline	–	1	5	1	0.020	0.032
NAC	–	5	2	–		

*P*1 value: Shows the difference between the nontreated and NAC groups; Mann-Whitney *U* test. *P*2 value: Shows the difference between the saline and NAC groups; Mann-Whitney *U* test. NAC, *N*-Acetylcysteine.

TABLE 3. Severity of Inflammation

Variables	No Infiltration (0) N	Mild (+) N	Moderate (++) N	Severe (+++) N	*P*1 Value	*P*2 Value
Nontreated	–	3	4	–		
Saline	–	3	4	–	0.019	0.019
NAC	1	6	0	–		

*P*1 value: Shows the difference between the nontreated and NAC groups; Mann-Whitney *U* test. *P*2 value: Shows the difference between the saline and NAC groups. Mann-Whitney *U* test. NAC, *N*-Acetylcysteine.

© 2015 Mutaz B. Habal, MD

Copyright © 2015 Mutaz B. Habal, MD. Unauthorized reproduction of this article is prohibited.

TABLE 4. Comparison of Epithelial and Subepithelial Thickness Positivity

Variables	ETI (+) N-percentage (%)	STI (+) N-percentage (%)
Nontreated	6 (% 85.7)	6 (% 85.7)
Saline	6 (% 85.7)	6 (% 85.7)
NAC	4 (% 57.1)	2 (% 28.6)
P value, Chi-squared test	0.366	0.032

ETI, epithelial thickness index; NAC, *N*-Acetylcysteine; STI, subepithelial thickness index.

In our study, the STI values in the NAC group were significantly lower compared with the nontreated and control saline groups. This finding was associated with a small number of inflammatory cell infiltration in subepithelial layer and decrease subepithelial thickness. The ETI values, however, were lower in the NAC group according to other 2 groups but the difference was not significant.

Khalmaturova et al[3] reported that the ETI and STI values established a significant difference between the dexamethasone and control groups, and the dexamethasone group had less subepithelial edema formation and inflammatory cell infiltration. They suggested that systemic dexamethasone administered after mucosal injury may have beneficial effects on postinjury wound healing.

Kinis et al[6] found that the STI values in the CAPE group were significantly lower compared with the nontreated and saline groups. The authors suggested that this finding was associated with the mild hypertrophy in the subepithelial layers and shows inflammation-reducing effects of CAPE. They found that the ETI values, however, were similar to the ones in the nontreated and saline groups and lower in the CAPE group, but the difference was not significant.

In our study, the ETI and STI values were found similar to those found by Kinis et al[6] and Khalmaturova et al.[3] Depending on these findings, we consider that NAC reduces the inflammatory response against the mechanic trauma in the nasal mucosa and this effect may play a crucial role in the postoperative wound healing.

In our study, the severity of inflammation, similar to those found by Kinis et al[6] and Khalmaturova et al[3] was lower in the NAC group compared with the other groups. Moreover, the severity of inflammation caused by fibrosis, neovascularization and inflammatory cell infiltration in the epithelial and subepithelial sites was significantly lower in the NAC group compared with the other groups. Moreover, the severity of inflammation caused by mechanical trauma was also lower in the NAC group.

We conclude that the administration of NAC following mucosal trauma may have beneficial effects for mucosal wound healing, less edema formation and adhesion, and milder loss of goblet cells and ciliated cells. NAC is an inexpensive drug and can be obtained easily, and using NAC after nasal surgeries such as septoplasty and sinus surgery may have positive effects for the success of surgery. Other animal models with longer observation times, however, need to be studied to better analyze the effects of NAC on the mucosal ciliary regeneration.

ACKNOWLEDGMENTS

The authors thank Dr. Yilmaz Palanci, Assistant Professor of Public Health, Dicle University School of Medicine, for his valuable contribution to the statistical analysis.

REFERENCES

1. Jeong GN, Jo GJ, Jo UB, et al. Effects of repeated welding fumes exposure on the histological structure and mucins of nasal respiratory mucosa in rats. *Toxicol Lett* 2006;167:19–26
2. Lindberg S. Morphological and functional studies of the mucociliary system during infection in the upper airways. *Acta Otolaryngol Suppl* 1994;515:22–24
3. Khalmuratova R, Kim DW, Jeon SY. Effect of dexamethasone on wound healing of the septal mucosa in the rat. *Am J Rhinol Allergy* 2011;25:112–116
4. Khalmuratova R, Jeon SY, Kim DW, et al. Wound healing of nasal mucosa in a rat. *Am J Rhinol Allergy* 2009;23:33–37
5. Jorissen M, Bachert C. Effect of corticosteroids on wound healing after endoscopic sinus surgery. *Rhinology* 2009;47:280–286
6. Kınıs V, Ozbay M, Akdag M, et al. Effects of caffeic acid phenethyl ester on wound healing of nasal mucosa in the rat: an experimental study. *Am J Otolaryngol Head Neck Med Surg D 2014* 482–486
7. Rocksen D, Lilliehook B, Larsson R, et al. Differential anti-inflammatory and anti-oxidative effects of dexamethasoneand *N*-acetylcysteine in endotoxin-induced lung inflammation. *Clin Exp Immunol* 2000;122:249–256
8. Palacio JR, Markert UR, Martínez P. Anti-inflammatory properties of *N*-acetylcysteine on lipopolysaccharide-activated macrophages. *Inflamm Res* 2011;60:695–704
9. Wu XY, Luo AY, Zhou YR, et al. *N*-acetylcysteine reduces oxidative stress, nuclear factor-κB activity and cardiomyocyte apoptosis in heart failure. *Mol Med Rep* 2014;10:615–624
10. Institute of Laboratory Animal Research, Commission on Life Sciences, National Research Council. The Guide for the Care and Use of Laboratory Animals. 7th ed. Washington, DC: National Academy of Sciences; 1996
11. Sadowska AM, Manuel-y-Keenoy B, De Backer WA. Antioxidant and anti-inflammatory efficacy of NAC in the treatment of COPD: discordant in vitro and in vivo dose-effects: a review. *Pulm Pharmacol Ther* 2007;20:9–22
12. Watelet JB, Bachert C, Gevaert P, et al. Wound healing of the respiratory mucosa: a review. *Am J Rhinol* 2002;16:77–84
13. Dorsett-Martin WA. Rat models of skin wound healing: a review. *Wound Repair Regen* 2004;12:591–599
14. Rowe-Jones JM, Medcalf M, Durham SR. Functional endoscopic sinus surgery: 5 years follow up and results of a prospective, randomized, stratified, double-blind, placebo controlled study of ostoperative fluticasone propionate aqueous nasal spray. *Rhinology* 2005;43:2–10
15. Kang IG, Yoon BK, Jung JH, et al. The effect of high-dose topical corticosteroid therapy on prevention of recurrent nasal polyps after revision endoscopic sinus surgery. *Am J Rhinol* 2008;5:497–501
16. Şimşek G, Ciftci O, Karadag N, et al. Effects of topical phenytoin on nasal wound healing after mechanical trauma: an experimental study. *Laryngoscope* 2014;124:449–454
17. Kashani MM, Saberi H, Hannani M. Prevention of acoustic trauma-induced hearing loss by *N*-acetylcysteine administration in rabbits. *Arch Trauma Res* 2013;1:145–150
18. Ozcan C, Görür K, Cinel L, et al. The inhibitory effect of topical *N*-acetylcysteine application on myringosclerosis in perforated rat tympanic membrane. *Int J Pediatr Otorhinolaryngol* 2002;63: 179–184
19. Grinberg L, Fibach E, Amer J, et al. *N*-acetylcysteine amide, a novel cell-permeating thiol, restores cellular glutathione and protects human red blood cells from oxidative stress. *Free Radic Biol Med* 2005;38: 136–145
20. Fox ES, Brower JS, Bellezzo JM, et al. *N*-acetylcysteine and alpha-tocopherol reverse the inflammatory response in activated rat Kupffer cells. *J Immunol* 1997;158:5418–5423
21. Finamor IA, Ourique GM, Pês TS, et al. The protective effect of *N*-acetylcysteine on oxidative stress in the brain caused by the long-term intake of aspartame by rats. *Neurochem Res* 2014;39: 1681–1690

© 2015 Mutaz B. Habal, MD

Copyright © 2015 Mutaz B. Habal, MD. Unauthorized reproduction of this article is prohibited.

22. Arredondo de Arreola G, López Serna N, de Hoyos Parra R, et al. Morphogenesis of the lateral nasal wall from 6 to 36 weeks. *Otolaryngol Head Neck Surg* 1996;114:54–60
23. Afzelius BA, Gargani G, Romano C. Abnormal length of cilia as a possible cause of defective mucociliary clearance. *Eur J Respir Dis* 1985;66:173–180
24. Ortuğ C. Scanning electron microscopic findings in respiratory nasal mucosa following cigarette smoke exposure in rats. *Ann Anat* 2003;185:207–210
25. Athanasiadis T, Beule AG, Robinson BH. Effects of a novel chitosan gel on mucosal wound healing following endoscopic sinüs surgery in a sheep model of chronic rhinosinusitis. *Laryngoscope* 2008;118:1088–1094

One-Stage Cleft Lip and Palate Repair in an Older Population

Ethem Guneren, MD, Halil Ibrahim Canter, MD, PhD,† Kemalettin Yildiz, MD,* Resit Burak Kayan, MD,* Mustafa Aykut Ozpur, MD,‡ Emre Gonenc Baygol, MD,§ Haci Omer Sagir, MD,† Ismail Melih Kuzu, MD,* Onur Akman, MD,* and Serap Arslan, MD*||*

Background: In underdeveloped countries one-stage definitive repair of cleft lip and palate is considered for late-presenting patients.

Materials and Methods: A total of 25 patients with unoperated cleft lip and palate more than 2 years of age were enrolled in this study for one-stage simultaneous repair of cleft lip and palate. According to Veau-Wardill-Kilner push-back technique, 2 flap palatoplasties were performed for palatal repairs; all of the lips were repaired with the Millard II rotation-advancement technique.

Results: The authors experienced no perioperative or postoperative life-threatening complications. With respect to the registered operation periods, longer times were required to perform these double operations, but this elongation is shorter than the sum of the periods if the 2 operations had been performed separately. Although the authors were unable to evaluate the late postoperative results because the authors could not follow-up the patients after they were discharged the day after surgery, the early results related to the success of the operation without any surgical complication were prone to meet the parents' and patients' expectations.

Discussion: The authors presented their experiences with many volunteer cleft lip and palate trips to third world countries; however the structure of this article is not a new hypothesis and data based to support a scientific study, but observations are objective to get a conclusion. To perform one-stage definitive repair of the cleft lip and palate in late-presented patients was the reality that they had only 1 chance to undergo these operations. According to the terms and conditions of this challenging operation, one-stage simultaneous repair of cleft lip and palate is a more demanding and time-consuming procedure than is isolated cleft lip repair or cleft palate repair. Although technically challenging, single-stage repair of the whole deformity in late-presenting patients is a feasible, reliable, successful, and safe procedure in authors' experience.

From the *Department of Plastic and Reconstructive Surgery, Bezmialem Vakif University, Instanbul; †Plastic and Reconstructive Surgery, Acibadem University, Istanbul; ‡Plastic and Reconstructive Surgery, Government Hospital, Adiyaman; §Plastic and Reconstructive Surgery, Government Hospital, Kirklareli, Turkey; and ||Turkiye Hospital, Instanbul.

Received July 24, 2014.
Accepted for publication April 9, 2015.

Address correspondence and reprint requests to Ethem Güneren, Bezmialem Vakif University, Istanbul, Turkey;. E-mail: eguneren@gmail.com

The authors report no conflicts of interest.

Copyright © 2015 by Mutaz B. Habal, MD

ISSN: 1049-2275
DOI: 10.1097/SCS.0000000000001881

Key Words: Abroad surgery, all-in-one-stage repair, charity, cleft lip, cleft lip and palate, cleft palate, late-presenting patients, simultaneous operation, surgical camp

Cleft lip and palate deformity is the second most frequently seen congenital anomaly.[1] Nasoalveolar molding (ie, preoperative infant orthopedics), multistage surgical interventions in early childhood, speech therapy, dental restoration, and orthognathic surgery represent the standard of care for excellent surgical outcomes in developed countries. In third world countries, however, patients who got chance to have an operation have only 1 bullet to fire.[2] Therefore, discussions on the excellence of surgical cleft repair are difficult in such situations. Late-presenting patients are even more demanding. One-stage definitive repair of cleft lip and palate anomaly should be considered in most of these patients. Surgery is also challenging because of the wide variations among the clefts at advanced ages and suboptimal surgical conditions while striving for optimal outcomes. No revision operations can be planned because these operations were usually performed in nongovernmental, charity organization, surgical camps at one time in these countries.[3–11]

One-stage simultaneous repair of cleft lip and palate anomaly was first described by Kaplan et al.[12–14] There are several simultaneous primary repair techniques for cleft lip and palate, such as cleft lip and simple posterior soft palate palatoplasty[15]; repair of unilateral clefts of the lip and primary palate[16]; nose, anterior palate, and lip repair[17]; repair of the lip and hard palate, and lip and hard and soft palate[18]; bilateral cleft lip and nose repair[19]; repositioning of the premaxilla and repair of bilateral cleft lip deformity[20]; cleft lip and cleft hard palate repair with vomer flaps[21]; and combined lip and palatal repair with Orticochea sphincter repair.[22]

Bardach et al[23–25] studied the craniomaxillofacial effects of one-stage simultaneous repair of acquired cleft lip and palate deformity in animals, although this did not realistically simulate the congenital anomaly. Their results showed that simultaneous repair had adverse effects on maxillofacial growth. Results of clinical studies, however, are even more controversial; whereas some studies have revealed no adverse effects of one-stage simultaneous repair of cleft lip and palate,[26] others have demonstrated craniomaxillofacial growth retardation.[27–29]

Although technically challenging, single-stage repair of the whole deformity in late-presenting patients is a feasible, reliable, successful, and safe procedure.[4–6,8,9,20,27,28] The aim of this study was to present the terms and conditions of one-stage definitive repair of late-presenting cleft lip and palate in our experiences.

MATERIALS AND METHODS

Patients

We participated several plastic surgery camps in different countries in Asia, Middle East, and Africa between 2007 and

© 2015 Mutaz B. Habal, MD

Copyright © 2015 Mutaz B. Habal, MD. Unauthorized reproduction of this article is prohibited.

2014. These camps were organized by the Turkish International Cooperation and Development Agency, and supported by the Turkish Branch of Doctors World Wide Organization, which is a nonprofit, nongovernmental charity. All of the patients were treated free of charge. We called these surgical camps the Smiling Children Projects for similarity to other such camps including the Smile Train, Operation Smile, Save Smile, and etc.

Initially, all of the patients in that region were assessed by a visiting/pioneer doctor of the charity. The team and equipment were then prepared accordingly depending on the list of the scheduled patients. The terms and conditions of the operation facilities are out of the scope of this study, but basic vital conditions were established properly. Because of ethical considerations, we do not declare the names of the hospitals or countries in this article. The registered files of the patients have been saved in the archives of the association. Informed consent was obtained in native languages of the patients.

Surgery

According to Veau-Wardill-Kilner push-back technique, 2 flap palatoplasties were performed for palatal repairs, regardless of whether the patient had a complete or incomplete cleft. Vomerine flap was used in appropriate patients to facilitate and secure the closure. Most anterior part at alveolar bone region of complete clefts left untouched. After removal of the mouth retractor, the hyperextended position of the head was neutralized for lip repair. All of the lips were repaired with the Millard II rotation-advancement technique regardless of whether they had complete or incomplete clefts. C flaps were used for columellar lengthening, medial rotation of ala along the alar wing incision was done in flared cases and releasing and suspending alar cartilage at the same time can correct nasal deformity. After nasal base, vestibular mucosa and muscle repair, lip mucosa was repaired in a double-breasted fashion.

RESULTS

Twenty-seven plastic surgery camps were conducted by the senior author of this study, who is certified by the European Board of Plastic Reconstructive and Aesthetic Surgery. A total of 1371 cleft operations were performed, 540 were incomplete or complete—unilateral or bilateral cleft lip, 309 were incomplete or complete cleft palate, and 522 were complete or incomplete—unilateral or bilateral cleft lip and palate. Patients with cleft lip and palate more than 2 years of age and suitable for one-stage simultaneous repair were enrolled in this study for one-stage simultaneous repair of cleft lip and palate (n = 25). In our series, the youngest patient was 2-year-old, and the oldest was 42-year-old. The mean age was 10 years. Eleven of 25 patients were women. Nine patients were bilateral. A total of 6 of 16 unilateral clefts were placed on right side (Table 1).

With respect to the registered operation periods, one-stage repair of cleft lip and palate takes longer time to perform compared with repair of either cleft lip or palate alone. Although one-stage simultaneous repair of cleft lip and palate requires a long period to perform, we fortunately experienced no perioperative or postoperative complications associated with anesthesia. In addition, neither bleeding-related nor wound-related problems occurred. We were unable to evaluate the late postoperative results because we could not follow-up the patients after they were discharged the day after surgery. Sample patients are shown in figures (Figs. 1–4).

TABLE 1. Distribution of Cases Among Cleft Types, Ages, and Sex

	Clefts	Age	Sex
1	Left unilateral complete cleft lip and palate	2	F
2	Left unilateral complete cleft lip and palate	5	M
3	Bilateral complete cleft lip and palate (Figure 1)	12	M
4	Right unilateral complete cleft lip, and cleft palate	7	M
5	Left unilateral complete cleft lip and palate (Figure 2)	42	F
6	Bilateral complete cleft lip and palate	17	M
7	Left unilateral complete cleft lip and palate	3	F
8	Left unilateral complete cleft lip and palate	19	M
9	Right unilateral complete cleft lip and palate (Figure 3)	8	F
10	Left unilateral complete cleft lip and palate	10	M
11	Bilateral complete cleft lip and palate	13	F
12	Left unilateral complete cleft lip and palate	3	M
13	Bilateral incomplete cleft lip and incomplete cleft palate (Figure 4)	4	M
14	Bilateral complete cleft lip and palate	4	M
15	Left unilateral complete cleft lip and palate	10	M
16	Bilateral complete cleft lip and palate	19	F
17	Bilateral complete cleft lip and palate	17	F
18	Right complete cleft lip, and incomplete cleft palate	4	M
19	Bilateral complete cleft lip and palate	4	F
20	Left unilateral complete cleft lip and palate	19	F
21	Bilateral complete cleft lip and palate	14	M
22	Left unilateral complete cleft lip and palate	6	M
23	Right unilateral complete cleft lip and palate	3	F
24	Right unilateral complete cleft lip and palate	9	M
25	Right unilateral complete cleft lip and palate	12	F

DISCUSSION

The treatment algorithm of cleft lip and/or cleft palate has been well established and multidisciplinary multistage treatment has been accepted in most respectable cleft centers. Although one-stage simultaneous repair of cleft lip and cleft palate is not a frequently performed operation, the specific indication of one-stage simultaneous repair along with the advantages and drawbacks are herein discussed.[2] Moreover, as one-stage simultaneous repair of cleft lip and cleft palate is done for late-presenting patients, treated during charity activities in third world countries, not only the operative technique but also the operative conditions and facilities, organizational details, and gained experience during these activities has been presented in detail.

The main factor to perform one-stage definitive repair of the cleft lip and palate in our series was the reality that these patients had only 1 chance to have this operation. Unfortunately, neither plastic surgeons nor well-educated health professional are available to deliver this health service to these patients in these countries. Moreover, neither those countries have high-quality hospitals to deliver that care nor the patients could afford the operation fees.[3–5,9,10,20,22,30,31]

As we had only 1 chance to touch these patients to make a difference in their life, everything was set for it; that is, most reliable palatal and cleft lip repair procedures were chosen to decrease the necessity of revision procedures, absorbable suture materials were used to avoid suture removal, prophylactic and postoperative antibiotics were prescribed to decrease the risk of infections, etc.

FIGURE 1. A-B, Intra- and postoperative views of a 12 year old boy with bilateral complete cleft lip and palate.

© 2015 Mutaz B. Habal, MD

Copyright © 2015 Mutaz B. Habal, MD. Unauthorized reproduction of this article is prohibited.

FIGURE 2. A-B, Pre- and postoperative views of a 42 years old female patient with left unilateral complete cleft lip and palate.

FIGURE 3. A-B, Pre- and postoperative views of an 8 year old girl with right unilateral complete cleft lip and palate.

The Veau-Wardill-Kilner push-back palatoplasty was chosen for palatal repair technique because it is easy, rapid, and safe technique.[30] Although it is strongly recommended in the literature, we did not insert ventilation tubes to the ears because it would have further complicated the procedure and would have necessitated the otolaryngologic follow-up in treatment process.[32] The Millard II rotation-advancement technique was performed for the repair, as it is a cut-as-you-go method, easy to perform, more adjustable and reliable technique.

One-stage simultaneous repair of cleft lip and palate is technically more demanding and time-consuming procedure than is isolated cleft lip repair or cleft palate repair[31]; however, a one-stage procedure still takes less time to perform than does separate performance of cleft lip repair and cleft palate repair.

There is a common belief among the majority of surgeons dealing specifically with cleft lip/palate surgery that early one-stage simultaneous repair of the hard and soft palates adversely affects maxillofacial development. Although this proposition has not been proven in long-term clinical studies, it is accepted that any type of palatal repair has a detrimental effect on craniomaxillofacial growth to some extent. Although palatal repair procedures have been simulated in animal studies, the actual clinical scenario is different.[23–25] In addition to the lack of normal tissue insertions and/or placements, there is the presence of a variety of degrees of hypoplasia, which is termed developmental hypoplasia from an embryologic point of view. True insertion of the muscles to the bones and their regular function aid development.[26–29,30–34] In addition to developmental hypoplasia, the trauma of the surgical intervention has inevitable adverse effects on growth. Because of the lack of long-term follow-up, it is not possible to make a comment on effect of our surgery in developmental maxillofacial growth of our patients. On the contrary, because some of our patients had already gone through adolescence at the time of surgery, we do not expect any relevant association between the surgery and their facial developmental pattern.

FIGURE 4. A-D: Pre-, intra-, and postoperative views of a 4 year old boy with bilateral incomplete cleft lip and incomplete cleft palate.

It is well known that the performance of anterior palate repair after cleft lip repair in patients with complete cleft lip and palate may be very difficult. Such an anterior palate repair procedure requires wide, extensive, and difficult dissection. Additionally, the risks of wound infection, wound dehiscence, complete wound disruption, recurrent oronasal fistula formation, and maxillary hypoplasia increase.[17,21] Therefore, one-stage simultaneous repair of cleft lip and palate may be a reliable treatment option that ensures complete recovery in 1 session. We found that cleft repair was easier to perform when beginning from the posterior region and progressing forward with wide exposure of all of the anatomical structures. This made it possible to use any excess tissue for neighboring structures instead of discarding it.

Parents' and patients' satisfaction with surgeries performed abroad has also been discussed in the literature with respect to various ethnicities.[3,6,7–9,21,35–37] We experienced high parents' and patients' satisfaction rate in this series, which may be due to the fact that they may not have had any other chances to undergo any other operation and/or they have initially low expectation rates for the surgical outcomes.

The most challenging aspect of these voluntary humanity missions was the logistic planning of the mission. Although team member doctor visited initially the district of the county to determine the number of the patients who would be operated and the facilities of the local hospitals, it was not possible to guess the real scenario in our first few trips. We initially determined the number of the days that the team will stay in that area, surgical instruments and surgical supplies, etc, according to our first assessment. Then by the time the team arrived, the news was heard not only in that specific district of the country but spread out to whole country and the numbers of the patients blowout. The days that we planned to stay there were enough to handle all of the applications for surgery. Even if the team members were ready to operate till midnight, the surgical supplies that could not be obtained from local market were depleted. Additionally, there was not enough heath care professional both in terms of number and medical quality to handle and serve the enormous number of postoperative cases. In our initial assessment, we have only determined the capability of the sterilization facility of the local hospital but not the speed of their sterilization capacity. It became obvious that sterilization facilities were far behind our requirements once we began to operate in terms of resterilization of the instruments. Finally, we decided to stick to our initial plan and to restrict the number of patients to the limit that we could deliver the best medical care without risking their life or surgical outcomes. In the following missions, we decided to travel with at least 25% excess of the estimated surgical supplies. Additionally, the voluntary surgical residents and nurses who

© 2015 Mutaz B. Habal, MD

Copyright © 2015 Mutaz B. Habal, MD. Unauthorized reproduction of this article is prohibited.

wanted to be involved in preoperative preparation and postoperative care of the patients were welcomed as team member to these missions. It was requested from local authorities not to exaggerate the arrival of the team on local news. We began to carry our portable autoclave sterilizer unit and high-level disinfecting solution for the disinfection of our surgical instruments with us in our missions. A team member doctor was left behind for few more days to ensure safety and well being of the patients in early postoperative period.

The surgical advantages of one-stage definitive repair of cleft lip and palate in late-presenting patients are as follows:

- It is possible to repair the cleft as a whole because of easier handling and dissection of well-developed, mature tissues, which have greater strength to retain the sutures.
- It is possible with fewer airway disturbances.
- Maxillary growth retardation is not a consideration in advanced age groups.
- Although it takes longer time to perform a one-stage combined procedure, it is still shortening than the sum of the periods if the 2 operations had been performed separately.
- Overall hospitalization period in combined procedure is less than the sum of the hospitalization periods of the 2 separate operations.
- Use of a large vomer flap facilitates closure of the hard palate.
- Rapid improvement occurs in the psychologic and social conditions of patients and parents.
- The surgical results are prone to better meet the parents' and patients' expectations because they have more realistic expectations.

The disadvantages of one-stage definitive repair of cleft lip and palate in late-presenting patients are as follows:

- Correction of the anterior part of the nasal deformity is difficult because adults have less elasticity and more severe deformity of the nasal cartilage.
- Although cheiloplasty under local anesthesia can reduce cost, time, and manpower in late-presented patients, simultaneous palatoplasty requires general anesthesia.

Our "all-in-one-session" principle could be taken into consideration in selected patients, who are more than the age of routine operations and have no other chance to be operated again. When we operate in third world countries, there is no question of delivering the same standards of care to the patients there that we deliver to our patients in our own country.

REFERENCES

1. Millard RD. Cleft craft. The incidence of clefts in the world. 1:57–68. calder.med.miami.edu/Ralph_Millard/ebooks.html
2. Murthy J. Management of cleft lip and palate in adults. *Indian J Plast Surg* 2009;42:S116–S122
3. Aziz SR, Rhee ST, Redai I. Cleft surgery in rural Bangladesh: reflections and experiences. *J Oral Maxillofac Surg* 2009;67:1581–1588
4. Hodges S, Wilson J, Hodges A. Plastic and reconstructive surgery in Uganda: 10 years experience. *Paediatr Anaesth* 2009;19:12–18
5. Morioka D, Yoshimoto S, Udagawa A, et al. Primary repair in adult patients with untreated cleft lip-cleft palate. *Plast Reconstr Surg* 2007;120:1981–1988
6. Gupta K, Bansal P, Dev N, et al. Smile Train project: a blessing for population of lower socio-economic status. *J Indian Med Assoc* 2010;108:723–725
7. Uetani M, Jimba M, Niimi T, et al. Effects of a long-term volunteer surgical program in a developing country: the case in Vietnam from 1993 to 2003. *Cleft Palate Craniofac J* 2006;43:616–619
8. Luyten A, D'haeseleer E, Budolfsen D, et al. Parental satisfaction in Ugandan children with cleft lip and palate following synchronous lip and palatal repair. *J Commun Disord* doi: 10.1016/j.jcomdis.2013.03.001
9. Olasoji O, Arotiba T, Dogo D. Experience with unoperated cleft lip and palate patients in a Nigerian teaching hospital. *Trop Doct* 2002;32:33–36
10. Schwarz R, Bhai Khadka S. Reasons for late presentation of cleft deformity in Nepal. *Cleft Palate Craniofac J* 2004;41:199–201
11. Onah II, Opara KO, Olaitan PB, et al. Cleft lip and palate repair: the experience from two West African sub-regional centres. *J Plast Reconstr Aesthet Surg* 2008;61:879–882
12. Kaplan I, Dresner J, Gorodischer C, et al. The simultaneous repair of cleft lip and palate in early infancy. *Br J Plast Surg* 1974;27:134–138
13. Kaplan I, Taube E, Ben-Bassat M, et al. Further experience in the early simultaneous repair of cleft lip and palate. *Br J Plast Surg* 1980;33:299–300
14. Kaplan I, Ben-Bassat M, Taube E, et al. A ten-year follow-up of simultaneous repair of cleft lip and palate in infancy. *Ann Plast Surg* 1982;8:227–228
15. Lo LJ, Huang CS, Chen YR, et al. Palatoalveolar outcome at 18 months following simultaneous primary cleft lip repair and post palatoplasty. *Ann Plast Surg* 1999;42:581–588
16. Carstens MH. The sliding sulcus procedure: simultaneous repair of unilateral clefts of the lip and primary palate: a new technique. *J Craniofac Surg* 1999;10:415–429
17. Laberge LC. Unilateral cleft lip and palate: simultaneous early repair of the nose, anterior palate and lip. *Can J Plast Surg*. 2007;15:13–18.
18. De Mey A, Franck D, Cuylits N, et al. Early one-stage repair of complete unilateral cleft lip and palate. *J Craniofac Surg* 2009;20S2:1723–1728
19. Penfold C, Dominguez-Gonzalez S. Bilateral cleft lip and nose repair. *Br J Oral Maxillofac Surg* 2011;49:165–171
20. Lee UL, Cho JB, Choung PH. Simultaneous premaxillary repositioning and cheiloplasty in adult patients with unrepaired bilateral cleft lip and palate. *Cleft Palate Craniofac J* 2013;50:231–236
21. Ferdous KM, Selak AJ, Islam MK, et al. Repair of cleft lip and simultaneous repair of cleft hard palate with vomer flap in unilateral complete cleft lip and palate: a comparative study. *Pediatr Surg Int* 2010;26:995–1000
22. Schwarz RJ. Combined repair of lip and palate with pharyngoplasty for late presenting clefts. *Scand J Plast Reconstr Surg Hand Surg* 2006;40:210–213
23. Bardach J, Roberts DM, Yale L, et al. The influence of simultaneous cleft lip and palate repair on facial growth in rabbits. *Cleft Palate J* 1980;17:309–318
24. Bardach J, Kelly KM, Jakobsen JR. Simultaneous cleft lip and palate repair: an experimental study in beagles. *Plast Reconstr Surg* 1988;82:31–41
25. Bardach J, Kelly KM, Salyer KE. A comparative study of facial growth following lip and palate repair performed in sequence and simultaneously: an experimental study in beagles. *Plast Reconstr Surg* 1993;91:1008–1016
26. Liao YF, Mars M. Long-term effects of palate repair on craniofacial morphology in patients with unilateral cleft lip and palate. *Cleft Palate Craniofac J* 2005;42:594–600
27. Fudalej P, Obloj B, Miller-Drabikowska D, et al. Midfacial growth in a consecutive series of preadolescent children with complete unilateral cleft lip and palate following a one-stage simultaneous repair. *Cleft Palate Craniofac J* 2008;45:667–673
28. Savaci N, Hoşnuter M, Tosun Z, et al. Maxillofacial morphology in children with complete unilateral cleft lip and palate treated by one-stage simultaneous repair. *Plast Reconstr Surg* 2005;115:1509–1517
29. Fudalej P, Hortis-Dzierzbicka M, Obloj B, et al. Treatment outcome after one-stage repair in children with complete unilateral cleft lip and palate assessed with the Goslon Yardstick. *Cleft Palate Craniofac J* 2009;46:374–380
30. Kwari DY, Chinda JY, Olasoji HO, et al. Cleft lip and palate surgery in children: anaesthetic considerations. *Afr J Paediatr Surg* 2010;7:174–177
31. Adenekan AT, Faponle AF, Oginni FO. Anesthetic challenges in orofacial cleft repair in Ile-Ife, Nigeria. *Middle East J Anesthesiol* 2011;21:335–339

© 2015 Mutaz B. Habal, MD

Copyright © 2015 Mutaz B. Habal, MD. Unauthorized reproduction of this article is prohibited.

32. Guneren E, Ozsoy Z, Ulay M, et al. A comparison of the effects of VWK palatoplaty and Furlow Z-plasty operations on ET function. *Cleft Palate Craniofac J* 2000;37:266–270
33. Hodges AM. Combined early cleft lip and palate repair in children under 10 months: a series of 106 patients. *J Plast Reconstr Aesthet Surg* 2010;63:1813–1819
34. Guneren E, Uysal OA. The quantitative evaluation of palatal elongation after Furlow palatoplasty. *J Oral Maxillofac Surg* 2004;62:446–450
35. Reekie T. The effect of South Asian ethnicity on satisfaction with primary cleft lip and or palate repair. *J Plast Reconstr Aesthet Surg* 2011;64:189–194
36. Murray L, Hentges F, Hill J, et al. Cleft Lip and Palate Study Team The effect of cleft lip and palate, and the timing of lip repair on mother-infant interactions and infant development. *J Child Psychol Psychiatry* 2008;49:115–123
37. McQueen KA, Magee W, Crabtree T, et al. Application of outcome measures in international humanitarian aid: comparing indices through retrospective analysis of corrective surgical care cases. *Prehosp Disaster Med* 2009;24:39–46

Effect of the Rhinoplasty Technique and Lateral Osteotomy on Periorbital Edema and Ecchymosis

Caner Kiliç, MD, Ümit Tuncel, MD,* Ela Cömert, MD,* and Ziya Şencan, MD†*

Aim: The present study aimed to compare edema and ecchymosis in the early and late postoperative periods following the application of different surgical techniques (open and endonasal) and different types of lateral osteotomy (internal and external).

Methods: The files and photographs of a total of 120 patients whose records were regularly maintained/updated and who underwent septo-rhinoplasty operation with the same surgeon were retrospectively evaluated. Sixty-nine (57.5%) patients were women and 51 (43.5%) were men. The patients were divided into 4 different groups according to the operations they underwent as follows—Group I: open technique septorhinoplasty + internal/continuous lateral osteotomy; Group II: endonasal rhinoplasty + internal/continuous lateral osteotomy; Group III: open technique septorhinoplasty + external/perforating lateral osteotomy; and Group IV: endonasal rhinoplasty + external/perforating lateral osteotomy. Postoperative edema and ecchymosis, and lateral nasal wall mucosal damage because of osteotomy were evaluated.

Results: Postoperative second day edema and ecchymosis scores were statistically significantly better in patients in Group II compared with the patients in Group I ($P = 0.010$ and $P = 0.004$, respectively). Postoperative first day edema and postoperative seventh day ecchymosis scores were statistically significantly better in the patients in Group IV compared with the patients in Group III ($P = 0.025$ and $P = 0.011$, respectively). Intraoperative bleeding was similar in all groups. The nasal tip was more flexible in patients who underwent closed technique rhinoplasty. Unilateral mucosal damage occurred in 3 patients (4%) with internal lateral osteotomy, whereas no mucosal damage was present in patients with external osteotomy.

Conclusions: The difference in the rate of edema and ecchymosis in the early postoperative period between the closed technique rhinoplasty and the open surgical approach was statistically significant, whereas osteotomy did not cause a significant difference. According to these results, the authors suggest endonasal surgery to prevent the development of edema and ecchymosis, whereas the choice of lateral osteotomy should be dependent on the experience of the surgeon.

Key Words: Ecchymosis, edema, nose, osteotomy

Because the nose is one of the most important organs of the aesthetic integrity of the face, many surgical procedures have been defined and applied to beautify this organ from the past to the present.[1] However, many complications developing secondary to different surgical techniques have resulted in rising problems between the surgeons and the patients.

Ecchymosis and edema developing in and around the eye in the early postoperative period are complications creating the most important morbidity of this surgery. The degree of edema and ecchymosis around the eye can vary from a slight color change to a severe form that impairs the vision of the patient.[2,3] This negative clinical situation may result from the social environment of the patients, from becoming distanced with family if they are parents with children, and from the lengthening of the hospitalization period.

Patients generally ask questions whether swelling would occur in and around their eyes and about the degree of swelling if it occurs after aesthetic nasal surgery as much as questions about the new look of their nose after the surgery. Surgeons, on the contrary, attempt to provide answers that would minimize the anxiety of the patients in light of the surgical procedures to be performed and the medical products that will be used.

Edema and ecchymosis after rhinoplasty may occur in different degrees according to some avoidable/changeable and unavoidable factors such as coagulation disorders and excess subcutaneous fat tissue of the patient, the surgical procedure performed, the type of the osteotomy, length of the operation, location differences of the arteria angularis and drug use before surgery.[4,5] Therefore, the results of various studies have been conducted on subjects such as comparing internal and external lateral osteotomy, open and closed rhinoplasty techniques, the effects of steroid, decongestants, and local heparinoids.[1,6–8]

The present study aimed to compare the differences in the development of edema and ecchymosis in the early and late postoperative periods after different surgical approaches (open and endonasal techniques) and different lateral osteotomy types (internal/continuous and external/perforating), while maintaining the changeable parameters equivalent.

MATERIALS AND METHOD

This retrospective study included 120 patients whose records were regularly maintained/updated and who underwent septorhinoplasty

From the *Department of Otorhinolaryngology, Ankara Dr. Abdurrahman Yurtaslan Oncology Training and Research Hospital; and †Elmadağ Government Hospital, Ankara, Turkey.
Received January 26, 2015.
Accepted for publication April 9, 2015.
Address correspondence and reprint requests to Caner Kiliç, Department of Otorhinolaryngology, Ankara Dr. Abdurrahman Yurtaslan Oncology Training and Research Hospital, Ankara, Turkey 06200; E-mail: canerkilic80@gmail.com
The authors report no conflicts of interest.
Copyright © 2015 by Mutaz B. Habal, MD
ISSN: 1049-2275
DOI: 10.1097/SCS.0000000000001885

Copyright © 2015 Mutaz B. Habal, MD. Unauthorized reproduction of this article is prohibited.

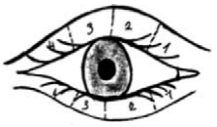

FIGURE 1. Scale for periorbital ecchymosis: 0 (none), (+)1 (in the medial canthus), (+)2 (extending to the pupil), (+)3 (past the pupil), (+)4 (extending to the lateral canthus).

operation with the same surgeon between May 2010 and February 2014. Sixty-nine (57.5%) patients were women and 51 (43.5%) were men.

The patients were divided into 4 groups according to the operation they underwent as follows—Group I: patients who underwent open technique septorhinoplasty and internal/continuous lateral osteotomy; Group II: patients who underwent endonasal rhinoplasty and internal/continuous lateral osteotomy; Group III: patients who underwent open technique septorhinoplasty and external/perforating lateral osteotomy; and Group IV: patients who underwent endonasal rhinoplasty and external/perforating lateral osteotomy. The number of patients in each group was 35 patients in Group 1, 35 patients in Group II, 25 patients in Group III, and 25 patients in Group IV.

Patients who underwent nasal dorsum surgery for nasal humps (originating from the cartilage or bone) and who did not have any planned nasal tip surgery were included into the study. All of the patients had undergone septoplasty. Coagulation parameters were within normal ranges in all patients and they had no history of drug use or cigarette smoking. Dexamethasone 10 mg was administered intravenously in all patients 30 minutes before the operation. Hypotensive anesthesia was performed with remifentanil.

Because ecchymosis is known in the literature to be at its peak level on the postoperative second day,[9] postoperative second and seventh day edema and ecchymosis were scored using photographs taken with the permission of the patients. Postoperative edema and ecchymosis were evaluated, and records of lateral nasal wall mucosal damage were assessed using a 0° endoscope at the end of the operation. Edema and ecchymosis scoring were performed using the staging system previously defined in the literature (Figs. 1–2).[7]

Surgical Technique

Skin flaps were prepared using an inverted V columellar image skin incision for open technique rhinoplasty and intercartilaginous incision for endonasal rhinoplasty. Nasal bone periosteum was elevated using a periosteal elevator. Following this, the upper lateral cartilages were separated from the septum using scissors; the cartilage dorsum was then removed using the scissors, whereas the bone dorsum was removed using a 6 mm guarded osteotome. To prevent inverted V deformity from forming, a spreader graft or autospreader flap was used. High-low-high internal and external lateral osteotomies were performed at the last stages of the operations. Internal lateral and external osteotomies were performed using 4 mm curved guarded and 3 mm unguarded osteotomes, respectively. Periosteal elevations were not performed before lateral osteotomies because they are known to increase edema and ecchymosis.[9] Columellar skin was sutured using a 5/0 prolene suture at the end of the surgery whereas endonasal incisions were not sutured.

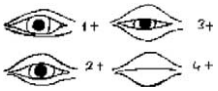

FIGURE 2. Scale for eyelid edema: 0 (none), (+)1 (minimal), (+)2 (covering to the iris), (+)3 (extending to the pupil), (+)4 (massive edema).

TABLE 1. Second Day Postoperative Edema and Ecchymosis Scores of Groups

Edema	Group I n (%)	Group II n (%)	Group III n (%)	Group IV n (%)
Grade 1	13 (37)	24 (68)	6 (24)	13 (52)
Grade 2	15 (42)	8 (22)	9 (36)	7 (28)
Grade 3	4 (11)	2 (5)	6 (24)	5 (20)
Grade 4	3 (8)	1 (2)	4 (16)	–
Ecchymosis				
Grade 1	7 (20)	18 (51)	6 (24)	10 (40)
Grade 2	16 (46)	12 (34)	10 (40)	9 (36)
Grade 3	8 (23)	4 (11)	5 (20)	3 (12)
Grade 4	4 (11)	1 (2)	4 (16)	2 (11)

Statistical Analysis

Windows SPSS (statistical package for social sciences) 15.0 package program (SPSS Inc, Chicago, IL) was used for statistical analysis. Normal distribution in the groups was tested with the Kolmogorov-Smirnov test. The Wilcoxon test was used to analyze the significance of the differences between different postoperative days. Differences between the groups were analyzed using the Mann- Whitney U test. Calculated values of $P < 0.05$ were considered statistically significant.

RESULTS

The age of the patients ranged between 18 and 44 years with a mean age of 28.6 (±7.928) years. Edema and ecchymosis scores on the postoperative second and seventh days were evaluated in all groups according to the ages of the patients. There were no statistically significant differences in the mean age of the patients between the groups ($P = 0.472$, $P = 0.758$, $P = 0.565$, $P = 0.755$, respectively, for Group I, II, III, and IV).

Edema and ecchymosis scores on the postoperative second day in patients with endonasal surgery were better compared with the patients who underwent the open technique surgery (Table 1).

Postoperative seventh day edema and ecchymosis scores were similar (Table 2).

Edema and ecchymosis scores on the postoperative second day in patients with internal lateral osteotomy were better (Table 1), whereas there were no significant differences between the edema and ecchymosis scores on the postoperative seventh day (Table 2).

TABLE 2. Seventh Day Postoperative Edema and Ecchymosis Scores of Groups

Edema	Group I n (%)	Group II n (%)	Group III n (%)	Group IV n (%)
Grade 1	29 (83)	32 (91)	18 (72)	23 (92)
Grade 2	6 (17)	3 (9)	7 (28)	2 (8)
Grade 3	–	–	–	
Grade 4	–	-	–	–
Ecchymosis				
Grade 1	28 (80)	29 (83)	14 (56)	22 (88)
Grade 2	5 (14)	4 (12)	9 (36)	3 (12)
Grade 3	2 (5)	2 (5)	2 (8)	–
Grade 4	–	–	–	–

© 2015 Mutaz B. Habal, MD

Copyright © 2015 Mutaz B. Habal, MD. Unauthorized reproduction of this article is prohibited.

TABLE 3. According to Edema and Ecchymosis of the Groups Were Compared Statistically to Score

	Group I–II/*P* value	Group III–IV/*P* value	Group I–III/*P* value	Group II–IV/*P* value
Edema day 1	*0.010	*0.025	0.114	0.168
Ecchymosis day 1	*0.004	0.068	0.318	0.938
Edema day 7	0.288	0.195	0.994	0.288
Ecchymosis day 7	0.775	*0.011	0.059	0.537

* $P < 0.05$ for Mann-Whitney U test.

Edema and ecchymosis scores in all groups on the postoperative seventh day were statistically significantly different than the scores of the postoperative first day ($P < 0.001$) (Tables 1 and 2).

The first postoperative day edema and ecchymosis scores in Group II were statistically significantly better compared with the scores in Group I ($P = 0.010$ and $P = 0.004$, respectively).

Postoperative first day edema and postoperative seventh day ecchymosis scores were statistically significantly better in patients in Group IV compared with the patients in Group III ($P = 0.025$ and $P = 0.011$, respectively) (Table 3).

Osteotomy lines were endoscopically evaluated at the end of the operations. No lateral nasal wall mucosal damages were detected in the external lateral osteotomy approach, whereas 3 patients (4%) had unilateral lateral nasal wall mucosal laceration at the superior level of the lower concha with the internal lateral osteotomy approach.

DISCUSSION

Edema and ecchymosis are common problems that are encountered by every surgeon after septorhinoplasty. These complaints may cause transient vision disorders and long-term and even permanent increased pigmentation. Different surgical approaches have been reported in the literature to decrease these complaints to a minimal level.[10] A variety of medical analyses[11] and different anesthetic agents have been used for this purpose.[12] Nevertheless, there is no consensus on the mechanism of production of these complaints because it is believed to be multifactorial.

Corticosteroids have been suggested to decrease edema and ecchymosis and dexamethasone used for this purpose is the most powerful agent with its acceptable half-life.[2] Dexamethasone was reported to be effective in decreasing edema and ecchymosis in the early postoperative period when given approximately 30 minutes before the operation in a dose of 10 mg intravenously; however, no significant statistical effect was observed in the late postoperative period. Corticosteroids have been reported to exert these effects by decreasing inflammation through capillary vessel dilatation and preventing the early process of the inflammatory response including fibrin accumulation, lymphocyte migration, and phagocytic activity.[13] The researchers of the present study administered 10 mg dexamethasone intravenously 30 minutes before the operation in all patients in order not to create a difference between the patients.

Saedi et al, in their study in which they found significant effects of preoperative steroids and postoperative decongestant use on the rate of development of edema and ecchymosis, reported that there was no statistically significant effect of age on the development of edema and ecchymosis.[2]

Intraoperative bleeding, postoperative edema, and ecchymosis have been reported to be increased in the presence of hypertension. These postoperative complaints were observed to decrease in patients who were administered controlled hypotensive anesthesia with remifentanil.[12] The authors of the present study also used controlled hypotensive anesthesia with remifentanil to prevent blood pressure measurement differences.

Postoperative edema has been reported to be increased in patients who undergo open technique septorhinoplasty in the literature.[14] Saedi et al reported that the rate of development of edema and ecchymosis decreased after closed technique surgery; however, this difference was not found to be statistically significant.[2] The authors of the present study observed better scores of edema and ecchymosis in Group II and Group IV on postoperative days 2 and 7; however, changes in the postoperative second day edema and ecchymosis in Group II and postoperative second day edema and postoperative seventh day ecchymosis in Group IV were statistically significant.

Lateral osteotomy is an indispensable step of rhinoplasty performed to close the nasal dorsum angle and narrow the nasal pyramid.[15] Differences in the scores of edema and ecchymosis because of internal and external osteotomies have been reported in the literature; however, there is no overall consensus. Giacomarra et al,[16] in their study that they performed for this purpose, studied 142 patients who underwent external lateral osteotomy and reported that the level of edema and ecchymosis was lower with the easier technique. Nasal mucosal damage was also reported to be lower because of external osteotomy in cadaver studies and thus it was concluded that the possibility of perioperative bleeding, postoperative edema, and ecchymosis were all estimated to be lower with this technique.[17,18] On the contrary, Mottura reported a lesser degree of edema and ecchymosis in patients who underwent rhinoplasty with internal osteotomy[19] Murakami et al also reported a lesser degree of edema and ecchymosis after internal osteotomy.[20] In a different study, the authors obtained better edema and ecchymosis scores with internal osteotomy that was performed using a 2 mm osteotome.[21] The scores were better in the groups with internal osteotomy in the present study. There were no statistically significant differences, however, between the groups. When the mucosa was evaluated endoscopically at the end of the operation, mucosal laceration was found to be present in 3 patients (4%) who underwent the internal lateral osteotomy technique, whereas there was no mucosal damage after the lateral osteotomy technique. The results in the present study were better compared with the cadaver studies performed.

Closed technique rhinoplasty is recommended in patients excluding those with asymmetric tip deformity, ptotic nasal tip, severe projection problems, trauma, and patients who have excess scar formation because of prior surgery.[22,23] According to our own experience and information gained from the literature, auto or alloplastic grafting using spreader, auto spreader, columellar strut and alar batten can easily be performed with closed technique rhinoplasty.[23] As a result of this kind of surgery, the duration of operation and exposure to anesthetic agents are decreased, columellar skin sutures, which the patients are very much afraid of (because of the painful sensation), can be avoided, scar formation is not seen because there will be no columellar skin incision and the degree of edema and ecchymosis will be lower, which all allow

© 2015 Mutaz B. Habal, MD

Copyright © 2015 Mutaz B. Habal, MD. Unauthorized reproduction of this article is prohibited.

increased patient comfort postoperatively. Consequently, return to social life and accommodation to daily routines will be shorter in duration.

CONCLUSIONS

Edema and ecchymosis scores in the early and late postoperative periods were found to be better in patients who underwent closed technique rhinoplasty. The difference was found to be statistically significant, however, only in the early postoperative period. The scores of patients with internal lateral osteotomy were better compared with those with external osteotomy; however, there was no statistical significance. The authors suggest endonasal surgery in terms of development of edema and ecchymosis and lateral osteotomy should be selected by surgeons according to their experience.

REFERENCES

1. Xu F, Zeng W, Mao X, et al. The efficacy of melilotus extract in the management of postoperative ecchymosis and edema after simultaneous rhinoplasty and blepharoplasty. *Aesth Plast Surg* 2008;32:599–603
2. Schmidt JH, Caffee HH. The efficacy of methylprednisolone in reducing flap edema. *Plast Reconstr Surg* 1990;86:1148–1151
3. Koc S, Gurbuzler L, Yaman H, et al. The effectiveness of steroids for edema, ecchymosis and intraoperative bleeding in rhinoplasty. *Am J Rhinol Allergy* 2011;25:95–98
4. Gryskiewicz JM, Gryskiewicz KM. Nasal osteotomies: a clinical comparison of the perforating methods versus the continuous technique. *Plast Reconstr Surg* 2004;113:1445–1456
5. Saedi B, Sadeghi M, Fekri K. Comparison of the effect of corticostreroid therapy and decongestant on reducing rhinoplasty edema. *Am J Rhinol Allergy* 2011;25:141–144
6. Kelles M, Erdem T, Fırat Y, et al. Efficacy of local heparinoids on preventing edema and ecchymosis after rhinoplasty. *Kulak Burun Bogaz Ihtis Derg* 2010;20:191–194
7. Sinha V, Gupta D, More Y, et al. External vs. internal osteotomy in rhinoplasty. *Indian J Otolaryngol Head Neck Surg* 2007;59:9–12
8. Kara CO, Kara CO, Kara IG, et al. Does creating a subperiosteal tunnel influence the periorbital edema and ecchymosis in rhinoplasty? *J Oral Maxillofac Surg* 2005;63:1088–1090
9. Erişir F, Oktem F, İnci E. Effects of steroids on edema and ecchymosis in rhinoplasty. *Turk Arch ORL* 2001;39:171–175
10. Alajmi MA, Al-Abdulhadi KA, Al-Noumas HS, et al. Results of intravenous steroid injection on reduction of postoperative edema in rhinoplasty. *Indian J Otolaryngol Head Neck Surg* 2009;61:266–269
11. Kosucu M, Omur S, Besir A, et al. Effects of perioperative remifentanil with controlled hypotension on intraoperative bleeding and postoperativeedema and ecchymosis in open rhinoplasty. *J Craniofac Surg* 2014;25:471–475
12. Griffies WS, Kennedy K, Gasser C, et al. Steroids in rhinoplasty. *Laryngoscope* 1989;99:1161–1164
13. Cizmeci MO, Kuvat SV. Choosing the operative techniqe and step in rhinoplasty. *J Plast Surg-Special Topics* 2010;2:12–15
14. Rees TD, La Trenta. The osteocartilaginous vault. In: Aesthetic Plastic Surgery. Philadelphia: WB Saunders, 1994:79–158.
15. Giacomarra V, Russolo M, Arnez ZM, et al. External osteotomy in rhinoplasty. *Laryngoscope* 2001;111:433–438
16. Rohrich R, Minoli J, Adam WP, et al. The lateral nasal osteotomy in rhinoplasty: an anatomic endoscopic comparison of the external versus the internal approach. *Plast Reconstr Surg* 1997;99:1309–1312
17. Kuran I, Ozcan H, Usta A, et al. Comparison of four different types of osteotomes for lateral osteotomy: a cadaver study. *Aesthetic Plast Surg* 1996;20:323–326
18. Mottura AA. Internal lateral nasal osteotomy: double guarded osteotome and mucosa tearing. *Aesthetic Plast Surg* 2011;35:171–176
19. Murakami CS, Larrabee WF Jr. Comparison of osteotomy techniques in the treatment of nasal fractures. *Facial Plast Surg* 1992;8:209–219
20. Yucel OT. Which type of ostetomy for edema and ecchymosis: external or internal? *Ann Plast Surg* 2005;55:587–590
21. Sheen JH. Closed versus open rhinoplasty and the debate goes on. *Plast Reconstr Surg* 1997;99:859–862
22. Williams EF, Lam SM. A systematic, graduated approach to rhinoplasty. *Facial Plast Surg* 2002;18:215–222
23. Seyhan A. Method for middle vault reconstruction in primary rhinoplasty: upper lateral cartilage bending. *Plast Reconstr Surg* 1997;100:1941–1943

Orthoptic Sequelae Following Conservative Management of Pure Blowout Orbital Fractures: Anecdotal or Clinically Relevant?

Ken Steinegger, MD,[*] Raoul De Haller, MD,[†] Delphine Courvoisier, PhD,[‡] and Paolo Scolozzi, MD, DDS[§]

Abstract: The aim of this study was to prospectively assess the prevalence of orthoptic anomalies following conservative management of pure blowout orbital fractures and to evaluate their clinical relevance. Clinical and radiologic data of patients with unilateral conservatively managed pure blowout orbital fractures with a minimum follow-up of 6 months were reviewed. Eligible patients were contacted and invited to undergo an extended ophthalmologic examination as follows: distance and near visual acuities, Hertel exophthalmometry, corneal light reflex (Hirschberg test), ductions and versions in the 6 cardinal fields of gaze, eye deviation with prisms and alternate cover test in all of the 9-gaze directions with Maddox rod, degrees of incyclo/excyclotorsion with right and left eye fixation, horizontal and vertical deviation with Hess-Weiss coordimetry, degree of horizontal/vertical and incyclo/excyclotorsion deviation with Harms wall deviometry, and vertical deviation with Bielschowsky head-tilt test. Of the 69 patients contacted, 49 declined to participate given that they were asymptomatic. Twenty patients agreed to undergo the examination. One patient complained of minimal double vision limited to the extreme downgaze. Four patients had asymptomatic ocular motility disturbances limited to the extreme gaze. Seven patients had asymptomatic horizontal heterophoria. These disturbances did not interfere with daily or professional activities in any of the patients. The current study

From the [*]University Ophthalmology Department, Hôpital Ophtalmique Jules-Gonin, University of Lausanne, Lausanne; [†]Neuro-Ophthalmology and Strabology Unit, Department of Clinical Neurosciences, Division of Ophthalmology, University Hospital and Faculty of Medicine of Geneva; [‡]CRC and Division of Clinical Epidemiology, Department of Health and Community Medicine; and [§]Division of Oral and Maxillofacial Surgery, Department of Surgery, University of Geneva and University Hospitals of Geneva, Geneva, Switzerland.

Received August 24, 2014.
Accepted for publication April 14, 2015.

Address correspondence and reprint requests to Paolo Scolozzi, Division of Oral and Maxillofacial Surgery, Department of Surgery, University of Geneva and University Hospitals of Geneva, Geneva, Switzerland; E-mail: paolo.scolozzi@hcuge.ch

The authors report no conflicts of interest.

Copyright © 2015 by Mutaz B. Habal, MD

ISSN: 1049-2275
DOI: 10.1097/SCS.0000000000001886

Copyright © 2015 Mutaz B. Habal, MD. Unauthorized reproduction of this article is prohibited.

demonstrated that conservative management of pure orbital blowout fractures can result in orthoptic anomalies. These sequelae were restricted to a very limited portion of the binocular field of the vision and were not found to be clinically relevant.

Key Words: Nonsurgical treatment, ocular motility, orthoptic examination, pure orbital fracture

Orbital fractures are encountered in up to 40% of craniofacial traumas and have been classically classified as either pure, when limited to the orbital walls, or impure, when associated with a concomitant involvement of the orbital rim, such as found in complex midfacial fractures (eg, orbitozygomatic, nasoorbitoethmoidal or Le Fort II type fractures).[1–5] Orbital fractures can result in severe functional and aesthetic complications such as visual impairment, diplopia, infraorbital sensory nerve function, and enophthalmos.[6–11] The indications for surgical or conservative treatment still remain controversial with no consensual and well-established guidelines.[4,9,12] Immediate or early surgery is clearly indicated in patients presenting with an immediate annoying diplopia on primary gaze, an early aesthetically unacceptable enophthalmos and/or a hypoglobus. In the majority of cases, however, the indication for surgery results from the association of nonstandardized clinicoradiologic findings, including the degree of diplopia and enophthalmos, and the type (linear or comminuted) and size of the fracture's defect. The decision substantially varies from surgeon to surgeon.[4,9,12]

The current literature has mainly focused on the different surgical techniques used to restore the preoperative bony orbital volume and shape, and the association between orbital volume and development of enophthalmos, rather than quantitatively evaluating the possible ocular motility disturbances by detailed orthoptic and strabologic examinations.[7,13–17] The global prevalence of long-term residual diplopia after orbital fractures has been reported to be between 15% and 82% and between 0% and 12% in the specific group of patients treated nonsurgically.[4,8] In most studies, extraocular motility disorder, change in globe position, and enophthalmos were only grossly assessed and rarely well documented and followed up, even though in many cases the indications for surgery were based on these clinical findings.[4,10,11,18–23] Moreover, only very few studies have reported on the nonsurgical management of blowout fractures, with very limited information regarding both the possible long-term oculomotor sequelae and the specific opthalmologic examination used.[4,10,11,18–23]

The purpose of this study was to assess the prevalence of orthoptic anomalies in patients presenting with pure orbital fractures managed conservatively and to define whether these anomalies should be considered as anecdotal findings or as clinically relevant anomalies.

MATERIALS AND METHODS

This retrospective cohort study was granted permission from our local ethical board and conducted in accordance with the Helsinki Declaration of 1975, as revised in 2000. Clinical charts and computed tomography scans of all of the patients presenting to the University Hospital of Geneva, Switzerland, for the evaluation and management of pure blowout orbital fractures from 2008 to 2012 were reviewed. Eighty-six patients with a unilateral pure blowout orbital fracture conservatively managed and with a minimum follow-up of 6 months were selected. Conservative management is defined within our department based upon the following criteria:

- Orbital wall defect size of $<50\%$ of the entire orbital floor as measured according to the computational method previously described by Schouman et al[24] and no evidence of soft tissue herniation on computed tomography scan;
- No immediate ocular motility restriction in ≥ 1 field of gaze or annoying diplopia at the 10-day follow-up visit. Ocular movements are evaluated by careful assessment of ductions and versions in the 6 cardinal fields of gaze by asking the patient to follow the examiner's finger without moving the head;
- No enophthalmos immediately obvious to the naked eye or <3 mm difference between the globe projection of the 2 eyes measured by Hertel exophthalmometry at the 10-day follow-up visit.

Patients were excluded from the study if they had an impure orbital fracture, a bilateral fracture, a previous orbital and/or ophthalmologic surgical treatment, monocular vision, or nonstereoscopic vision.

All of the selected patients were invited to undergo an extended ophthalmologic examination. We were unable to contact 17 patients. The 69 remaining patients were first asked about the presence or absence of diplopia, the type of diplopia (horizontal, vertical, oblique), the frequency of occurrence (everyday, >1 hour a day, $>50\%$ of the day, permanently) and in which direction of gaze it occurred or it worsened. Of these, 49 (ie, 71%) reported that they were asymptomatic, and thus they declined to participate in the extended ophthalmologic examination. The remaining 20 patients accepted our invitation and were assessed by an experienced strabologist using the following examinations: distance and near visual acuities, Hertel exophthalmometry, corneal light reflex (Hirschberg test), ductions and versions in the 6 cardinal fields of gaze, eye deviation with prisms and alternate cover test in all of the 9-gaze directions with Maddox rod, degrees of incyclo/excyclotorsion with right and then left eye fixation, horizontal and vertical deviation with Hess-Weiss coordimetry, degree of horizontal/vertical and incyclo/excyclotorsion deviation with Harms wall deviometry, and vertical deviation with Bielschowsky head-tilt test.

The other variables reviewed included age and sex, type of fracture, time between trauma and examination, pre- and postoperative symptoms, and residual visual axis deviations.

Statistical Analysis

Data were analyzed using the PropCIs package of R statistical software (v. 3.0.2) (The R Foundation for Statistical Computing, Vienna, Austria) to compute Clopper-Pearson exact confidence intervals (CI) around the proportions.

RESULTS

Orbital pure fractures presented by the 69 patients (56 Caucasians, 10 Africans, and 3 Asians) were classified as follows: 31 orbital floors, 23 medial walls, 4 lateral walls, and 11 combined fractures (medial wall/floor). The mean age of the 69 patients at the time of the trauma was 44.5 years (range 8–87 years) with a male predominance ($n = 47$; 68%).

Of the 69 patients contacted, only 1 complained of double vision limited to the extreme downgaze, which did not interfere with daily activities (proportion: 1.5%, 95% CI: 0.0–7.9). Twenty patients agreed to undergo the examination. One patient was excluded due to an abnormal retinal correspondence with right eye suppression for near vision and left eye suppression for far vision. The follow-up period ranged from a minimum of 6 months to a maximum of 48 months (average 24 months). Data concerning the remaining 19 patients who received comprehensive evaluation are summarized in Tables 1 and 2.

None of the 19 patients had an enophthalmos (proportion: 0.0%, 95% CI: 0.0–17.6%) nor incyclo/excyclotorsion deviation on

© 2015 Mutaz B. Habal, MD

Copyright © 2015 Mutaz B. Habal, MD. Unauthorized reproduction of this article is prohibited.

TABLE 1. Baseline Data and Initial Opthalmologic Evaluation on 19 Patients Receiving Comprehensive Evaluation

Patient No.	Sex	Age (years)	Race/Ethnicity	Cause	Fracture Location	Visual Activity	Diplopia*	Enophthalmos†
1	F	65	Caucasian	Traffic accident	Isolated right medial orbital wall	N	No	No
2	M	42	Caucasian	Assault	Isolated left medial orbital wall	N	No	No
3	F	58	African	Traffic accident	Isolated right orbital floor	N	No	No
4	M	13	Caucasian	Assault	Isolated right medial orbital wall	N	No	No
5	M	35	Caucasian	Work accident	Isolated right lateral orbital wall	N	No	No
6	M	45	Caucasian	Traffic accident	Combined right medial orbital wall and orbital floor	N	No	No
7	F	61	Caucasian	Traffic accident	Isolated right orbital floor	N	No	No
8	M	37	Caucasian	Fall	Isolated right orbital floor	N	No	No
9	F	23	African	Assault	Isolated right lateral orbital wall	N	No	No
10	M	35	African	Assault	Isolated left medial orbital wall	N	No	No
11	M	35	Caucasian	Assault	Combined left medial orbital wall and orbital floor	N	No	No
12	M	74	African	Traffic accident	Isolated right orbital floor	N	No	No
13	M	8	Caucasian	Fall	Isolated left orbital floor	N	No	No
14	F	49	Caucasian	Fall	Combined left medial orbital wall and orbital floor	N	No	No
15	M	28	Caucasian	Sport accident	Isolated left orbital floor	N	No	No
16	M	24	Caucasian	Sport accident	Isolated right orbital floor	N	No	No
17	M	25	Caucasian	Fall	Combined right medial orbital wall and orbital floor	N	No	No
18	F	15	Caucasian	Traffic accident	Isolated left lateral orbital wall	N	No	No
19	M	75	Caucasian	Fall	Combined right medial orbital wall and orbital floor	N	No	No

*Evaluated by assessment of ductions and versions in the 6 cardinal fields of gaze by asking the patient to follow the examiner's finger without moving the head.
†Evaluated by Hertel exophthalmometry.

TABLE 2. Follow-Up Opthalmologic Evaluation on 19 Patients Receiving Comprehensive Evaluation

Patient No.	Follow-Up (months)	Visual Activity	Diplopia*	Enophthalmos†	Hirschberg Test	Maddox Rod Test	Incyclo/ Excyclotorsion	Hess-Weiss Coordimetry	Harms Wall Deviometry	Bielschowsky Head-Tilt Test
1	31	N	No	No	N	Esophoria	N	Esophoria; Left eye upward gaze limitation	Esophoria; Left eye upward gaze limitation	N
2	7	N	No	No	N	N	N	N	N	N
3	41	N	No	No	N	N	N	N	N	N
4	31	N	No	No	N	N	N	N	N	N
5	9	N	No	No	N	Esophoria	N	Esophoria; Right eye abduction limitation	Esophoria	N
6	25	N	Extreme downward gaze	No	N	N	N	Right eye adduction limitation	N	N
7	12	N	No	No	N	N	N	N	N	N
8	13	N	No	No	N	N	N	Esophoria	N	N
9	42	N	No	No	N	Esophoria	N	Esophoria	Esophoria	N
10	32	N	No	No	N	N	N	Exophoria	N	N
11	31	N	No	No	N	N	N	N	N	N
12	37	N	No	No	Right eye upward gaze limitation	Right eye hypotropia	N	Right eye hypotropia; Right eye upward gaze limitation	Right eye hypotropia	Right eye hypotropia
13	48	N	No	No	N	N	N	N	N	N
14	29	N	No	No	N	N	N	N	N	N
15	6	N	No	No	N	Exophoria	N	Exophoria	Exophoria	N
16	12	N	No	No	Right eye upward gaze limitation	Right eye upward gaze limitation	N	N	N	N
17	6	N	No	No	N	N	N	Exophoria	Exophoria	N
18	12	N	No	No	N	N	N	N	N	N
19	6	N	No	No	N	N	N	N	N	N

*Evaluated by assessment of ductions and versions in the 6 cardinal fields of gaze by asking the patient to follow the examiner's finger without moving the head.
†Evaluated by Hertel exophthalmometry.

© 2015 Mutaz B. Habal, MD

Copyright © 2015 Mutaz B. Habal, MD. Unauthorized reproduction of this article is prohibited.

cyclotorsion test (proportion: 0.0%, 95% CI: 0.0–17.6%). Nine had orthophoria (proportion: 47.4%, CI: 24.4–71.1%), 4 had esophoria (proportion: 21.1%, 95% CI: 6.1–45.6%), 3 had exophoria (proportion: 15.8%, 95% CI: 3.4–39.6%), and 4 had gaze limitation (proportion: 26.3%, 95% CI: 9.1–51.2%) as follows: a right eye limitation in extreme abduction gaze (right lateral orbital fracture); a right eye limitation in extreme adduction gaze (right combined floor and medial wall fracture); a right eye hypotropia and limitation in extreme upgaze (right orbital floor fracture); and a minimal right eye limitation in extreme upgaze (right orbital floor fracture) (Table 2).

DISCUSSION

The present study analyzed the orthoptic outcomes following conservative management of pure blowout orbital fractures. Our findings showed that of 19 patients reporting symptoms following this treatment, 4 developed a certain degree of ocular motility restriction limited to the very extreme gaze and 7 had asymptomatic horizontal heterophoria with no gaze limitation; however, these anomalies were so discrete that they were only detectable by a detailed orthoptic evaluation and did not result in any interference with daily or professional activities. Unfortunately, these results could only be approximately compared with other data in the literature, given the absence of similar studies using such an extended follow-up orthoptic assessment. To the best of our knowledge, the literature contains only 5 references to the quantitative evaluation of ocular motility outcome in the specific subgroup of blowout fractures conservatively managed. In 1974, Putterman et al[21] were the first to report on the oculomotor assessment in 57 patients (28 studied retrospectively and 29 prospectively) presenting with blowout fractures that were nonsurgically treated. They performed the evaluation of diplopia by using an alternate cover test in all of the 9-gaze directions with Maddox rod and prisms. They did not perform Hess-Weiss coordimetry or a Harms wall deviometry. Seven patients among the 28 retrospectively evaluated were found to present diplopia (1 in primary gaze and 6 in extreme gaze position) and 4 were found to present some degree of abnormal vertical deviation. No specific details were given concerning either the follow-up time or the severity of the vertical deviation and the possible interference with daily activities related to these anomalies. Only 3 of 29 patients prospectively followed presented with long-term diplopia (>6 months) that was limited to the extreme gaze only. Interestingly, the authors concluded that "since these positions are rarely used, none was troubled by it." Catone et al[20] retrospectively evaluated 27 patients with untreated orbital fractures. Diplopia was assessed in primary gaze or peripheral gaze but without eye deviation with prisms and alternate cover test in all of the 9-gaze directions with Maddox rod and without Hess-Weiss coordimetry.[20] Only 12 patients returned for the follow-up examination.[20] The investigators found only 1 patient (8.3%) with persistent vertical diplopia in extreme upward gaze.[20] Catone et al[20] also pointed out that minimal diplopia in extreme gaze is generally not to be considered significant. Given the incomplete ophthalmologic evaluation performed in this study, no specific details regarding possible other orthoptic "stigmata" were available. Nishida et al[19] performed a quantitative evaluation of ocular motility using Hess-Weiss coordimetry but without eye deviation with prisms and the alternate cover test in all of the 9-gaze directions with Maddox rod, and they compared nonsurgically with surgically managed pure orbital fractures. They analyzed 23 nonsurgical patients. They found residual diplopia in 4 patients at 25 degrees upward with none of the patients complaining of daily serious binocular vision problems. Pansell et al[22] performed an orthoptic evaluation of 23 cases using the prism cover test, the test of stereovision and measurement of convergence. They found only 1 patient presenting with abnormal ocular motility, which was due to a known strabismus present before the orbital fracture.[9] Gosse et al[23] looked at the pattern of ocular motility between surgical and nonsurgical cases, but unfortunately they did not explain how they evaluated ocular motility.

Although the selected criteria for nonsurgical management of orbital fractures are certainly important parameters influencing the final outcome, curiously only 1 study detailed the criteria used.[9]

The current study has demonstrated that the conservative management of pure orbital fractures is not free of orthoptic sequelae; however, the observed restrictions of the globe motility found in 4 patients were limited to extreme directions of gaze, which are only exceptionally used in the binocular field of the vision in everyday life. Moreover, limitations in such extreme gaze directions are automatically compensated for most of the time by a reflex head movement. This also explains why classically, as happened to our patients, these limitations may have gone unnoticed, and thus were only revealed by a detailed examination given that they are not associated with the development of annoying diplopia. The same reflection applies to the heterophoric anomalies found in 4 patients, which were not associated with any visual disturbances and were completely asymptomatic. It is interesting to note that the ocular motility assessment as reported in the literature would have allowed the detection of anomalies in only 2 of 4 patients, and no detection of horizontal or vertical heterophoria.

In conclusion, the current results seem to confirm that orthoptic sequelae following conservative management of pure orbital blowout fractures should be considered as clinically irrelevant accidental findings. Nevertheless, it should be stressed that such discrete objective anomalies also have the potential of causing disturbances, especially in patients who rely more often on extreme gaze for professional or hobby-related reasons. Undoubtedly, these results should be interpreted with caution given the limited number of patients, and it is not possible to draw any definitive conclusion, which hopefully may be provided at the end of an ongoing prospective study in our department.

REFERENCES

1. Smith B, Regan WF Jr. Blow-out fracture of the orbit; mechanism and correction of internal orbital fracture. *Am J Ophthalmol* 1957;44:733–739
2. Cramer LM, Tooze FM, Lerman S. Blowout fractures of the orbit. *Br J Plast Surg* 1965;18:171–179
3. Ellis E 3rd, el-Attar A, Moos KF. An analysis of 2,067 cases of zygomatico-orbital fracture. *J Oral Maxillofac Surg* 1985;43:417–428
4. Brady SM, McMann MA, Mazzoli RA, et al. The diagnosis and management of orbital blowout fractures: update 2001. *Am J Emerg Med* 2001;19:147–154
5. Cole P, Boyd V, Banerji S, et al. Comprehensive management of orbital fractures. *Plast Reconstr Surg* 2007;120:57S–63S
6. Manson PN, Clifford CM, Su CT, et al. Mechanisms of global support and posttraumatic enophthalmos. I. The anatomy of the ligament sling and its relation to intramuscular cone orbital fat. *Plast Reconstr Surg* 1986;77:193–202
7. Manson PN, Grivas A, Rosenbaum A, et al. Studies on enophthalmos. II. The measurement of orbital injuries and their treatment by quantitative computed tomography. *Plast Reconstr Surg* 1986;77:203–214
8. al-Qurainy IA, Stassen LF, Dutton GN, et al. Diplopia following midfacial fractures. *Br J Oral Maxillofac Surg* 1991;29:302–307
9. Burnstine MA. Clinical recommendations for repair of isolated orbital floor fractures: an evidence-based analysis. *Ophthalmology* 2002;109:1207–1210
10. Mazock JB, Schow SR, Triplett RG. Evaluation of ocular changes secondary to blowout fractures. *J Oral Maxillofac Surg* 2004;62:1298–1302

© 2015 Mutaz B. Habal, MD

Copyright © 2015 Mutaz B. Habal, MD. Unauthorized reproduction of this article is prohibited.

11. Brucoli M, Arcuri F, Cavenaghi R, et al. Analysis of complications after surgical repair of orbital fractures. *J Craniofac Surg* 2011;22:1387–1390
12. Ellis E 3rd, Tan Y. Assessment of internal orbital reconstructions for pure blowout fractures: cranial bone grafts versus titanium mesh. *J Oral Maxillofac Surg* 2003;61:442–453
13. Bite U, Jackson IT, Forbes GS, et al. Orbital volume measurements in enophthalmos using three-dimensional CT imaging. *Plast Reconstr Surg* 1985;75:502–508
14. Charteris DG, Chan CH, Whitehouse RW, et al. Orbital volume measurement in the management of pure blowout fractures of the orbital floor. *Br J Ophthalmol* 1993;77:100–102
15. Whitehouse RW, Batterbury M, Jackson A, et al. Prediction of enophthalmos by computed tomography after 'blow out' orbital fracture. *Br J Ophthalmol* 1994;78:618–620
16. Ploder O, Klug C, Voracek M, et al. Evaluation of computer-based area and volume measurement from coronal computed tomography scans in isolated blowout fractures of the orbital floor. *J Oral Maxillofac Surg* 2002;60:1267–1272
17. Fan X, Li J, Zhu J, et al. Computer-assisted orbital volume measurement in the surgical correction of late enophthalmos caused by blowout fractures. *Ophthal Plast Reconstr Surg* 2003;19:207–211
18. Lee SH, Lew H, Yun YS. Ocular motility disturbances in orbital wall fracture patients. *Yonsei Med J* 2005;46:359–367
19. Nishida Y, Hayashi O, Miyake T, et al. Quantitative evaluation of ocular motility in blow-out fractures for selection of nonsurgically managed cases. *Am J Ophthalmol* 2004;137:777–779
20. Catone GA, Morrissette MP, Carlson ER. A retrospective study of untreated orbital blow-out fractures. *J Oral Maxillofac Surg* 1988;46:1033–1038
21. Putterman AM, Stevens T, Urist MJ. Nonsurgical management of blow-out fractures of the orbital floor. *Am J Ophthalmol* 1974;77: 232–239
22. Pansell T, Alinasab B, Westermark A, et al. Ophthalmologic findings in patients with non-surgically treated blowout fractures. *Craniomaxillofac Trauma Reconstr* 2012;5:1–6
23. Gosse EM, Ferguson AW, Lymburn EG, et al. Blow-out fractures: patterns of ocular motility and effect of surgical repair. *Br J Oral Maxillofac Surg* 2010;48:40–43
24. Schouman T, Courvoisier DS, Imholz B, et al. Computational area measurement of orbital floor fractures: reliability, accuracy and rapidity. *Eur J Radiol* 2012;81:2251–2254

New Screw Design for Securing Buried Distractors Usefulness and Ease of Removal

Rodrigo Fariña, DDS,[*] *Andrés Hinojosa, DDS,*[†] *Martín Sánchez, DDS,*[†] *and Sergio Olate, DDS*[‡]

From the [*]Maxillofacial Department, Hospital del Salvador, Hospital San Borja Ariiarán, Profesor of Maxillofacial Surgery Universidad de Chile; [†]Resident in Oral and Maxillofacial Surgery, Hospital del Salvador, Santiago; and [‡]Maxillofacial Department, Universidad de la Frontera, Temuco, Chile.

Received August 30, 2014.
Accepted for publication April 14, 2015.

Address correspondence and reprint requests to Rodrigo Fariña, Chilean Society of Oral and Maxillofacial Surgery, Providencia 2330, Appt 23, Santiago, Chile; E-mail: rofari@gmail.com

This study was approved by the Hospital del Salvador ethics board.
The authors report no conflicts of interest.

Copyright © 2015 by Mutaz B. Habal, MD

ISSN: 1049-2275
DOI: 10.1097/SCS.0000000000001887

Abstract: There are 2 types of distraction devices for mandibular distraction: buried and external. The advantage of buried devices is the stability, but the difficulty in removing the screws is the greatest disadvantage. To resolve this problem, an osteosynthesis screw (Fariña Screw) has been designed, which greatly facilitates its removal when buried distractors are used.

Key Words: Complications of removal of the distractor device, distraction osteogenesis, mandibular distraction, transport disc distraction

Osteogenic distraction is a process that allows the formation of new bone tissue in a space that is gradually separated using a distraction device. There are 2 types of distraction devices for mandibular distraction: buried and external.[1]

The advantages of buried devices are the stability of the device, the patient's comfort, the one-to-one ratio between the device's activation and the bone separation (smaller lever arm).[2]

External devices require insertion pins that leave behind an undesired scar, are unstable and pose a greater risk of the pins coming loose, in addition to causing discomfort among patients.[3]

The greatest disadvantages that buried devices present are the need for a second operation to remove them and the difficulty in removing the screws that hold the device in place. In vertical ramus mandibular distraction (hemifacial microsomia, transport disc distraction in temporomandibular joint ankylosis, etc), the neoformed bone usually covers the screw heads, especially in the proximal segment, which is also gradually moved in the cephalic direction during traction. When it comes to removing the device, once the consolidation process has concluded, it becomes very difficult to see and to remove this osteosynthesis material. The need to remove bone tissue covering the screws (with a bur) generally damages the screw head's shape, making its removal even more difficult.

To resolve this problem an osteosynthesis screw (Fariña Screw, FS) has been designed that facilitates its removal when buried distractors are used on vertical ramus mandibular distraction.

This adaptation reduces manipulation of the recently formed bone segment, avoids expanding the initial approach or the need to create a new approach (generally preauricular) to remove the conventional osteosynthesis material, and significantly cuts down on surgery time.

This study was approved by the Hospital del Salvador ethics board.

TECHNICAL DESCRIPTION

A screw (FS) made of surgical steel was designed, with a 2 mm diameter thread and 9 mm long, the head of which is hexagonal in shape and with a volume of $3 \times 3 \times 10$ mm (Figs. 1-2). The FS

FIGURE 1. The Fariña Screw.

FIGURE 2. Fariña Screw fixes the distractor device.

Copyright © 2015 Mutaz B. Habal, MD. Unauthorized reproduction of this article is prohibited.

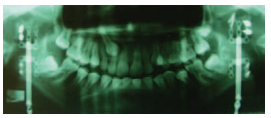

FIGURE 3. Panoramic x-ray showing Fariña Screw in bilateral temporomandibular joint ankylosis after gap arthroplasty and transport disc distraction.

FIGURE 4. Computed tomography scan showing Fariña Screw after the end of consolidation time of transport disc distraction (before removal of the distractor device).

FIGURE 5. Removal of the Fariña Screw through a simple and small incision on the skin, over the screw.

allows the distractor to be stabilized safely and to locate the precise location of the screw through external palpitation of the skin (Figs. 3-4), allowing it to be easily removed via a small incision directly above it (Fig. 5).

The FS has been successfully used in 7 patients, without difficulties.

REFERENCES

1. Padwa BL, Kearns GJ, Todd R, et al. Maxillary and mandibular distraction osteogenesis. *Int J Oral Maxillofac Surg* 1999;28:2–8
2. El-Bialy TH, Razdolsky Y, Kravitz ND, et al. Long-term results of bilateral mandibular distraction osteogenesis using an intraoral toothborne device in adult Class II patients. *Int J Oral Maxillofac Surg* 2013;42:1446–1453
3. Swennen G, Schliephake H, Dempf R, et al. Craniofacial distraction osteogenesis: a review of the literature. *Int J Oral Maxillofac Surg* 2001;30:89–1032001 International Association of Oral and Maxillofacial Surgeons

Morphometric Analysis of Styloid Process Using Multidetector Computed Tomography

Mehmet T. Yilmaz, PhD, Duygu Akin, MS,**
Aynur E. Cicekcibasi, MD, Anil D.A. Kabakci, MS,**
Muzaffer Seker, PhD, and Mehmet E. Sakarya, MD†*

Abstract: Styloid process (SP) is a cylindrical anatomical structure located at the anterior side of stylomastoid foramen. Normally, it is 20 to 25 mm in length and can vary with ageand sex. An elongated SP is an unusual source of craniofacial and cervical pain. In this study, the clinical role of morphometric data of SP was discussed.

In this study, 64-slice multidetector computed tomography images (Somatom Sensation 64, Siemens, Germany) from Radiology Department's archive of Necmettin Erbakan University were used. The examined images were collected from 100 patients (31 female and 69 male). Length of SP (SPL), SP width (SPW), distance between SP rooths (DBR), SP's angulation, and the distance between SP and internal carotid artery (SP-ICA) were measured.

Statistical differences were found regarding to the data of SPL, SPW, DBR, and SP-ICA left between sexes. No statistical significance was detected between right and left side SPL (paired *t* test; $P = 0.989$, $P > 0.05$). SP was observed as mostly type A1 (right %55, left %52). These parameters were also compared with those of previous studies.

The present study showed side and sex differences and types of SP. We believe that it was necessary to determine the normal range of values for different populations, and this knowledge will provide guidance to surgeons in the examination of this area.

Key Words: Morphometry, multidetector computed tomography, styloid process

INTRODUCTION

Styloid process (SP) is an important bone structure that is placed on the external surface of cranial base. SP is a long and cylindrical structure that stands out right in front of stylomastoid foramen, lateral to jugular foramen and carotid canal, united with inferior surface of petrous part of temporal bone.[1–6] SP is surrounded with important structures fromlateral to medial. At its lateral, it has facial nerve, hypoglossal nerve, occipital artery, and posterior belly of digastric as neighboring structures and at its medial internal carotid artery, internal jugular vein, and sphenomandibular ligament as neighboring structures.[3,7]

A great number of studies have been published regarding the length of SP (SPL). The first study was published by Eagle regarding mineralization symptoms of SP—stylohyoid ligament complex in 1937.[2,8] Eagle[9] defined the normal SPL for adults as 25 to 30 mm. Eagle syndrome, also known as elongated SP syndrome or carotid artery syndrome, defines the conditions related to either SP, which is longer than normal or stylohyoid and stylomandibular ligaments that are ossified. Symptoms presented due to elongated SP or calcification of stylohyoid ligament includes a specific facial pain, otalgia, dysphagia, vertigo, constant feeling of tonsillitis, pain in tongue base, and pain distributed through carotid arteries pathways.[10–13]

In this study, the determination of morphometric data such as SP sizes, medial angle, which is constructed with skull base, and

From the *Department of Anatomy; and †Department of Radiology, Meram Faculty of Medicine, Necmettin Erbakan University, Meram, Konya, Turkey.

Received September 5, 2014.
Accepted for publication April 14, 2015.

Address correspondence and reprint requests to Aynur E. Cicekcibasi, MD, Department of Anatomy, Meram Faculty of Medicine, Necmettin Erbakan University, 42080 Meram, Konya, Turkey;
E-mail: aynurcicekcibasi@yahoo.com.tr

This study conformed to Helsinki Declaration.
The authors report no conflicts of interest.

Copyright © 2015 by Mutaz B. Habal, MD

ISSN: 1049-2275
DOI: 10.1097/SCS.0000000000001888

Copyright © 2015 Mutaz B. Habal, MD. Unauthorized reproduction of this article is prohibited.

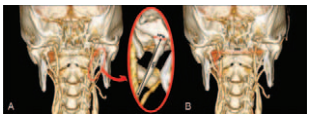

FIGURE 1. (A) Styloid process length (SPL) and styloid process width (SPW). (B) Distance between SP rooths (DBR) and the angle (SPA) formed between the line consisted between tip of styloid process and vagina processus styloidei and the line that unites the rooths of both sides of styloid processes (DBR).

distance from internal carotid artery by multi-detector computed tomography (MDCT) in living individuals, and determination of the effects of sex on the subject were intended. Also classification and possible variations were studied and clinical importance was emphasized.

MATERIALS AND METHODS

This study was conducted on carotid angiography images of a total of 100 patients consisted of 69 male (mean age: 65.23 ± 9.90; 45–86 age ranged) and 31 female (mean age: 61.35 ± 10.78; 43–80 age ranged) who applied to Department of Radiology, Necmettin Erbakan University. Furthermore, the patient groups were formed according to age (<60 age group and ≥60 age group). The history of any kind of cranial operation, any kind of cranial trauma, and remarkable bone deformation was excluding criteria for the patients. The necessary permissions were acquired from Non-invasive Clinical Researches Ethic Board of Meram Faculty of Medicine with April 13, 2012 dated and 2012/84 numbered decision.

Sixty-four-channeled MDCT machine was used (Somatom Sensation 64, Siemens, Erlangen, Germany). The total of 100-cc contrast agent was applied to patients with 22-gauge granules from one of their superficial forearm veins at 3 to 4 cc/s, and at portal phase (60–65 s later from the zero point, the beginning of contrast agent infusion) carotidangiography images were obtained. The images were transferred to the workstation (Leonardo Workstation, Siemens Medical Solutions, Erlangen, Germany). The axial, coronal, sagittal, and inspace images were used and data were assessed in centimeters as unit of length.

Morphometric measurements of SP were performed on 3D volume-rendered images by the same person. SPL, defined as the length from tip of the SP to the root of the SP (Fig. 1), SP width (SPW), defined as the width of SP after it leaves sheath of SP Fig. 1), distance between SP rooths (DBR) (Fig. 1), and the angle formed between the line consisted between tips of SP and sheath of SP and the line that unites the rooths of both sides SPs (SPA) (Fig. 1) were measured.

The distance measurements between SP and internal carotid artery were carried out onmultiplanar reconstructed images. After images of SPs from both sides were acquired onsagittal plane, the distance between internal carotid artery and the tip of SP (SP-ICA) (Fig. 2) was measured.

We used the classification regarding shapes (Fig. 3) and SPL and stylohyoid ligament formed by several researchers.[3,12,14–18]

Type A: normal SP appearance
Type A1: shorter SP (<25 mm)
Type A2: longer SP (25–40 mm)

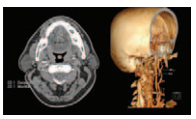

FIGURE 2. The distance between internal carotid artery and the tip of styloid process (SP-ICA).

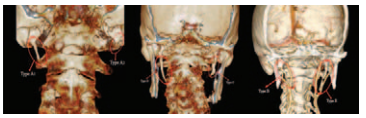

FIGURE 3. Types of styloid process.

Type B: elongated SP (>40 mm)
Type C: bended SP
Type D: segmented (SP + partial ossification of stylohyoid ligament)
Type E: SP pseudo-arthrosis
Type F: SP and stylohyoid ligament ossified through distal and adhered on lesser horn of hyoid bone

The obtained data from the study was assessed by using SPSS 15.0 (Statistical Package for Social Science; SPSS Inc, Chicago, IL) program. The mean values of the data, standard deviations, maximum and minimum values were determined. The differences between morphometric values of SP of male and female patients were compared using independent sample *t* test and data from morphometric measurements acquired from right and left sides of the individuals were compared using paired sample *t* test. Pearson correlations were used to confirm the relationship between the variables. The 95% confidence intervals were calculated and $P < 0.05$ was considered statistically significant.

RESULTS

Sixty-four percent of the patients included in the study were male and 31% were female. The mean age of all patients was determined as 63.95 ± 10.23 years (Table 1). The mean SPL of right side (SPLright) was determined as 2.30 ± 0.86 cm (male: 2.45 ± 0.90, female: 1.98 ± 0.69 cm), SPL of the left side (SPLleft) was determined as 2.31 ± 0.78 cm (male: 2.47 ± 0.79, female: 1.94 ± 0.60 cm) (Tables 1 and 2). SP' angulation of right side (SPAright) was found as 71.96 degree in males and 71.12 degree in females, whereas SPA of the left side (SPAleft) was observed as 71.44 degree in males and 70.79 degree in females. Statistical differences were found regarding SPLright, SPLleft, SPWright, SPWleft, DBR, and SP-ICA left between sexes (Table 2).

The obtained data from male, female, and all patients showed no statistical significance between right and left sides ($P > 0.05$) (Table 3). In both age groups, the whole data were found higher

TABLE 1. Minimum, Maximum, Mean Values, and Standard Deviations of the Obtained Data in all Patients (Mean ± SD, cm, degree)

	N	Minimum (Min)	Maximum (max)	Mean ± SD
Age	100	43.00	86.00	63.95 ± 10.23
SPL_{right}	100	0.34	4.69	2.30 ± 0.86
SPL_{left}	100	0.34	4.78	2.31 ± 0.78
SPW_{right}	100	1.17	6.20	4.02 ± 1.08
SPW_{left}	100	1.30	7.65	3.86 ± 1.07
DBR	100	6.75	9.55	8.14 ± 0.57
SPA_{right}	100	47.50 degree	86.30 degree	71.7 ± 6.19 degree
SPA_{left}	100	53.90 degree	95.10 degree	71.24 ± 6.90 degree
$SP\text{-}ICA_{right}$	100	0.17	1.81	0.74 ± 0.37
$SP\text{-}ICA_{left}$	100	0.14	2.12	0.81 ± 0.35

DBR = Distance between styloid process rooths, SPA_{left} = Left angulation of the styloid process, SPA_{right} = right angulation of the styloid process, $SP\text{-}ICA_{left}$ = distance between internal carotid artery and the tip of left styloid process, $SP\text{-}ICA_{right}$ = distance between internal carotid artery and the tip of right styloid process, SPL_{left} = left styloid process length, SPL_{right} = right styloid process length, SPW_{left} = left styloid process width; SPW_{right} = right styloid process width.

© 2015 Mutaz B. Habal, MD

Copyright © 2015 Mutaz B. Habal, MD. Unauthorized reproduction of this article is prohibited.

TABLE 2. The Comparison of the Obtained Data According to Sex (Mean ± SD, cm, degree)

	Male		Female		
	N	Mean ± SD	N	Mean ± SD	P
SPL_{right}	69	2.45 ± 0.90	31	1.98 ± 0.69	0.009
SPL_{left}	69	2.47 ± 0.79	31	1.94 ± 0.60	0.001
SPW_{right}	69	4.25 ± 1.04	31	3.50 ± 1.00	0.001
SPW_{left}	69	4.07 ± 1.10	31	3.40 ± 0.85	0.003
DBR	69	8.31 ± 0.56	31	7.76 ± 0.37	0.000
SPA_{right}	69	71.96 ± 6.67 degree	31	71.12 ± 5.02 degree	0.539
SPA_{left}	69	71.44 ± 7.38 degree	31	70.79 ± 5.71 degree	0.668
$SP\text{-}ICA_{right}$	68	0.79 ± 0.36	31	0.71 ± 0.38	0.302
$SP\text{-}ICA_{left}$	69	0.88 ± 0.37	31	0.67 ± 0.25	0.006

DBR = distance between styloid process rooths, SPA_{left} = left angulation of the styloid process, SPA_{right} = right angulation of the styloid process, $SP\text{-}ICA_{left}$ = distance between internal carotid artery and the tip of left styloid process, $SP\text{-}ICA_{right}$ = distance between internal carotid artery and the tip of right styloid process, SPL_{left} = left styloid process length, SPL_{right} = right styloid process length, SPW_{left} = left styloid process width, SPW_{right} = right styloid process width.

in males compared with females. Rest of the data were observed higher in ≥60 age group except for SPAleft (Table 4).

We observed that 55% of all patients had type A1 SP, 30% type A2, 3% type B, 3% type C, 1% type D, and 8% type E on their right side and 52% type A1, 28% type A2, 3% type B, 6% type C, 1% type D, and 10% type E-shaped SPs on their left side, whereas type F was not observed on either side (Table 5). Between SPLright, SPLleft, SPWright, SPWleft, and age groups, significant positive correlations were observed, whereas there were significant negative correlations between SPLright, SPLleft, SPWright, SPWleft, DBR, SP-ICA left, and sex (Table 6).

DISCUSSION

SP is a cylindrical shaped bone structure placed at inferior surface of petrous part of temporal bone and in front of stylomastoid foramen. This structure is a surface for ligaments (stylohyoid ligament, stylomandibular ligament) and muscles (stylopharyngeus muscle, stylohyoid muscle, and styloglossal muscle) to attach. The stylohyoid ligament attaches to the lesser horn of the hyoid bone and seems like extension of SP.[19–21]

Many studies regarding the SPL can be seen in the literature.[3,5,7,12,22–28] The mean SP length was measured on 484 patients whose ages were ranged between 40 and 44 as 29.49 mm on right side and 29.92 mm on the left side on panoramic radiography (PR) images[26]; on 521patients as 23–36 mm[25]; 32.75 mm on 60–79 age group[27]; and 698 patients with mean ageof 34.9 males were measured as approximately 38.1 mm while females were measured as 36.6 mm in average.[24]

TABLE 3. The Comparison of the Right and Left Parameters of SP (Mean ± SD, cm, degree)

	Male	Female	Total Patients
SPL_{right} and SPL_{left}	0.835	0.682	0.989
SPW_{right} and SPW_{left}	0.145	0.554	0.118
SPA_{right} and SPA_{left}	0.551	0.789	0.515
$SP\text{-}ICA_{right}$ and $SP\text{-}ICA_{left}$	0.116	0.567	0.243

DBR = distance between styloid process rooths, SPA_{left} = left angulation of the styloid process, SPA_{right} = right angulation of the styloid process, $SP\text{-}ICA_{left}$ = distance between internal carotid artery and the tip of left styloid process, $SP\text{-}ICA_{right}$ = distance between internal carotid artery and the tip of right styloid process, SPL_{left} = left styloid process length, SPL_{right} = right styloid process length, SPW_{left} = left styloid process width, SPW_{right} = right styloid process width.

Mansour and Young[12] reported after assessment of PR images of 670 patients ages between 8 and 67 years that the mean SP length was 29.20 mm that SP length slowly increased until the age of 30 and stayed at the same length for some time and increased as a small rate near the age of 60.

Onbaş et al[5] reported SP length as 26.8 mm on MDCT images of 283 patients whose ages were ranged between 18 and 77 years and Andrei et al[22] reported SP length as 35.09 mm on 44 patients' CT images. In our study, SP length was determined as 2.30 cm on right side and 2.31 cm on the left side in average. When 2 studies were compared, these values were a little lower than the findings of Onbaş et al whose patients' mean age was lower than our patients'.

Yavuz et al[28] observed 51 elongated SPs on radiological images of 30 patients (27 females, 3 males; mean age = 48.2) and reported that SP length was ranged between 3.5 and 8 cm. In the control group (28 females, 3 males, mean age = 45.5) mean of SP length was 2.8 cm on the right side and 2.6 cm on the left side.

In 80 cadavers, SP length was observed between 15.2 and 47.7 mm.[29] Promthale et al[7] reported average of normal SP length as 21.73 mm, average of elongated SP length as 34.74 mm, and total average of SP length as 24.12 mm in 176 Thai skulls (aged 18–92) and 150 cadavers(aged 22–95) and reported the SP length as shorter compared with Turks based on the data obtained from the control group of the study conducted by Yavuz et al.[28] Also Promthale et al[7] detected that elongated SP rate was higher in the ≥60 age group. The data acquired from our study were closer to the data from the study of Promthale et al.[7] The other data were observed higher in ≥60 age group except for SPAleft (Table 4).

There were many studies conducted regarding the relation between age, sex, and SP length.[12,25,27,30–33] In our study, significant positive correlations between right and left side SP length and age groups were observed (rright = 0.342, rleft = 0.230). In addition, this relationship was more significant on the right side compared with the left. Also in our study, a significant relationship between sex and SP length was observed (rright = 0.258, rleft = 0.321). In all age groups, SP length was found higher in males compared with females (Table 6).

Ilguy et al[31] suggested the idea that in Eagle Syndrome, caused by longer and wider SP, SP angle, deviation, and ossification rate could be important. Direction and the angle of the elongated SP causing irritation on the surrounding parapharyngeal anatomical structures were reported in several studies.[28,34,35] Kosar et al[4] designated the angle between the transverse line uniting SP and the line appears between the rooths of SP as medial angle on the 3D images originated from axial CT scans of 11 male and 11 female patients aged between 24 and 80 years and detected that angle on the right side as 66.0 degree (male: 67.4 degree; female: 64.6 degree) and on the left side as 69.0 degree (male: 69.2 degree; female: 68.8 degree). Onbas et al[5] defined the angle as transverse angle, which is described as medial angle by Kosar et al,[4] and detected the mean value of this angle as 72.7 degree on MDCT images of 283 patients.

In our study based on the same measurement reference points, mean of this angle was observed as 71.7 degree (male: 71.96 degree; female: 71.12 degree) on the right side and 71.24 degree (male: 71.44 degree; female: 70.79 degree) on the left side (Table 1). It has been detected that the data acquired from our study were consistent with the data from the study of Onbaş et al[5] and higher than the values that Kosar et al[4] acquired from their study.

The correlation between the right and left medial angle was found to be insignificant.[4] In our study, the correlation

© 2015 Mutaz B. Habal, MD
Copyright © 2015 Mutaz B. Habal, MD. Unauthorized reproduction of this article is prohibited.

TABLE 4. Minimum, Maximum, Mean Values, and Standard Deviations of the Obtained Data According to Age Groups in all Patients (Mean ± SD, cm, degree)

	Total Patients			Male		Female	
	n	Min	Max	Mean ± SD	n	Mean ± SD	n	Mean ± SD
<60 Age group								
Age	31	43	59	51.68 ± 5.31	18	52.11 ± 4.98	13	51.08 ± 5.88
SPL_{right}	31	0.34	4.29	1.87 ± 0.92	18	2.17 ± 1.01	13	1.46 ± 0.61
SPL_{left}	31	0.34	4.18	2.04 ± 0.94	18	2.49 ± 0.96	13	1.43 ± 0.44
SPW_{right}	31	1.17	5.89	3.53 ± 1.34	18	3.96 ± 1.32	13	2.93 ± 1.16
SPW_{left}	31	1.3	5.38	3.33 ± 0.88	18	3.62 ± 0.89	13	2.93 ± 0.73
DBR	31	7.14	9.32	8.08 ± 0.54	18	8.35 ± 0.51	13	7.70 ± 0.32
SPA_{right}	31	47.5°	86.3°	71.15 ± 7.53°	18	71.19 ± 8.82°	13	71.09 ± 5.62°
SPA_{left}	31	55.6°	95.1°	71.31 ± 7.94°	18	72.45 ± 8.42°	13	69.72 ± 7.24°
$SP\text{-}ICA_{right}$	31	0.32	1.64	0.74 ± 0.32	18	0.75 ± 0.30	13	0.72 ± 0.35
$SP\text{-}ICA_{left}$	31	0.29	1.4	0.79 ± 0.28	18	0.86 ± 0.30	13	0.67 ± 0.22
≥60 Age group								
Age	69	60	86	69.46 ± 6.36	51	69.71 ± 6.37	18	68.78 ± 6.43
SPL_{right}	69	0.64	4.69	2.51 ± 0.76	51	2.56 ± 0.84	18	2.35 ± 0.46
SPL_{left}	69	0.7	4.78	2.43 ± 0.67	51	2.47 ± 0.74	18	2.31 ± 0.39
SPW_{right}	69	2.04	6.2	4.24 ± 0.87	51	4.36 ± 0.92	18	3.91 ± 0.64
SPW_{left}	69	1.61	7.65	4.11 ± 1.06	51	4.24 ± 1.12	18	3.75 ± 0.78
DBR	69	6.75	9.55	8.17 ± 0.58	51	8.30 ± 0.58	18	7.81 ± 0.40
SPA_{right}	69	58.6 degree	84.9 degree	71.94 ± 5.54 degree	51	72.23 ± 5.81 degree	18	71.15 ± 4.71 degree
SPA_{left}	69	53.9 degree	91.6 degree	71.21 ± 6.41 degree	51	71.08 ± 7.02 degree	18	71.57 ± 4.35 degree
$SP\text{-}ICA_{right}$	69	0.17	1.81	0.78 ± 0.39	51	0.80 ± 0.38	18	0.71 ± 0.40
$SP\text{-}ICA_{left}$	69	0.14	2.12	0.83 ± 0.39	51	0.88 ± 0.39	18	0.68 ± 0.29

DBR = distance between styloid process rooths, SPA_{left} = left angulation of the styloid process, SPA_{right} = right angulation of the styloid process, $SP\text{-}ICA_{left}$ = distance between internal carotid artery and the tip of left styloid process, $SP\text{-}ICA_{right}$ = distance between internal carotid artery and the tip of right styloid process, SPL_{left} = left styloid process length, SPL_{right} = right styloid process length, SPW_{left} = left styloid process width, SPW_{right} = right styloid process width.

between right and the left medial angle was not found to be statistically significant in male, female and all patient groups (Table 3).

Gözil et al[3] classified SP on CT images of 58 female and 47 male patients aged between 18 and 86 years. They observed 24.8% A1, 32.4% A2, 6.7% B, 7.6% C, 24.8% D, 3.8% E, and 0% F types of SP on the right side and 25.7% A1, 32.4% A2, 7.6% B, 4.8% C, 17.1% D, 10.5% E, and 1.9% F types on the left side. Mansour and Young[12] detected SP length >40 mm as 21.1%, <40 mm as 35%, bended SP rate as 4.5% in the study they conducted on PR images of 670 patients.[12] In our study, SPs >40 mm were classified as type B, and type B SP rate was observed as 3% on the left and right sides (Table 5). Also the bended SP rate, which is classified as type C in our study, was observed as 3% on the right and 6% on the left side and these findings were similar to the findings of Mansour andYoung[12] acquired from their study.

SP was observed as mostly type A1 on our study (right 55%, left 52%) (Table 5). The type D rate observed in the study of Gözil et al[3] (right 24.8%, left 17.1%) is found to be greatly higher compared with our findings of type D SP (right 1%, left %1).

The SPL, its angulation, and distance from internal carotid artery are greatly variable. Carotid artery syndrome is a clinical manifestation of the compression applied to the artery by the elongated SP. This syndrome is related to pain and ischemic symptoms. Carotid artery dissection and temporary cerebral ischemia caused by the pressure of elongated SP in close distance to the carotid artery are rare but seen cases.[36–39] In our study, the distance between SP and carotid artery was found to be statistically insignificant on the right side ($P > 0.05$), but it was statistically significant on the left ($P < 0.05$). In contrast to other studies regarding to SP, in our study, morphometric measurements (length, width, angle), SP internal carotid artery distance measurements, and classification of SP were carried out on same cases. Another study in which these

TABLE 5. Type Classification of Styloid Process and Percentages (According to Gözil et al's Classification)

	Male		Female		Total	
	Right	Left	Right	Left	Right	Left
A1	34 (%49.28)	31 (%44.93)	21 (%67.74)	21 (%67.74)	55 (%55)	52 (%52)
A2	25 (%36.23)	25 (%36.23)	5 (%16.13)	3 (%9.68)	30 (%30)	28 (%28)
B	3 (%0.43)	3 (%0.43)	0 (%0)	0 (%0)	3 (%3)	3 (%3)
C	0 (%0)	2 (%2.9)	3 (%9.68)	4 (%12.90)	3 (%3)	6 (%6)
D	1 (%1.45)	1 (%1.45)	0 (%0)	0 (%0)	1 (%1)	1 (%1)
E	6 (%8.7)	7 (%10.15)	2 (%6.45)	3 (%9.68)	8 (%8)	10 (%10)
F	0 (%0)	0 (%0)	0 (%0)	0 (%0)	0 (%0)	0 (%0)

© 2015 Mutaz B. Habal, MD

Copyright © 2015 Mutaz B. Habal, MD. Unauthorized reproduction of this article is prohibited.

TABLE 6. The Correlation Between Data of SP

		SP-ICA$_{left}$	SP-ICA$_{right}$	SPA$_{left}$	SPA$_{right}$	DBR	SPW$_{left}$	SPW$_{right}$	SPL$_{left}$	SPL$_{right}$	Sex	Age Group
Age group	*R*	0.069	0.048	−0.007	0.06	0.079	0.340**	0.305**	0.230*	0.342**	−0.158	1
	P	0.495	0.636	0.946	0.555	0.438	0.001	0.002	0.021	0.000	0.115	
Sex	*R*	−0.271**	−0.104	−0.043	−0.062	−0.448**	−0.292**	−0.322**	−0.321**	−0.258**	1	
	P	0.006	0.302	0.668	0.539	0.000	0.003	0.001	0.001	0.009		
SPL$_{right}$	*R*	−0.063	0.013	−0.155	−0.135	0.216*	0.176	0.513**	0.710**	1		
	P	0.530	0.901	0.124	0.180	0.031	0.079	0.000	0.000			
SPL$_{left}$	*R*	−0.048	−0.125	0.187	−0.091	0.187	0.279**	0.395**	1			
	P	0.635	0.215	0.063	0.368	0.063	0.005	0.000				
SPW$_{right}$	*R*	−0.087	−0.120	0.000	0.051	0.094	0.603**	1				
	P	0.390	0.235	0.998	0.613	0.354	0.000					
SPW$_{left}$	*R*	0.062	−0.064	0.074	0.191	0.055	1					
	P	0.539	0.525	0.466	0.058	0.586						
DBR	*R*	0.174	0.043	−0.213*	−0.284**	1						
	P	0.084	0.668	0.033	0.004							
SPA$_{right}$	*R*	0.088	0.226*	0.423**	1							
	P	0.385	0.024	0.000								
SPA$_{left}$	*R*	0.277**	0.168	1								
	P	0.005	0.095									
SP-ICA$_{right}$	*R*	0.301**	1									
	P	0.002										
SP-ICA$_{left}$	*R*	1										
	P											

*Correlation is significant at the 0.05 level (2-tailed).
**Correlation is significant at the 0.01 level (2-tailed).
DBR = distance between styloid process rooths, SPA$_{left}$ = left angulation of the styloid process, SPA$_{right}$ = right angulation of the styloid process, SP-ICA$_{left}$ = distance between internal carotid artery and the tip of left styloid process, SP-ICA$_{right}$ = distance between internal carotid artery and the tip of right styloid process, SPL$_{left}$ = left styloid process length, SPL$_{right}$ = right styloid process length, SPW$_{left}$ = left styloid process width, SPW$_{right}$ = right styloid process width.

parameters were studied together in same case group was not found in the literature. The obtained data have shown that SP has variable anatomical structural features. This variability can affect the surrounding anatomical structures and cause non-specific symptoms including pain in cervicocranial region, temporomandibular pain, difficulty in swallowing (dysphagia), foreign subject feeling in throat. Although these kinds of complaints usually occur due to other reasons, it can be caused by Eagle Syndrome as well. We believe that the knowledge of the morphometric data and anatomical variances of SP would help clinicians to correctly diagnose the case.

REFERENCES

1. Başekim CÇ, Mutlu H, Güngör A, et al. Evaluation of styloid process by three-dimensional computed tomography. *Eur Radiol* 2005;15:134–139
2. Campos D, Silva T, Kipper J, et al. Ossification of styloid ligament and its clinical implication: a report of human cases. *Braz J Morphol Sci* 2011;28:137–139
3. Gözil R, Yener N, Calgüner E, et al. Morphological characteristics of styloid process evaluated by computerized axial tomography. *Ann Anat* 2001;183:527–535
4. Kosar M, Atalar M, Sabanciogullari V, et al. Evaluation of the length and angulation of the styloid process in the patient with pre-diagnosis of Eagle syndrome. *Folia Morphol (Warsz)* 2011;70:295–299
5. Onbas O, Kantarci M, Karasen RM, et al. Angulation, length, and morphology of the styloid process of the temporal bone analyzed by multidetector computed tomography. *Acta Radiol* 2005;46:881–886
6. Paraskevas GK, Raikos A, Lazos LM, et al. Unilateral elongated styloid process: a case report. *Cases J* 2009;2:9135
7. Promthale P, Chaisuksunt V, Rungruang T, et al. Anatomical consideration of length and angulation of the styloid process and their significances for eagle's syndrome in Thais. *Siriraj Med J* 2012;64(Suppl 1):30–33
8. Eagle WW. The symptoms, diagnosis and treatment of the elongated styloid process. *Am Surg* 1962;28:1–5
9. Eagle WW. Elongated styloid process: further observations and a new syndrome. *Arch Otolaryngol* 1948;47:630–640
10. Diamond LH, Cottrell DA, Hunter MJ, et al. Eagle's syndrome: a report of 4 patients treated using a modified extraoral approach. *J Oral Maxillofac Surg* 2001;59:1420–1426
11. Erol B. Radiological assessment of elongated styloid process and ossified stylohyoid ligament. *J Marmara Univ Dent Fac* 1996;2:554–556
12. Monsour PA, Young WG. Variability of the styloid process and stylohyoid ligament in panoramic radiographs. *Oral Surg Oral Med Oral Pathol* 1986;61:522–526
13. Schroeder WA. Traumatic Eagle's syndrome. *Otolaryngol Head Neck Surg* 1991;104:371–374
14. Chandler JR. Anatomical variations of the stylohyoid complex and their clinical significance. *Laryngoscope* 1977;87:1692–1701
15. Guo B, Jaovisidha S, Sartoris D, et al. Correlation between ossification of the stylohyoid ligament and osteophytes of the cervical spine. *J Rheumatol* 1997;24:1575–1581
16. Langlais RP, Miles DA, Van Dis ML. Elongated and mineralized stylohyoid ligament complex: a proposed classification and report of a case of Eagle's syndrome. *Oral Surg Oral Med Oral Pathol* 1986;61:527–532
17. Lengelé BG, Dhem AJ. Length of the styloid process of the temporal bone. *Arch Otolaryngol Head Neck Surg* 1988;114:1003–1006
18. Satyapal K, Kalideen J. Bilateral styloid chain ossification: case report. *Surg Radiol Anat* 2000;22:211–212
19. Camarda AJ, Deschamps C, Forest DI. Stylohyoid chain ossification: a discussion of etiology. *Oral Surg Oral Med Oral Pathol* 1989;67:508–514
20. Fini G, Gasparini G, Filippini F, et al. The long styloid process syndrome or Eagle's syndrome. *J Cranio Maxill Surg* 2000;28:123–127

© 2015 Mutaz B. Habal, MD

Copyright © 2015 Mutaz B. Habal, MD. Unauthorized reproduction of this article is prohibited.

21. Gossman J Jr, Tarsitano JJ. The styloid-stylohyoid syndrome. *J Oral Surg* 1977;35:555
22. Andrei F, Motoc AG, Didilescu AC, et al. A 3D cone beam computed tomography study of the styloid process of the temporal bone. *Folia Morphol (Warsz)* 2013;72:29–35
23. Frommer J. Anatomic variations in the stylohyoid chain and their possible clinical significance. *Oral Surg Oral Med Oral Pathol* 1974;38:659–667
24. Gokce C, Sisman Y, Ertas ET, et al. Prevalence of styloid process elongation on panoramic radiography in the Turkey population from cappadocia region. *Eur J Dent* 2008;2:18–22
25. Jung T, Tschernitschek H, Hippen H, et al. Elongated styloid process: when is it really elongated? *Dentomaxillofac Rad* 2004;33:119–124
26. Kaufman SM, Elzay RP, Irish EF. Styloid process variation: radiologic and clinical study. *Arch Otolaryngol* 1970;91:460–463
27. Rizzatti-Barbosa CM, Ribeiro MC, Silva-Concilio LR, et al. Is an elongated stylohyoid process prevalent in the elderly? A radiographic study in a Brazilian population. *Gerodontology* 2005;22:112–115
28. Yavuz H, Caylakli F, Yildirim T, et al. Angulation of the styloid process in Eagle's syndrome. *Eur Arch Otorhinolaryngol* 2008;265:1393–1396
29. Moffat D, Ramsden R, Shaw H. The styloid process syndrome: aetiological factors and surgical management. *J Laryngol Otol* 1977;91:279–294
30. Bozkir M, Boga H, Dere F. The evaluation of elongated styloid process in panoramic radiographs in edentulous patients. *Turk J Med Sci* 2009;29:481–486
31. Ilgüy M, Ilgüy D, Güler N, et al. Incidence of the type and calcification patterns in patients with elongated styloid process. *J Int Med Res* 2005;33:96–102
32. MacDonald-Jankowski D. Calcification of the stylohyoid complex in Londoners and Hong Kong Chinese. *Dentomaxillofac Radiol* 2001;30:35–39
33. Okabe S, Morimoto Y, Ansai T, et al. Clinical significance and variation of the advanced calcified stylohyoid complex detected by panoramic radiographs among 80-year-old subjects. *Dentomaxillofac Radiol* 2006;35:191–199
34. Ghosh LM, Dubey SP. The syndrome of elongated styloid process. *Auris Nasus Larynx* 1999;26:169–175
35. Strauss M, Zohar Y, Laurian N. Elongated styloid process syndrome: intraoral versus external approach for styloid surgery. *Laryngoscope* 1985;95:976–979
36. Chuang W, Short J, McKinney A, et al. Reversible left hemispheric ischemia secondary to carotid compression in Eagle syndrome: surgical and CT angiographic correlation. *AJNR Am J Neuroradiol* 2007;28:143–145
37. Piagkou M, Anagnostopoulou S, Kouladouros K, et al. Eagle's syndrome: a review of the literature. *Clin Anat* 2009;22:545–558
38. Soo OY, Chan YL, Wong KS. Carotid artery dissection after prolonged head tilting while holding a newborn baby to sleep. *Neurology* 2004;62:1647–1648
39. Zuber M, Meder J, Mas J. Carotid artery dissection due to elongated styloid process. *Neurology* 1999;53:1886–1887

Delayed Hypersensitive Process in Subacute Subdural Hematoma

Zhiqiang Tao, MD, Shenghong Ding, MD, Maotong Hu, MD, and Jianwei Li, MD

Abstract: The authors report 2 patients with subacute subdural hematoma (sASDH). An inflammatory process is known to be involved in the development of traumatic subdural effusion (TSE) evolving into chronic subdural hemorrhage (CSDH), but a similar event has not been previously described in acute subdural hematoma (ASDH) evolving into sASDH. In our cases, dexamethasone (DXM) and other conservative treatments were administered to our first patient with dramatic clinical outcome, and a postoperative pathologic examination of the neomembrane of the sASDH in the second patient was done, which showed marked inflammatory process with T-lymphocytes and neutrophils infiltration. The good response to DXM in the first patient and the definite laboratory result of the second patient and their radiologic presentations, as well as a review of relevant literature, suggest that a T-lymphocyte-mediated, delayed hypersensitive reaction triggered by undissolved blood clot may be the driving force of ASDH developing into sASDH, which starts after the seventh day, and peaked by the end of the second week of the clinical course.

Key Words: Delayed hypersensitivity, dexamethasone, inflammation, subacute subdural hematoma, T-lymphocyte

Acute subdural hematoma (ASDH) at the subacute stage, which is referred to as subacute subdural hematoma (sASDH), is a comparatively underinvestigated disease with very few papers focused on the mechanism of its clinical characteristics and management.[1–7] In this article, we describe 2 patients with a definite diagnosis of sASDH to boost our understanding of its clinical characteristics.

CLINICAL REPORT

Patient 1: A 20-year-old man was admitted to our department with complaints of headache, dizziness, nausea, and vomiting. He had sustained a head trauma at his left temporal region with a short period of unconsciousness followed by same symptoms described above (2 days before). He had been transferred to a local hospital, where a computerized tomography (CT) scanning had not found obvious abnormality (Fig. 1A). Consequently, he had been discharged when his symptoms relieved. These symptoms, however, had relapsed, which made him present to the hospital again. On admission, neurologic examination revealed a conscious adult male with unlimited limb movements, whereas CT demonstrated an ASDH at the right frontoparietal region with subarachnoid hemorrhage (SAH) (Fig. 1B). He was then turned to our hospital and treated with hemostatic agents only in light of his bearable symptoms and mild signs. Magnetic resonance imaging (MRI) on the fifth day after injury showed a low-intensity subdural mass at the right frontotemporoparietal region in T2-weighted images (T2WI) (Fig. 1C). Ironically, on the ninth day after the accident, he complained an exacerbated headache and vomited twice. Five micrograms of dexamethasone (DXM) was dripped intravenously twice on that day, which miraculously resolved his symptoms on the next day. Withdrawal of DXM on the 11th day made his symptoms relapse on the 12th day again. No conspicuous pathologic signs

From the Department of Neurosurgery, Yiwu Central Hospital, Wengzhou Medical College, Yiwu, China.
Received January 25, 2015.
Accepted for publication April 14, 2015.
Address correspondence and reprint requests to Zhiqiang Tao, MD, Department of Neurosurgery, Yiwu Central Hospital, Wengzhou Medical College, Yiwu 322000, China. E-mail: 266181@163.com
The authors report no conflicts of interest.
Copyright © 2015 by Mutaz B. Habal, MD
ISSN: 1049-2275
DOI: 10.1097/SCS.0000000000001889

Copyright © 2015 Mutaz B. Habal, MD. Unauthorized reproduction of this article is prohibited.

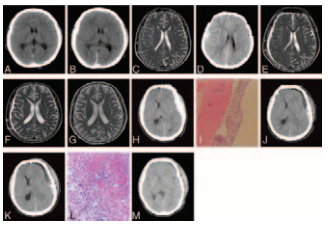

FIGURE 1. A: a CT scan of the 1st patient on the day of injury revealed no significant abnormality; B: a CT scan of the 1st patient on the 2nd day after head trauma; C: a MRI T2WI of the 1st patient on the 5th day after head injury; D: an emergent CT scan of the 1st patient on the 13rd day after head injury; E: a T2WI of the 1st patient on the 15th day of the course; F: a subsequent T2WI of the 1st patient showed marked shrinkage of the right subdural mass; G: the latest T2WI of the 1st patient of the first patient; H: a CT scan of the 2nd patient on admission; I: neo-membrane formation obtained during the first surgery of the 2nd patient under microscopic examination showed extensive T-lymphocyte infiltration (hematoxylin-eosin stain, original magnification×400); J: a CT scan of the 2nd patient on the 14th day after the first complaining; K: a more marked midline shift was revealed in CT imaging on the 14th day after the first complaining; L: T-lymphocytes and neutrophils infiltration accompany with plasma effusion was found in the neo-membrane tissue obtained during the second surgery under microscopic examination (hematoxylin-eosin stain, original magnification×400); M: a CT scan of the patient on the 15th day.

were discovered during his neurologic examination and an emergent CT scan demonstrated a homogeneous density hematoma with a high-density clot in it (Fig. 1D). The headache symptom became more serious and was accompanied by vomiting frequently on the 13th day. Therefore, DXM was instituted to him again according to the previous protocol, which relieved his symptoms rapidly. On the 15th day of the course, MRI was performed again, which demonstrated a homogeneously high-intensity subdural hematoma in T2WI (Fig. 1E) as opposed to the MRI findings on the fifth day. DXM was ceased on the 16th day. Subsequent serial MRI showed a gradual disappearance of the subdural mass in T2WI (Fig. 1F-G), and the patient was discharged without neurologic deficit 30 days.

Patient 2: A 57-year-old man presented to our department complaining about paroxysmal headaches at his left frontotemporal region with vomiting in the second time. At the first time, he suffered the agony because of drinking alcohol 3 days before and alleviated after vomiting. In spite of the failure of eliciting any meaningful physical findings, CT scanning revealed an ASDH, which covered the left frontoparietotemporal region with obvious midline shift (Fig. 1H). He was admitted and 125 μL of a 20% mannitol solution was dripped intravenously for 4 times per day, which can relieve his headache effectively. The ninth day after injury saw the worsening of his headaches, anorexia and a deterioration of his mental state. On the 11th day, neurologic examination found him to be delirious. Craniotomy, surgical removal, and subdural drainage placement of subdural hematoma were performed on that day. On opening of the subdural hematoma, neomembrane formation was noticed and dissected to have pathologic examination (Fig. 1I). Postoperative CT imaging on the 13th day after injury revealed a separated-density subdural hematoma with midline shift similar to the initial CT scan (Fig. 1J) and the total amount of drainage volume was 30 mL and the patient remained febrile and confused. A CT scan on the 14th day after the first complaining showed an even more serious enlargement of subdural fluid collections with marked midline shift (Fig. 1K). Patient appeared apathetic and weak. A second surgery was performed immediately, where a thicker neomembrane was found with intensive lymphocytes together with neutrophils and plasma effusion as revealed by microscopic examination (Fig. 1L). The second postoperative period was uneventful. The total subdural drainage volume after the second craniotomy on the 15th day was 110 mL, and then it fell to 10 mL throughout the next 2 days. The subdural hematoma was barely seen in CT on the 15th day (Fig. 1M). The patient was discharged without neurological deficits.

DISCUSSION

ASDH is generally considered as a result of vascular rupture,[8] but the subsequent events are not as very clear. Traditionally, it is widely accepted that the clinical course of ASDH developing into sASDH is subjected to lysis of the ASDH, damaged vessels rebleeding into the subdural cavity, the presence of osmotic gradient forcing cerebrospinal fluid (CSF) into it and/or a torn arachnoid membrane producing a leakage of CSF.[7] But neither rebleeding nor leakage of CSF can be detected in the second patient throughout his 2 perioperative periods. Moreover, the regular fluctuating (rather than linear) radiological presentations, the time of the peak symptoms, and the good response to steroids of the sASDH we observed suggested that the sASDH may undergo a special inflammatory pathway.

The similar clinical courses of the current 2 patients, may reflect the common pathophysiological features of sASDH, which is reinforced by the observation reported by Morinaga et al.[9] Recently, the antigen-presentation function was discovered in arachnoid cells, where basic expression of human leukocyte antigen-DR (HLA-DR) was detected and a potential to activate T-lymphocytes is confirmed when stimulated by bloody CSF.[10] Because arachnoid and dura mater are firmly attached to each other, and share the dural border layer cells,[11] the border layer cells adherent to the dura mater may respond to the lytic components of the ASDH and therefore serve as the antigen-presentation cells (APCs) to motivate the enlisted T-lymphocytes in the newly formed vessels. In addition, a time regular pattern of activation of T-lymphocytes-induced inflammatory pathway was also recorded in literature,[10] which showed that the activity of T-lymphocytes peaked approximately after 7 days of coculturing arachnoid cells with bloody CSF in vitro. Interestingly, clinical conditions were seen approximately at the end of second week after head injury. This happened to be close to the time of the neomembrane vessel formation plus the time of the peaked activation of T-lymphocytes as discovered in laboratory findings.[10] Our operational findings in the second patient confirmed the existence of neomembrane and its laboratory examination also revealed extensive infiltration of T-lymphocytes, both of which indicated the important role played by the inflammatory process in the natural course of sASDH. Consequently, we hypothesize that ASDH progress to sASDH via T-lymphocyte-induced type IV hypersensitivity triggered by remaining blood clot components in subdural cavity or adjacent brain tissues, instead of posttraumatic bleeding.

With regard to the management of sASDH, aside from careful observations, surgery has routinely been suggested to be the first-line approach, with burr-hole surgery preferable. In addition, in the first patient, the cease of DXM administration happened on the 11th day of the course, which soon produced the deterioration on the 12th day, and the second cease of DXM use on the 16th day after injury did not lead to any deterioration. The clinical course illustrated a continuous hypersensitive reaction at the 11th day, which sharply decreased on the 16th day. In addition, the unfavorable drainage in the second patient after the first operation failed to reduce the subdural size hinted the inflammatory reaction existed during the 11th to 14th day as before. Consequently, we hypothesize that a possible recommendatory use of DXM in sASDH should during 14th to 16th days in the course to cover the whole process of the delayed hypersensitivity.

CONCLUSIONS

In sum, most patients with ASDH can be cured by conservative therapy with complete absorption of their subdural hemorrhage

© 2015 Mutaz B. Habal, MD

Copyright © 2015 Mutaz B. Habal, MD. Unauthorized reproduction of this article is prohibited.

(SDH), but expansion of SDH, which appears as low-intensity masses in CT scan, or subdural fluid collection in MRI, may be seen in some patients after the seventh day after injury. Of the latter cases, the majority sustained the worst symptoms and had surgery between the 13th and 14th day of the course, which perhaps constitute the clinical entity of sASDH. Of course, more clinical and experimental efforts are needed to confirm and elaborate the exact relation between sASDH and T-lymphocyte-mediated inflammatory response to improve the clinical outcome of patients with sASDH.

REFERENCES

1. Hassen GW, Kalantari H. Diplopia from subacute bilateral subdural hematoma after spinal anesthesia. *West J Emerg Med* 2012;13:108–110
2. Izumihara A, Yamashita K, Murakami T. Acute subdural hematoma requiring surgery in the subacute or chronic stage. *Neurol Med Chir* 2013;53:323–328
3. Lee SM, Park HS, Choi JH, et al. Ruptured mycotic aneurysm of the distal middle cerebral artery manifesting as subacute subdural hematoma. *J Cerebrovasc Endovasc Neurosurg* 2013;15:235–240
4. Lollis SS, Wolak ML, Mamourian AC. Imaging characteristics of the subdural evacuating port system, a new bedside therapy for subacute/chronic subdural hematoma. *Am J Neuroradiol* 2006;27:74–75
5. Galvez JC, Hecht S. Subacute subdural hematoma in a Karate instructor after noncontact head trauma. *Curr Sports Med Rep* 2011;10:11–13
6. Echlin F. Traumatic subdural hematoma; acute, subacute and chronic; an analysis of 70 operated cases. *J Neurosurg* 1949;6:294–303
7. Kuwahara S. Diffusion-weighted imaging of traumatic subdural hematoma in the subacute stage. *Neurol Med Chir* 2005;45:464–469
8. Miller JD, Nader R. Acute subdural hematoma from bridging vein rupture: a potential mechanism for growth. *J Neurosurg* 2014;120:1378–1384
9. Morinaga K. Subacute subdural hematoma: findings in CT, MRI and operations and review of onset mechanism. *No Shinkei Geka* 1995;23:213–216
10. Xin ZL, Wu XK, Xu JR, et al. Arachnoid cell involvement in the mechanism of coagulation-initiated inflammation in the subarachnoid space after subarachnoid hemorrhage. *J Zhejiang Univ Sci B* 2010;11:516–523
11. Heula AL, Sajanti J, Majamaa K. Procollagen propeptides in chronic subdural hematoma reveal sustained dural collagen synthesis after head injury. *J Neurol* 2009;256:66–71

Finite-Element Analysis of a New Designed Miniplate which is Used via Intraoral Approach to the Mandible Angle Fracture: Comparison of the Different Fixation Techniques

Fatih Mehmet Coskunses, DDS, PhD,[*] *Ismail Doruk Kocyigit, DDS, PhD,*[†] *Fethi Atil, DDS, PhD,*[†] *Umut Tekin, DDS, PhD,*[†] *Berkay Tolga Suer, DDS, PhD,*[‡] *Hakan Hifzi Tuz, DDS, PhD,*[§] *Ozkan Ozgul, DDS, PhD,*[||] *and Ayberk Yagiz*[¶]

Abstract: The mandible is the largest facial bone as well as the most commonly fractured bone in the maxillofacial region. Despite numerous studies conducted to identify optimal treatment modalities and plates configurations for intraoral and transoral approaches, no definitive conclusion has been reached.

This study used finite element analysis (FEA) to assess 4 scenarios for treatment of an angle fracture (6-hole noncompression miniplate; 6-hole single plate/Champy's technique, 3D strut plate; 2 parallel 4-hole noncompression miniplates). Analysis included segmental displacement and Von Mises Stress evaluations of a 3D reconstruction of a human mandible.

Von Mises Stress values for plates did not vary significantly among treatment groups. Moreover, no significant differences were observed in cumulative displacement of segments subjected to vertical and horizontal loads, with all treatment configurations demonstrating clinical acceptability.

Key Words: Finite element analysis, mandible fracture, new designed miniplate

The most common bone injuries are mandible fractures, which account for 23–97% of all facial fractures.[1,2] Common causes of mandible fracture include physical assault, sports activities, motor vehicle accidents, industrial accidents, warfare, and falls.[3] Factors affecting fracture include the direction and amount of force as well as the biomechanical and anatomical properties of bone. The primary aim of treatment should be the reestablishment of function and form as quickly as possible. Rigid internal fixation can provide stability, reducing the risk of malunion and infection due to postoperative displacement of segments and improving quality of life for patients who would otherwise require intermaxillary fixation.[4]

The angle is one of the sites most frequently fractured as a result of a traumatic event involving the mandible.[5] Such fractures are commonly treated using miniplate osteosynthesis.[6,7] Successful use of a 3D strut – a single plate composed of 2 curved miniplates buttressed with perpendicular strut bars – and an increased number of screws have been confirmed in the literature.[8,9] In addition, Alkan et al[10] has recommended 2 parallel miniplates as an alternative to conventional treatment of mandibular angle fractures. This is usually achieved with a 6-hole miniplate and monocortical screws placed above or just below the superior border of the mandible and is referred to as Champy's technique. The authors of the present study have designed a new noncompression miniplate to be used with monocortical screws in an intraoral approach that would offer similar advantages to Champy's technique, but is also able to displace the lateral forces exerted on the miniplate.

From the *Department of Oral and Maxillofacial Surgery, Kocaeli University, Kocaeli; †Department of Oral and Maxillofacial Surgery, Kirikkale University, Kirikkale; ‡Department of Oral and Maxillofacial Surgery, Gulhane Military Medical Academy, Haydarpasa Teaching Hospital, Istanbul; §Department of Oral and Maxillofacial Surgery, Hacettepe University; ||Department of Oral and Maxillofacial Surgery, Ufuk University; and ¶Ay Tasarim, Ankara, Turkey.

Received January 27, 2015.

Accepted for publication April 14, 2015.

Address correspondence and reprint requests to Fatih Mehmet Coskunses, DDS, PhD, Assistant Professor, Kocaeli University, Faculty of Dentistry, Department of Oral and Maxillofacial Surgery, Yuvacik Yerleskesi Pasadagi Mah. Akcakesme Sok. No:5 41190 Basiskele/Kocaeli, Turkey; E-mail: fcoskunses@gmail.com

This study was supported by the Kirikkale University Research Foundation (Project #2012-110).

The authors report no conflicts of interest.

Copyright © 2015 by Mutaz B. Habal, MD

ISSN: 1049-2275

DOI: 10.1097/SCS.0000000000001890

Copyright © 2015 Mutaz B. Habal, MD. Unauthorized reproduction of this article is prohibited.

Finite element analysis (FEA) is a computational technique originally developed by engineers to model the mechanical behavior of structures such as buildings, aircraft, and engine parts.[11] FEA can provide stress and displacement analysis of materials with known properties and boundary conditions and has been shown to provide accurate analysis of the biomechanical behavior of bone.[12,13] Previous studies have used FEA and mechanical tests to evaluate various configurations of miniplates used for trauma or other reconstruction scenarios.[10,14,15]

This study used 3D FEA to evaluate and compare segmental displacement and Von Mises (VM) Stress values for a new miniplate, Champy's technique, a 3D strut plate and 2 parallel miniplates in mandible angle fractures.

MATERIALS AND METHODS

Modeling

Cone-beam computed tomography (CBCT) was used to obtain a 3D scanned image of a mandible bone. A model was constructed from 575 slices, each with a section range of 0.4 mm at the neutral position and a 512 × 512 pixel resolution. Images were recorded in Digital Imaging and Communications in Medicine (DICOM) format and transferred to the MIMICS 12.1 3D image-processing software (Materialise, Leuven, Belgium). A model of a hemimandible was created using a semi-full solid bone mask with a predefined threshold. Cancellous bone was modeled using the software's "Erode" feature to remove 3 pixels from the bone edge, and trabecular bone was modeled by manual editing. Boolean operations were performed to subtract the cancellous and trabecular bone masks to create the cortical bone model using the scanned information of the patient's own cortical bone. Geomagic Studio 10 software tools (eg spike, intersection) were used to correct the surface roughness of the cortical and trabecular bone, and the images were imported in the IGES format to the Solidworks software program (Dassault Systems SolidWorks Corp,). The Solidworks software was also used to generate solid 3D models of titanium plates and screws and to simulate a mandibular angle fracture. A caliper was used to measure the implant dimensions, and the modeled implants were virtually inserted into the fracture models.

Material Properties

Cortical and cancellous bone and implant models were assumed to be homogeneous, linear, elastic, and isotropic. Implants were modeled as the Ti–6Al–4 V titanium alloy. Elastic modulus and Poisson ratios of all materials were obtained from the literature[16] and are given in Table 1.

Loading Forces and Contact Conditions

CAD models were imported into the FEA software (ANSYS WORKBENCH 15.0) to simulate vertical and horizontal forces to the mandible. Models were meshed with 3-dimensional quadratic tetrahedral elements of 1 mm and 2 mm, respectively, for implant and bone. Bonding contact was defined as occurring between bone tissue and implants, with the exception of the osteotomy interfaces.

TABLE 1. Elastic Modulus and Poisson Ratios of Materials

Materials	Elastic Modulus (*E*) (MPa)	Poisson Ratio
Cortical bone[16]	8700	0.33
Cancellous bone[16]	500	0.30
Titanium alloy (Ti–6Al–4V)[16]	110,000	0.34

Vertical and horizontal forces of 100 N were applied based on the literature, which indicates masticatory forces ranging from 75 to 300N.[17,18] To decrease the model size and processing time, only a hemimandible was modeled, with symmetrical loading applied to the mandible median sagittal plane.

Plate and Screw Configurations

Four types of plate and screw configurations were modeled, as follows – Group 1: a newly designed 6-hole noncompression titanium miniplate (Trimed Titanium Implant Systems; Trimed, Ankara, Turkey); Group 2: a single straight, 6-hole noncompression titanium miniplate (Champy principle) (Trimed Titanium Implant Systems; Trimed, Ankara, Turkey); Group 3: an 8-hole 3D strut plate (Trimed Titanium Implant Systems; Trimed, Ankara, Turkey); Group 4: 2 parallel 4-hole noncompression titanium miniplates (Trimed Titanium Implant Systems; Trimed, Ankara, Turkey).

RESULTS

Displacement of Segments

An application of a vertical load of 100N resulted in displacements of the fracture segments by 0.00147 mm in Group 1 (Fig. 1), 0.00081 mm in Group 2 (Fig. 1), 0.00140 mm in Group 3, and 0.00071 mm in Group 4 (Fig. 2).

An application of a horizontal load of 100N resulted in displacements of 0.00234 mm in Group 1, 0.00267 mm in Group 2, 0.00293 mm in Group 3, and 0.00161 mm in Group 4 (Fig. 2).

Von Mises Stresses

An application of a vertical load of 100N produced VM stress values of 6.57 MPa on the plates in Group 1, 5.68 MPa in Group 2, 5.61 MPa in Group 3, and 3.95 MPa in Group 4 (Fig. 3) (Fig. 4).

An application of a horizontal load of 100N produced VM stress values of 5.32 MPa on the plates in Group 1, 3.20 MPa in Group 2, 3.52 MPa in Group 3, and 5.06 MPa in Group 4 (Fig. 3) (Fig. 4).

DISCUSSION

Mandible angle fractures are commonly occurring facial fractures that have a high incidence of postsurgical complications, making them a frequent topic of study.[8,9] In the case of mandibular fracture, the aim of treatment is to achieve the necessary reduction and stabilization to re-establish a functional occlusion, reducing morbidity and obviating the need for intermaxillary fixation (IMF).

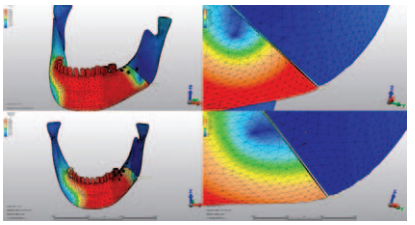

FIGURE 1. Displacements of the fracture segments with the result of vertical load: above left/right: Group 1; below left/right: Group 2.

FIGURE 2. Displacement of the segments in millimeters.

© 2015 Mutaz B. Habal, MD

Copyright © 2015 Mutaz B. Habal, MD. Unauthorized reproduction of this article is prohibited.

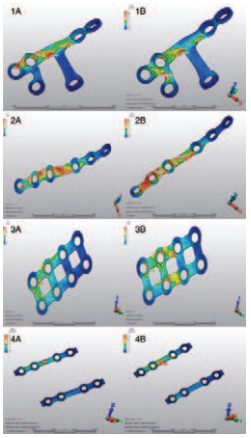

FIGURE 3. VM stresses of the plates with the application of vertical and horizontal loads: vertical load/left (A); horizontal load/right (B).

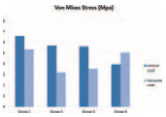

FIGURE 4. Von Mises Stress values of miniplates.

Studies have put forward a variety of recommendations for establishing accurate reduction and stable fixation, with different treatment modalities, including various plating techniques. Except for cases of comminuted and complicated fractures, intraoral approaches are considered preferable to IMF and extra oral approaches. Whereas extra oral approaches involve an external incision and potential nerve complication, IMF may be associated with a compromise of the oropharyngeal airway, inadequate nutritional intake and associated weight loss, thinning of the temporomandibular joint articular cartilage, ankyloses, and patient noncompliance.[19]

Five years after Michelet et al[20] published their technique for intraoral open reduction with intermaxillary fixation using a single noncompression miniplate adapted to the superior border along the external oblique ridge of the mandible, Champy et al[21] published a biomechanical study demonstrating the ideal osteosynthesis line based on what later became known as Champy's principle. Champy's technique, which entails the placement of a single noncompression miniplate at the superior border of the mandible, has been reported to result in the lowest morbidity rates, with the fewest postoperative complications of all techniques used to treat mandible angle fractures.[20,21] Although Champy's technique is preferred by surgeons because the size and adaptability of the miniplate make it easy to fix via an intraoral approach, Kroon et al[22] have reported Champy's technique to be associated with poor resistance to torsional forces, poor rigidity, and poor stability in angle fracture prompting researchers to turn their attention to new methods that aim to overcome these disadvantages.

A biomechanical study by Suer et al[15] evaluated the same new plate design assessed in the present study, namely a noncompression titanium miniplate similar to the one used on the external oblique ridge in the conventional Champy's technique, but with the addition of lateral extensions. The study found the new design to offer improved stability in the case of mandible angle fracture. Another biomechanical study by Alkan et al[10] found more favorable biomechanical behavior with the placement of 2 miniplates when compared to both Champy's technique and the monoplanar plate placement; based on these results, the authors suggested that 2 miniplates would provide better anatomical repositioning and more stable fixation of mandible angle fractures. Sehgal et al[23] conclude that use of 3D titanium miniplates showed similar results when compared to use of two standard titanium miniplates. Similarly, biomechanical clinical studies by Choi et al[24] and Schierle et al[25] found placement of a second miniplate at the inferior border provided stable fixation under functional loading. However, other studies reported an unacceptable rate of complications with the use of miniplates at both the superior and inferior borders of the mandible, but no difference in stability between 1 and 2 plate configurations.[6,26] Furthermore, placement of a second miniplate has been reported to increase operating time, costs, postoperative morbidity, and risk of bacterial contamination.[26,27] Given the discrepancies in the literature, this study aimed to determine whether the addition of lateral extensions to a miniplate similar to that used in Champy's technique would improve stability in the case of mandible angle fracture. Two other designs – namely, parallel miniplates and a 3D strut plate – were also evaluated.

The accuracy of 3D FEA in assessing plating techniques used in the treatment of facial fractures has been confirmed in different studies.[28,29] The procedure is able to demonstrate the complexities of stress behavior that characterize actual clinical conditions.[16] The present study measured VM stress, a trait used to evaluate ductile material such as titanium, as well as segmental displacement.

Excessive mobilization can result in nonunion of fracture segments and prevent proper bone healing. Cox et al[30] reported segmental displacement in excess of 0.15 mm to result in failure of bone healing, with tissue formation proceeding from granulation tissue to connective tissue, woven bone, and, ultimately, compact bone. The present study found segmental displacement to be at clinically acceptable levels for direct bone healing with all plate configurations tested.

Similarly, despite significant differences in VM stress values on miniplates of different configurations with both vertical and horizontal loads, none of the treatment designs in the present study would produce clinical failure. Biomechanical stability of the new miniplate design, Champy's technique, two parallel miniplates, and the 3D strut plate was found to be similar when subjected to lateral as well as horizontal displacing forces. Thus, the new design appears to offer another plating technique that can be used with a simple intraoral approach and with few major complications, such as facial nerve injury or visible scar tissue. In contrast, the use of either the 8-hole 3D strut miniplate or two parallel miniplates for fixation of mandible angle fractures would be more difficult, requiring a transbuccal approach in most cases.

In conclusion, results of the present FEA study, although not entirely reflective of clinical conditions, suggest a new design for a titanium miniplate offers similar resistance and stability to existing modalities and thus represents a useful alternative in the treatment of noncomminuted, noncomplicated and minimally displaced mandible angle fractures. Further prospective clinical studies are required to determine the effectiveness of this new plate design under actual clinical conditions.

REFERENCES

1. Vetter JD, Topazian RG, Goldberg MH, et al. Facial fractures occurring in a medium-sized metropolitan area: recent trends. *Int J Oral Maxillofac Surg* 1991;20:214–216
2. Haug RH, Prather J, Indresano AT. An epidemiologic survey of facial fractures and concomitant injuries. *J Oral Maxillofac Surg* 1990;48: 926–932

© 2015 Mutaz B. Habal, MD

Copyright © 2015 Mutaz B. Habal, MD. Unauthorized reproduction of this article is prohibited.

3. Torreira MG, Fernandez JR. A three-dimensional computer model of the human mandible in two simulated standard trauma situations. *J Craniomaxillofac Surg* 2004;5:303–307
4. Fox AJ, Kellman RM. Mandibular angle fractures. *Arch Fac Plast Surg* 2003;5:464–469
5. Chacon GU, Dillard F, Clelland N, et al. Comparison of strains produced by titanium and poly D,L-lactide acid plating systems to in vitro forces. *J Oral Maxillofac Surg* 2005;63:968–972
6. Ellis E 3rd. Treatment methods for fractures of the mandibular angle. *Int J Oral Maxillofac Surg* 1999;28:243–252
7. Regev E, Shiff JS, Kiss A, et al. Internal fixation of mandibular angle fractures: a meta-analysis. *Plast Reconstr Surg* 2010;125:1753–1760
8. Feledy J, Caterson EJ, Steger S, et al. Treatment of mandibular angle fractures with a matrix miniplate: a preliminary report. *Plast Reconstr Surg* 2004;114:1711–1716
9. Guimond C, Johnson JV, Marchena JM. Fixation of mandibular angle fractures with a 2.0 mm 3-dimentional curved angle strut plate. *J Oral Maxillofac Surg* 2005;63:209–214
10. Alkan A, Celebi N, Ozden B, et al. Biomechanical comparison of different plating techniques in repair of mandibular angle fractures. *Oral Surg Oral Med Oral Pathol Oral Radiol Endod* 2007;104:752–756
11. Aquilina P, Chamoli U, Parr WC, et al. Finite element analysis of three patterns of internal fixation of fractures of the mandibular condyle. *Br J Oral Maxillofac Surg* 2013;51:326–331
12. Hart RT, Hennebel VV, Thongpreda N, et al. Modeling the biomechanics of the mandible: a three-dimensional finite element study. *J Biomech* 1992;25:261–286
13. Korioth TW, Versluis A. Modeling the biomechanical behavior of the jaws and their related structures by finite element (FE) analysis. *Crit Rev Oral Biol Med* 1997;8:90–104
14. Haug RH, Fattahi TT, Goltz M. A biomechanical evaluation of mandibular angle fracture plating techniques. *J Oral Maxillofac Surg* 2001;59:1199–1210
15. Suer BT, Kocyigit ID, Kaman S, et al. Biomechanical evaluation of a new design titanium miniplate for the treatment of mandibular angle fractures. *Int J Oral Maxillofac Surg* 2014;43:841–845
16. Maurer P, Holweg S, Johannes S. Finite element analysis of different screw diameters in the sagittal split osteotomy of the mandible. *J Craniomaxillofac Surg* 1999;27:365–372
17. Haraldson T, Carlsson GE. Bite force and oral function in patients with osseointegrated oral implants. *Scand J Dent Res* 1977;85:200–208
18. Uckan S, Veziroglu F, Soydan SS, et al. Comparison of stability of resorbable and titanium fixation systems by finite element analysis after maxillary advancement surgery. *J Craniofac Surg* 2009;20:775–779
19. Fernandez JR, Gallas M, Burquera M, et al. A three-dimensional numerical simulation of mandible fracture reduction with screwed miniplates. *J Biomech* 2003;36:329–337
20. Michelet FX, Deymes J, Dessus B. Osteosynthesis with miniaturized screwed plates in maxillo-facial surgery. *J Maxillofac Surg* 1973;1: 79–84
21. Champy M, Lodde JP, Schmitt R, et al. Mandibular osteosynthesis by miniature screwed plates via a buccal approach. *J Maxillofac Surg* 1978;6:14–21
22. Kroon FH, Mathisson M, Cordey JR, et al. The use of miniplates in mandibular fractures. An in vitro study. *J Craniomaxillofac Surg* 1991;19:199–204
23. Sehgal S, Ramanujam L, Prasad K, et al. Three-dimensional v/s standard titanium miniplate fixation in the management of mandibular fractures: a randomized clinical study. *J Craniomaxillofac Surg* 2014;42:1292–1299
24. Choi BH, Yoo JH, Kim KN, et al. Stability testing of a two miniplate fixation technique for mandibular angle fractures. An in vitro study. *J Craniomaxillofac Surg* 1995;23:123–125
25. Schierle HP, Schmelzeisen R, Rahn B, et al. One- or two-plate fixation of mandibular angle fractures. *J Craniomaxillofac Surg* 1997;25: 162–168
26. Siddiqui A, Markose G, Moos KF, et al. One miniplate versus two in the management of mandibular angle fractures: a prospective randomised study. *Br J Oral Maxillofac Surg* 2007;45:223–225
27. Kumar S, Prabhakar V, Rao K, et al. A comparative review of treatment of 80 mandibular angle fracture fixation with miniplates using three different techniques. *Indian J Otolaryngol Head Neck Surg* 2011;63: 190–192
28. Han UA, Kim Y, Park JU. Three-dimensional finite element analysis of stress distribution and displacement of the maxilla following surgically assisted rapid maxillary expansion. *J Craniomaxillofac Surg* 2009;37: 145–154
29. Ishak MI, Kadir MR, Sulaiman E, et al. Finite element analysis of zygomatic implants in intrasinus and extramaxillary approaches for prosthetic rehabilitation in severely atrophic maxilla. *Int J Oral Maxillofac Implants* 2013;28:151–160
30. Cox T, Kohn MW, Impelluso T. Computerized analysis of resorbable polymer plates and screws for the rigid fixation of mandibular angle fractures. *J Oral Maxillofac Surg* 2003;61:481–487

Clinical Characteristics and Treatment of Trigeminal Neuralgia Following Herpes Zoster

Guo-wei Li, MD, Qing Lan, PhD, and Wen-chuan Zhang, MD

Objective: The aim of this study was to illustrate the clinical characteristics and treatment of trigeminal neuralgia following herpes zoster.

Methods: From August 1, 2011 to August 1, 2013, 23 consecutive patients with trigeminal neuralgia following herpes zoster underwent microvascular decompression (MVD) at our cranial nerve disease center. All patients underwent preoperative MRI evaluation, intraoperative observation, and clinical effect evaluation. Clinical data were collected and analyzed in our center.

Results: V2 division was the most commonly affected branch. Unlike pretrigeminal neuralgia (PTN), trigger zone was only found in a small part of patients (21.7%). Unlike PTN, the adhesions and compressions between trigeminal nerve and offending vessels were usually not serious; trigeminal nerve usually is atrophic; superior cerebellar artery was the most common offending vessels (65.2%). Of 23 patients, 19 experienced pain relief (82.6%), 1 patient suffered from hearing loss, and another one suffered from cerebrospinal fluid leak; no severe complications were found. During follow-up period, no recurrence was found (3 lost).

Conclusions: For patients who suffered from trigeminal neuralgia following herpes zoster, trigger zone was only found in a small part of patients. The trigeminal nerve usually is atrophic; microvascular decompression was equally applied to these patients if vessel compression was confirmed.

From the Department of Neurosurgery, Second Affiliated Hospital of Soochow University, Suzhou, China.
Received March 1, 2015.
Accepted for publication April 19, 2015.
Address correspondence and reprint requests to Qing Lan, PhD, No 1055 Sanxiang Road, Suzhou, Jiangsu, China 215004.
E-mail: lgw19880729@163.com
The authors report no conflict of interest.
Copyright © 2015 by Mutaz B. Habal, MD
ISSN: 1049-2275
DOI: 10.1097/SCS.0000000000001893

Copyright © 2015 Mutaz B. Habal, MD. Unauthorized reproduction of this article is prohibited.

Key Words: Adhesion, compression, herpes zoster, microvascular decompression, secondary trigeminal neuralgia

In most instances, zoster produces cutaneous pain at the time of the infection. Although it is reported that herpes zoster virus is usually associated with trigeminal neuralgia (TN), sometimes also implicated in the etiology of TN,[4] the definite pathogenetic of this association has not been illuminated yet. For most patients, neuralgia usually disappears 1 month after herpes zoster heals up, but a small number of patients suffer from long-term postherpetic neuralgia.[3,5] Whether these patients share vascular compression as generally accepted for primary TN and their treatment remains controversial. For now, there are only scattered reports about TN following herpes zoster, mainly limited to single case report. In this article, 23 consecutive patients with TN following herpes zoster who referred to our hospital were retrospectively analyzed, to illustrate the clinical characteristics and treatment of TN following herpes zoster.

PATIENTS AND METHODS

Patient Population

From August 1, 2011 to August 1, 2013, 23 consecutive patients with TN following herpes zoster underwent microvascular decompression (MVD) in our hospital. The age of patients ranged from 35 to 81 years (mean age, 61.7 years); the pain duration ranged from 11 to 32 months (mean 21.09 months). Three divisions of trigeminal nerve were affected in 5 patients (21.7%), 2 divisions were affected in 13 patients (56.5%), and 1 division was affected in 5 patients (21.7%). V1 was affected in 12 patients (52.2%), V2 was affected in 19 patients (82.6%), and V3 was affected in 15 patients (65.2%); the V2 division was the most commonly affected branch. All patients suffered from facial pain whereas trigger zone was found in 5 patients. Eighteen patients underwent pill treatment previously, 3 patients underwent acupuncture previously, and 2 patients underwent radio frequency previously; no one is treated successfully or underwent surgical treatment before they were admitted to our center (Table 1).

Magnetic Resonance Imaging

3.0-Tesla magnetic resonance imaging (MRI) scanner (General Electric Vectra, IGF Medical, Milwaukee, WI, USA) was employed for neuroradiologic examination for each patient before surgery, to evaluate the vessel condition. During this examination, three-dimensional time-of-flight (3D-TOF) sequence was adopted; intracranial lesions could also be excluded (Fig. 1).

The Operation

For all the patients, we performed MVD as described[10]: A suboccipital superior-lateral cerebellar approach via a retromastoid craniectomy was operated in all patients. After the dura was opened and sutured back, a direct corridor along the petrotentorial bone was created. With microscopic visualization, all arachnoids around the nerve and vessels were sharply dissected. The trigeminal nerve should be circumferentially inspected along its entire intracranial course from root entry zone at the brainstem laterally to its entrance into the Meckel cave. Offending vessels should be separated once they were found compressing trigeminal nerve. Finally, insert Teflon between offending vessels and trigeminal nerve.

Clinical Effect Evaluation

Surgical effects included pain relief, which we divided as "excellent" (at least 98% pain free), "good" (75% or greater pain free), and "failure" (less than 75% pain free). The follow-up duration was limited to 12 months.

TABLE 1. Patient Population, Symptom Observation, Intraoperative Findings, and Follow-Up Results

ID	Sex/Age	Duration (m)	Division	Trigger	previous treatment	MRI	Neuro thin/atrophy	Offending vessel	Pain relief	Complication	Clinical effect	Follow-up (m)
1	Male/63	17	V2,V3	No	Pills	Positive	Yes	SCA	Yes	No	Excellent	12
2	Male/48	14	V1,V2	No	Pills	Positive	Yes	SCA	Yes	No	Excellent	12
3	Female/41	21	V1	No	Pills	Positive	Yes	AICA	No	No	Failed	12
4	Female/46	23	V2,V3	No	Pills	Positive	Yes	SCA	Yes	No	Excellent	Lost
5	Male/37	25	V1,V2,V3	Yes	Pills	Positive	Yes	Vein	Yes	No	Excellent	12
6	Male/68	11	V3	Yes	Pills	Positive	Yes	AICA	Yes	No	Excellent	12
7	Female/71	13	V1,V2	No	Pills	Positive	Yes	SCA	Yes	No	Good	12
8	Female/63	32	V1,V2,V3	No	Acupuncture	Positive	Yes	Vein	No	No	Failed	12
9	Male/79	29	V2,V3	No	Pills	Positive	Yes	SCA	Yes	No	Excellent	12
10	Female/62	26	V2	No	Acupuncture	Positive	No	SCA	Yes	No	Excellent	12
11	Male/71	20	V1,V2,V3	No	Pills	Positive	Yes	SCA	Yes	No	Excellent	12
12	Male/76	18	V1,V2	Yes	Pills	Positive	Yes	Vein	No	No	Failed	12
13	Female/81	24	V1,V2,V3	No	Pills	Positive	Yes	SCA	Yes	Yes	Good	12
14	Female/63	12	V1,V2	No	Pills	Positive	Yes	SCA	Yes	No	Excellent	12
15	Male/74	19	V2,V3	No	RF	Positive	Yes	SCA	Yes	No	Excellent	12
16	Male/59	24	V2,V3	No	Pills	Positive	No	SCA	Yes	No	Excellent	12
17	Female/35	32	V3	No	RF	Positive	Yes	AICA	Yes	No	Excellent	Lost
18	Male/65	25	V1,V2	Yes	Pills	Positive	Yes	SCA	Yes	No	Excellent	12
19	Male/73	17	V1,V2,V3	No	Pills	Positive	Yes	Vein	No	Yes	Failed	12
20	Female/61	12	V2,V3	No	Pills	Positive	Yes	Vein	Yes	No	Excellent	12
21	Male/70	30	V3	No	Acupuncture	Positive	Yes	SCA	Yes	No	Excellent	12
22	Female/52	28	V1,V2	No	Pills	Positive	No	SCA	Yes	No	Good	12
23	Male/61	13	V2,V3	Yes	Pills	Positive	Yes	SCA	Yes	No	Excellent	Lost

© 2015 Mutaz B. Habal, MD

Copyright © 2015 Mutaz B. Habal, MD. Unauthorized reproduction of this article is prohibited.

RESULTS

MRI Findings

See Figure 1.

Intraoperative Findings

During surgical procedures, we found that vessel compression or adhesion in these patients usually were not very serious; nerve translocation only existed in a few patients. Trigeminal nerve usually is atrophic, which was probably caused by herpes zoster infection (Figs. 2-4).

Clinical Effect

Postoperatively, the symptom of pain completely disappeared once patients awoke from the anesthesia in 16 cases. According to the evaluation scale mentioned above, the results were ''excellent''; the pain mostly relieved in 3 patients, defined as good; 4 patients have not reached a satisfying pain relief, defined as failure, the remission rate was 82.6%; 1 patient suffered from hearing loss and another one suffered from cerebrospinal fluid leak. During follow-up period, no recurrence was found (3 lost) (Table 1).

DISCUSSION

Trigeminal nerve is a syndrome characterized by paroxysmal facial pain, which is a typical pain distributed in the zone dominated by trigeminal nerve. It is reported that there is an annual incidence of 12.6 per 100,000 person-years.[7,11,13] Usually, TN is divided into primary or secondary ones; compared with primary TN, the secondary ones are rare in clinic, which are usually associated with hypoesthesia, impairment of other cranial nerves, or of the central nervous system. Lesions in cerebellopontine angle area and malignant skull base tumors are the common pathogenesis for secondary TN. Besides this, oral and maxillofacial surgeons found that approximately 20% herpes zoster patients suffered from TN, but for now no consecutive cases have ever been retrospectively studied.

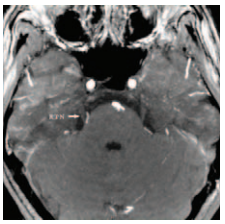

FIGURE 1. Vascular image could be revealed around right trigeminal nerve.

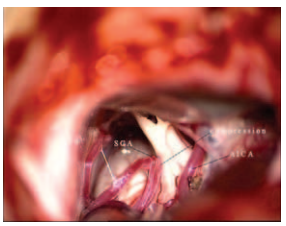

FIGURE 2. Superior cerebellar artery compressed trigeminal nerve in the first zone; anterior cerebellar artery compressed trigeminal nerve in the second zone. We notice that the compression and adhesion between nerve and artery were not serious, no nerve translocation was found, at the same time trigeminal nerve suffered mild delicate and atrophic, which was probably caused by herpes zoster infection.

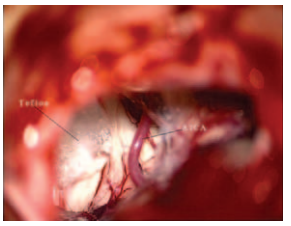

FIGURE 3. Insert Teflon between trigeminal nerve and SCA to relieve compression.

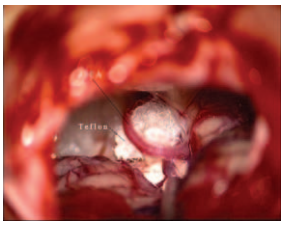

FIGURE 4. Insert Teflon between trigeminal nerve and AICA to relieve compression.

Since 1967, when Jannetta brought forward microvascular compression theory,[6] microvascular decompression has been wildly applied to treat pretrigeminal neuralgia (PTN) patients.[2,8] Unlike PTN, the treatment for TN following herpes zoster is mainly limited to oral or vein medications, including antiviral drugs, antidepressants, anticonvulsants and painkillers, acyclovir, carbamazepine, tricyclic antidepressants, which are usually the first choice.[1,9,12] Local application such as lidocaine are also used for treatment. Besides these, radio frequency and γ-knife were used for severe patients who were failed in drug therapy.[14]

Based on these, we considered that these patients shared unique clinical characteristics and if the preoperative MRI showed positive vessel image, microvascular decompression was equally applied to the patients.

Through symptom observation, we found V2 division was the most commonly affected branch. Unlike PTN, trigger zone was only found in a small part of patients (21.7%); all patients showed positive vessel image in MRI (Table 1).

Through intraoperative observation, we found that unlike PTN, the adhesions and compressions between trigeminal nerve and offending vessels were usually not serious. TN usually suffered delicate and atrophic; superior cerebellar artery was the most common offending vessels (65.2%, Figs. 2-4, Table 1).

Based on the above observation, we considered that herpes virus infection would lead to TN degeneration; thus, nerve suffered from demyelination. This change makes trigeminal nerve more sensitive to neurovascular compression. Therefore, these patients had severe symptoms despite the fact that the compression and adhesion were not serious. For these cases, we should perform microvascular decompression once vessel compression was confirmed.

Through surgical outcomes evaluation, we found that of 23 patients, 19 experienced pain relief (82.6%), 1 patient suffered hearing loss, and another one suffered from cerebrospinal fluid leak, no severe complications were found. During follow-up period, no recurrence was found (3 lost) (Table 1).

CONCLUSIONS

Based on the above analysis, we concluded that for patients suffered from TN following herpes zoster, trigger zone was only found in a small part of patients. The TN usually suffered delicate and

© 2015 Mutaz B. Habal, MD

Copyright © 2015 Mutaz B. Habal, MD. Unauthorized reproduction of this article is prohibited.

atrophic; microvascular decompression was equally applied to these patients if vessel compression was confirmed.

REFERENCES

1. Backonja MM. Use of anticonvulsants for treatment of neuropathic pain. *Neurology* 2002;59 (5 suppl 2):S14
2. Borucki L, Szyfter W, Wrobel M, et al. Neurovascular conflicts. *Otolaryngol Pol* 2006;60:809–815
3. Eller JL, Raslan AM, Burchiel KJ. Trigeminal neuralgia: definition and classification. *Neurosurg Focus* 2005;18:E3
4. Gilden DH, Kleinschmidt-DeMasters BK, LaGuardia JJ, et al. Neurologic complications of the reactivation of varicella-zoster virus. *N Engl J Med* 2000;342:635–645
5. Gilden DH, Mahalingam R, Dueland A, et al. Herpes zoster: pathogenesis and latency. *Prog Med Virol* 1992;39:19–75
6. Jannetta PJ. Arterial compression of the trigeminal nerve at the pons in patients with trigeminal neuralgia. *J Neurosurg* 1967;107:216–219
7. Koopman JS, Dieleman JP, Huygen FJ, et al. Incidence of facial pain in the general population. *Pain* 2009;147:122–127
8. Kureshi SA, Wilkins RH. Posterior fossa reexploration for persistent or recurrent trigeminal neuralgia or hemifacial spasm: surgical findings and therapeutic implications. *Neurosurgery* 1998;43:1111–1117
9. Li Q, Chen N, Yang J, et al. Antiviral treatment for preventing postherpetic neuralgia. *Cochrane Database Syst Rev* (2)2009Art.No:CD00686
10. Li ST, Wang X, Pan Q, et al. Studies on the operative outcomes and mechanisms of microvascular decompression in treating typical and atypical trigeminal neuralgia. *Clin J Pain* 2005;21:311–316
11. Merskey H, Bogduk N. Classification of chronic pain. Descriptors of chronic pain syndromes and definitions of pain terms. 2nd ed. Seattle: IASP Press; 1994:222
12. Roxas M. Herpes zoster and postherpetic neuralgia: diagnosis and therapeutic considerations. *Altern Med Rev* 2006;11:102–113
13. Tenser RB. Herpes zoster infection and postherpetic neuralgia. *Curr Neurol Neurosci Rep* 2001;1:526–532
14. Urgosik D. Treatment of postherpetic trigeminal neuralgia with the gamma knife. *J Neurosurg* 2000;93 (suppl 3):165–168

Vision Loss due to Central Retinal Artery Occlusion Following Embolization in a Case of a Giant Juvenile Nasopharyngeal Angiofibroma

Mihir Trivedi, MBBS, Roshani J. Desai, MS,* Nayana A. Potdar, MS,* Chhaya A. Shinde, MS,* Vivek Ukirde, MD,† Maunil Bhuta, MD,† and Akshay Gopinathan Nair, DNB*‡*

Abstract: Juvenile nasopharyngeal angiofibroma (JNA) is a benign, vascular, and locally aggressive tumor that arises in the nasal cavity, extending into the nasopharynx and often in to the orbit. It may rarely present to the ophthalmologist with proptosis and optic neuropathy. Preoperative embolization of JNA is done before surgical resection. In this communication, the authors report a rare occurrence of ipsilateral central retinal artery occlusion (CRAO) following embolization with polyvinyl alcohol in a 13-year-old boy with right-sided JNA. Retrospective review of the angiograms pointed out to a suspicious communication between the external carotid artery and the ophthalmic vessels. Pre-embolization detailed study of the angiograms is necessary to avoid such devastating complications. Although rare, vision loss is a possible complication arising from embolization of nasopharyngeal and intracranial tumors, and all patients undergoing these procedures should be informed of the risk of visual loss because it has a lasting impact on the quality of life.

Key Words: Central retinal artery occlusion, embolization, juvenile nasopharyngeal angiofibroma, polyvinyl alcohol, proptosis

Juvenile nasopharyngeal angiofibroma (JNA) is an uncommon, benign, vascular, and locally aggressive tumor that predominantly occurs in adolescent boy. Although the presenting symptom is usually painless nasal obstruction or epistaxis, other symptoms may develop depending on the size and extent of the tumor mass.[1] Stern et al[2] in their review of JNA reported that proptosis was noted in 14% of cases of JNA, whereas decreased visual acuity and partial ophthalmoplegia occurred in 5% and 2% of the cases, respectively. Surgery is the mainstay of treatment of JNA. Preoperative embolization and newer surgical approaches result in less hemorrhage and complete resection of the tumor.[1] Although CRAO has been reported as a result of embolization of nasal vessels for intractable epistaxis[3,4], there have been only 3 previously documented cases of CRAO resulting in visual loss as a result of embolization for a nasopharyngeal angiofibroma.[5–7]

CLINICAL REPORT

A 13-year-old boy presented to our clinic with a history of outward protrusion of the right eye and diplopia since 2 months. He also had a history of repeated right-sided nasal bleeds since 1 year. His other complaints included nasal stuffiness and snoring. His history was significant as he had undergone a transmaxillary excision of a nasal mass through a lateral rhinotomy, 10 months before presentation. There was no history of toothache and the patient's dental history was noncontributory. On examination, his visual acuity was 6/9, N6 OD and 6/6, N6 OS. Color vision was normal in both eyes, when recorded with Ishihara pseudoisochromatic plates. Grade I RAPD was present in the right eye. Right-sided axial proptosis was noted in the right eye with minimal upward dystopia (Fig. 1A). Hertel exophthalmometry measurements were 28 mm in the right eye and 18 mm in the left eye. Vertical diplopia present in all gazes except downgaze suggestive of a mechanical compression inferiorly. On dilated fundus examination, there was disc hyperemia with elevated margins seen suggestive of compressive optic neuropathy in the right eye.

No visual field defects were seen on 30-2 automated visual fields. A computed tomography (CT) scan showed a large

From the *Departments of Ophthalmology; †Radiodiagnosis, Lokmanya Tilak Municipal General Hospital and Medical College, Sion, Mumbai; and ‡Ophthalmic Plastic Surgery and Neuro-Ophthalmology, Advanced Eye Hospital and Institute, Navi Mumbai, India.

Received March 25, 2015.
Accepted for publication May 3, 2015.

Address correspondence and reprint requests to Akshay Gopinathan Nair, DNB, Department of Ophthalmology, Lokmanya Tilak Municipal General Hospital and Medical College, Sion, Mumbai 400 022, India; E-mail: akshaygn@gmail.com

The authors report no conflicts of interest.

Copyright © 2015 by Mutaz B. Habal, MD

ISSN: 1049-2275
DOI: 10.1097/SCS.0000000000001936

Copyright © 2015 Mutaz B. Habal, MD. Unauthorized reproduction of this article is prohibited.

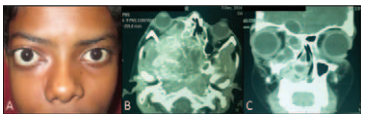

FIGURE 1. A, External photograph depicting the right-sided proptosis. Note the external scar from the previous surgery. B and C, CT scan depicting the extent and aggressive nature of the tumor with its epicenter in the postoperative bed in the right pterygopalatine fossa and the right sphenopalatine foramen.

heterodense, destructive, soft tissue lesion with its epicenter in the postoperative bed in the right pterygopalatine fossa and the right sphenopalatine foramen (Fig. 1B-C). The mass measuring $47 \times 42 \times 54$ mm had completely occupied the entire right nasal cavity with destruction of the medial wall of the orbit; the mass was compressing the globe and causing proptosis. Furthermore, there was extension into the right maxillary antrum crossing the midline and displacing the nasal septum. Axial cuts showed extension of the tumor mass into the nasopharynx. An otorhinolaryngology consult was sought and correlating the clinical and imaging findings of previous histopathologic reports, a diagnosis of recurrent JNA was made. The plan was to embolize the tumor using polyvinyl alcohol (PVA) particles to reduce the size of the tumor, which would also relieve the mechanical compression on the optic nerve before excision. Subsequently, digital subtraction angiography and selective endovascular embolization of the right internal maxillary artery with 150 to 250 mm PVA particles was carried out. Following the procedure, the patient complained of loss of vision in the right eye and vision was recorded as no perception of light. On fundus examination, a hyperemic disc with ischemic areas around the optic disc and a cherry red spot were found in the right eye. Therefore, a diagnosis of CRAO was made (Fig. 2). Ocular massage was initiated and continued for 15 minutes and paracentesis was also performed under topical anesthesia. He also received oral acetazolamide 250 mg immediately, which was continued BD for 2 days. The vision recorded on the next day was perception of light with inaccurate projection of rays. Twelve days following the initial embolization, the patient underwent excision of the residual mass. The vision, however, did not improve. Retrospective study of the angiograms showed the presence of a choroidal blush when then external carotid angiogram was performed suggestive of a communication between the external carotid and the ophthalmic artery, which was possibly overlooked before the embolization (Fig. 3). This communication could have led to the flow of PVA into the ophthalmic vasculature leading to CRAO.

DISCUSSION

In a retrospective analysis of 167 cranial base meningiomas that were embolized with PVA, Rosen et al[8] found a 1.8% risk of retinal artery occlusion despite superselective angiography. Casasco et al[7] reported a case of a 18-year-old boy with a left-sided JNA where the technique followed was direct intratumoral injection of permanent liquid polymerizing agent that causes embolization. The mixture injected was a combination of Histoacryl, Lipiodol, and tantalum

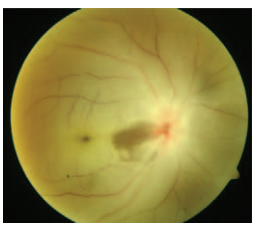

FIGURE 2. Fundus photograph showing the ischemic retina, attenuated vessels, and the area supplied by the cilioretinal artery demarcated separately.

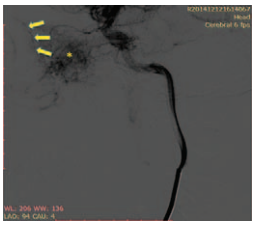

FIGURE 3. Angiogram of the external carotid vascular system showing the vascular angiofibroma (asterisk mark); note the appearance of a carotid blush indicating the presence of a communication between the external carotid vasculature and the ophthalmic artery.

powder. In their case, a small amount of Histoacryl entered the ophthalmic artery, resulting in an acute loss of vision in the left eye.

Ramezani et al[6] reported a case of a 23-year-old man with right-sided JNA who developed CRAO following preoperative embolization with PVA. They reported, however, that a retrospective review of the angiograms revealed the presence of a suspicious collateral artery between the external carotid artery and ophthalmic vessels on the left side, which had not been noticed before embolization. They suggested that the embolus passed mostly via this collateral artery to the left central retinal artery whereas tumor embolization was being carried out through the left-side arteries.[6]

Onerci et al reported a case of a child with JNA who developed CRAO following preoperative embolization. In their case, however, they could not demonstrate any responsible communicating artery and therefore assumed the existence of a branch of the internal maxillary artery supplying the intraorbital contents and the retina in their case.[5]

Considering the long-standing duration of tumor, its vascular nature and the potential for angiogenesis in JNA,[9] it is prudent to expect the presence of collateral vessels in such cases. The different mechanisms in which PVA embolization can cause CRAO can be varied: the presence of congenital variations in vasculature, overforceful injection, which can result in a reflux into the internal carotid system,[10] or collaterals, which may arise because of the tumor's aggressive and vascular nature.[5]

Our case is rare and unusual but potentially avoidable. We, therefore, agree with the recommendations of Ramezani et al[6] that careful evaluation of angiograms for detection of any abnormal collateral vessels or any vascular anomaly before embolization is extremely important. Furthermore, we believe that vision loss is a possible complication arising from embolization of nasopharyngeal and intracranial tumors and all patients undergoing these procedures should be informed of the risk of visual loss because it has long-term consequences and impact on the quality of life. Ophthalmologists and ENT specialists, alike should be sensitive to the possibility of this uncommon rare but devastating complication occurring after PVA embolization for JNA.

REFERENCES

1. Mishra S, Praveena NM, Panigrahi RG, et al. Imaging in the diagnosis of juvenile nasopharyngeal angiofibroma. *J Clin Imaging Sci* 2013;3 (suppl 1):1
2. Stern RM, Beauchamp GR, Berlin AJ. Ocular findings in juvenile nasopharyngeal angiofibroma. *Ophthalmic Surg* 1986;17:560–564
3. Mames RN, Snady-McCoy L, Guy J. Central retinal and posterior ciliary artery occlusion after particle embolization of the external carotid artery system. *Ophthalmology* 1991;98:527–531
4. Ashwin PT, Mirza S, Ajithkumar N, et al. Iatrogenic central retinal artery occlusion during treatment for epistaxis. *Br J Ophthalmol* 2007;91:122–123

© 2015 Mutaz B. Habal, MD

Copyright © 2015 Mutaz B. Habal, MD. Unauthorized reproduction of this article is prohibited.

5. Onerci M, Gumus K, Cil B, et al. A rare complication of embolization in juvenile nasopharyngeal angiofibroma. *Int J Pediatr Otorhinolaryngol* 2005;69:423–428
6. Ramezani A, Haghighatkhah H, Moghadasi H, et al. A case of central retinal artery occlusion following embolization procedure for juvenile nasopharyngeal angiofibroma. *Indian J Ophthalmol* 2010;58:419–421
7. Casasco A, Houdart E, Biondi A, et al. Major complications of percutaneous embolization of skull-base tumors. *Am J Neuroradiol* 1999;20:179–181
8. Rosen CL, Ammerman JM, Sekhar LN, et al. Outcome analysis of preoperative embolization in cranial base surgery. *Acta Neurochir (Wien)* 2002;144:1157–1164
9. Saylam G, Yücel OT, Sungur A, et al. Proliferation, angiogenesis and hormonal markers in juvenile nasopharyngeal angiofibroma. *Int J Pediatr Otorhinolaryngol* 2006;70:227–234
10. Vitek J. Idiopathic intractable epistaxis: endovascular therapy. *Radiology* 1991;181:113–116

© *2015 Mutaz B. Habal, MD*

Copyright © 2015 Mutaz B. Habal, MD. Unauthorized reproduction of this article is prohibited.